

Analytische Chemie

**Degradation of Crude Oil in the Environment:
Toxicity Arising Through Photochemical Oxidation in the
Aqueous Phase**

Inaugural-Dissertation
zur Erlangung des Doktorgrades
der Naturwissenschaften im Fachbereich Chemie und Pharmazie
der Mathematisch-Naturwissenschaftlichen Fakultät
der Westfälischen Wilhelms-Universität Münster

vorgelegt von

Eiman Mohamed Fathalla

aus Alexandria, Ägypten

-2007-

Dekan:	Prof. Dr. Ekkehardt Hahn
Erster Gutachter:	Prof. Dr. Jan T. Andersson
Zweiter Gutachter:	Prof. Dr. Uwe Karst
Tag der mündlichen Prüfungen:	5 December 2007
Tag der Promotion:	5 December 2007

To My Parents and My Husband

Table of contents

1. Introduction.....	1
1.1. Petroleum as energy source.....	1
1.2. Sources of oil in the sea.....	1
1.3. Crude oil composition.....	4
1.4. Introduction of sulfur in crude oil.....	5
1.5. Processes affecting the impact of oil releases.....	7
1.5.1. Spreading.....	8
1.5.2. Dispersion.....	8
1.5.3. Evaporation.....	9
1.5.4. Emulsification.....	9
1.5.5. Dissolution.....	10
1.5.6. Sinking and sedimentation.....	10
1.5.7. Tar ball formation.....	11
1.5.8. Biodegradation.....	11
1.5.9. Combined processes.....	12
1.5.10. Photochemical degradation.....	12
1.5.10.1. Types of photo-oxidation reactions.....	13
1.5.10.2. Photochemical mechanisms and oil weathering.....	15
1.6. Desulfurization and photo-oxidation.....	17
1.6.1. Hydrodesulfurization.....	17
1.6.2. Photochemical desulfurization.....	18
2. Stand of the research.....	20
2.1. Photo-oxidation of benzo[<i>b</i>]thiophene.....	20
2.2. Photo-oxidation of monomethylbenzo[<i>b</i>]thiophenes.....	21
2.2.1. Photo-oxidation of 2-methylbenzo[<i>b</i>]thiophene.....	21
2.2.2. Photo-oxidation of 3-methylbenzo[<i>b</i>]thiophene.....	22
2.2.3. Photo-oxidation of 4-methylbenzo[<i>b</i>]thiophene.....	22
2.2.4. Photo-oxidation of 5-methylbenzo[<i>b</i>]thiophene.....	22
2.2.5. Photo-oxidation of 6-methylbenzo[<i>b</i>]thiophene.....	23
2.2.6. Photo-oxidation of 7-methylbenzo[<i>b</i>]thiophene.....	23
2.3. Photo-oxidation of 2,3-dimethylbenzo[<i>b</i>]thiophene.....	23
2.4. Photo-oxidation of dibenzo[<i>b</i>]thiophene.....	23

2.5. Photo-oxidation of 4-methyldibenzo[<i>b</i>]thiophene.....	24
2.6. Photo-oxidation of 4,6-dimethyldibenzo[<i>b</i>]thiophene.....	24
2.7. Summary.....	25
3. Analytical techniques for the characterization of polar and non-polar photoproducts of polycyclic aromatic sulfur heterocycles.....	26
3.1. Liquid chromatography.....	26
3.1.1. Group separation into saturates, aromatics, resins and asphaltenes (SARA)...	26
3.1.2. Group separation into saturates, monoaromatics and polyaromatics.....	26
3.2. High performance liquid chromatography (HPLC).....	26
3.2.1. Separation of the aromatic fraction into PAHs and PASHs.....	26
3.2.2. Separation of PASHs according to the number of rings.....	27
3.3. Photo-oxidation apparatus.....	27
3.4. Liquid-liquid extraction.....	28
3.5. Derivatization.....	28
3.6. Gas chromatography.....	29
3.7. Mass spectrometry.....	29
4. Phototoxicity.....	30
4.1. Definition of toxicity.....	30
4.2. Toxicity tests.....	30
4.3. Types of toxicity tests.....	30
4.3.1. Acute toxicity (short-term testing).....	30
4.3.2. Chronic toxicity (long-term testing).....	31
4.4. Suitable organisms for toxicity tests.....	31
4.5. Classification of environmental pollutants.....	31
4.6. Types of phototoxicity.....	34
4.7. Phototoxicity of single compounds.....	35
4.8. Toxicity-based fractionation.....	37
5. High resolution mass spectrometry.....	38
5.1. Electrospray ionization.....	38
5.2. Mass analyzers.....	38
5.2.1. Definitions.....	39
5.2.1.1. Resolution.....	39
5.2.1.2. Mass resolving power.....	39

5.2.1.3. Mass accuracy.....	39
5.2.2. Types of mass spectrometers.....	40
5.2.2.1. Quadrupole.....	40
5.2.2.2. Ion trap.....	40
5.2.2.3. Multiple quadrupoles.....	41
5.2.2.4. Time of flight.....	41
5.2.2.5. Fourier transform ion cyclotron resonance (FT-ICR).....	43
5.3. Data interpretation.....	44
5.3.1. Nominal mass series	44
5.3.2. Kendrick mass defect.....	45
5.3.3. Multiple sorting.....	45
5.4. Limitations of electrospray ionization.....	47
5.5. Summary.....	48
6. Objectives.....	49
7. Application of toxicity-based fractionation techniques for the identification of the most phototoxic fraction of crude oil.....	50
7.1. <i>Daphnia magna</i> as toxicity test organism.....	51
7.2. Culture of <i>Daphnia magna</i>	52
7.3. Toxicity tests using <i>Daphnia magna</i>	53
7.3.1. Toxicity of crude oil.....	54
7.3.2. Toxicity of photo-oxidized aliphatic, monoaromatic and polyaromatic fractions.....	56
7.3.3. Toxicity of photo-oxidized PAHs and PASHs.....	60
7.3.4. Toxicity of photo-oxidized PASH subfractions I and II.....	63
7.3.5. Toxicity of polar and non-polar photoproducts of PASHs after 37 hours irradiation.....	66
7.3.6. Toxicity of polar and non-polar photoproducts of PASHs after 10 days irradiation.....	68
7.4. Summary.....	70
8. Characterization of polar photoproducts of PASHs.....	71
8.1. Experimental section.....	71
8.1.1. Crude oil fractionation.....	71
8.1.2. Ligand exchange chromatography.....	71

8.1.3. Photo-oxidation of the PASH fraction.....	71
8.1.4. Extraction of polar photoproducts.....	72
8.1.5. Derivatization of polar photoproducts 1.....	72
8.1.6. Identification of polar photoproducts 1.....	72
8.1.7. Analysis of polar photoproducts 2.....	72
8.2. Results and discussion.....	73
8.2.1. Characterization of polar photoproducts 1.....	73
8.2.1.1. Derivatization.....	73
8.2.1.2. Silylation.....	74
8.2.1.3. Identification of polar photoproducts 1.....	75
8.2.1.4. Identification of novel non-condensed cyclohexyl compounds.....	88
8.2.2. Characterization of polar photoproducts 2 (PP2).....	89
8.3. Summary.....	96
9. Characterization of PASHs after photo-oxidation.....	97
9.1. Characterization of PASHs after 10 days photo-oxidation by GC-MS.....	97
9.1.1. Experimental section.....	97
9.1.1.1. Crude oil fractionation.....	97
9.1.1.2. Standard compounds.....	97
9.1.1.3. Fractionation of the aromatic fraction into PAHs and PASHs.....	97
9.1.1.4. Photo-oxidation of the PASH fraction.....	97
9.1.1.5. Liquid-liquid extraction.....	98
9.1.2. Results and discussion.....	99
9.1.2.1. The dark control.....	99
9.1.2.2. PASHs after 10 days photo-oxidation.....	103
9.2. Characterization of PASHs after 2 and 10 days photo-oxidation by FT-ICR MS..	106
9.2.1. Experimental section.....	106
9.2.1.1. Crude oil fractionation.....	106
9.2.1.2. Photo-oxidation of the aromatic fraction.....	106
9.2.1.3. Liquid-liquid extraction.....	106
9.2.1.4. Sulfur selective methylation.....	107
9.2.1.5. High resolution mass spectrometry.....	108
9.2.1.6. Data analysis.....	109
9.2.2. Results and discussion.....	109
9.2.2.1. Characterization of monosulfur PASHs.....	109

9.2.2.2. Characterization of disulfur PASHs.....	116
9.3. Summary.....	120
10. Summary.....	121
11. Zusammenfassung.....	126
12. Appendix.....	130
12.1. Synthesis of Pd(II)-ACDA silica gel.....	130
12.1.1. Synthesis of 2-amino-1-cyclopentene-dithiocarboxylic acid (ACDA).....	130
12.1.2. Synthesis of aminopropanosilica gel.....	130
12.1.3. Synthesis of ACDA-functionalized silica gel.....	131
12.2. Synthesis of Pd(II)-mercaptopropano silica gel.....	131
12.3. Instrumental parameters.....	132
12.3.1 HPLC instrumentation.....	132
12.3.2. Gas chromatographs.....	132
12.3.3. FT-ICR MS.....	134
12.4. Materials.....	135
12.5. Abbreviations.....	137
13. References.....	139

1. Introduction

1.1. Petroleum as energy source

As the population of the world increases and developing nations become more industrialized, the demand for energy increases. Oil is currently the dominant energy fuel and is expected to remain so over the next several decades (see Figure 1.1). Historically, the industrialized nations have been the major consumers of oil. However, by the year 2020, consumption in the developing countries is expected to increase to be nearly equal to that of the industrialized countries and this increase is expected to be related to the transportation sector.

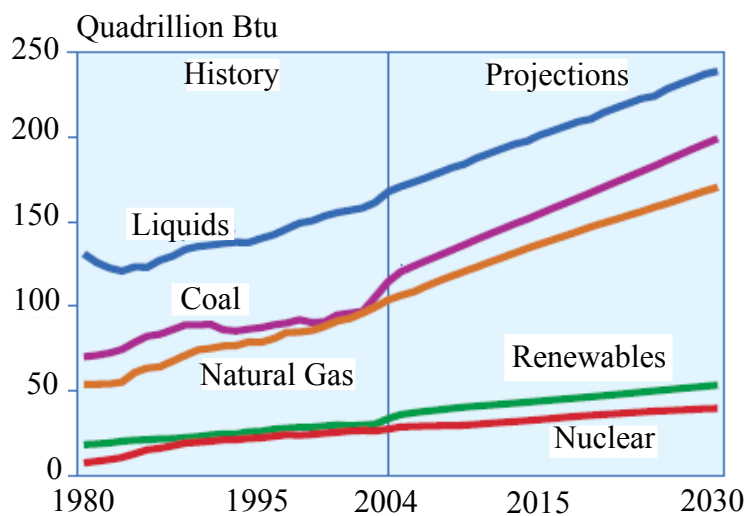


Figure 1.1. Graph showing the history and projections of the world energy consumption in British thermal units (Btu). The increasing demand for petroleum (liquids) can be seen in the projections [1].

Hence, crude oil represents an important part of the current fossil fuels energy mixture. However, as crude oil is extracted, refined, transported, distributed, or consumed, spills and other releases occur. In addition, natural seepage of crude oil from geologic formations below the seafloor to the overlying water column also takes place. Therefore, understanding the behaviour of petroleum in the environment is an important key for understanding the potential effect of releases of crude oil or its products on the marine environment.

1.2. Sources of oil in the sea

Three billion metric tonnes of crude oil are annually produced worldwide with approximately half of this total transported by sea [2]. Oil entering marine environments each year from all

sources (excluding biosynthesis) is estimated to be about 2.145 million metric tonnes (Table 1.1). Oil enters marine waters from both natural and anthropogenic sources including natural seeps, industrial waste waters, urban and river runoff, tanker spills, losses during marine transportation, leakages from refineries, production facilities and marine terminals. By inspecting the data given in Table 1.1, it is clear that the marine input of petroleum from anthropogenic sources (1.918 million tonnes/year) exceeds that from natural sources (0.27 million tonnes/year) excluding biosynthesis [3].

Petroleum inputs into worldwide marine waters can be categorized into four major groups: natural seeps, petroleum extraction, petroleum transportation and petroleum consumption.

Natural seeps of petroleum

Natural seeps are natural phenomena in which crude oil seeps from the geologic strata beneath the seafloor to the overlying water column. Although natural seeps indicate the existence of potentially economic reserves of petroleum, they release vast amounts of crude oil annually and hence change the nature of the marine ecosystems around them. They are therefore responsible for over 60 % of the petroleum entering the marine environment worldwide [4].

Extraction of petroleum

The world production of oil rose from 8.5 million tonnes in 1985 to 11.7 million tonnes in 2000 and during that time, the number of offshore oil and gas platforms have also risen [4]. Historically, oil and gas exploration and production of petroleum were considered to be among the important sources of spills. For instance, 476000 tonnes of crude oil were released into the Gulf of Mexico in 1979 in a blow out representing one of the largest marine spill in the world. However, during the past decade, the production technology and safety training of personnel have greatly improved which lead to a decrease in the number of blowouts and daily operational spills. Nowadays, accidental spills from platforms represent only about 3 % worldwide [4].

Transportation of petroleum

Releases from petroleum transportation can vary in size from small operational releases that occur regularly to major spills associated with tanker accidents such as the *Exxon Valdez* and is estimated to be less than 13 percent worldwide [4]. However, the spills arising from

transportation are down for several reasons, among them, the use of new technology and safety procedures and the application of regulations which have increased liability on responsible parties and forbidden the use of old vessels. Even though, the risk of spills in regions with less stringent safety procedures or maritime inspection practices still exists.

Table 1.1. Sources of oil pollution in marine environments ^a

<i>Source</i>	<i>Oil industry</i>	<i>Other</i>	<i>Total</i>
Transportation			
Tanker operations	0.143		
Tanker accidents	0.110		
Dry docking	0.004		
Other shipping operations		0.229	
Other shipping accidents		0.018	
			0.504
Fixed installations			
Offshore oil production	0.045		
Coastal refineries	0.091		
Thermal loading	0.027		
			0.163
Other sources			
Industrial waste		0.181	
Municipal waste		0.635	
Urban runoff		0.109	
River runoff		0.036	
Atmospheric fallout		0.272	
Ocean dumping		0.018	1.251
Natural inputs		0.227	0.227
Biosynthesis			
Marine phytoplankton	23,582		
Atmospheric fallout	91-93,630		

^a Values in million metric tonnes per year. From [2].

Consumption of petroleum

“From 1985 to 2000, global oil consumption increased from 9.3 to 11.7 million tonnes per day, an increase of more than 25 percent” [4]. Releases taking place during the consumption of petroleum either from cars, boats, marine vessels, or airplanes, contribute to the vast majority of petroleum introduced through human activity. In addition, activities on land contribute to the pollution of rivers and streams, which eventually empty to the sea. It was also found that land-based inputs are highest near urbanized areas and refinery production and that the threat of pollution from urban areas is expected to rise in the future.

1.3. Crude oil composition

The chemical composition of crude oils can vary tremendously from different producing regions, and even from within a particular formation. Crude oils consist of complex mixtures of hydrocarbons and non-hydrocarbons that range from small, volatile compounds to large, non-volatile ones. Thousands of different chemical compounds have been identified in crude oils. Ultrahigh-resolution Fourier transform ion cyclotron resonance mass spectrometry (FT-ICR MS) has recently revealed that crude oil contains heteroatom-containing (N, O, S) organic components having more than 20000 distinct elemental compositions [5]. In general, petroleum components are generally classified into four classes: saturates, alkenes, aromatics, resins and asphaltenes (also called SARA analysis).

Saturates, which represent the predominant class of hydrocarbons in most crude oils, consist of straight and branched chain alkanes (also called paraffins) and cycloalkanes (also called naphthenes). Saturates also include biomarker terpanes and steranes, which are branched cycloalkanes consisting of multiple condensed five- or six-carbon rings, and sesquiterpanes and diamondoids, which are smaller cyclic biomarkers, that are used for the source identification of lighter petroleum products [6].

Alkenes, also known as olefins, are partially unsaturated hydrocarbons containing one or multiple double carbon-carbon bonds. Although these compounds are rare in crude oil, they may be present in some petroleum products and could have been formed during the refining process.

Aromatics in petroleum include at least one benzene-ring hydrocarbons such as benzene, toluene, and ethylbenzene, and o-, m-, and p-xylene isomers and other alkyl-substituted

benzene compounds in addition to polycyclic aromatic compounds (PAHs), polycyclic aromatic sulfur heterocycles (PASHs) and other heterocycles which consist of at least two benzene rings.

Polar compounds are those compounds containing nitrogen, oxygen, or sulfur atoms. Heavy oils generally contain more aromatic polar compounds. In the petroleum industry, the smaller polar compounds are called resins and the big ones are called asphaltenes. Asphaltenes are the oil constituents precipitated from oils and bitumen either by natural processes or in laboratory by addition of excess n-pentane or n-hexane and this depends on the solution properties of petroleum residues in various solvents [7].

In addition, crude oils contain widely many trace metals such as V, Ni, Fe, Al, Na, Ca and Cu in varying concentrations.

1.4. Introduction of sulfur in crude oil

The amount of sulfur in crude oils plays an important role in determining their prices. Moreover, sulfur compounds are the most abundant non-hydrocarbon constituents in petroleum. The sulfur content is in the range 0.5-3.0 % in most crudes, but is up to 8 % in the vacuum residue of heavy crude oils [8]. However, the incorporation of sulfur into crude oil has not been clearly understood until now, although many hypotheses have been proposed. All are collectively termed organic sulfur compounds. These hypotheses are based on biosynthesis and formation during early diagenesis.

Most of the sulfur present in crude oils is organically bound sulfur while elemental sulfur and hydrogen sulfide usually represent a very minor portion of the total sulfur [9]. Some sulfur may be derived from amino acids in the original contributing organic matter in sediments [10]. However, most primarily sulfur in oils originates from early diagenetic reactions between the deposited organic matter and aqueous sulfide species such as hydrogen sulfide or polysulfides [11].

Sulfides are produced by sulfate-reducing bacteria, such as *Desulfovibrio*, primarily in highly reducing to anoxic marine sediments. Two sinks compete for sulfide in sediments: metals and organic matter. High- and low-sulfur crude oils are derived from high- and low-sulfur

kerogens, respectively [12]. In addition, biodegradation can lead to an increase in the sulfur content in oils by the preferential removal of saturated hydrocarbons.

Sulfur compounds in crude oils are distributed over a wide range of molecular structures: aliphatic thiols, mono- and disulfides are sometimes present [13, 14], but a large amount of sulfur occurs in aromatic structures, especially as alkylated thiophene benzologues [15]. However, Schmid et al. [16] and Sinninghe Damsté et al. [17] have described the presence of long chain dialkylthiacyclopentanes in oils, while Payzant et al. [18] have identified terpenoid sulfides in petroleum. Moreover, Sinninghe Damsté et al. [17] and Valisolalao et al. [19] have tentatively identified steroid and hopanoid thiophenes in petroleum. Sinninghe Damsté et al. [20] have also cited the presence of various highly branched isoprenoid thiophenes in sediments and immature oils. These compounds appear to result from the selective incorporation of sulfur into isoprenoid alkenes during diagenesis. A few typical structures of both aliphatic and aromatic sulfur compounds are presented in Figure 1.2.

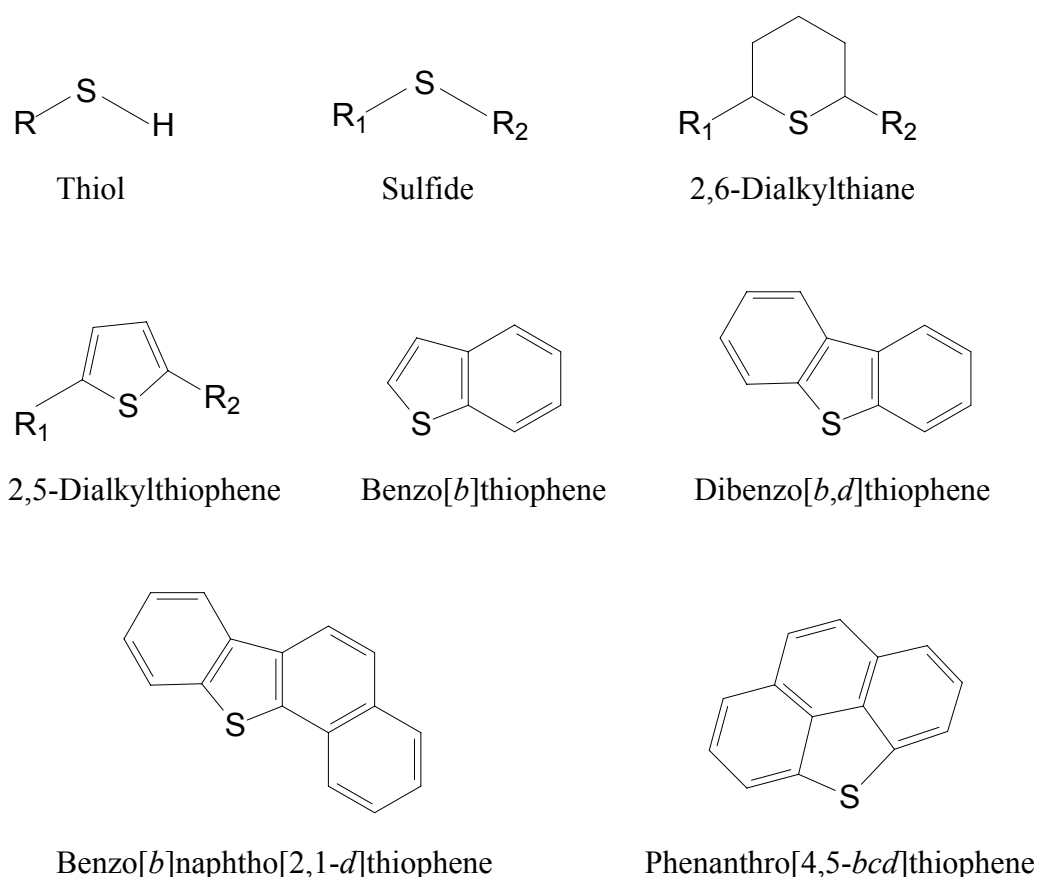


Figure 1.2. Typical organic sulfur compounds found in crude oils.

1.5. Processes affecting the impact of oil releases

Clark [3] stated that 92 % of the world's water pollution by petroleum and petroleum products is directly related to human activities and one eighth of this is due to tanker accidents. In addition, the extent of contamination is dependent upon the rate of continuous input of petroleum into the environment as well as upon the rate at which the environment can clean itself. Although between five hundred thousand and one million tons of oil were released in the "Gulf war" spill in 1991 [21], the quantity of dissolved organic matter in the Persian Gulf had returned to its initial level one year after the spill [22]. This implies that oil oxidation and removal take place by efficient processes. Table 1.2 gives a list of major spills.

Table 1.2. List of largest oil spills ordered by tonnes. One tonne of crude oil = 7.33 barrels (from [23])

<i>Spill / Tanker</i>	<i>Spill place</i>	<i>Year</i>	<i>Oil spilled</i> <i>×10³ (tonnes)</i>
Gulf War oil spill	Persian Gulf	1991	780-1,500
Ixtoc I oil well	Gulf of Mexico	1979	454-480
Atlantic Empress / Aegean Captain	Trinidad and Tobago	1979	287
Fergana valley	Uzbekistan	1992	285
Nowruz oil field	Persian Gulf	1983	260
ABT Summer	Angola	1991	260
Castillo de Bellver	South Africa	1983	252
Amoco Cadiz	France	1978	223
Haven tanker	Italy	1991	144
Odyssey	Canada	1988	132
Sea Star	Gulf of Oman	1972	115
Torrey Canyon	United Kingdom	1967	80-119
Irenes Serenade	Greece	1980	100
Urquiola	Spain	1976	100
Prestige	Galicia, Spain	2002	63
Exxon Valdez	Alaska, USA	1989	37
Jiyeh power station oil spill	Lebanon	2006	20-30

Studies completed in the last 20 years showed that there is no correlation between the size of a release and its impact. The effects of a petroleum release depend on different factors such as the rate of release, the nature of the petroleum and the local physical and biological character of the exposed ecosystem. In addition, some petroleum components can be more toxic than others. For instance, polycyclic aromatic hydrocarbons are known to be among the toxic components of petroleum, and their initial concentration is an important factor in the impact of a given release. Thus, toxic compounds such as PAHs or other compounds present in crude oil or refined products can have adverse effects on biota even at very low concentrations.

Oil or petroleum products spilled on water undergo changes in physical and chemical properties that are called “weathering.” Weathering processes occur at different rates but begin immediately after oil is released into the environment. Both weathering processes and their rates depend more on the type of oil than on the environmental conditions. Most weathering processes depend on the temperature and they often become very slow as the temperature approaches zero.

Next, an overview of the different weathering processes acting on crude oil will be illustrated.

1.5.1. Spreading

After oil is spilled in the marine environment, it begins to spread out over the sea surface as a single slick. The speed of spreading is dependent to a great extent upon the viscosity of the oil. Low viscosity oils spread more quickly than high viscosity ones. Nevertheless, slicks quickly spread to cover large areas of the sea surface. After a few hours, the slick begins to break up and starts to form narrow bands because of winds, wave action and water turbulence. The factors that affect the rate at which the oil spreads include the temperature, water currents, tidal streams and wind speeds. The spreading and breaking up of the oil is more rapid when the environmental conditions become more severe.

1.5.2. Dispersion

All or part of a slick can be broken up into fragments and droplets of varying sizes by the action of waves and turbulence at the sea surface. The small droplets remain suspended in the sea water while the large ones tend to rise back to the surface, where they start to reform a slick or to spread out as a very thin film. At this stage, the oil has a greater surface area than

before dispersion occurred and hence remained suspended in the water, which promotes other natural processes such as dissolution, biodegradation and sedimentation to occur.

The speed at which oil disperses depends to a high extent on the nature of the oil and the sea state. The lighter the oil and the rougher the sea is, the more rapid the dispersion of the oil is.

1.5.3. Evaporation

In the first days after an oil spill, lighter components (low molecular weight components) of the oil evaporate to the atmosphere [24, 25]. In general, in temperate conditions, those components of the oil with a boiling point under 200 °C tend to evaporate within the first 24 hours. Evaporation is usually limited to molecules with less than about 15 carbon atoms [25, 26], however, under high aeration in water, as happened in the spill from the OSSA II pipeline on the Bolivian Altiplano in January 2000, this evaporation can extend into molecules with >30 carbon atoms [27].

The amount and speed of evaporation is highly dependent upon the volatility of the oil. Oil containing a high percentage of light and volatile compounds will evaporate more than that containing a large amount of heavier compounds. For example, petrol, kerosene, diesel oils and all light products evaporate almost completely in a few days while a heavy fuel oil will hardly undergo evaporation (Figure 1.3). It has also been found that light crude oils lose 75 % of their initial volume in the first few days of an oil spill, medium crudes lose 40 % while heavy oils lose less than 10 % of their volume due to evaporation [4]. Moreover, the rate of evaporation increases as the environmental conditions become more severe as in the case of rougher seas, high wind speeds and high temperatures.

1.5.4. Emulsification

Emulsification of crude oils is the process whereby sea water droplets become suspended in the oil. The emulsion thus formed is usually very viscous and more persistent than the original oil and is often called chocolate mousse because of its appearance. Due to the formation of these emulsions, the volume of pollutant increases between three and five times. This makes mechanical oil removal from the water surface more difficult and slows and delays other processes which would allow the oil to dissipate such as microbiological degradation and sediment penetration [29, 30]. Oils with a high asphaltene content (greater than 0.5 %) tend to form stable emulsions and may persist for many months after the oil spill while those oils

having a low content of asphaltenes are less likely to form emulsions and are more likely to disperse [31, 32].

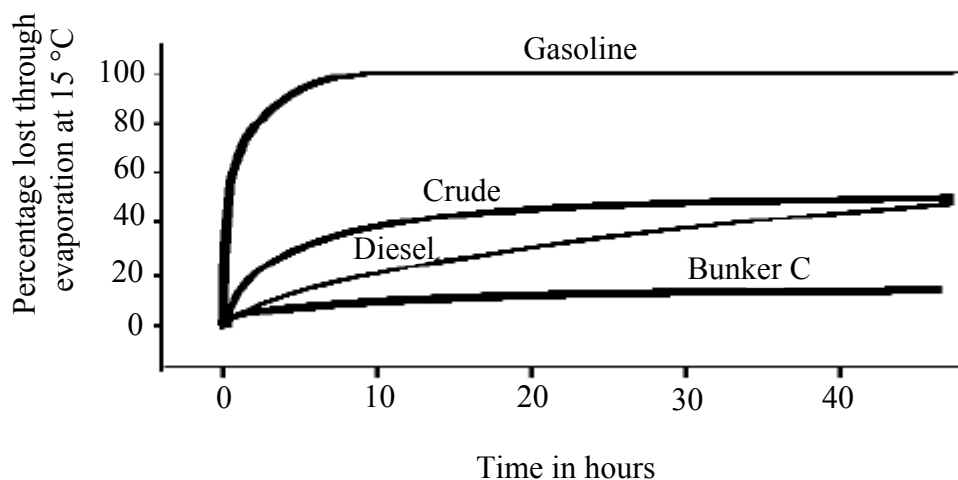


Figure 1.3. Evaporation rates of different types of oil at 15 °C (adapted from [28]).

1.5.5. Dissolution

Dissolution is responsible for the loss of a small portion of oil, but it is still considered an important behaviour parameter for the soluble components of oil, especially the monoaromatic compounds. In addition, as the size and substitution of the compounds in a crude oil increases, their solubility decrease. On the other hand, aliphatic compounds have very low solubility in comparison to that of the aromatic ones [33].

1.5.6. Sinking and sedimentation

Oil masses that are denser than water are transported to the bottom of the sea by a process called sinking. In general, very few crudes are dense enough or weather sufficiently, so that their residues will sink in the marine environment. Sinking usually occurs when the oil becomes adherent to particles of sediment or organic matter. Sinking can take place when oil stranded on sandy shorelines becomes mixed with sand and other sediments and then is washed off the beach back into the sea. In addition, residues formed after the combustion of oil can be sufficiently dense to sink.

The settling of suspended sediments, onto which sorption of oil has taken place, out of the water column and their accumulation on the seafloor is called sedimentation. Shallow waters are often the most suitable ones for sedimentation.

1.5.7. Tar ball formation

The fates of persistent oil residues include the shoreline stranding resulting from spills near to shore and the tar ball formation resulting from releases in offshore waters.

After the various physical and chemical processes that floating oil can undergo following an oil spill, oil can coagulate into residues called tar balls. Tar balls can be as large as pancakes, or as small as coins. They usually consist of a solid outer crust surrounding a softer, less weathered interior. Tar balls are usually problematic as they can persist in the marine environment for a long time, can travel hundred of miles from the original oil spill site and can deposit on shorelines and along shipping routes [34-36].

1.5.8. Biodegradation

Sea water contains a wide range of micro-organisms that can partially or completely degrade oil to water soluble compounds and eventually to carbon dioxide and water. There are many types of micro-organisms that tend to degrade a particular group of compounds in crude oil.

Bacteria and fungi, and to a lesser extent, heterotrophic phytoplankton, utilize hydrocarbons as a carbon source to produce energy, while subsequently degrading the long-chained molecules in a metabolic process called oxidative phosphorylation, or respiration [37]. Moreover, there are different types of microorganisms that use other metabolic pathways such as nitrate reduction and sulphate reduction to degrade hydrocarbons into carbon dioxide and water. However, a consortium of bacterial strains usually uses multiple metabolic pathways in order to degrade complex hydrocarbons such as branched alkanes and multicyclic compounds (polycyclic aromatic and aliphatic hydrocarbons) [38].

The efficiency of biodegradation is affected by several factors including the amount of nutrients (nitrogen and phosphorus) in the water, the temperature and the concentration of oxygen present. Therefore, biodegradation usually takes place at oil-water interface where oxygen is available. Moreover, as a result of dispersion, the surface area of the oil increases and hence the area available for biodegradation also increases.

The rates of biodegradation depend on the ability of micro-organisms to get into contact with hydrocarbons and on the bacterial metabolic processes taking place within the cell. Atlas et al. [39] and Leahy et al. [40] reported that saturated alkanes are biodegraded faster than aromatic compounds and that branched alkanes, multi-ring and substituted aromatics and cyclic compounds are biodegraded after alkanes and smaller-sized aromatics. On the other hand, Prince [41] showed that polar petroleum compounds containing sulfur and nitrogen are the most resistant ones to microbial degradation.

1.5.9. Combined processes

The processes described previously are summarised in Figure 1.4. All come into play as soon as oil is spilled, although their relative importance varies with time. The processes of spreading, evaporation, dispersion, emulsification and dissolution are most important during the early stages of a spill whilst photo-oxidation, sedimentation and biodegradation are more important later on and determine the ultimate fate of the oil.

1.5.10. Photochemical degradation

Photo-oxidation is a major factor of crude oil removal from the environment and this was shown in studies of the *Exxon Valdez* where as much as 70 % of the crude was found to be photooxidized in the water or in the atmosphere [42]. The oxidized products resulting from the photochemical transformation have a big effect on the viscosity, the mousse formation and the physical properties of weathered petroleum. Moreover, photo-oxidation can lead to the destruction of existing toxic components, to the generation of new toxic components and to the formation of water soluble products.

Photolysis plays an important role in the mousse formation that begins some time after an oil spill [43]. As crude oil films are exposed to sunlight, their interfacial tension rapidly decreases and chocolate mousse starts to form which lead to the stabilization of the water-in-oil emulsions [44-46]. It has been also reported that the formation of emulsions depends on the amount of asphaltene present and that this amount increases upon irradiation [44, 45, 47]. In addition, Desmaison et al. [48] suggested that an increase in emulsion viscosity occurs due to the structural organization of the asphaltenes.

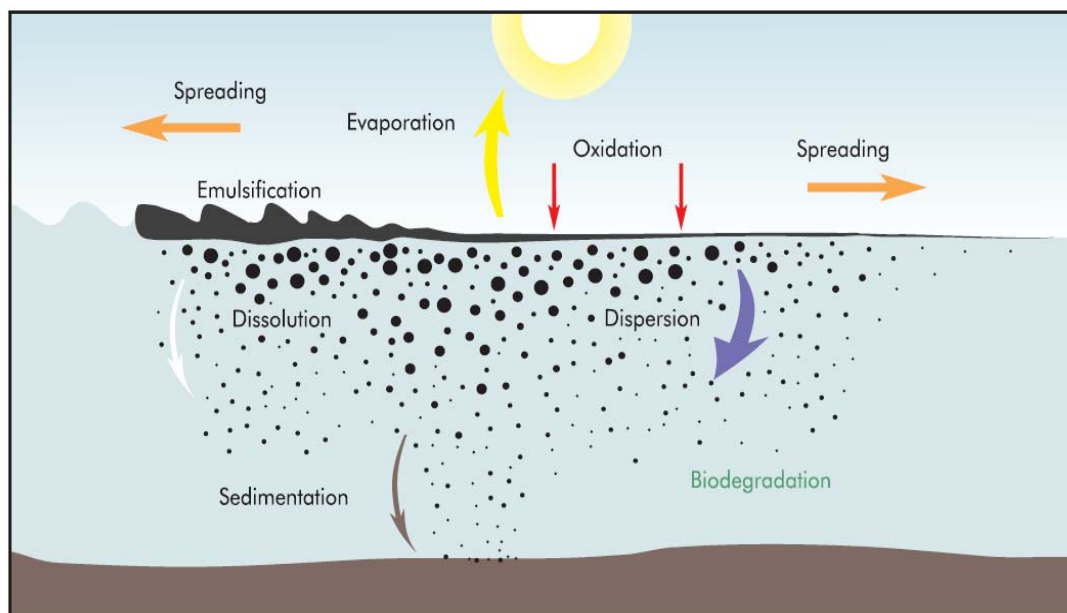


Figure 1.4. Processes acting on spilled oil (from [49]).

Moreover, the oil solubility has been shown to increase by the artificial or solar irradiation of oil films [45, 50]. This increase range from 32 to 295 ppm for a No. 2 fuel oil [51], from 4 to 40 ppm for light crudes [52, 53], but is much lower for highly viscous crudes [54]. This increased solubility is due to the formation of aliphatic and aromatic polar compounds from all petroleum fractions such as ketones [55], alcohols [56], hydroperoxides [57-59], sulfoxides [60], phenols [58, 59] and carboxylic acids [53, 58, 59]. Therefore, the photochemical oxidation of petroleum and petroleum products is an important process in transferring the organic matter from the oil phase into the water column.

As most crude petroleum absorb strongly in the ultraviolet and visible regions of the solar spectrum, photochemical processes can also lead to the thinning of the oil slick which occur by the increase in the area exposed to sunlight. To exemplify, the solar spectrum and the absorption spectrum of a Brazilian petroleum are shown in Figure 1.5.

1.5.10.1. Types of photo-oxidation reactions

The transformation of pollutants in the aquatic environment is due to a number of different photochemical processes. These processes are direct photolysis and indirect or “sensitized” photolysis.

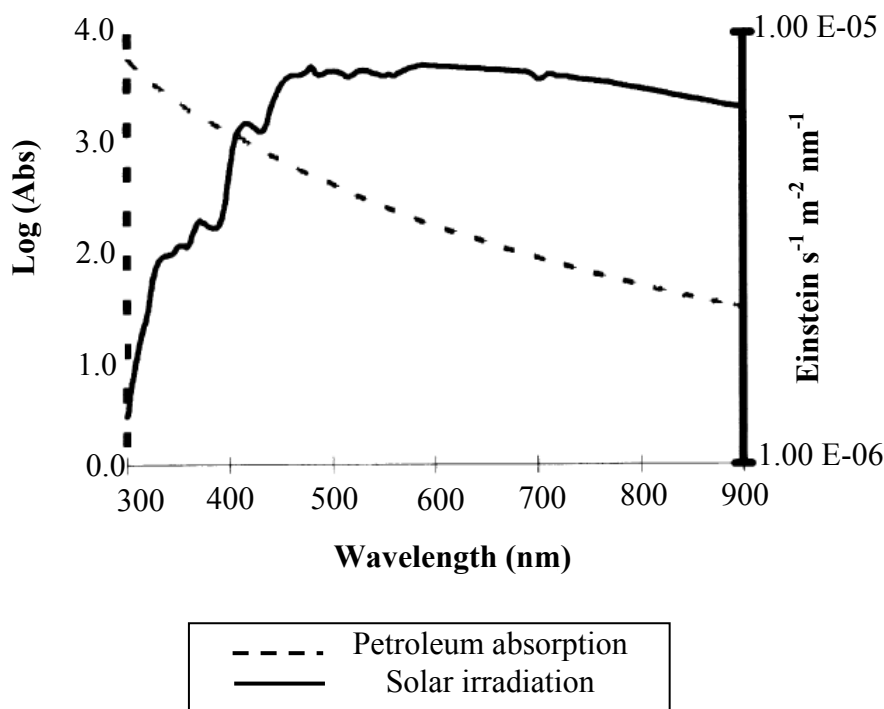


Figure 1.5. Solar spectrum and absorbance of a typical crude petroleum (from [61]).

1.5.10.1.1. Direct photolysis

A compound that absorbs light energy and as a result, its chemical structure can be altered, undergoes direct photolysis. Compounds containing light-absorbing entities called chromophores such as alkenes or aromatic rings, with unsaturated carbon/carbon bonds or fatty acids with carbonyl groups, as well as nitrosamines, benzidines, chlorinated organics and some metal complexes are susceptible to direct photolysis [62].

In order to photolyse any compound in the laboratory, the "right" experimental conditions should be applied. For instance, mercury-vapor lamps and xenon arc lamps are commonly used in laboratory experiments to approximate sunlight. However, because the light emitted from these sources contains wavelengths less than 290 nm, Pyrex filters are used to filter the light. In addition, a cooling system is usually utilized as these light sources generate heat. Moreover, when the compound to be irradiated is less soluble in water, a mixture of water and a polar solvent such as acetonitrile or methanol can be used [63].

1.5.10.1.2. Indirect photolysis

Compounds unable to undergo direct photolysis due to the absence of chromophores in their molecules may be photolyzed indirectly via sensitized photolysis or photo-oxidation [64].

During indirect photolysis, another compound present in the environment, namely the photosensitizer (e.g., quinones, humic acid, flavins, as well as trace metals, nitrate, nitrite, and hydrogen peroxide) [64], absorbs light energy and then transfers it either indirectly via various reactive intermediates such as oxidants or directly to the compound of interest causing its structural alteration. Examples of oxidants commonly found in aquatic environments are the peroxy radical ($\text{RO}\cdot$), hydroxy radical ($\text{HO}\cdot$), singlet oxygen ($^1\text{O}_2$), ozone (O_3), and triplet diradicals [65]. In addition, many dyes, pigments and aromatic hydrocarbons may act as sensitizers [66].

Photosensitizers have been used in different photo-oxidation studies. For instance, naphthalene derivatives have sensitized the oxidation of alkyl benzenes [67] and xanthone has been used in the photo-oxidation of hexadecane [68].

Anthraquinone, which has been found in sea water [69], has been used as a sensitizer in several studies. The water soluble fraction of gasoline was readily photodegraded in the presence of anthraquinone giving alcohols, aldehydes and ketones [70]. The photosensitized oxidation of aqueous solutions of n-tetradecane and petroleum samples gave formaldehyde, acetaldehyde and acetone [71]. Anthraquinone has also been used in the photodegradation of nonylbenzene [72], monoalkylated benzenes [73], pentadecane [74], nonlinear hydrocarbons [75, 76] and cycloalkanes [77].

1.5.10.2. Photochemical mechanisms and oil weathering

In order that a molecule undergoes photochemical changes, irradiation of light in the UV–visible range must occur within the system. In marine photochemistry, the source of radiation is sunlight. The sun emits visible light (400–800 nm) and infrared radiation in addition to ultraviolet (UV) radiation consisting of UV-A (320–400 nm) and UV-B (290–320 nm). The intensity of UV irradiation at the Earth's surface is dependent upon the season, time of day, latitude, thickness of the atmosphere and the ozone layer, altitude, and cloud cover.

As soon as a molecule absorbs a photon, it transfers from the low-energy ground state to a higher energy electronically excited state (Figure 1.6) [78]. Almost all stable molecules are singlets having paired electrons in their ground states. The first excited state is also a singlet, however, most singlet excited states are short-lived species. Therefore, they lose their excess electronic energy either as thermal reversion to the ground state, with emission of heat; or

as fluorescence (emission of a photon with lower energy than that of the exciting photon) and return to the singlet ground state; or as internal conversion (intersystem crossing)-transformation of the singlet to a lower energy triplet excited state with unpaired electrons.

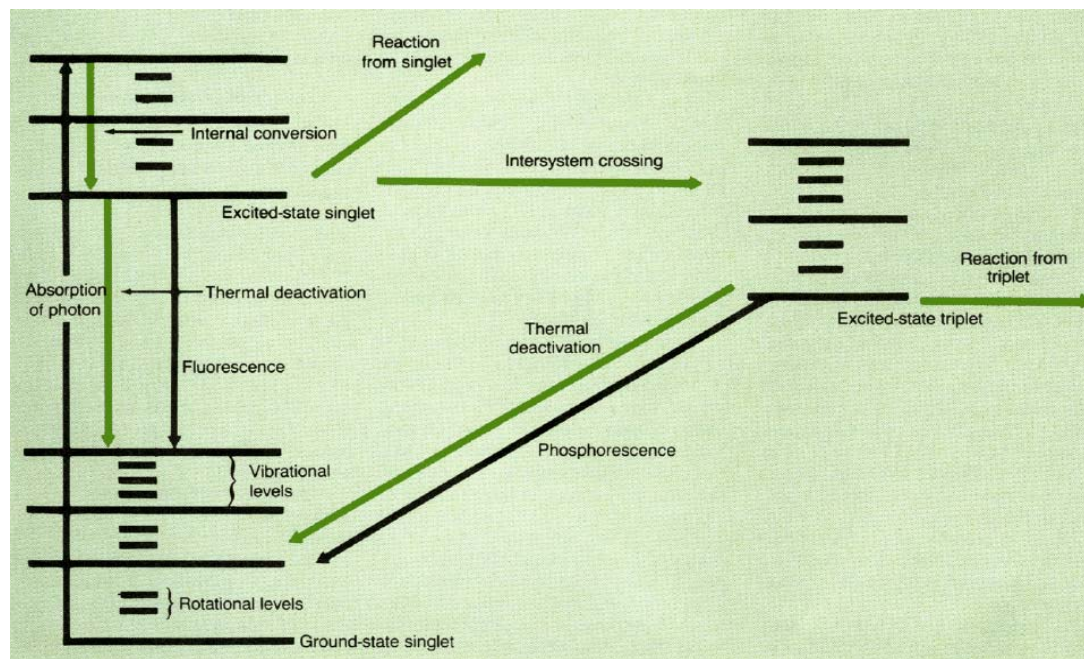


Figure 1.6. Photochemical processes (from [78]).

Molecules in the triplet excited states are known to have longer lifetimes than singlets. The excited triplet states of these molecules (donor) can collide with a different molecule in the ground state (acceptor) leading to the promotion of the acceptor to an excited state and the return of the donor molecule to the ground state. Compounds capable of this energy transfer are called photosensitizers. Because oxygen is readily available in natural waters, this energy can be transferred to oxygen molecules generating singlet oxygen, $^1\text{O}_2$. This formation has been demonstrated in the photo-oxidation study of dimethylnaphthalenes in which the authors have explained the formation of the photoproducts via singlet oxygen mechanism [57].

Molecules in the triplet state also may take part in photochemically promoted electron-transfer reactions. For instance, the superoxide radical anion, O_2^- , is formed through an electron transfer from a photoexcited molecule to molecular oxygen. In water, O_2^- is partly protonated to its conjugate acid, HOO^\cdot which can undergo disproportionation to oxygen and hydrogen peroxide (H_2O_2).

It has been reported that H_2O_2 forms in various natural-waters exposed to sunlight [65]. Hydrogen peroxide undergoes decomposition by light and trace metals such as iron to form the reactive hydroxyl radical ($\text{HO}\cdot$). As the hydroxyl radical is a very powerful oxidizing species, it reacts very rapidly with most organic compounds and also with many inorganic ions. Moreover, an organic free radical can be produced from the reaction of $\text{HO}\cdot$ and an organic molecule which can then react quickly with nearby organic molecules or with oxygen.

Photo-oxidation via free radicals has been suggested in model studies such as the sensitized oxidation of alkyl benzenes [67, 73], hexadecane [68], pentadecane [74], nonlinear hydrocarbons [75, 76] and cycloalkanes [77].

A combination of singlet oxygen and free radical induced photo-oxidation mechanisms have also been proposed to explain the products in some studies such as in the photolysis of thiophene oxides in which the photolysis has regenerated the thiophene and eliminated atomic oxygen [79] which has then abstracted hydrogen and formed free radicals.

1.6. Desulfurization and photo-oxidation

Sulfur-containing compounds in petroleum are receiving recently great attention throughout the world as they are converted into sulfur oxides by combustion and are thus one of the main sources of acid rain and air pollution. Current E.U. specifications for diesel fuel mandates that the sulfur concentration must be less than 50 ppm, but future values will certainly be much tightened. The easiest way to limit the amount of sulfur dioxide emitted into the air is to limit the amount of sulfur in fuel. In this regard, many approaches have been attempted including hydrodesulfurization (HDS), photochemical and bio-desulfurization methods. However, at present, hydrodesulfurization is the process currently used to remove sulfur from petroleum fractions.

1.6.1. Hydrodesulfurization

HDS is the process that uses hydrogen gas to reduce the sulfur in petroleum fractions to hydrogen sulfide, which can then be easily separated from the fuel. However, HDS is costly as the reaction is usually operated at high temperature (300-350 °C) and pressure (50-100 atm) in addition to the use of sophisticated and expensive catalysts such as sulfided Co/Mo/ Al_2O_3 or sulfided Ni/Mo/ Al_2O_3 [80, 81].

Although HDS is the current method used for the removal of sulfur, it is highly effective only for certain sulfur compounds as thiols, sulfides and disulfides [82, 83]. Alkylated benzothiophenes and dibenzothiophenes have been found to be more resistant to HDS treatment than mecaptans and sulfides, with alkyl substitutions in position 1, 4 and 6 on the DBT ring leading to higher resistance [84-86].

1.6.2. Photochemical desulfurization

The high cost of HDS and its failure to remove certain sulfur compounds in fuels are driving the search for more efficient desulfurization methods including photochemical desulfurization.

Photochemical desulfurization is a process that removes sulfur from fossil fuels by a photochemical reaction. It has been proposed as an attractive alternative to HDS as it has several advantages over the catalytic technique:

- (1) No catalysts are needed.
- (2) No hydrogen is required.
- (3) It is easy to operate and to control the reaction.
- (4) The process is energy-saving since the reaction occurs at room temperature and under atmospheric pressure.
- (5) The deep desulfurization of refractory sulfur compounds such as 4-methyldibenzothiophene (4-MDBT) and 4,6-dimethyldibenzothiophene (4,6-DMDBT) as well as DBT may be feasible.

In the early 1990s, Moza et al. [87] reported on the photodegradation of aromatic sulfur compounds dissolved in n-hexane and spread as a thin liquid film on water. Irradiation by a medium-pressure mercury lamp brought about the oxidation of the DBT to its sulfoxide, which then moved into the water phase.

Moreover, Hirai et al. [88] investigated the desulfurization of DBT, 4-MDBT and 4,6-DMDBT by a combination of photochemical reaction and liquid-liquid extraction using an organic/water two-phase system and this process was extended for benzothiophenes and alkyl sulfides [89]. DBTs, dissolved in a tetradecane solution, were photodecomposed by the use of a high-pressure mercury lamp and were removed to the water phase as sulfate anion at conditions of room temperature and atmospheric pressure. The order of reactivity for the

DBTs was $DBT < 4\text{-MDBT} < 4,6\text{-DMDBT}$, thus indicating a different tendency from that reported for the hydrodesulfurization method. However, the desulfurization yield of commercial light oil, was only 22 % following 30 h irradiation. This low yield was caused mainly by the depression of the photoreaction of DBT by the presence of naphthalene (NAP) in the light oil probably because of triplet energy transfer from photoexcited DBT to ground-state NP. In order to overcome this problem, the desulfurization was improved by introducing benzophenone, a triplet photosensitizer, into the light oil and hydrogen peroxide into the water phase [90]. Hydrogen peroxide was found to be effective, since it acts as a weak oxidizing agent for the photoexcited DBT and to some extent interrupts the energy transfer from the excited DBT to the naphthalene. In these studies, the basic idea for desulfurization was the photodecomposition of sulfur-containing compounds in the light oil phase, followed by the transfer of the resultant oxidized compounds into the aqueous phase. Thus, Shiraishi et al. [91] achieved a decrease in sulfur content in the light oil from 0.2 wt % to less than 0.05 wt % by 48 hours of photoirradiation using H_2O_2 and benzophenone.

In addition, Shiraishi and Hirai [92] applied the previous photochemical process for the desulfurization of a light oil in the presence of benzophenone-modified silica gel as a heterogeneous triplet photosensitizer. By the use of this process, the sulfur content of light oil was reduced from 0.18 to less than 0.05 wt % by 60 hours of photoirradiation and the nitrogen-containing compounds present in light oil were removed simultaneously with the sulfur-containing compounds.

2. Stand of the research

Large amounts of crude oil and petroleum products are introduced into the environment every year. As already described in chapter 1, physical processes like evaporation, dissolution and adsorption move the compounds from the site of introduction but only microbial and photochemical processes alter them chemically, ultimately leading to a mineralization and their removal from the environment. Although the polycyclic aromatic sulfur heterocycles represent an important part of the aromatic fraction of crude oils and in some cases are even more abundant than the polycyclic aromatic hydrocarbons [93], much attention was directed to the photo-oxidation of PAHs. Therefore, only very little is so far known about the photo-oxidation of polycyclic aromatic sulfur heterocycles. This chapter will give an overview about the photo-oxidation of PASH compounds that were described in the literature together with their photoproducts.

2.1. Photo-oxidation of benzo[*b*]thiophene

Benzo[*b*]thiophene (BT) was selected for the first studies since it is the simplest PASH possible [94]. As BT has a fairly low boiling point (221 °C), it was expected that under oil-spill conditions, it would fairly rapidly evaporate before substantial photo-oxidation occurs, as Lichtenthaler et al. [95] reported that compounds of boiling point below about 250 °C are rapidly lost through evaporation. In addition, as a model substance for alkylated derivatives, it could be studied without possible complications arising from the oxidation of alkyl groups. The photolysis was performed by Andersson and Bobinger [94] in a two-phase system consisting of water and a tetradecane solution of benzo[*b*]thiophene as a simulated oil matrix using a middle-pressure mercury lamp producing light mainly above 300 nm. The products of the photo-oxidation of BT were benzothiophene-2,3-quinone and benzonaphtho[2,1-*d*]thiophene. This four-ring heterocycle is known to result if BT is irradiated in the solid state [96]. However, when the sample was irradiated for a long time, this product disappeared with the formation of a new photoproduct, which was identified as 2-sulfobenzoic acid. This was in analogy with the photochemical oxidation of aromatic compounds like phenanthrene which are known to yield quinones [97] and as quinones are frequently used as photosensitizers, this product might thus have acted to increase the efficiency of photo-oxidation. Surprisingly, products from the oxidation of the sulfur atom, such as the sulfoxide or the sulfone were not observed. The photo-oxidation pathway of BT is shown in Figure 2.1.

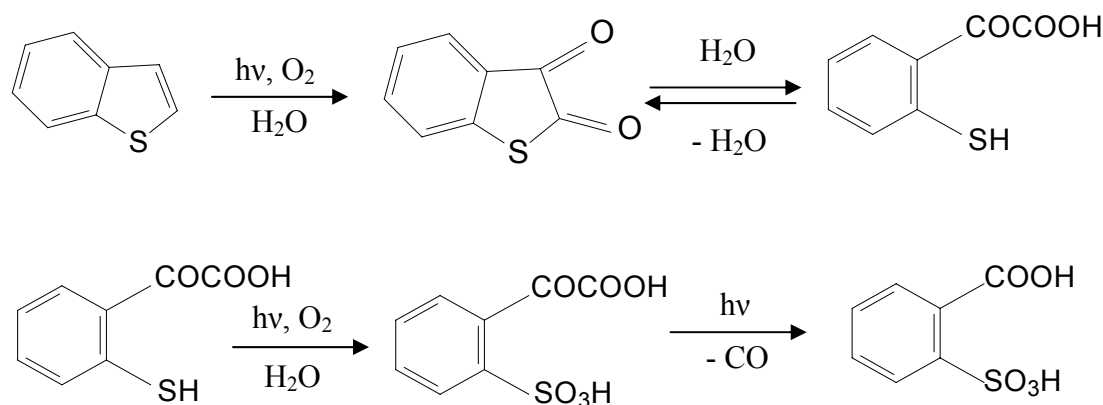


Figure 2.1. Photo-oxidation pathway of benzo[*b*]thiophene (from [94]).

Shiraishi et al. [98] have identified the acidic products of BTs and DBTs produced during a new photochemical desulfurization process employing high-pressure mercury lamp and two phase liquid-liquid extraction system. The authors reported that BT was first converted to benzo[*b*]thiophene-2,3-dione which undergoes hydrolysis, oxygenation on the sulfur atom and loss of CO leading in the end to the formation of 2-sulfobenzoic acid, which is in agreement with Andersson and Bobinger results [94].

2.2. Photo-oxidation of monomethylbenzo[*b*]thiophenes

Bobinger and Andersson [99, 100] have studied the photo-oxidation of different monomethylated benzo[*b*]thiophenes. They have carried out the photochemical oxidations in aqueous solutions with 20 % methanol added in order to achieve a sufficiently high concentration of the benzo[*b*]thiophenes ascertaining that in preliminary experiments the methanol did not influence the product distribution.

2.2.1. Photo-oxidation of 2-methylbenzo[*b*]thiophene

The major product from the photo-oxidation of 2-methylbenzo[*b*]thiophene was 2-sulfobenzoic acid with benzo[*b*]thiophene-2-carbaldehyde and benzo[*b*]thiophene-2-carboxylic acid as minor products. Traces of benzenesulfonic acid were also found. A thorough search among the minor products revealed that the probable precursor of the aldehyde is the corresponding alcohol, 2-hydroxymethylbenzo[*b*]thiophene. In addition, 2,3-diformylbenzo[*b*]thiophene was identified as a minor product. Since this compound contains one carbon atom more than the starting compound, Andersson and Bobinger [100] presumed that it was formed through the cleavage of a photochemical dimer.

2.2.2. Photo-oxidation of 3-methylbenzo[*b*]thiophene

3-Formylbenzo[*b*]thiophene emerged as the major product from the photo-oxidation of 3-methylbenzo[*b*]thiophene in the neutral fraction (Figure 2.2) with very low amounts of hydroxylated methylbenzo[*b*]thiophene. Again, 2-sulfobenzoic acid was one of the major products in the acidic fraction with the detection of a new product, 2-acetylbenzenesulfonic acid. The minor products found were benzenesulfonic acid and benzo[*b*]thiophene-2,3-dicarboxylic acid, the latter resulting from the photochemical cleavage of a putative dimer as was the case for 2,3-diformylbenzo[*b*]thiophene from 2-methylbenzo[*b*]thiophene.

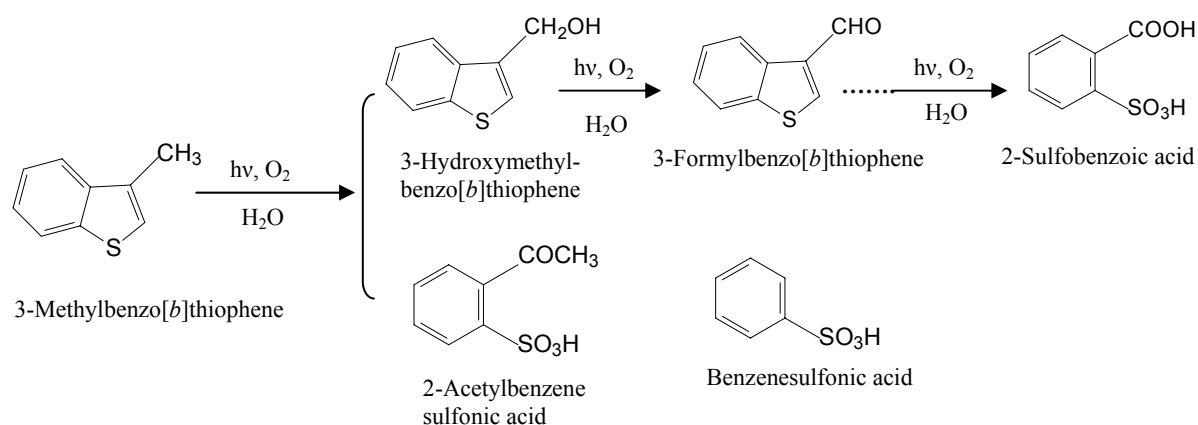


Figure 2.2. Degradation pathway of 3-methylbenzo[*b*]thiophene (from [99]).

Shiraishi et al. [98] also obtained 2-sulfobenzoic acid, benzenesulfonic acid and 2-acetylbenzenesulfonic acid as acidic products from the photochemical desulfurization of 3-methyl BT in addition to traces of 3-formylbenzo[*b*]thiophene.

2.2.3. Photo-oxidation of 4-methylbenzo[*b*]thiophene

The identified products in the neutral fraction were 4-methylbenzo[*b*]thiophene-2,3-quinone, 4-formylbenzo[*b*]thiophene, and 3-acetyl-2-formylthiophene which arised through the oxidative ring opening of the benzo ring and retention of the 4-methyl group, whereas those identified in the acidic fraction were 2-methyl-6-sulfobenzoic acid, 2-formyl-6-sulfobenzoic acid and 3-sulfophthalic acid.

2.2.4. Photo-oxidation of 5-methylbenzo[*b*]thiophene

The neutral products were dominated by 5-methylbenzo[*b*]thiophene-2,3-quinone with small amounts of thiophenecarboxylic acid and 5-formylbenzo[*b*]thiophene, while 5-methyl-2-

sulfobenzoic acid, 5-methyl-2-sulfobenzaldehyde, 4-methylbenzenesulfonic acid and 4-sulfoisophthalic acid, formed through oxidation of the 5-methyl group to a carboxylic acid, were among the acidic products obtained. Moreover, the acidic fraction contained thiophene-2,3-dicarboxylic acid, showing the possibility of a benzo ring cleavage, and 5-methylbenzo[*b*]thiophene-2,3-dicarboxylic acid.

2.2.5. Photo-oxidation of 6-methylbenzo[*b*]thiophene

The neutral products found were 6-methylbenzo[*b*]thiophene-2,3-quinone and 6-formylbenzo[*b*]thiophene in agreement with several of the other isomers and the acidic products were 4-methyl-6-sulfobenzoic acid and 3-toluenesulfonic acid.

2.2.6. Photo-oxidation of 7-methylbenzo[*b*]thiophene

The photo-oxidation of this compound led to the formation of 7-formylbenzo[*b*]thiophene and 2-acetyl-3-formylthiophene as neutral products, and 3-methyl-2-sulfobenzoic acid, 2-toluenesulfonic acid, thiophene-2,3-dicarboxylic acid, 2-formyl-6-methylbenzenesulfonic acid and 3-formyl-2-sulfobenzoic acid as acidic products.

2.3. Photo-oxidation of 2,3-dimethylbenzo[*b*]thiophene

Shiraishi et al. [98] showed that the photochemical desulfurization of 2,3-dimethyl BT gave the same acidic products obtained in case of 3-methyl BT, i.e. 2-sulfobenzoic acid, benzenesulfonic acid and 2-acetylbenzenesulfonic acid.

2.4. Photo-oxidation of dibenzo[*b*]thiophene

Bobinger et al. [101] investigated the photo-oxidation of dibenzo[*b*]thiophene in a mixture of methanol/water (1:2) using a mercury middle pressure lamp. In the same time, Traulsen et al. [102] also studied the photodegradation of dibenzo[*b*]thiophene by exposing a quartz vessel containing a solution of dibenzo[*b*]thiophene dissolved in membrane-filtered natural seawater to sunlight. The major products were 2-sulfobenzoic acid, formed through the opening of both a benzene and the thiophene ring, and benzothiophene-2,3-dicarboxylic acid formed through the oxidation of one of the benzo rings. A photochemical decarboxylation of the latter compound led to the formation of benzothiophene-2- and -3-carboxylic acid. Small amounts of 2-hydroxybiphenyl-2'-sulfinic acid- δ -sultine and thiophenetetracarboxylic acid were found together with an isomer of thiophenetricarboxylic acid and an isomer of thiophene-

dicarboxylic acid. As a consequence of the formation of sulfonic acids, it was observed that the pH value of the reaction solution dropped to quite low values.

However, during the photochemical desulfurization of DBT, only six acidic products were obtained including DBT sulfoxide, DBT sulfone, 2-sulfobenzoic acid, benzo[*b*]thiophene-2,3-dicarboxylic acid, dibenz[1,2-*c,e*]oxathiin-6-oxide and dibenz[1,2-*c,e*]oxathiin-6,6-dioxide [98].

Moreover, Shemer and Linden [103] carried out the photodegradation of dibenzothiophene as a single compound and in a mixture with fluorene and dibenzofuran using monochromatic low pressure (LP, 253 nm) and polychromatic medium pressure (200-400 nm) UV sources with and without the addition of hydrogen peroxide in natural and laboratory water. They observed a synergistic effect during direct photolysis using LP-UV and H₂O₂ of the mixture as compared to the photodegradation of a single component in an aqueous solution. Furthermore, natural water enhanced the direct photolysis compared to laboratory buffered water, whereas degradation of the compounds in the natural water was inhibited using the UV/H₂O₂ process. However, the authors were obviously interested in the kinetics and quantum yields of the compounds without studying the products formed.

2.5. Photo-oxidation of 4-methyldibenzo[*b*]thiophene

As 4-MDBT and 4,6-DMDBT are known to be the most difficult compounds to be desulfurized [84, 85], they have attracted Shiraishi et al. [98] to study their photochemical desulfurization. From the desulfurization process, Shiraishi et al. obtained four photoproducts which are 3-methyl-2-sulfobenzoic acid, 2-sulfobenzoic acid, 4-methyldibenzo[*b*]thiophene sulfone and 7-methylbenzo[*b*]thiophene-2,3-dicarboxylic acid.

2.6. Photo-oxidation of 4,6-dimethyldibenzo[*b*]thiophene

The photo-oxidation of dibenzothiophene and 4,6-dimethyldibenzothiophene sensitized by N-ethylquinolinium tetrafluoroborate (NMQ⁺ BF₄⁻) in oxygen-saturated acetonitrile solution was studied by Che et al. [104] using a 100-W mercury lamp. The oxidized products reported were predominantly composed of the corresponding sulfoxides and sulfones, which were produced via photoinduced electron transfer from the substrates to the excited singlet state of NMQ⁺.

In addition, the same previous products were obtained when DBT and 4,6-DMDBT were irradiated with visible light in O₂-saturated acetonitrile solutions in the presence of either 2-(4-methoxyphenyl)-4,6-diphenylpyrylium tetrafluoroborate or 10-methylacridine hexafluorophosphate as sensitizers [105].

However, the photochemical oxidation of 4,6-DMDBT led to the production of two nondesulfurized photoproducts, namely 3-methyl-2-sulfobenzoic acid and 4,6-DMDBT sulfone [98].

2.7. Summary

It could be concluded by investigating the photoproducts of BT, alkylated BTs, DBT and alkylated DBTs that there are three possible pathways for the photo-oxidation of these compounds. One pathway involves the oxidation of the methyl substituent(s) into an alcohol, an aldehyde and finally into a carboxylic group. Another pathway leads via opening of a benzene ring to the oxidation of the carbon atoms at the ring junction with thiophene and the formation of 2,3-thiophenedicarboxylic acid in case of BTs. Opening of both benzene rings in case of DBTs gives thiophenetetracarboxylic acid. The opening of the thiophene ring was also demonstrated by the detection of 2-sulfobenzoic acid in case of BT. The same product was obtained from DBT through the cleavage of both the benzene and thiophene rings. Finally, a minor pathway was also observed involving the oxidation of the sulfur atom in DBT giving the corresponding sulfoxide and sulfone. In addition, some products such as 2,3-diformylbenzothiophene were detected that seem to be derived from initial photodimers.

3. Analytical techniques for the characterization of polar and non-polar photoproducts of polycyclic aromatic sulfur heterocycles

The complexity of petroleum necessitates the utilization of a variety of chromatographic techniques to reduce its complexity by separating the sample into simpler fractions. Afterwards, these fractions can be photo-oxidized and the photoproducts of the most toxic fraction can be characterized e.g. by spectroscopic methods. Thus, this chapter gives an overview of the different analytical techniques applied in this work.

3.1. Liquid chromatography

3.1.1. Group separation into saturates, aromatics, resins and asphaltenes (SARA)

The initial and most common step in petroleum analysis of distilled fractions is the group separation of petroleum fractions into saturates, aromatics, resins and asphaltenes. Asphaltenes, highest molecular weight matter and insoluble in the lower n-alkanes, are removed by precipitation [106]. Then the saturate, aromatic, and resin (polar compounds) fractions can be separated on chromatographic columns packed with silica and/or alumina by stepwise elution with solvents of increasing polarity.

3.1.2. Group separation into saturates, monoaromatics and polyaromatics

In order to separate alkylbenzenes from the polyaromatic compounds, an alumina column was used with different mixtures of pentane and dichloromethane. The crude oil can be separated into an aliphatic, a one-ring aromatic and a polyaromatic fraction in one step on alumina column by eluting the aliphatics with pentane, the alkylbenzenes with a pentane/dichloromethane (50:1) mixture and the polyaromatic compounds with pentane/dichloromethane (3:1) mixture [107].

3.2. High performance liquid chromatography (HPLC)

3.2.1. Separation of the aromatic fraction into PAHs and PASHs

As the sulfur atom introduces an element of asymmetry into a PASH molecule and hence lead to the presence of a larger number of parent systems among PASHs than among PAHs [93], this characteristic can thus be exploited by using a suitable effective chromatographic phase.

Previous studies found that some sulfur aromatics are retained on a stationary phase containing palladium ions in normal-phase liquid chromatography [108]. This principle was improved using a bonded stationary phase which prevents slow loss (bleeding) of the Pd-metal center by complexation with silica-bonded 2-aminocyclopentene-1-dithiocarboxylic acid (ACDA) [109]. By using gas chromatography with a sulfur-selective detector, it has been shown previously that this method can be applied to the aromatic compounds in low boiling materials like diesel fuel. They are completely separated into a fraction 1 which only contains hydrocarbons and, after an increase in eluent polarity, a fraction 2 that only contains PASHs [110]. Therefore, the polyaromatic fraction of crude oil was further fractionated onto Pd(II)-ACDA stationary phase into polycyclic aromatic hydrocarbons and polycyclic aromatic sulfur heterocycles according to the number of condensed aromatic rings in the normal-phase mode [110].

3.2.2. Separation of PASHs according to the number of rings

Cyclodextrin phases have been extensively used for a long time in the separation of enantiomers [111]. However, the separation of polycyclic aromatic sulfur heterocycles according to their number of aromatic double bonds was recently accomplished on a β -cyclodextrin stationary phase [112]. As cyclodextrins are cyclic oligoglucoses and as the β -phase consists of seven glucose units in a ring with the hydroxy groups pointing outwards, it is assumed that the interaction between the solutes and the phase will take place through the hydroxyl groups on the outer surface of the cyclodextrin when the mobile phase used is cyclohexane. This interaction may resemble that taking place between PAHs and diol phases [113]. Hence, a β -cyclodextrin phase was used in this work for the separation of PASHs into two-ring fraction (benzothiophenes), three-ring fraction (dibenzothiophenes) and higher-ring fraction.

3.3. Photo-oxidation apparatus

In order to simulate the sunlight irradiation at the surface of the earth, a mercury middle pressure lamp equipped with a water cooling system (TQ150, 250 W, Heraeus, Germany) was used for the photo-oxidation experiments. It emits radiation in the 250-600 nm region. In addition, the different fractions of crude oil to be photo-oxidized were added to 100 ml water solution and were placed in 100 ml DURAN® glass measuring flasks to cut off all wavelengths below 300 nm to simulate sunlight. Moreover, all the flasks were covered to prevent vaporization and to maximize the photolysis yields.

3.4. Liquid-liquid extraction

Liquid-liquid extraction of organic compounds has been an effective method for concentrating trace compounds and for removing interfering components from environmental samples for a long time. For extraction, the sample is distributed between pairs of immiscible liquids in which the analyte and its matrix have different solubilities. Thus, certain analytes in water can be transformed directly into an organic solvent which is not miscible with water, such as cyclohexane or dichloromethane. A selected solvent or mixture of two solvents may be used for extraction, provided the extraction is at least 80 % efficient. The distribution of a compound between two immiscible liquid phases can be expressed in terms of its partition coefficient. For some systems, the partition coefficient may be made more favorable by adjusting the pH to prevent ionization of acids or bases, by forming ion pairs with ionizable solutes, by forming hydrophobic complexes with metal ions or by adding neutral salts to the aqueous phase to reduce the solubility of the analyte. Solvent extraction of aqueous solutions by manipulating the pH is widely used to fractionate samples into neutral, basic, weakly acidic and strongly acidic fractions [114].

After the photo-oxidation of the aliphatic, monoaromatic, polyaromatic, PAH and PASH fractions in aqueous solutions, polar and non-polar photoproducts are found. In order either to separate the polar products from the non-polar ones to perform the toxicity tests or to try to identify these products by their injection on gas chromatography with flame ionization detector (GC-FID) or gas chromatography coupled to mass spectrometry (GC-MS), liquid-liquid extraction was used to extract them from the aqueous solutions. First, the non-polar compounds were extracted into dichloromethane after making the aqueous phase basic (pH ~ 11). Then the the water solution was acidified by adding concentrated HCl to extract the carboxylic acids produced from the photo-oxidation of PASHs from water solutions using dichloromethane. However, because of the strong acidity of sulfonic acids, also produced from the photo-oxidation of PASHs, no solvent was able to extract them from the aqueous solutions. Hence, sulfonic acids were obtained here by the evaporation of the aqueous solution of the photo-oxidized products of PASHs remaining after the extraction of the carboxylic acids on the rotary evaporator.

3.5. Derivatization

Derivatization techniques include procedures in which the analyte chemical structure is changed using various derivatizing agents to enhance detectability or improve separation

efficiency. Derivatization is also employed to improve the limit of detection of an analytical procedure. In addition, the separation of the analytes is often easier to achieve not only because the reaction is selective and the formed derivatives may be detected selectively but also the derivatization can neutralize the activity of polar functional groups. Among other advantages, derivatization often improves the thermostability of thermally labile compounds and increases the volatility of low volatile compounds. Therefore, in order to identify the polar photoproducts (carboxylic acids) of PASHs, they were first subjected to silylation and then injected on GC-MS.

3.6. Gas chromatography

GC-MS is currently the most frequently used technique for determining trace organic compounds in environmental samples. Therefore, the different fractions of crude oil, after their separation by liquid chromatography, were injected onto GC-FID and GC-MS for the screening and identification of individual compounds.

3.7. Mass spectrometry

Quadrupole mass spectrometers with their ability to provide different options, the product ion, the parent ion and the neutral loss mode together with the high resolution time of flight mass spectrometers were used for the detection and identification of unknown polar photoproducts. In this work, carboxylic acids were detected first by electrospray ionization mass spectrometry (ESI-MS) in the negative mode by a loss of 44 amu $[M-CO_2]^-$ from the parent ions, then after silylation, were identified by GC-MS. Because of the strong acidity of sulfonic acids, their detection was performed by ESI-MS in the negative ion mode by a loss of 80 amu $[M-SO_3]^-$ from the parent anions. Afterwards, they were analyzed by time of flight-mass spectrometry (TOF-MS) for the identification of the different acids as this technique allows the determination of the molecular formula of unknown compounds.

As the polycyclic aromatic sulfur heterocycles are not only non-ionic, but also non-polar, they can not be ionized in ESI. Hence, after the photo-oxidation and extraction of the non-reacted PASHs from the aqueous solutions, they were subjected to methylation and then analysis by Fourier transform ion cyclotron resonance mass spectrometry (FT-ICR MS).

4. Phototoxicity

Recent environmental research has focused on the toxicity to aquatic organisms caused by the concurrent exposure to natural solar radiation and environmental contaminants. Exposure of living organisms to natural ultraviolet radiation alone, especially wavelengths in the UV-B range, was found to cause damage at the molecular, cellular and organismal levels [115]. However, the exposure of organisms to UV and specific contaminants can have more severe consequences [116, 117-123]. In addition, the increase in the levels of ultraviolet radiation reaching the earth due to ozone depletion will also increase the interactions of natural solar radiation and environmental contaminants and can lead to severe ecological effects [124-126].

In this chapter, an overview will be given on the types of toxicity tests, the different classes of pollutants, the phototoxicity types and experiments performed on different compounds and the toxicity-based fractionation methodology.

4.1. Definition of toxicity

Toxicity refers to the potential of a substance to produce an adverse or harmful effect on a living organism. A toxicant is an agent that can produce an adverse effect in a biological system, by either damaging its structure or function or by causing death. The adverse response may be expressed as abnormal mortality, reproduction or growth.

4.2. Toxicity tests

Toxicity tests determine the level of toxicity, if any, present in a chemical and the duration of exposure required for the toxicity to be expressed as adverse effects. Organisms are exposed in test chambers to various concentrations of the chemical. The toxicity effects, such as mortality and changes in reproduction are evaluated by comparing those organisms exposed to different dilutions of the chemical with other organisms (controls) exposed only to non-toxic dilution water.

4.3. Types of toxicity tests

4.3.1. Acute toxicity (short-term testing)

Acute toxicity tests are short-term tests designed to measure the effects of pollutants on species during a short portion of their life span. The tests typically running between 48 and 96 hours, and usually measure the effects of pollutants on the survival of a species. The results of

these tests are often reported as an 'EC₅₀', which is the effective concentration of a test sample that causes a 50 % reduction in survival.

4.3.2. Chronic toxicity (long-term testing)

In chronic tests, the organism is exposed to a chemical for a long time relative to its lifetime. Effects on growth, reproduction and survival are then investigated. As young organisms are more sensitive to chemicals than older ones, the tests usually start with very young organisms which are exposed to a chemical for as long a period of time as is practical. The tests often continue until reproduction begins as reproduction is generally a sensitive endpoint. In all of these tests, the health of the treated organisms is compared with that of control organisms. Except for the presence of the chemical, both the treated and control organisms are treated the same. As long as the exposed organisms can survive, grow and reproduce as well as or better than the control group, then the chemical is not harming them. In addition, chronic tests are used for low-level pollutants and high-risk situations.

4.4. Suitable organisms for toxicity tests

Species or life stages that are especially sensitive to pollutants are ideal for toxicity testing. For example, the early developmental stages of marine organisms are more sensitive than their adult equivalents. Because environmental stresses affecting larval development can have potentially serious consequences for the population and ecosystem, these early life stages are very useful for identifying harmful environmental effects. It also helps if the test organism has a wide geographic distribution, is an important part of the ecosystem, is recreationally, economically, or culturally significant (or all of these), and can be collected from the field throughout the year or maintained under laboratory conditions.

4.5. Classification of environmental pollutants

It has been long known that chemicals affecting an organism in the same way have the same "mode of action". However, it was not known which chemicals have the same mode of action, or even how many modes of action exist.

Hermens [127] have used quantitative structure-activity relationship studies to estimate the acute aquatic toxicity of chemicals by classifying them into four classes. These classes are: inert chemicals (baseline toxicity), less inert chemicals, reactive chemicals and specifically acting chemicals.

Inert chemicals

Chemicals that are not reactive and do not interact with specific receptors in an organism are called inert chemicals. They cause narcosis to the living organism, which is entirely dependent on the hydrophobicity of the chemical. Hence, in the absence of other modes of action, the toxicity of the chemical will increase with the increase in its hydrophobicity. This type of toxicity is called "baseline" toxicity or minimum toxicity.

Less inert chemicals

These are chemicals that possess hydrogen bond donor acidity, such as phenols and anilines [128]. Their mode of action is called "polar narcosis" [129] which is slightly more toxic than the baseline toxicity.

Reactive chemicals

Reactive chemicals act by different modes of action and thus have higher toxicity in comparison to baseline toxicity. This increase in their toxicity is due to that these chemicals react unselectively with certain chemical structures (e.g. epoxides, which react with sulfhydryl groups of cysteine residues of peptides), or chemicals that are metabolized into more toxic species [130, 131].

Specifically acting chemicals

These chemicals exhibit their toxicity by their interaction with specific receptor molecules, such as organic phosphorus esters [132].

In addition, recently, Verhaar et al. [133] classified the chemicals into one of the previous classes according to their structural characteristics. A chemical may belong to one of the above mentioned classes only when it can fulfil the following conditions: the compound should consist of carbon, hydrogen, nitrogen, oxygen, sulfur and/or halogens (excluding iodine), have a log K_{ow} (Log octanol-water partitioning coefficient) that lies between 0 and 6 and have a molecular mass of not more than 600 Daltons [134]. The classification of Verhaar et al. is as follows:

Class 1-type compounds (Narcosis or Baseline Toxicity)

This class includes:

- acyclic compounds not containing halogen at β -position from unsaturations

- monocyclic compounds substituted with halogens.
- monocyclic compounds that are unsubstituted or substituted with acyclic structures containing only carbon and hydrogen atoms.
- polycyclic compounds that are unsubstituted or substituted with acyclic structures containing only carbon and hydrogen atoms.
- linear ethers or monocyclic mono-ethers, but not epoxides or peroxides.
- aliphatic alcohols, but not allylic alcohols.
- alcohols with aromatic moieties, but not phenols or benzylic alcohols.
- ketones, but not α,β -unsaturated ketones.
- aliphatic secondary or tertiary amines.
- halogenated compounds, but not α or β halogen-substituted compounds.

Class 2-type compounds (Less inert compounds)

These compounds are:

- non- and weakly acidic phenols;
- anilines with one nitro substituent and/or one to three chlorine substituents, and/or alkyl substituents;
- mononitroaromatics with one or two chlorine substituents and/or alkyl substituents; primary alkylamines and pyridines with one or two chlorine substituents.

Class 3-type compounds (Unspecific reactivity)

Compounds belonging to this class include:

- compounds with a good leaving group at an α -position of a carbon-carbon double or triple bond.
- compounds with a good leaving group at an α -position of an aromatic ring.
- other compounds with a good leaving group at an α -position of a double or triple bond fragment.
- compounds containing an epoxide or aziridine function.
- compounds containing carbonyl, nitrile, amide, nitro or sulfone group at an α -position of a double or triple bond.
- compounds with a single, double or triple nitrogen-nitrogen linkage.
- activated nitriles, e.g. α -hydroxynitriles or allylic nitriles.

- acid anhydrides, lactones, acid halides, carbamoylhalides, ketenes, aldehydes, isocyanates, thiocyanates, isothiocyanates, disulphides, sulfonic esters, sulphuric esters, cyclic sulfonic/sulphuric esters, α -haloethers and β -haloethers.

Class 4-type compounds (Acting by a specific mechanism)

Examples of these compounds are dichloro-diphenyl-trichloroethane (DDT) and analogues, dithiocarbamates, organotin compounds and organophosphorothionate esters.

Compounds that do not belong to one of the previous four classes are termed “not possible to classify according to these rules”.

4.6. Types of phototoxicity

When determining the toxicity of contaminants in the environment, it is crucial to consider the effect of solar radiation in order to avoid an underestimation of their toxicity. The photomediated toxicity of environmental contaminants can be expressed through two mechanisms: photomodification (direct photo-oxidation) and photosensitization (indirect photosensitized oxidation) [135]. Photosensitization may occur when the organisms bioaccumulate photoactive chemicals and the toxic effects are then manifested upon exposure of the organisms to solar radiation [121, 136, 137]. On the other hand, phototoxicity may result from photomodification if the dissolved chemicals are photochemically transformed to oxidized compounds of higher toxicity (photoproducts) and subsequently absorbed by the organisms.

The extent of photomodification of contaminants can be a function of several variables, including photo-oxidation rate [123], amount of the contaminant irradiated and the volume and mixing characteristics of the surface water.

Generally, investigations of the photomediated toxicity of petroleum have focused on a few nonalkylated PAHs such as anthracene, however, other petroleum components such as heterocyclic aromatics may also contribute to the photomediated toxicity. In contrast to nonalkylated parent compounds, the alkylated forms of PAHs and other compounds are predominant in crude oils, refined petroleum products and their water accommodated fractions (WAFs).

4.7. Phototoxicity of single compounds

Because the photoproducts are more water soluble than the parent compounds, they are available in higher concentrations to the organisms in comparison to the the parent ones. This presents a great toxic risk because oxidized products are known to be more reactive and biologically damaging than their parent compounds [123, 138].

To evaluate the potential hazards of the photomodified compounds in petroleum, the toxicity of the photoproducts of some PAHs was determined as examples and compared sometimes with the toxicity of the PAH itself.

McConkey et al. [139] have exposed the marine bacteria *Photobacterium phosphoreum* and the aquatic plant *Lemna gibba* (duckweed) to solutions of phenanthrene (PHE) and its primary photoproduct 9,10-phenanthrenequinone (PHEQ). They found that for both *Photobacterium phosphoreum* and *Lemna gibba*, PHEQ was much more toxic than PHE.

This is in agreement with the results of Xie et al. [140] who also determined the toxicity of PHE and PHEQ, however, using *Daphnia magna* in presence and absence of copper and found that PHEQ was the more toxic of the two compounds.

To stress the role of photomodification, Lampi et al. [141] have tested the toxicity of 14 PAH photoproducts to *Daphnia magna* and observed that most of them were highly toxic. The most toxic compounds tested were two photoproducts of benzo[*a*]pyrene, namely 1,6- and 3,6-benzo[*a*]pyrenequinone followed by benzo[*a*]anthraquinone.

In order to assess the photoinduced toxicity of three PAHs, Ren et al. [123] exposed *Lemna gibba* to fluoranthene (FLA), pyrene (PYR) and naphthalene (NAP) solutions after their irradiation with UV light. They observed that the rates of photomodification of the three PAHs were rapid and that the photomodified PAHs were more toxic than the parent compounds.

Anthracene (ANT), benzo[*a*]pyrene (BAP), FLA, PHE, and PYR were photomodified by natural sunlight and the toxicity of the photoproducts were tested on the duckweed *Lemna gibba* [142]. After their photomodification in sunlight, the PAHs were incubated with the plants and the toxicity expressed over a period of 7 and 20 days was determined. The

mixtures of photomodified products derived from each PAH showed the following order of decreasing toxicity: PYR = FLA > PHE > ANT > BAP.

Mallakin et al. [143] identified the photo-oxidation products of ANT and assessed the toxicity of some selected photoproducts, prevalent among these were anthraquinone (ATQ) and hydroxy-anthraquinones. The toxicity of eight of these photoproducts (ATQ, 1-hydroxyATQ, 2-hydroxyATQ, 1,2-dihydroxyATQ, 1,4-dihydroxyATQ, 1,5-dihydroxyATQ, 1,8-dihydroxyATQ, 2,6-dihydroxyATQ) with four other structurally related ones (1,3-dihydroxyATQ, 1,2,4-trihydroxyATQ, 1,2,5,8-tetrahydroxyATQ and 1,2,10-trihydroxyATQ) was tested based on the growth inhibition of the duckweed *Lemna gibba*. All but one (2,6-dihydroxyATQ) of the compounds tested were found to be toxic showing that the resultant photoproducts were more toxic than the parent compounds.

In a separate experiment, Mallakin et al. [144] also demonstrated that the photo-oxidation products of ANT caused the inhibition of the photosynthetic activity and the electron transport in *Lemna gibba*.

Huang et al. [138] investigated the photoinduced toxicity of ANT, PHE and BAP to *Lemna gibba*, in which the inhibition of growth and extent of chlorosis were the toxicity end points and found that the photomodified PAHs were hazardous to the duckweed.

Ohe [145] studied the mutagenicity of the photoproducts of six PAHs in the presence of nitrite to *Salmonella typhimurium*. Irradiated samples of PYR, FLA, BAP and 5,6-benzoquinoline showed high mutagenic effects on *Salmonella*.

Ren et al. [146] applied ANT, BAP and FLA after their irradiation with UV-B light to the seeds of *Brassica napus* (Canola) and observed the toxicity effects on the germination efficiency, root and shoot growth and the chlorophyll content. The photomodified PAHs had a big impact on the root system of the plant and led to the inhibition of the root fresh weight. The order of toxicity of the photomodified compounds was as follows: ANT > BAP > FLA.

Schirmer et al. [147] showed that the toxicity of a creosote to the rainbow trout (*Oncorhynchus mykiss*) gill cells would substantially increase through the interaction of the

creosote with UV irradiation. The photomodified creosote showed high cytotoxicity to the fish measured as impairment of the mitochondrial electron transport.

4.8. Toxicity-based fractionation

In order to identify toxic compounds in complex environmental samples, toxicity testing and chemical analysis have been combined in an approach known as bioassay-directed chemical analysis. This approach is based on the “toxicity identification evaluation” procedure developed by the US-American Environmental Protection Agency (EPA) about one decade ago [148]. It starts with the separation of sample extracts into fractions followed by the determination of their toxicity by applying bioassays. This process of separation and testing can be repeated until the chemical complexity of the fractions is sufficiently reduced. The approach was originally established to investigate waste waters. However, it has now extended to all kinds of samples such as air [149], sediments [150, 151], effluents [152-154], pore water [155] and surface water [156]. The main aim of the toxicity-based fractionation technique is to pinpoint the exact chemicals producing the greatest risk in the environmental samples.

In an attempt to identify the compounds responsible for the phototoxicity of ANT, Brack et al. [157] applied a toxicity-based fractionation methodology using the bacterium *Vibrio fischeri*. The trace photoproduct, ANT-1,4-dione was identified among the phototoxic fractions and showed a very high toxicity which dominated that of all other ANT photoproducts. In addition, some fractions exhibited mutagenic activity that was attributable to 1-hydroxyANT-9,10-dione and 1,4-dihydroxyANT-9,10-dione.

Contaminated samples from Hamilton harbour (Hamilton, Ontario) were profiled using a bioassay-directed fractionation approach [158]. The fractions obtained from HPLC were tested for toxicity using short-term as well as long-term assays on the bacterium *Vibrio fischeri*. The photomodified PAHs were equally as toxic as intact PAHs.

5. High resolution mass spectrometry

Mass spectrometers with a resolution higher than $\sim 10,000$ $m/\Delta m$ are considered to be high-resolution instruments. This high resolution enables the determination of elemental compositions behind a mass signal. Time of flight (TOF) and, to a certain degree, triple quadrupole instruments are capable of resolutions up to about 20,000. In addition, the rapid development of Fourier transform ion cyclotron resonance (FT-ICR) instruments in recent years has offered ultra-high resolution ($> 250,000$) [159]. This chapter will give an overview about the instruments used in this work, starting with the electrospray ionization technique (ESI) used and then describing the mass analyzers and the data processing.

5.1. Electrospray ionization

Since its development by Yamashita and Fenn [160] in 1984, ESI has been widely used for the analysis of a variety of polar molecules ranging from < 100 Da up to and above 200 000 Da in molecular mass. ESI is a very soft method of ionization. The sample solution is introduced into the ionization source through a stainless steel capillary (75-100 μm internal diameter) at a flow rate of between $1 \mu\text{l min}^{-1}$ and 1ml min^{-1} , but more typically in the region $5\text{-}300 \mu\text{l min}^{-1}$. A strong electric field is applied to the liquid passing the capillary by applying a potential difference of 3 or 4 KV between the capillary and the counter electrode. As a consequence of this strong electric field, a charge accumulates at the liquid surface located at the end of the capillary, which will then break up to form highly charged droplets. As the solvent in the droplets evaporates, they shrink until they reach the point at which the repelling coulombic forces come close to their cohesion forces. At this point, a "Coulombic explosion" occurs and the droplets are ripped apart. This produces smaller droplets that can repeat the process, ultimately producing bare analyte ions.

5.2. Mass analyzers

The main function of the mass analyzer is to separate, or resolve, the ions formed in the ionization source by their mass to charge ratios (m/z). All mass analyzers employ electric fields, sometimes in conjunction with magnetic fields, to allow the discrimination between ions of different mass-to-charge ratio. This discrimination can be expressed through the resolution concept.

5.2.1. Definitions

5.2.1.1. Resolution

The resolution (R) of a mass analyzer, or its ability to separate two peaks, is defined as the ratio of the mass of a peak of interest, m , to the difference in mass between this peak and the adjacent peak of higher mass, Δm , i.e. $R = m / \Delta m$.

Two neighbouring peaks are assumed to be sufficiently separated when the valley separating their maxima has decreased to 10 % of their intensity. Hence, this is known as 10 % valley definition of resolution. The 10 % valley conditions are fulfilled if the peak width at 5 % relative height equals the mass difference of the corresponding ions, because then the 5 % contribution of each peak to the same point of the m/z axis adds to 10 %.

It should be noted that the attributive low resolution is generally used to describe spectra obtained at $R = 500-2000$. High resolution is appropriate for $R > 5000$.

5.2.1.2. Mass resolving power

The resolving power ($m/\Delta m_{50\%}$), used in FT-MS, is the ratio of mass to the width of the corresponding mass peak at half height.

5.2.1.3. Mass accuracy

The mass accuracy of a spectrometer is defined as the difference between the measured accurate mass of an ion and its calculated exact mass expressed relative to the measured mass. It is usually reported in parts per million (ppm).

Mass accuracy depends on many parameters such as resolving power, scan rate, scanning method, signal-to-noise ratios of the peaks, peak shapes, overlap of isotopic peaks at some nominal mass and mass difference between adjacent reference peaks. The experimental accurate mass should lie within an error range of ± 5 mmu for routine applications independent of the ionization method and the instrument used [161].

5.2.2. Types of mass spectrometers

5.2.2.1. *Quadrupole*

A quadrupole mass filter consists of four parallel metal rods. Two opposite rods have an applied potential of $(U+V\cos(\omega t))$ and the other two rods have a potential of $-(U+V\cos(\omega t))$, where U is a dc voltage and $V\cos(\omega t)$ is an ac voltage. The applied voltages affect the trajectory of ions traveling down the flight path centered between the four rods. As an ion enters the quadrupole assembly in the z -direction, an attractive force is exerted on it by one of the rods with its charge actually opposite to the ionic charge. If the voltage applied to the rods is periodic, attraction and repulsion in both the x - and y -directions are alternating in time, because the sign of the electric force also changes periodically in time. As the applied voltage is composed of a dc and a radiofrequency voltages, the overall ion motion results in a stable trajectory causing ions of a certain m/z value or m/z range to pass the quadrupole and to be detected thereafter. For given dc and ac voltages, only ions of a certain mass-to-charge ratio pass through the quadrupole filter and all other ions are thrown out of their original path. A mass spectrum is obtained by monitoring the ions passing through the quadrupole filter as the voltages on the rods are varied.

5.2.2.2. *Ion trap*

The ion trap, also called quadrupole ion trap, consists of three cylindrical electrodes, two end-caps and a ring. Each of these electrodes has hyperbolic geometry and, in the normal mode of use, an auxiliary oscillating potential of low amplitude is applied across the end-cap electrodes while an rf oscillating drive potential is applied to the ring electrode. Ions created within the ion trap either by injection of electrons or injection from an external source, pass into the analyzer, and depending upon the combination of the mass to charge ratio, the amplitudes of the potentials, the frequency of the drive potential and the internal dimensions of the electrode array, will have either “stable” trajectories and pass through the analyzer to the detector, or “unstable” trajectories and collide with the electrodes. Finally, in order of increasing mass to charge value, ions exit the ion trap through small holes in one of the end-cap electrodes and pass to the detector. Mass analysis in this way takes less than one tenth of a second, and the resolution obtained is comparable to that of a quadrupole.

The ion trap finds application in GC/MS and liquid chromatography-mass spectrometry and can be used with any other mass analyzers in hybrid systems.

5.2.2.3. *Multiple quadrupoles*

In the last few years, multiple, usually triple, quadrupoles have found increasing application in chemical analysis. They use the collisional induced dissociation of ions to provide an unambiguous analysis of trace components in complex mixtures. The first quadrupole is used to select one mass from the spectrum in the normal manner. The selected ions enter the second quadrupole which has only an rf voltage applied and where energetic collisions can occur with inert gas molecules. The second quadrupole drives both parents and daughters ions towards the third quadrupole for analysis. The dissociation spectrum that is observed depends upon the collision energy, on the average number of collisions and, to some extent, on the way the instrument is designed and constructed. Obviously there are two important factors that should be considered when designing such instruments: the efficiency of transmission as ions pass from one quadrupole to the next and the control over the ion energy.

5.2.2.4. *Time of flight*

Time of flight-mass spectrometry (TOF-MS) has been known since the 1950's [162]. The TOF-MS analyzers allow the separation of ions of different m/z ratios due to different times of their passing a fixed path in the instrument [163]. In order to achieve the separation, first, a packet of monoenergetic ions is selected from the ion beam by modulation, then the ions enter the flight tube after acceleration (a flight tube, typically 2×0.5 m length, kept at high vacuum). The time for the ions to reach the detector depends on their masses. A mass spectrum of a packet of ions is a plot of ion signals versus time calibrated to mass.

However, the use of TOF-MS analyzers has greatly increased after the development of the mass reflectron by Mamyrin et al. in 1973 [164]. The reflectron consists of electrostatic ion mirror that refocuses and reflects the ions back to the detector surface (Figure 5.1). The use of reflectron has led to the extension of the drift length resulting in a nearly constant flight time for ions with equal m/z . Hence, ions possessing high energy pass the flight tube fast, but spend more time in the reflectron while those having less energy pass more slowly and spend less time in the reflectron. Thus, ions of the same m/z arrive at the detector together. The m/z for a given ion can be determined from $m/z = 2 eV (t / L)^2$ where z is the charge on the ion, e is the charge of an electron in Coulomb, V is the voltage in volts, t is the flight time of the ion and L is the flight path length of the ion.

The TOF-MS technique has been widely used due to its high data acquisition speed, its high ion transmission and the quasi-simultaneous measurement of all masses for each ion packet extracted from the ion source (nanoseconds between adjacent masses). In addition, the system can accumulate thousands of mass spectra per second.

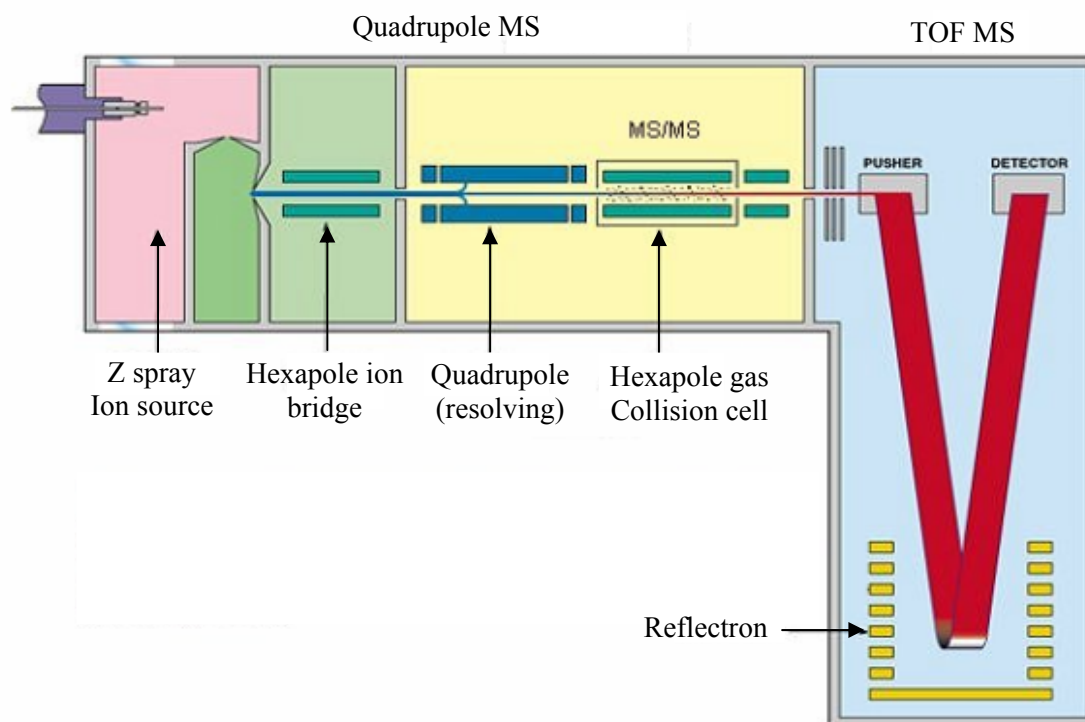


Figure 5.1. The Quadrupole-TOF mass spectrometer (from [165]).

The introduction of new ionization techniques to TOF-MS, such as electrospray ionization, has attracted a widespread interest to this technique that has been used for a rapid determination of low and high molecular weight compounds [166]. Electrospray TOF-MS has also been used with liquid chromatography [167] and capillary electrophoresis [168] for the identification and quantification of low and high molecular-weight species and with on-line liquid chromatography for the estimation of the exact masses of unknown organic compounds in complex mixtures [154].

TOF mass analysis has brought several advantages to ESI including mass range, speed, mass accuracy, and mass resolution. TOF has a theoretically unlimited mass range [169]. For instance, instruments typically extend well beyond 200,000 m/z . In addition, the best resolution that can be achieved is about 30,000, but in general 10,000 is observed.

5.2.2.5. *Fourier transform ion cyclotron resonance (FT-ICR)*

FT-ICR MS allows the determination of the elemental composition of individual components in unknown complex mixtures through its ultrahigh mass resolving power and mass accuracy [5, 170]. It reveals the heteroatom content, the degree of unsaturation (number of rings plus double bonds) and the carbon number distribution for numerous compound classes and types. Therefore, it finds more application in the field of petroleomics. For instance, it has been reported that negative ion ESI FT-ICR MS has resolved more than 10 000 compositionally distinct compounds (enabling assignment of chemical formulas) to more than 7500 species [171]. Therefore, a short description will be provided in order to demonstrate the operation principles involved in the separation of ions.

Ions are generated in a cell, which can be cubic (Figure 5.2) (edge of the cell approximately 2.5 cm), elongated (2.5 x 2.5 x 5 cm) or cylindrical (diameter and length 6 cm), located in a high-vacuum chamber (pressure $<1 \times 10^{-6}$ Pa) between the poles of an electromagnet or in a superconducting magnet. When an ion of velocity v enters a uniform magnetic field B perpendicular to its direction, it will move in a circular path by action of Lorentz force, the radius of which is determined by $r_m = (m v) / (z B)$ where z is the electric charge of an ion of mass m . Upon substitution with $v = r_m \omega$, the angular frequency ω_c becomes $\omega_c = (z B)/m$. Hence, the cyclotron angular frequency is independent of the ion's initial velocity, but a function of its mass, charge and the magnetic field. By applying a transverse electric field alternating at the cyclotron frequency f_c ($\omega_c = 2\pi f_c$), the ions are accelerated. Such a field is applied by a pair of radiofrequency (rf) electrodes placed on opposite sides of the orbit. As the ions accelerate, the radius of their orbit increases, and the resulting overall motion is spiral. The accelerated ions move up and down between the top and bottom of the detection plates of the cell, generating image currents in the circuit connecting these plates that can be amplified and digitized. The signal induced in the detection plates depends on the number of ions and their distance from the detection plates. If several different masses are present, then one must apply an excitation pulse that contains components at all of the cyclotron frequencies. This is done by using a rapid frequency sweep (chirp), an "impulse" excitation, or a tailored waveform. The image currents induced in the detection plates will contain frequency components from all of the mass-to-charge ratios. The various frequencies and their relative abundances are subjected to Fourier transformation to generate an ICR frequency-domain spectrum, which subsequently is converted into an FT-ICR mass spectrum.

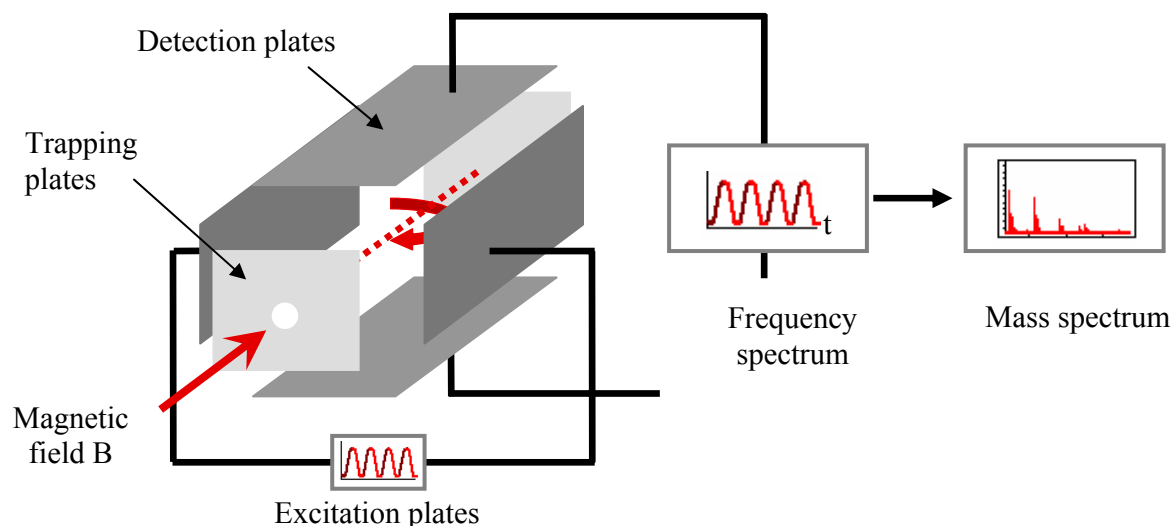


Figure 5.2. Schematic diagram of a cubic FT-ICR cell (from [172]).

5.3. Data interpretation

5.3.1. Nominal mass series (z^*)

It is almost impossible to make a complete analysis of each individual molecular species in a petroleum fraction due to the presence of an enormous number of isomers. Therefore, the analysis is usually accomplished by the groupings of the compound series (or compound types) according to the number of hydrogens relative to the number of carbons, i.e., $C_nH_{2n+z}=X$, where n is the number of carbon atoms, z is the “hydrogen deficiency” relative to mono-olefins or 1-ring naphthenes, X represents heteroatoms such as S, N and O. For example, C_6H_6 , C_7H_8 , and C_8H_{10} are benzene, toluene and xylenes/ ethyl benzene, respectively. They are classified as a $z = -6$ series. Another example is the $z = -10S$ series that includes benzothiophenes, methyl benzothiophenes and C_n -substituted benzothiophenes, etc. By using the concept of compound distribution in petroleum fractions as a function of z -series, all the components in a crude oil can be grouped into 14 families according to their nominal molecular masses [173]. The nominal mass series, z^* , of an ion is the remainder of its nominal mass divided by 14, minus 14, i.e., the modulus of (nominal mass/14) - 14. Each nominal mass yields a z^* value between -1 and -14. However, several compound types are included in each nominal mass series, z^* . For example, the $z^* = -6$ series contains compound types of $z = -6$ (benzenes), $-10S$ (benzothiophenes), -20 (phenylnaphthalenes), etc.

5.3.2. Kendrick mass defect

In the early 1960's, a new mass scale was introduced by Kendrick based on the mass assignment of a methylene group as exactly 14 mass units, instead of 14.01565 on the $^{12}\text{C} = 12.00000$ scale to express the organic mass spectral data [174]. The mass of an ion is converted from the IUPAC scale to the Kendrick mass scale as shown in equation 1

$$\text{Kendrick mass} = \text{IUPAC mass} \times (14.00000/14.01565) \quad \text{Eq. 1}$$

In order to gain information from the complex mass spectrum obtained, the Kendrick nominal mass (KNM) and the Kendrick mass defect (KMD) of individual ions are calculated. The Kendrick nominal mass is obtained by rounding the Kendrick mass to the nearest integer. The Kendrick mass defect can be obtained from equation 2:

$$\text{KMD} = \text{KNM} - \text{Kendrick exact mass} \quad \text{Eq. 2}$$

The Kendrick mass scale provides several advantages such as that the members of a homologous series (namely, compounds with the same heteroatom composition and number of rings plus double bonds, but different numbers of CH_2 groups) have an identical Kendrick mass defect. In addition, the mass defect of each member in each series (same class and same type) will be the same, which is not the case in the IUPAC scale where all the compounds in each series have a different mass defect. Homologous series are separated and grouped by sorting nominal Kendrick masses and KMDs as described below.

5.3.3. Multiple sorting

A multiple sorting technique based on nominal mass series and KMD was used as reported in the literature [175]. Mass peaks with their accurate masses are first sorted by z^* and separated into 14 groups with z^* ranging from -1 to -14. Within the same z^* group, the mass peaks are further sorted by their KMD. The pre-sorting of masses with z^* before sorting according to KMD can be understood by observing the following example. The difference in KMD between $\text{C}_{11}\text{H}_8\text{O}$ and $\text{C}_7\text{H}_6\text{S}$ is only 5 millimass units. However, the z^* for $\text{C}_{11}\text{H}_8\text{O}$ and $\text{C}_7\text{H}_6\text{S}$ is -12 and -4 respectively. Hence, the z^* values are well separated to distinguish between O- and S-containing heterocycles. A multiple sorting algorithm for data analysis is shown in Figure 5.3.

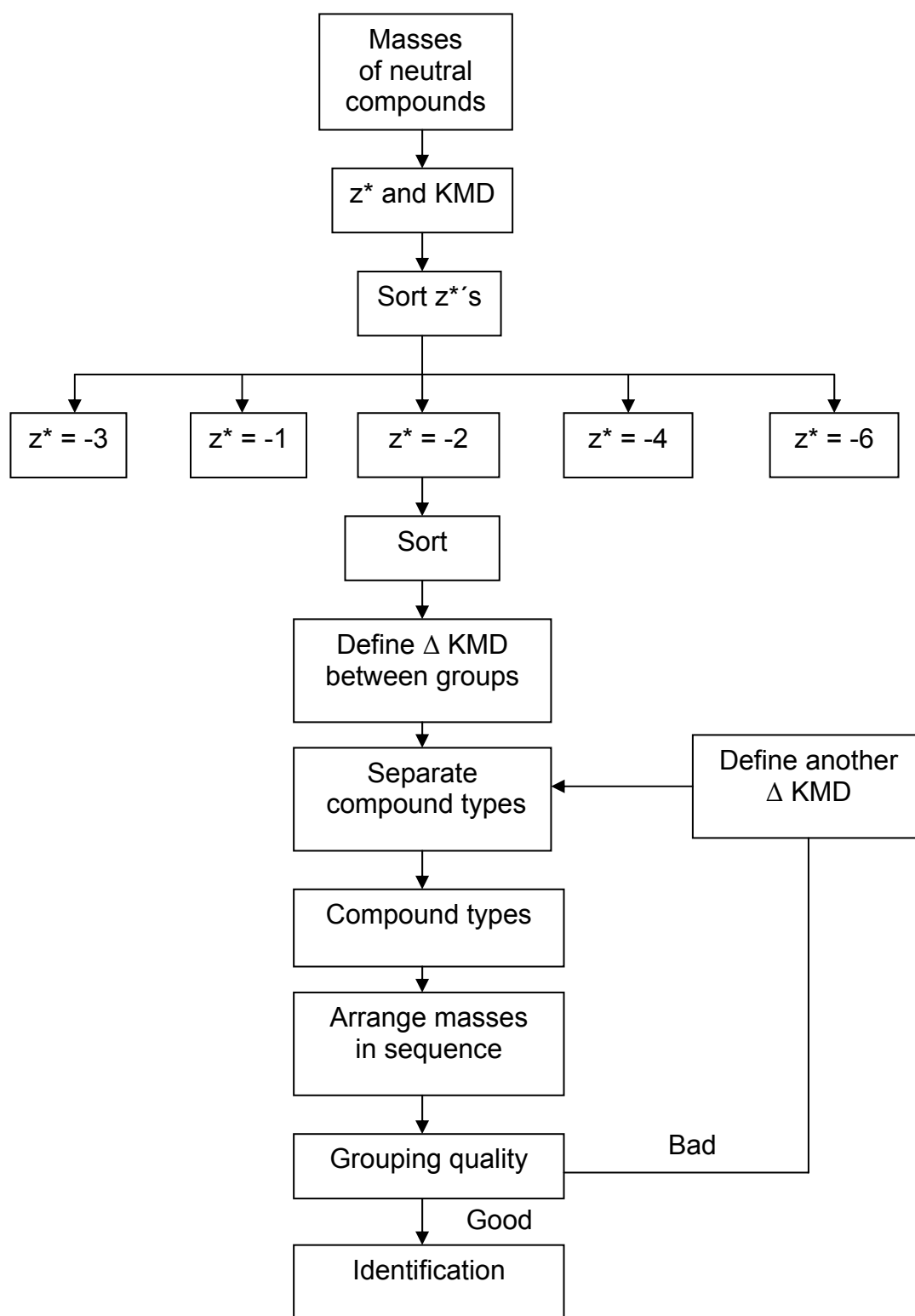


Figure 5.3. Flow diagram of multiple sorting algorithm (from [175]).

The composition of a sulfur-containing hydrocarbon can be expressed by the chemical formula $C_nH_{2n+z}S$. As z indicates of the number of rings plus double bonds present in the molecule, because each ring and each double bond means a reduction in the number of

hydrogens by 2, therefore, it is preferred in this work to use the double bond equivalent (DBE), which is the sum of rings (R) and double bonds (DB): $DBE = R + DB$, as a more direct measure of unsaturation.

5.4. Limitations of electrospray ionization

As the analysis of polar compounds, in general, suffers from their thermal instability, low volatility and inefficient ionization by traditional mass spectrometric ionization sources, electrospray ionization coupled to different mass analyzers offers a powerful tool for the identification of polar compounds. For instance, ESI coupled to high-field (9.4 T) FT-ICR MS has been used for the detailed characterization of heteroatomic species in crude oils and crude oil distillates [176] and complex environmental mixtures [177, 178]. Positive- or negative-ion electrospray selectively ionizes strongly basic or acidic polar heteroatomic compounds within the predominately hydrocarbon matrix of petroleum samples, thereby eliminating the need for pre-chromatographic isolation. In addition, by resolving mass differences down to ~ 1 mDa, FT-ICR MS provides unambiguous determination of molecular formulas for more than 20 polar compounds having the same nominal mass [179]. Nevertheless, a major disadvantage of ESI technique is that very little (usually no) fragmentation is produced although this may be overcome through the use of tandem mass spectrometric techniques.

However, the ionization of non-polar compounds with electrospray techniques is not very efficient [180, 181], hence, derivatized compounds are then desired. For PASHs, palladium(II) has been used as a sensitivity-enhancing reagent in standard resolution experiments with ESI ion trap MS [181]. However, this technique may show problems with samples of unknown sulfur content, because the concentration ratios of palladium(II) and sulfur seem crucial. In addition, instrumental parameters such as the flow rate for injection of the sample and the voltages must be finely tuned to suppress hydrocarbons. For such reasons, in this work, organic sulfur is derivatized to methylsulfonium salts to achieve selectivity toward sulfur aromatics in the presence of PAHs [182, 183]. The purpose of this derivatization is to form ions from the sulfur compounds that are efficiently ionized by ESI, before their introduction to the ionization source. The formation of charged ions of sulfur compounds, in the presence of a large number of PAHs that are not affected by the reaction, increases the selectivity for PASHs and lower to a great extent the problems of space charge effects in the ICR cell.

5.5. Summary

Since electrospray ionization technique selectively ionizes acidic and basic polar compounds, negative ion ESI-MS and tandem ESI-MS was used in this work for the characterization of polar photoproducts of PASHs. In addition, accurate mass measurements of the sulfonic acids were acquired using electrospray ionization time of flight mass spectrometry at a mass resolution of 9000 in order to identify the various sulfonic acids obtained. On the other hand, electrospray ionization is not suitable for the ionization of non-polar compounds such as PASHs. Hence, methylation of the PASHs was carried out before their characterization by ESI FT-ICR MS.

6. Objectives

Large amounts of crude oil are spilled into the environment every year. Upon sunlight exposure, crude oil components undergo structural modifications generally via photo-oxidation reactions leading to the formation of photomodified products. A great concern is currently increasing worldwide mainly because of the toxic potential of these photoproducts to the aquatic life as they are highly water soluble.

The objective of this work is to try to establish which class of compounds is mainly responsible for the highest toxicity of petroleum after sunlight irradiation and to identify the components of this class.

In this regard, a toxicity-based fractionation methodology will be applied using the microcrustacean *Daphnia magna*, which involves the fractionation of petroleum, the photo-oxidation of the different fractions separately and the toxicity testing of the water-soluble photoproducts of these fractions, in order to determine the most phototoxic class.

Furthermore, the low- and high-molecular weight parent components of the most phototoxic class will be characterized by Fourier transform ion cyclotron resonance mass spectrometry in order to understand their fate in the environment after photo-oxidation.

Moreover, the oxygenated photoproducts belonging to this toxic class will be analyzed by electrospray ionization-, time of flight- and gas chromatography-mass spectrometry to try to identify them.

7. Application of toxicity-based fractionation techniques for the identification of the most phototoxic fraction of crude oil

There is a large body of literature showing that the toxicity of certain PAHs is greatly enhanced when there is exposure to both PAHs and sunlight [141]. In addition to mortality, there are also studies showing that exposure to sunlight and PAHs caused a variety of sub-lethal effects in marine animals [184, 185]. In addition to the work with single compounds, there have been also laboratory studies on the photo-toxicity of water accommodated oils or with sediments containing oil. Fish (*Menidia beryllina*) exposed for 48 h in the dark to a water accommodated fraction of weathered middle distillate oil (1.5 mg/l of total petroleum hydrocarbons) showed no toxicity, however exposure to the WAF and solar radiation (48 h) resulted in 30 % toxicity [186].

Moreover, extensive studies of photomodification of anthracene have been performed in the past, but only by using the toxicity based fractionation technique, Brack et al. [157] were able to identify the metabolites causing the toxicity of photomodified anthracene including anthracene-1,4-dione, a previously unknown photoproduct of very high toxicity to *Vibrio fischeri*. They were also able to identify 1-hydroxyanthracene-9,10-dione and 1,4-dihydroxyanthracene-9,10-dione and assigned them as genotoxic compounds.

Therefore, it is important to discover the potential risk of the photoinduced toxicity of the different components of crude oils. Thus, identifying the phototoxic compounds present may be desirable to better understand the hazard posed to humans and the marine environment by chronic release of petroleum, especially the cumulative effects of petroleum-related toxic compounds, since not many compounds in the crude oil have yet been tested for their phototoxicity. Due to the enormous number of compounds found in crude oil, it is difficult to explicitly determine which compounds may be responsible for the highest observed photo-induced toxicity. To address this complex problem, toxicity-based fractionation techniques will be used to isolate highly phototoxic fractions from less phototoxic ones in order to isolate the most toxic fraction. Fractionation can be based on several physicochemical and chemical properties of the analytes including polarity, hydrophobicity, molecular size, planarity and/or the presence of specific functional groups. Finally, when the most phototoxic fraction will be known, it will be subjected to chemical identification.

To determine the fraction of highest phototoxicity in crude oil, the phototoxicity of the different fractions of crude oil should be investigated. Toxicity was measured as immobilization (or mortality) using the small Cladoceran *Daphnia magna* (Figure 7.1).

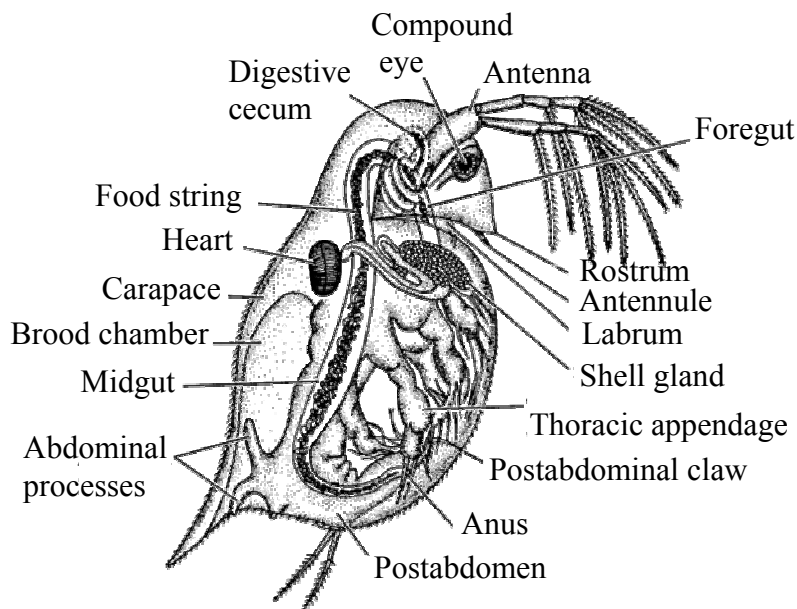


Figure 7.1. The toxicity test organism *Daphnia magna* (from [187]).

7.1. *Daphnia magna* as toxicity test organism

Daphnia was chosen for this study because it has been used for many years as a “standard” aquatic test species. Except for fish and algae, acute tests with *Daphnia* are among the most frequently performed studies in aquatic toxicology [188-190]. In addition, *Daphnia* tests are currently the only type of freshwater invertebrate bioassay that are formally endorsed by international organizations such as US EPA, the EEC (European Economic Community) and the OECD (Organization for Economic Cooperation and Development), and that are required by virtually every country for regulatory testing. Moreover, the choice of *Daphnia magna* for use as a standard test species was strongly influenced by the following factors:

- It can alternate the production of asexual and sexual (ephipial) eggs under certain environmental conditions, which allows the maintenance and testing of clones.
- It can be cultured in the laboratory.
- It represents the zooplankton community, a major element of the freshwater food chain.
- As a species of worldwide occurrence, the ecological relevance of the test results is recognized.

- It is assumed to be relatively sensitive compared with other freshwater invertebrates.

7.2. Culture of *Daphnia magna*

A successful culture of *Daphnia magna* depends on suitable water quality and nutrition. In other words, the composition of the medium and its temperature should allow normal development of the animals. In addition, in order to avoid exposing the daphnids to an additional shock at the beginning of the toxicity tests, these should not be conducted under conditions differing from those under which the animals were cultured. Thus, a synthetic medium is usually chosen as its composition is known and it is known not to contain any contaminants. That is why the OECD Test Guideline 202, Part II (1996 draft), has recommended the use of a fully defined medium to provide continuous culture of daphnids without any signs of reduced viability or reproduction [188]. Therefore, Elendt M4, reported among the adequate synthetic *Daphnia* media, was used in this work for culturing *Daphnia* (Standard Fresh Water) [188, 191]. The chemical composition of the culture medium is represented in Table 7.1.

Table 7.1. The chemical composition of *Daphnia magna* culture medium (Elendt M4)

<i>Constituent</i>	<i>Concentration</i> (mg/l)	<i>Constituent</i>	<i>Concentration</i> (mg/l)
CaCl ₂ .2H ₂ O	293.8	MnCl ₂ . 4 H ₂ O	0.361
MgSO ₄ . 7 H ₂ O	123.3	CoCl ₂ . 6 H ₂ O	0.01
K ₂ HPO ₄	0.0184	NaMoO ₄ . 2 H ₂ O	0.063
NaNO ₃	0.0274	NaCl	0.016
NaHCO ₃	64.8	CuCl ₂ . 2 H ₂ O	0.0165
Na ₂ SiO ₃ . 9 H ₂ O	1.0	ZnCl ₂	0.013
H ₃ BO ₃	2.86	Na ₂ SeO ₃	0.0022
KCl	5.8	NH ₄ VO ₃	0.0006
LiCl	0.31	FeSO ₄ . 7 H ₂ O	0.996
RbCl	0.071	KH ₂ PO ₄	0.0143
SrCl ₂ . 6 H ₂ O	0.15	Cyanocobalamin	0.001
KI	0.0033	Biotin	0.0008
Na ₂ EDTA. 2 H ₂ O	2.5	Thiaminehydrochloride	0.075

Culturing *Daphnia* has started after the hatching of ephippia from the Daphtokit F magna. Ephippia are dormant eggs protected by a chitinous capsule that can be stored for long periods of time without losing their viability. In order to hatch the eggs into neonates, the contents of the vial of ephippia was poured into a microsieve and rinsed with tap water to eliminate all traces of the storage medium. The eggs are then transferred into a Petri dish containing 20 ml of Standard Fresh Water, preaerated by air bubbling. Finally, the Petri dish was covered and incubated at 20 °C for 3 days under continuous illumination of 6000 lux. The neonates produced were then cultured to be used for toxicity tests.

Daphnia typically live 40 to 56 days, varying according to species and environmental conditions. Each brood typically holds 6-10 eggs, which turn into embryos and are released within few days. Juveniles reach sexual maturity in 6 to 10 days. A healthy population of *Daphnia* consists mostly of females that have been produced asexually.

The culture can become stressed if the population density gets too high or if there is a food shortage, poor water quality or extreme temperatures. Under stressful conditions, *Daphnia* produce more male embryos and begin to reproduce sexually. The resulting resting eggs will not hatch until they have gone through a certain sequence of environmental changes, including several freeze/thaw cycles. So, in order to maintain a steady supply of *Daphnia*, stressful conditions should be avoided. In addition, an optimal culture growth is obtained under the following conditions: at pH 7-8.6, temperature between 20 and 25 °C, dissolved oxygen > 6 mg/l, water hardness between 160 to 180 mg CaCO₃/l and by using a lighting cycle of 16 hours light and 8 hours darkness.

7.3. Toxicity tests using *Daphnia magna*

Toxicity tests were performed according to the OECD guidelines for testing of chemicals using the neonates (not older than 24 h) obtained from the culture [188]. The bioassays are conducted in disposable multiwell test plates with 30 test wells (see Figure 7.2). Each plate is provided with 4 wells for the controls and 4 wells (A, B, C, D) for each toxicant concentration. Additionally, the plates are provided on the left side with a column of "rinsing wells" to prevent dilution of the toxicant during the transfer of the neonates from the culture vessel to the test wells. The wells are labelled vertically as rows X (for the controls) and 1 to 5 for the toxicant dilutions. Each well of the test plates has to be filled with 10 ml toxicant solution (or Standard Fresh Water in the control column). Twenty actively swimming

neonates (2 hours pre-fed with dry algae) are transferred from the culture vessel with a micropipette into each rinsing well and then exactly 5 neonates are transferred from the rinsing wells into each of the 4 wells of each column. This transfer was also performed in the order of increasing toxicant concentrations. The Multiwell plate is then covered and incubated in darkness at 20 °C. After 24 h and 48 h incubation, the number of dead and immobilized test organisms is then determined. An organism is defined to be immobile if it was not able to swim within 15 sec after gentle agitation of the liquid [192].

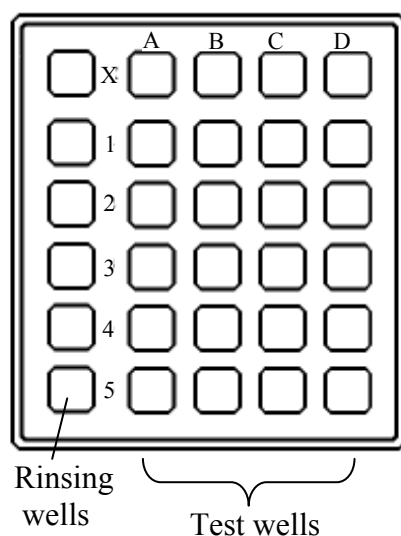


Figure 7.2. Multiwell test plate used in *Daphnia* toxicity tests.

7.3.1. Toxicity of crude oil

7.3.1.1. Photo-oxidation of Egyptian crude oil by sunlight and mercury lamp

1.01 mg of an Egyptian crude oil was added to 100 ml distilled water in a measuring flask, stirred for half an hour and then the flask was irradiated by sunlight for 37 hours. The irradiation experiment took place in July 2005 on the roof surface of the Institute of Inorganic and Analytical Chemistry where there were nearly no clouds. Another 1.01 mg of crude oil was added to 100 ml distilled water, stirred for half an hour and then the measuring flask was irradiated this time by the mercury lamp (described in section 3.3) for 37 hours.

7.3.1.2. Preparation of non-irradiated crude oil sample

1.01 mg of the Egyptian crude oil was added to 100 ml distilled water, stirred for half an hour, the flask was then wrapped in an aluminium foil and kept in the dark for 37 hours.

7.3.1.3. Toxicity measurements of sunlight-, lamp-irradiated and non-irradiated crude oil

10 ml of the solution, resulting from the photo-oxidation of the crude oil after 37 hours sunlight irradiation, was placed in each of the four wells (A, B, C, D) in row 1 of the multiwell plate. The *Daphnia* from the culture maintained in the laboratory were used, where twenty neonates (less than 24 hr old) were transferred from the culture to the rinsing well (containing Standard Fresh Water) at the left side of row 1. Five neonates were then transferred from the rinsing well into each of the four wells in row 1 containing the photo-oxidized sun-irradiated crude oil solution. The previous procedure was performed, using the photo-oxidized lamp-irradiated crude oil solution which was placed in row 2 of the multiwell plate. The same previous procedure was repeated again, but this time using the solution of the crude oil kept in dark in row 3. Finally, the multiwell plate was then covered and incubated in darkness at 20°C. After 24 and 48 h incubation, the number of dead and immobilized organisms was determined. A negative control consisting of the same test conditions and test organisms but with Standard Fresh Water instead of the toxicant solution, was maintained concurrently with the toxicity tests.

As can be seen in Figure 7.3, the non-irradiated crude oil was the least toxic with no observable effect on *Daphnia* after 24 hours and exerting 35 % toxicity after 48 hours. Both sunlight- and lamp-irradiated crude oil solutions were similar in their toxicity effects on daphnids where the % immobility was 50 % for both of them after 48 hours. This indicates that the lamp gives a simulated sunlight irradiation and that it can be used for further photo-oxidation experiments.

The next step will be the fractionation of the crude oil into fractions and their photo-oxidation with the mercury lamp followed by the toxicity determination of each photo-oxidized fraction.

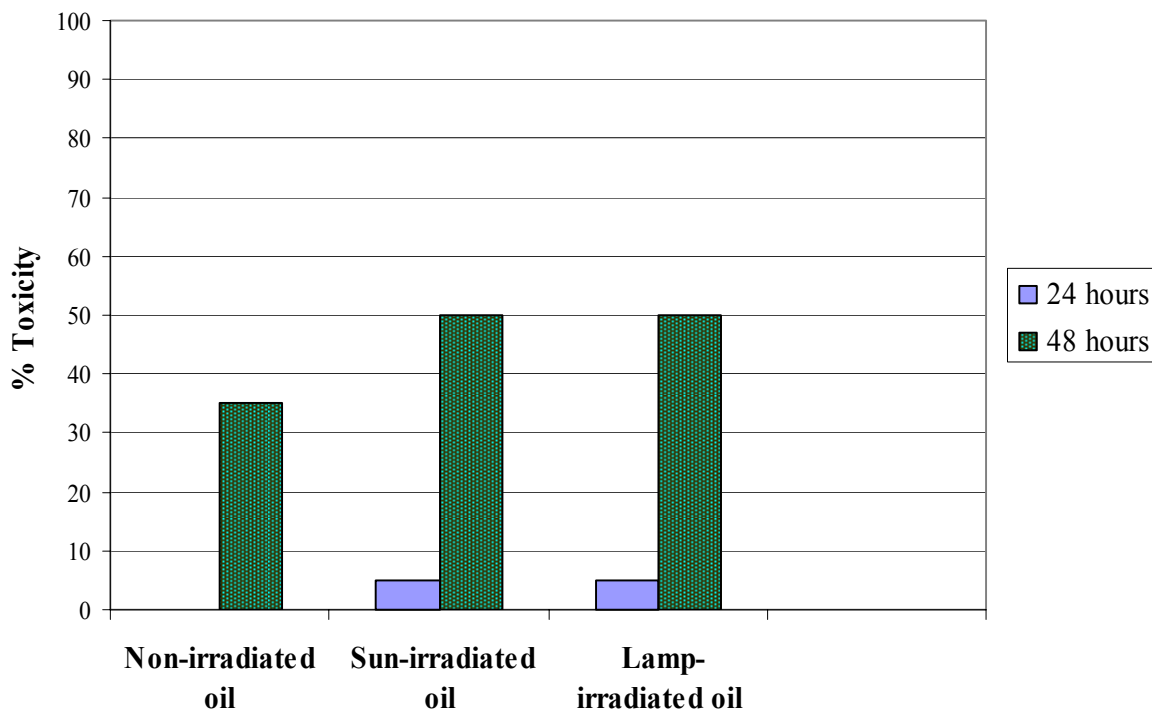


Figure 7.3. Toxicity of non-irradiated (kept in dark), sun-irradiated and lamp-irradiated Egyptian crude oil on *Daphnia magna* after 24 and 48 hours.

7.3.2. Toxicity of photo-oxidized aliphatic, monoaromatic and polyaromatic fractions

7.3.2.1. Fractionation of crude oil into aliphatic, monoaromatic and polyaromatic fractions

A chromatographic column (90 mm x 8 mm) was packed with 5 g alumina (activated at 450 °C for 12 h, 2 % water added then stored at 155 °C). The oil sample (90 mg) was fractionated using n-pentane (20 ml) to elute the saturated hydrocarbon fraction, n-pentane/dichloromethane (50:1, v/v, 15 ml) to elute monoaromatics and n-pentane/dichloromethane (3:1, v/v, 30 ml) to elute polyaromatics [107]. Afterwards, the fractions were analyzed by GC-FID. The GC-FID chromatograms of the aliphatic, monoaromatic and polyaromatic fractions are given in Figure 7.4, 7.5 and 7.6 respectively.

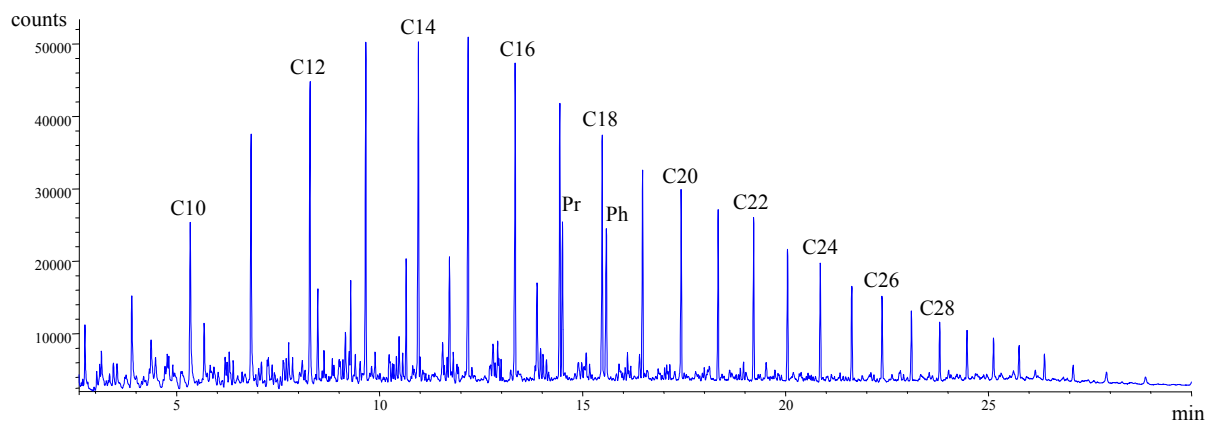


Figure 7.4. GC-FID chromatogram of the aliphatic fraction of the Egyptian crude oil (Pr: Pristane, Ph: Phytane).

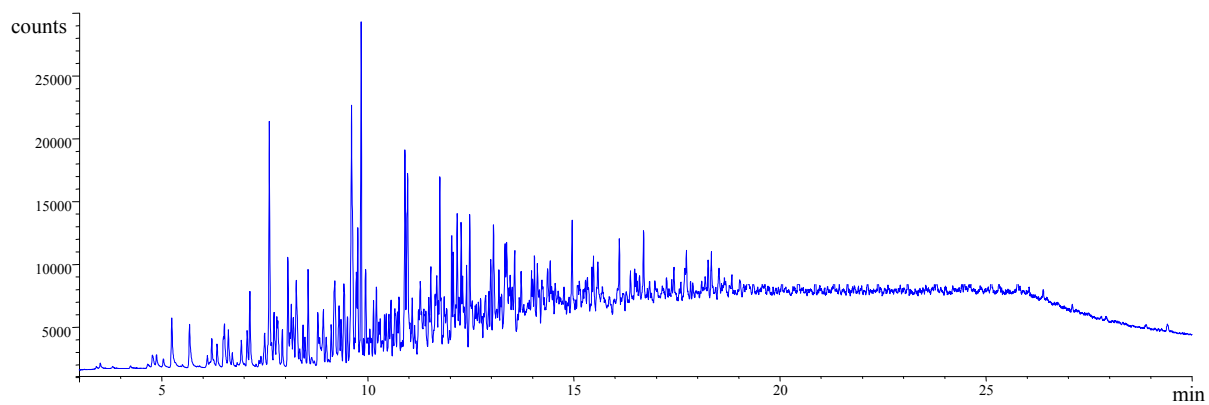


Figure 7.5. GC-FID chromatogram of the monoaromatic fraction of the Egyptian crude oil.

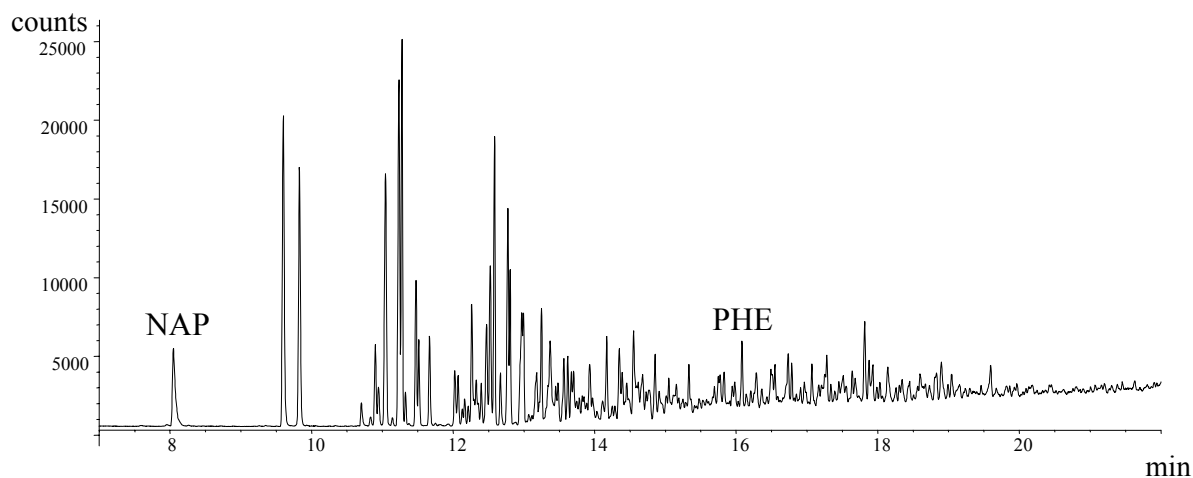


Figure 7.6. GC-FID chromatogram of the polyaromatic fraction of the Egyptian crude oil (NAP = naphthalene, PHE = phenanthrene).

7.3.2.2. Toxicity measurements of photo-oxidized aliphatic, monoaromatic and polyaromatic fractions

0.97 mg of aliphatic, monoaromatic and polyaromatic fractions of crude oil were dissolved in 150 μ l of tetradecane and added to 100 ml distilled water separately. Each one of these solutions was photo-oxidized by the mercury lamp for 37 hours. After photo-oxidation, each solution was placed in a separatory funnel in order to separate the tetradecane layer from the water layer, as tetradecane was found to cause the death of *Daphnia* because they get trapped in it. A dilution series (100 % - 50 % - 25 % - 12.5 % - 6.25 %) of each fraction was prepared by serial dilution 1:1 of the water layer with Standard Fresh Water.

The toxicity effects of the aliphatic, monoaromatic and polyaromatic fractions of crude oil are shown in Figure 7.7, 7.8 and 7.9 respectively. By comparing the three figures, it is clear that the highest concentration (0.97 mg/ 100 ml) was the most lethal, causing immobilization or mortality of all the daphnids in both the monoaromatic and polyaromatic fractions and of 90% of them in the aliphatic fraction after 48 hours. In addition, it can be seen that in all fractions, there was an increase in the immobilization of *Daphnia* with increasing concentration starting from the concentration of 0.06 mg/ 100 ml being the least toxic one. Hence, it appears that the polyaromatic fraction exhibited the highest toxicity among the other fractions.

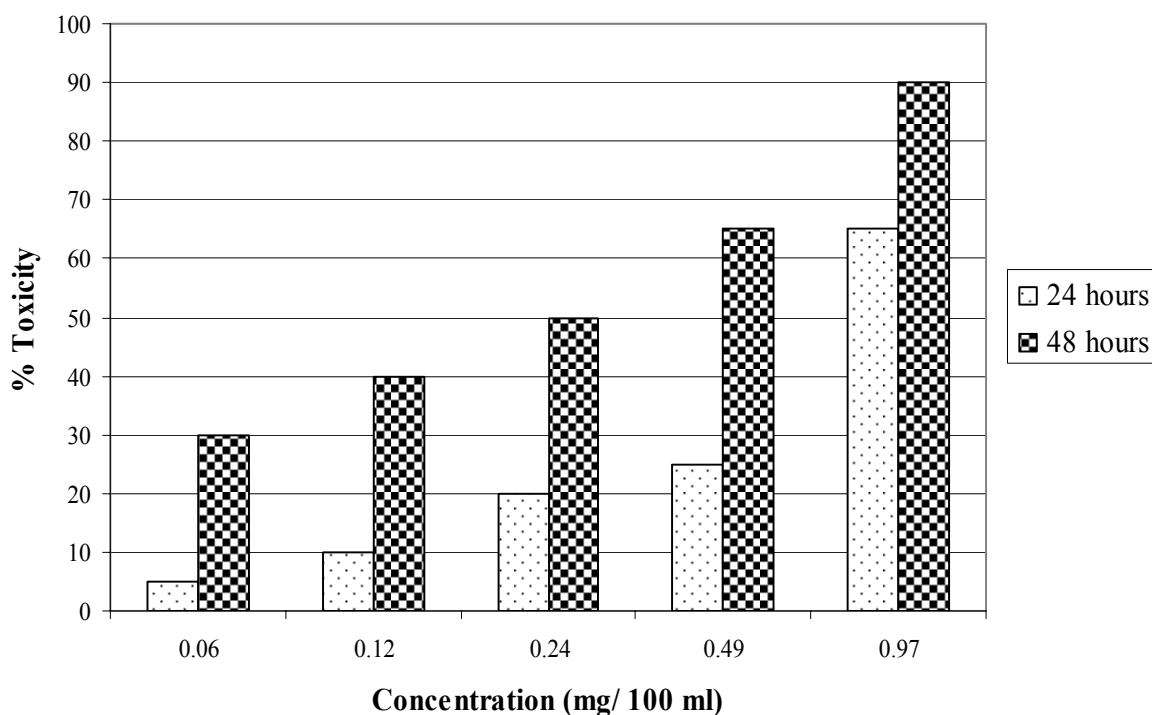


Figure 7.7. Toxicity of aliphatic fraction of Egyptian crude oil after 37 hours photo-oxidation.

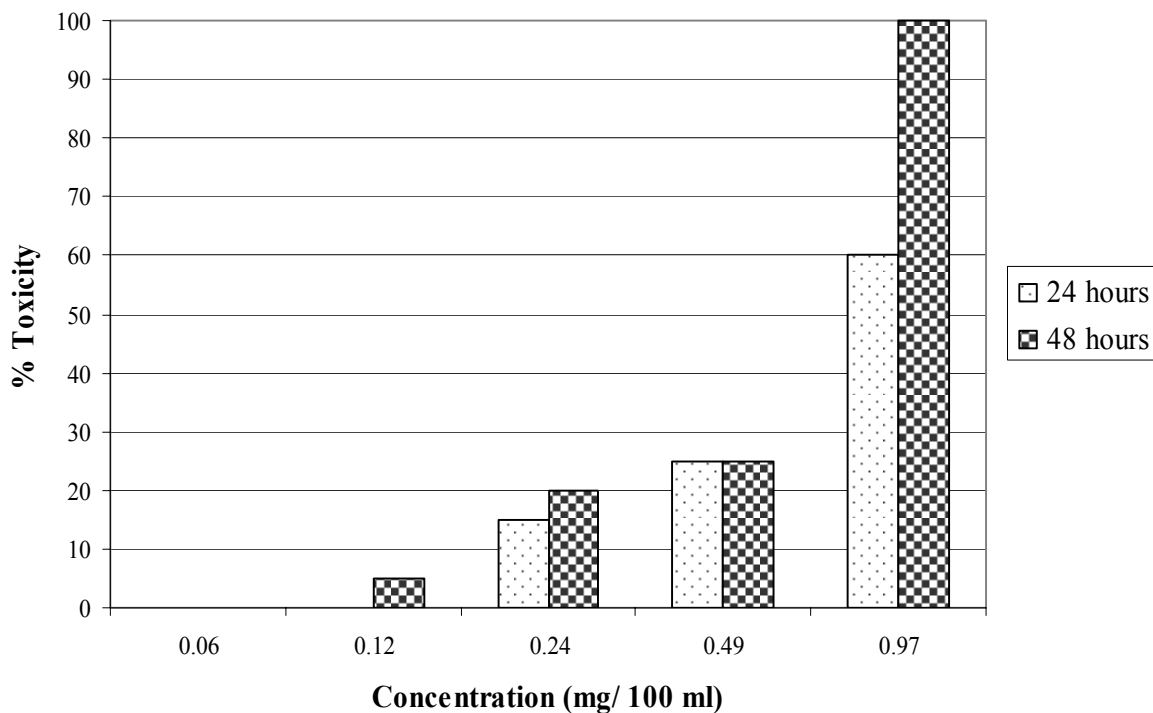


Figure 7.8. Toxicity of monoaromatic fraction of Egyptian crude oil after 37 hours photo-oxidation.

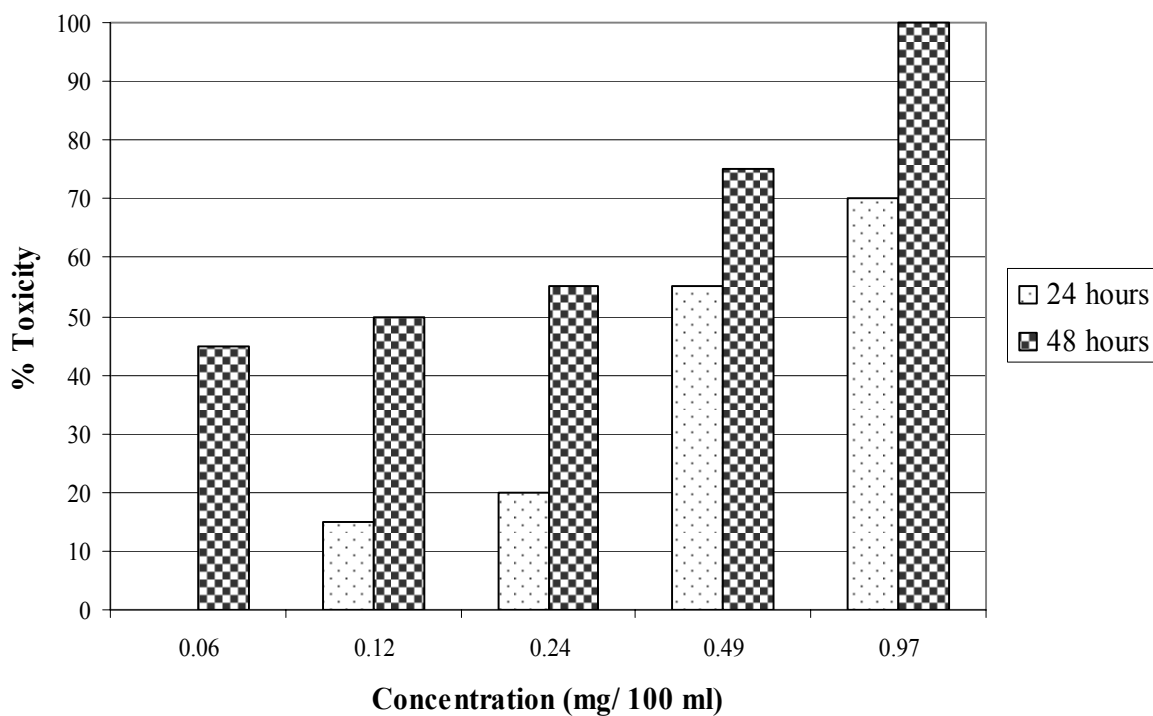


Figure 7.9. Toxicity of polyaromatic fraction of Egyptian crude oil after 37 hours photo-oxidation.

7.3.3. Toxicity of photo-oxidized PAHs and PASHs

7.3.3.1. Fractionation of polyaromatic fraction into PAHs and PASHs

In order to reduce the chemical complexity of the polyaromatic fraction, HPLC fractionation was used. The stationary phase, a Pd(II)-containing complex based on 2-amino-1-cyclopentene-1-dithiocarboxylate (Pd-ACDA) covalently bonded to silica gel was used for ligand exchange chromatography so that the polyaromatic fraction is separated into PAHs and PASHs. Hence, about 250 μ l (10 mg) of the polyaromatic fraction were injected on the Pd(II)-bonded silica gel. The first fraction (PAHs) was eluted with cyclohexane: dichloromethane (7:3 v/v) for 12 minutes and the second fraction (PASHs) was eluted after addition of 1 % isopropanol to the previous mobile phase (Figure 7.10). The flow rate maintained throughout the whole separation was 3 ml/min. Afterwards, both fractions were injected on GC-FID and GC-MS for their investigation and their GC-MS chromatograms are given in Figures 7.11 and 7.12.

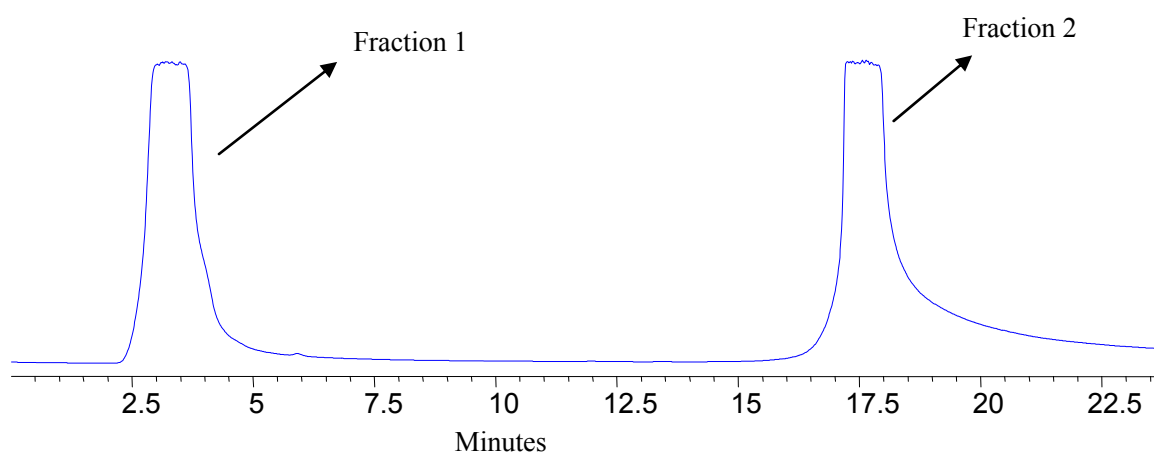


Figure 7.10. Fractionation on Pd(II)-bonded phase of the polyaromatic fraction of the Egyptian crude oil.

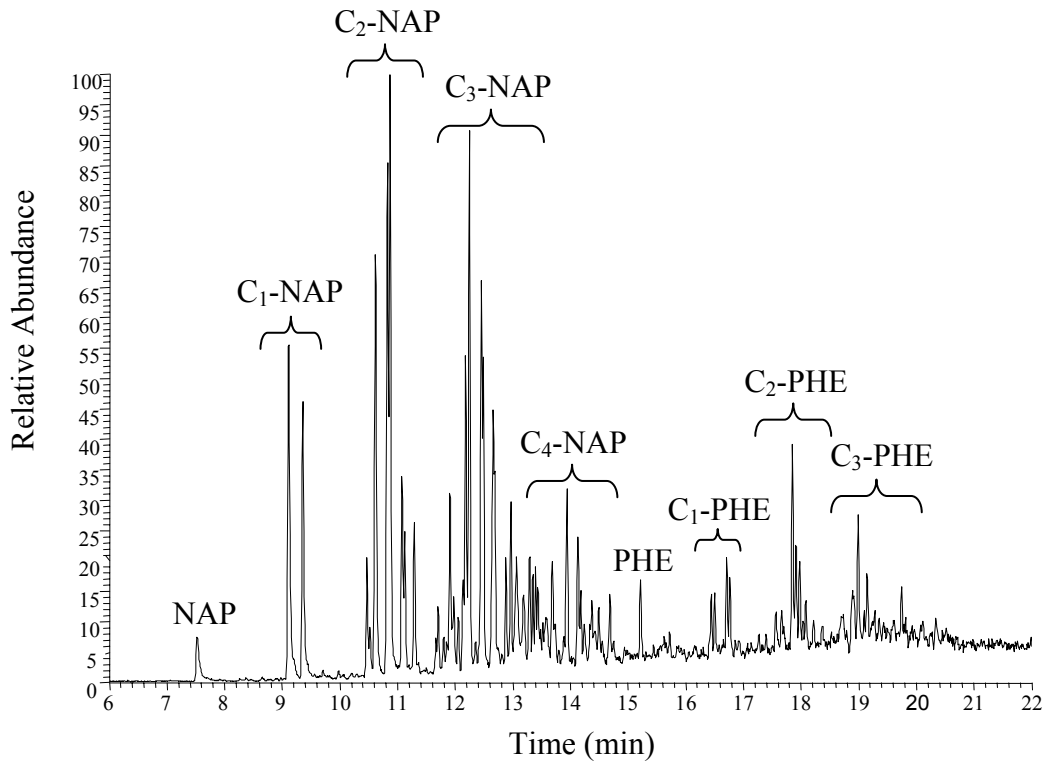


Figure 7.11. GC-MS chromatogram of PAH fraction (C₀-C₄ naphthalenes (NAP) and C₀-C₃ phenanthrenes (PHE)).

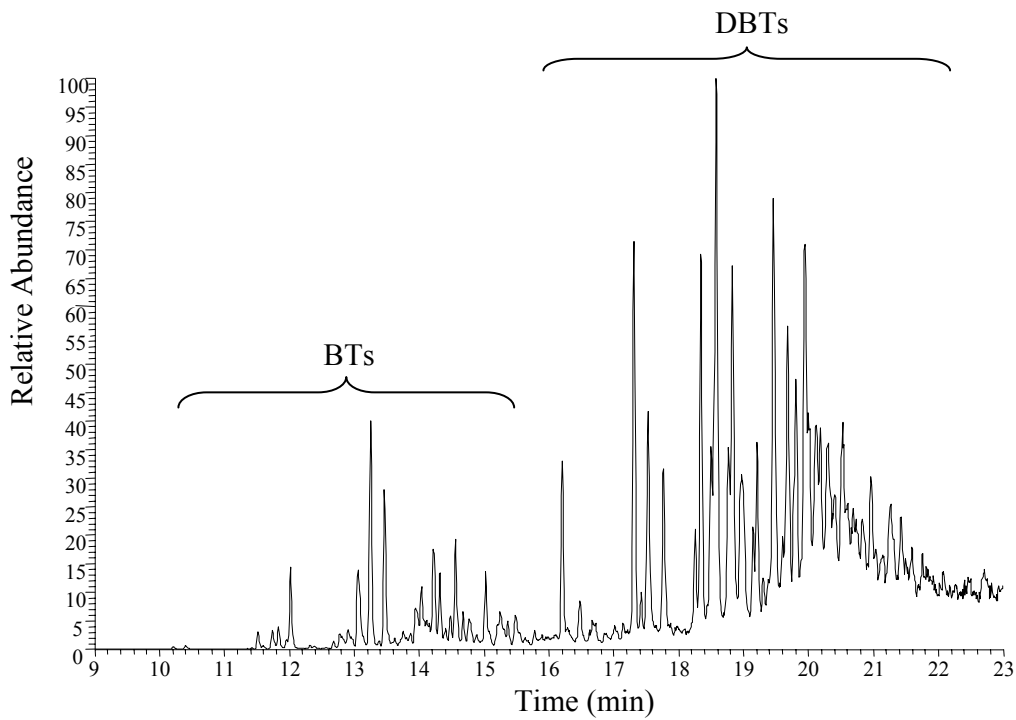


Figure 7.12. GC-MS chromatogram of PASH fraction (C₁-C₄ benzothiophenes (BTs) and C₀-C₄ dibenzothiophenes (DBTs)).

7.3.3.2. Toxicity measurements of photo-oxidized PAHs and PASHs

1.01 and 1.55 mg of PAHs and PASHs were dissolved in 150 μ L tetradecane and added to 100 ml distilled water separately. After the irradiation of each solution by the mercury lamp for 37 hours, the tetradecane layer from each solution was separated from the water layer in a separatory funnel and the aqueous solutions were then used for the determination of their toxicity.

The toxicity of the PAH fraction of crude oil is shown in Figure 7.13. The highest concentration (1.55 mg/ 100 ml) is the most lethal one causing 60 % and 90 % immobility after 24 and 48 hours respectively, whereas the concentration of 1.01 mg/ 100 ml resulted in 25 % and 70 % immobility after 24 and 48 hours respectively. On the other hand, PASH fraction of crude oil caused greater effects on *Daphnia* (Figure 7.14). All the daphnids were killed within 48 hours when subjected to a 1.55 mg/ 100 ml solution. These results clearly show that the PASH fraction of crude oil is more toxic than the PAH one and hence was subjected to further fractionation.

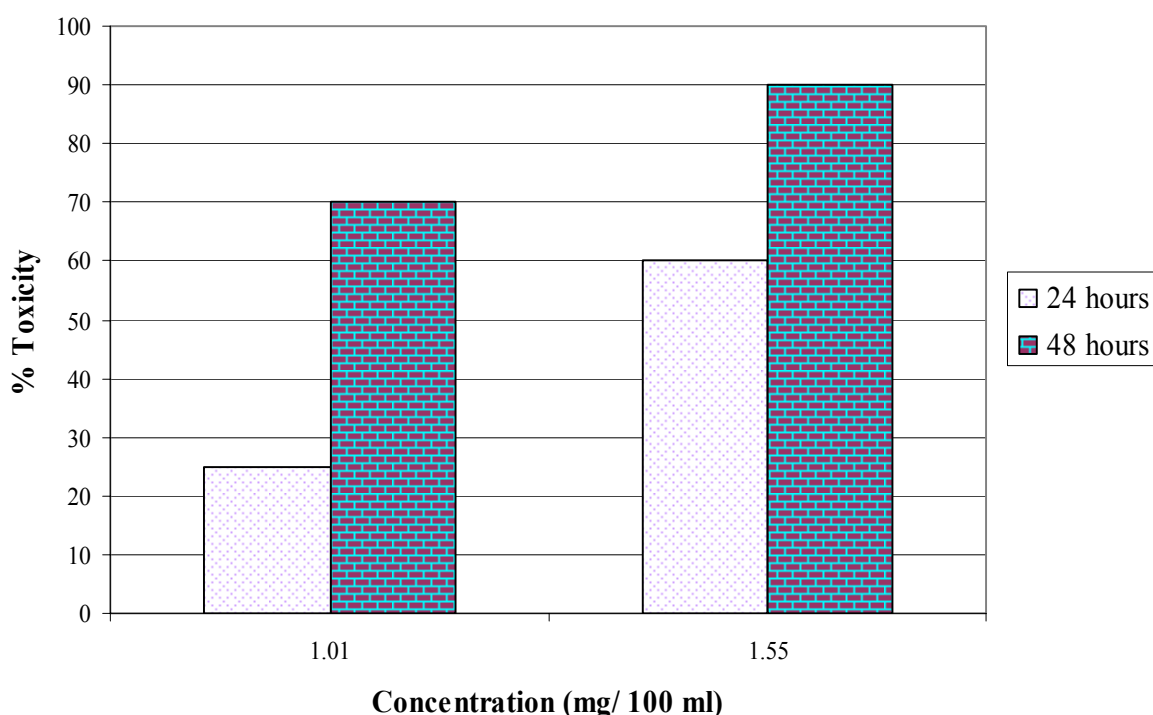


Figure 7.13. Toxicity of PAH fraction after 37 hours irradiation.

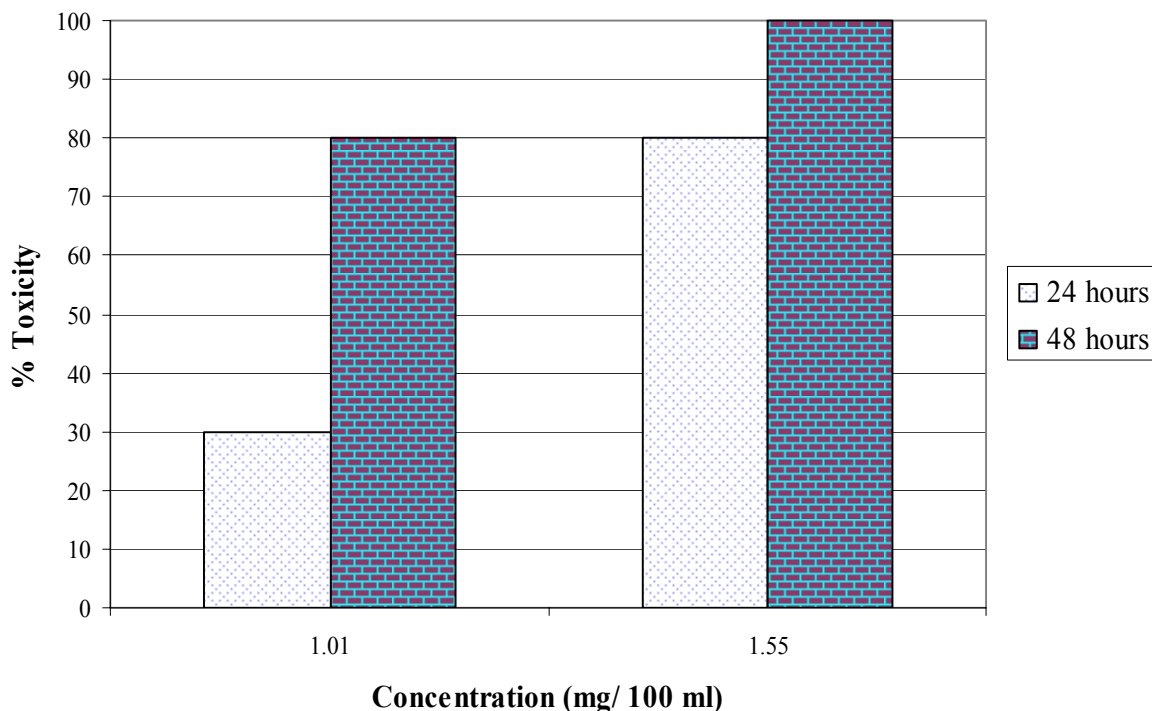


Figure 7.14. Toxicity of PASH fraction after 37 hours irradiation.

7.3.4. Toxicity of photo-oxidized PASH subfractions I and II

7.3.4.1. Fractionation of PASHs into three subfractions

The PASH fraction was further fractionated using a β -cyclodextrin column which was reported to separate the PASHs according to the number of condensed aromatic rings [112]. 100 μ l (1 mg) of PASHs were injected on two β -cyclodextrin columns (150 mm x 4.6 mm) connected in series and three subfractions were obtained by using 0.5 % t-butyl methyl ether in cyclohexane as mobile phase with a flow rate of 1 ml/min. The column oven temperature was maintained at 50°C. UV-visible detection was performed at 254 nm. The retention times for the fractions were as follows: subfraction (1): 2.5-5.9 min, subfraction (2): 5.9-9.1 min and subfraction (3): 9.1-25 min (Figure 7.15). The three subfractions were then analyzed by GC-MS.

After the investigation of the three subfractions eluted from β -cyclodextrin column on GC-MS, it appeared that subfraction 1 and 2 contained the benzothiophenes (two-ring compounds) while subfraction 3 contained the dibenzothiophenes (three-ring) and higher ring compounds. Thus, subfraction 1 and 2 were combined as subfraction I, which was

concentrated and tested for its phototoxicity with fraction 3, designated now as subfraction II (Figure 7.16).

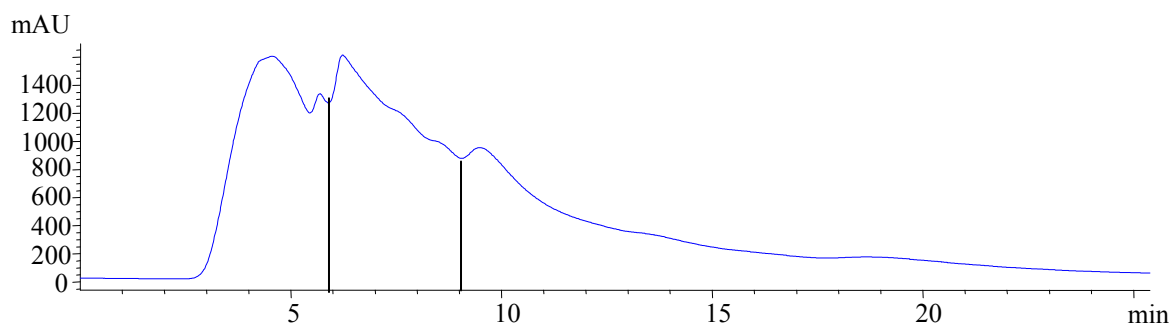


Figure 7.15. Fractionation of the PASH fraction of the Egyptian crude oil on β -cyclodextrin column.

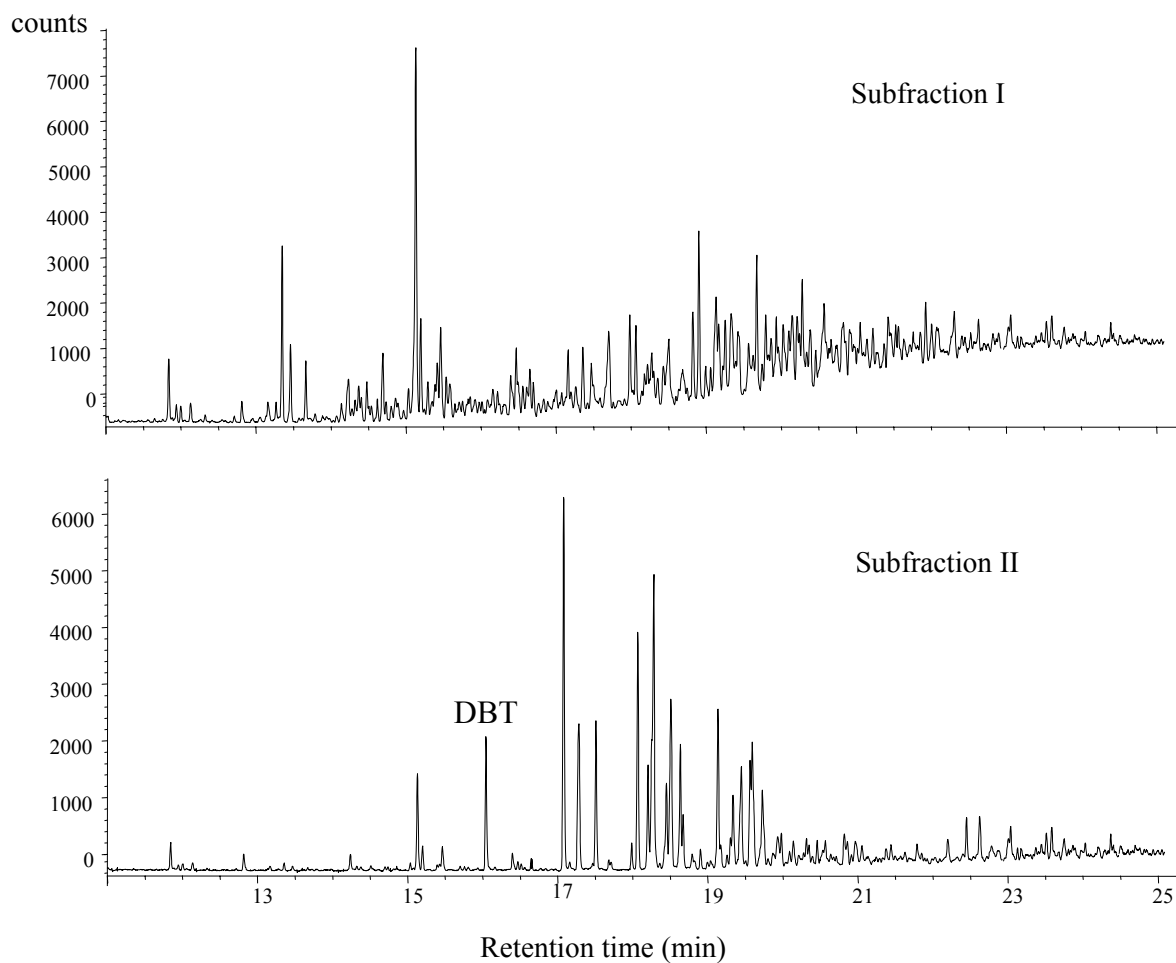


Figure 7.16. GC-FID chromatogram of subfraction I and II.

7.3.4.2. Toxicity measurements of photo-oxidized PASH subfractions I and II

0.20 and 0.38 mg of PASH subfraction I and II were dissolved in 100 μ l tetradecane and added to 100 ml distilled water each separately. The solutions were irradiated for 37 hours and then the tetradecane layer was separated from each solution using a separatory funnel. Afterwards, the water layer was used for the toxicity tests. Unexpectedly, both subfractions showed almost the same phototoxic effect on *Daphnia* as can be seen in Figure 7.17 and 7.18. Although the toxicity test of both subfractions was repeated, it gave the same identical results.

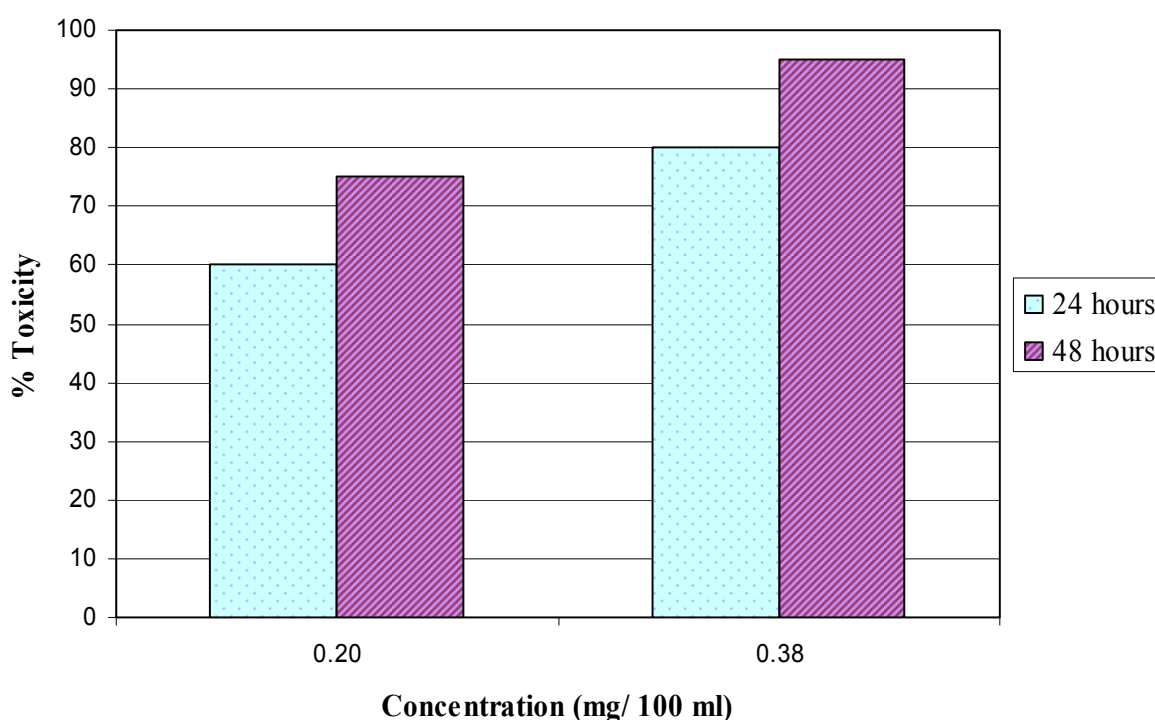


Figure 7.17. Toxicity of subfraction I of PASHs after 37 hours irradiation.

As can be seen from Figure 7.17 and 7.18 both subfractions I and II showed nearly the same toxicity effect. Since these results did not determine which photo-oxidized PASH fraction is more toxic than the other, another separation protocol was conducted, namely the separation of PASH photoproducts, based on their polarity properties, into polar and non-polar photoproducts in an attempt to find the most phototoxic compounds in the PASH fraction.

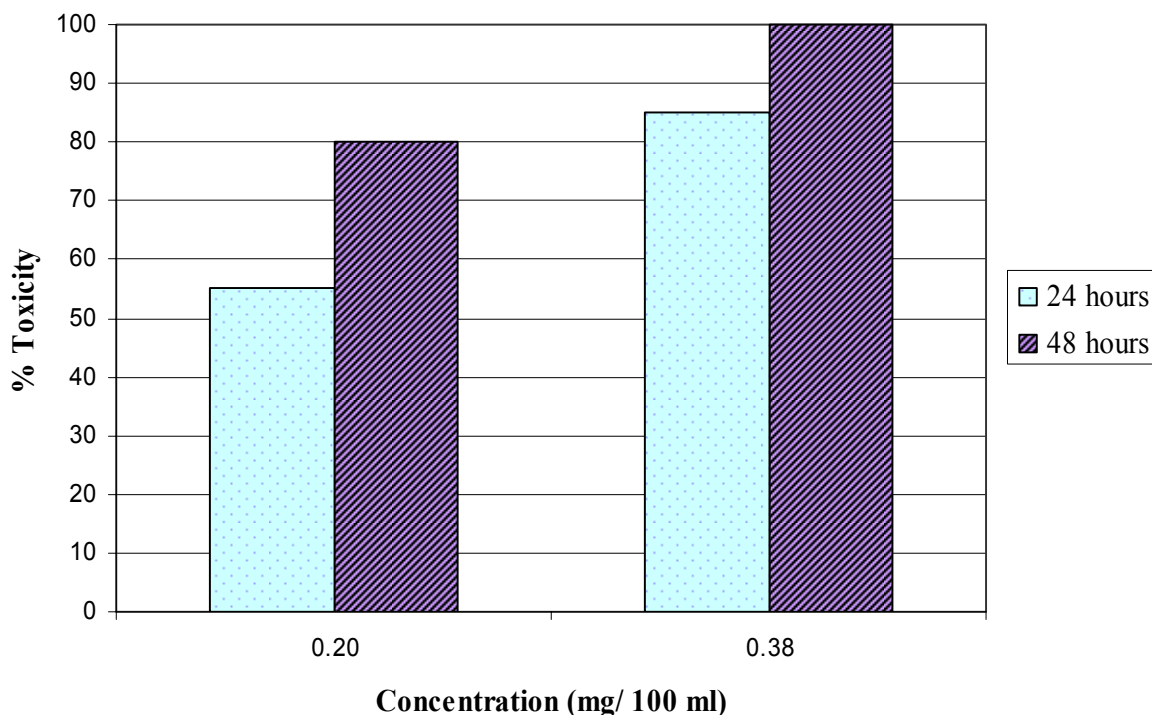


Figure 7.18. Toxicity of subfraction II of PASHs after 37 hours irradiation.

7.3.5. Toxicity of polar and non-polar photoproducts of PASHs after 37 hours irradiation

7.3.5.1. Separation of the photo-oxidized fraction of PASHs into polar and non-polar compounds after 37 hours irradiation

0.40, 0.88 and 1.20 mg of PASHs were dissolved in 1 ml pentane, added to 100 ml distilled water and then photo-oxidized for 37 hours. After the photo-oxidation, the non-polar products from each solution were extracted in pentane in a separatory funnel, whereas the polar products remained in water. The pentane layer containing the non-polar products, for each concentration, was added to 100 ml water and the pentane was then removed by rotary evaporator resulting in the non-polar products in water. Any traces of pentane in the original water layer were removed by rotary evaporator. The water solutions containing the polar and non-polar products for each PASH concentration were used lately for the toxicity tests of the photoproducts.

7.3.5.2. Toxicity measurements of polar and non-polar photoproducts of PASHs after 37 hours irradiation

After the separation of polar and non-polar photoproducts of each solution of the three concentrations (0.40, 0.88 and 1.20 mg) in 100 ml distilled water, the toxicity tests were performed using these solutions (Figure 7.19 and 7.20).

As can be seen in Figure 7.19, the non-polar photoproducts exhibited 5 % and 5 %; 65 % and 100 %; and 95 % and 100 % mortality to *Daphnia* exposed to 0.40, 0.88 and 1.20 mg/ml after 24 and 48 hours respectively. However, the same concentrations of the polar products gave only 0 % and 0 %; 55 % and 90 %; and 70 % and 95 % mortality after 24 and 48 hours respectively (Figure 7.20) which show that the non-polar products may be somewhat more toxic than the polar ones.

Although the previous observations indicated that the toxicity of non-polar photoproducts is higher than that of polar ones after short-term (37 hours) photolysis, the photo-oxidation of the PASH fraction was continued for 10 days and the toxicity of the polar and non-polar products were investigated to ensure that possible long-term effects were not overlooked by early termination of the photo-oxidation.

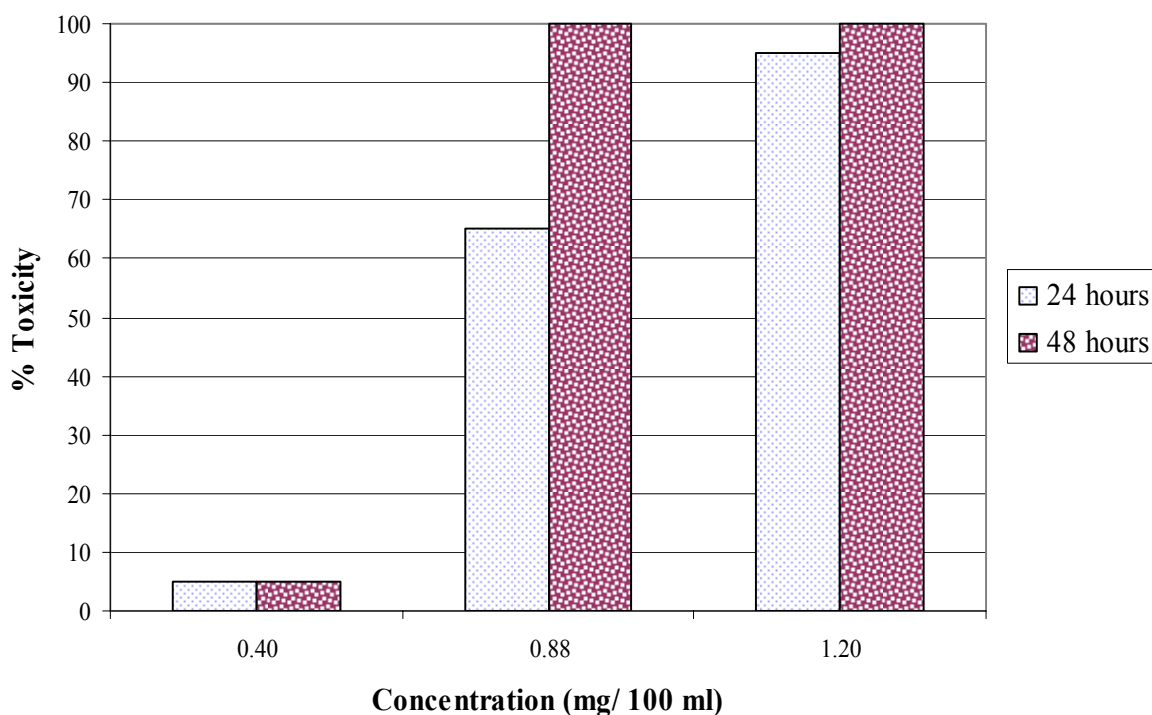


Figure 7.19. Toxicity of non-polar products of PASHs after 37 hours photo-oxidation.

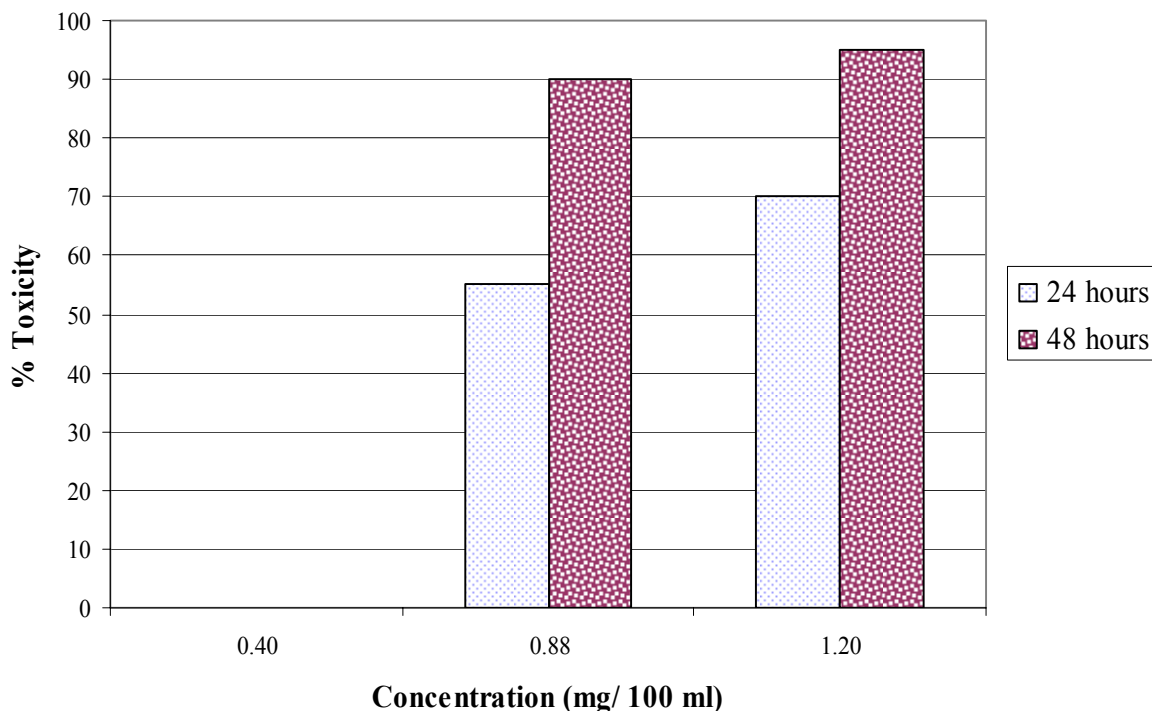


Figure 7.20. Toxicity of polar products of PASHs after 37 hours photo-oxidation.

7.3.6. Toxicity of polar and non-polar photoproducts of PASHs after 10 days irradiation

7.3.6.1. Separation of photo-oxidized fraction of PASHs into polar and non-polar compounds after 10 days irradiation

After the dissolution of 0.30, 0.41 and 0.88 mg of PASHs in 1 ml pentane and added to 100 ml distilled water separately, the solutions were photo-oxidized for 10 days. After the photo-oxidation, the same procedure for the separation of polar and non-polar photoproducts as in section (7.3.5.1) was followed.

7.3.6.2. Toxicity measurements of polar and non-polar photoproducts of PASHs after 10 days irradiation

The toxicity of polar and non-polar photoproducts of 0.30, 0.41 and 0.88 mg PASHs were determined after their separation in water following the same procedure previously mentioned in section 7.3 and they are illustrated in Figure 7.21 and 7.22 respectively.

By comparing Figure 7.21 and 7.22, it is obvious that the toxicity of the polar products has increased and exceeded that of the non-polar ones for all the tested concentrations. In case of

the polar photoproducts, 100 % mortality was observed for daphnids exposed to 0.41 and 0.88 mg/ 100 ml after 24 and 48 hours whereas as for the non-polar photoproducts, 100 % mortality was observed for the same concentrations but only after 48 hours. Hence, a significant increase in mortality occurred among daphnids exposed to 0.40 and 0.88 mg/ 100 ml of polar photoproducts after 10 days photo-oxidation. Thus, mortality increased from 0 % and 90 % (after 48 hours) after 37 hours irradiation (Figure 7.20) to 100 % and 100 % for 0.41 and 0.88 mg/ 100 ml solutions after 10 days photo-oxidation.

Based on the last results, it is evident that by increasing the time of photo-oxidation, it leads to an increase in the amount of polar photoproducts formed and consequently to an increase in their toxicity effects on *Daphnia* relative to the non-polar photoproducts.

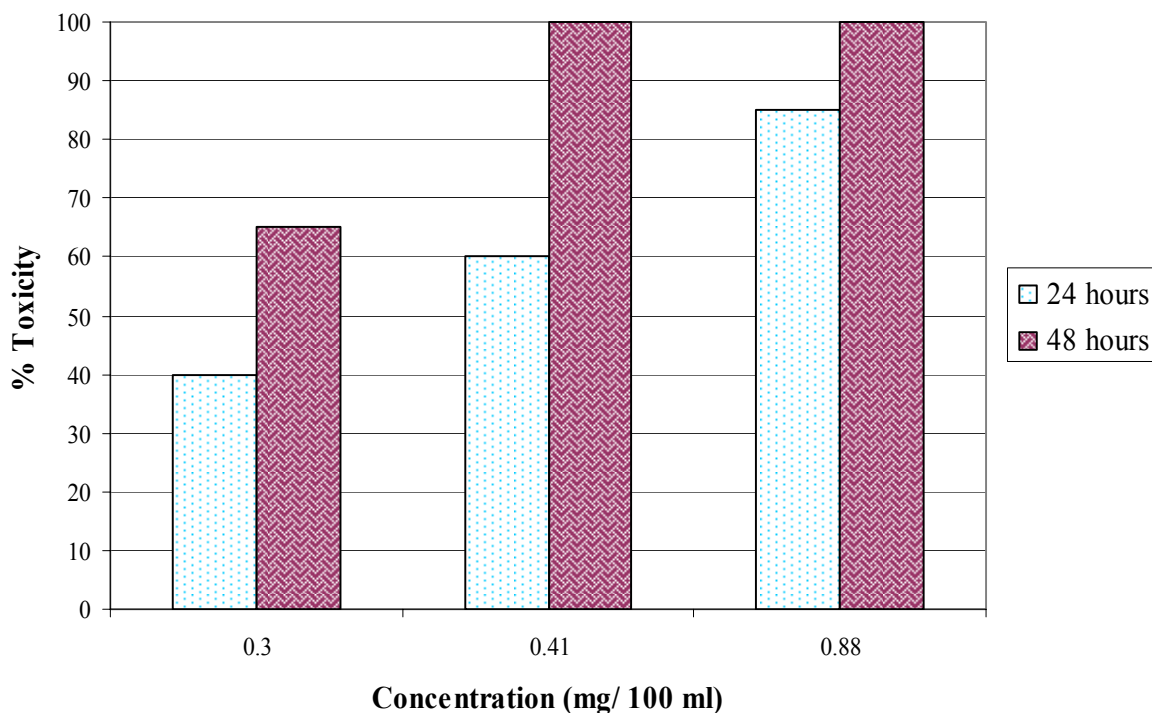


Figure 7.21. Toxicity of non-polar photoproducts of PASHs after 10 days photo-oxidation.

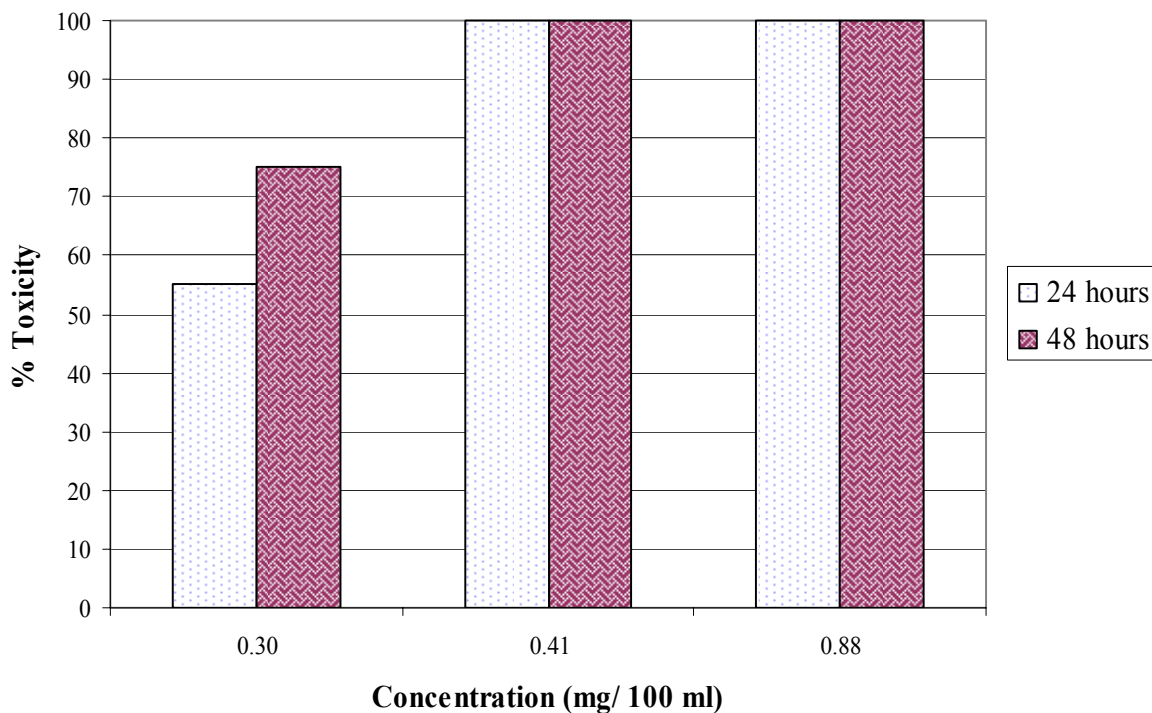


Figure 7.22. Toxicity of polar photoproducts of PASHs after 10 days photo-oxidation.

7.4. Summary

A toxicity-based fractionation method for identifying the most phototoxic fraction of petroleum has been developed by application of a *Daphnia* biotest for acute toxicity. Moreover, special toxicity patterns of fractions and subfractions of crude oil have been obtained and the polar photoproducts of the polycyclic aromatic sulfur heterocycles were found to be the most significant toxicants. This may be due to that the polar photoproducts of PASHs are more water soluble than the non-polar ones, their concentrations in the water could be higher, resulting in increased bioavailability. Furthermore, these oxygenated compounds are still sufficiently lipophilic to partition into biological membranes [193]. This combination of good bioavailability and high bioconcentration potential indicate that polar photoproducts present a real risk when they are present in the environment. The extent of this risk is currently unknown, however, because the photoproducts have never been included in environmental surveillance programs. These toxic photoproducts will be the focus of our subsequent instrumental analyses and chemical identification in addition to the polycyclic aromatic sulfur heterocycles.

8. Characterization of polar photoproducts of PASHs

It was demonstrated that photo-oxidation is responsible for the stabilization of water in oil emulsions "chocolate mousse" [46] and the increase of the oil solubility in water [45, 50]. These phenomena are due to the formation of a variety of oxygenated compounds including aliphatic and aromatic ketones, aldehydes, sulfoxides, carboxylic acids, fatty acids, esters, hydroperoxides, quinones and aliphatic and aromatic alcohols [53, 56-60, 194, 195].

In the present work, it is aimed to identify the polar photoproducts of polycyclic aromatic sulfur heterocycles which were found to be causing the highest toxicity of crude oil.

8.1. Experimental section

8.1.1. Crude oil fractionation

About 1 g of an Egyptian crude oil (1 % sulfur) was fractionated by column chromatography into saturates and aromatics. A gravity-fed chromatographic column (200 mm x 28 mm) was packed with 20 g silica gel and 35 g alumina. Before using silica and alumina, they were activated at 180 °C for 16 hours separately. The saturate fraction was collected using 120 ml n-heptane as eluent and the aromatic one was eluted by 360 ml of a mixture of n-heptane and toluene (2:1). The aromatic fraction was then subjected to a class separation into the PAHs and the PASHs using ligand exchange chromatography on a stationary phase containing a Pd(II) complex as described below.

8.1.2. Ligand exchange chromatography

The Pd(II)-containing complex based on 2-amino-1-cyclopentene-1-dithiocarboxylate covalently bonded to silica gel was used for the fractionation of the aromatic fraction of the Egyptian crude oil into PAHs and PASHs as already described in section 7.3.3.1.

8.1.3. Photo-oxidation of the PASH fraction

About 32 mg of the PASHs fraction were dissolved in 2 ml cyclohexane and floated as a film on 50 ml distilled water saturated with oxygen and irradiated for one month with the mercury lamp. Traces of anthraquinone were added as photosensitizer to the PASH solution prior to photo-oxidation.

8.1.4. Extraction of polar photoproducts

The aqueous solution containing the photoproducts of PASHs was acidified to pH 1 using concentrated hydrochloric acid and the polar photoproducts 1 (PP1) were extracted with 5×10 ml dichloromethane. The PP1 extract was dried over anhydrous sodium sulphate, concentrated by rotary evaporator to 2 ml and dried under a stream of nitrogen. The residual aqueous solution, remaining after the extraction of PP1, was completely dried by rotary evaporator to give the polar photoproducts 2 (PP2).

8.1.5. Derivatization of polar photoproducts 1

The PP1 were dissolved in the smallest volume of a mixture of chloroform/ methanol (1:1 v/v) and then derivatized to their trimethylsilyl (TMS) derivatives by their reaction with N-methyl-N-(trimethylsilyl)-trifluoroacetamide at 70 °C for 30 min and then were subjected to GC-MS analysis, using the quadrupole GC-MS consisting of an Agilent 6890 GC and a Waters Micromass (Manchester, U.K.) QuattroMicro mass spectrometer, and tandem mass spectrometry (ESI-MS/MS) operated in the electrospray negative mode.

8.1.6. Identification of polar photoproducts 1

The PP1 were identified by comparison of their gas chromatographic retention times and mass spectra with those of authentic standards after their derivatization to trimethylsilyl derivatives or by comparison of their mass spectra with reference mass spectra (NIST mass spectra database). The standard compounds used were cyclohexylacetic acid, cyclohexanecarboxylic acid, octanoic acid, decanoic acid, tetradecanoic acid and benzoic acid.

8.1.7. Analysis of polar photoproducts 2

The PP2 after drying were subjected to electrospray tandem mass spectrometry (ESI-MS/MS) analyses performed on a Quattro LCZ triple quadrupole mass spectrometer (Waters-Micromass, Manchester, UK) in the electrospray positive and negative ion mode. Determination of the elemental compositions of PP2 was performed on a MicroTof mass spectrometer (Bruker Daltonics, Bremen).

The detailed analysis scheme is presented in Figure 8.1.

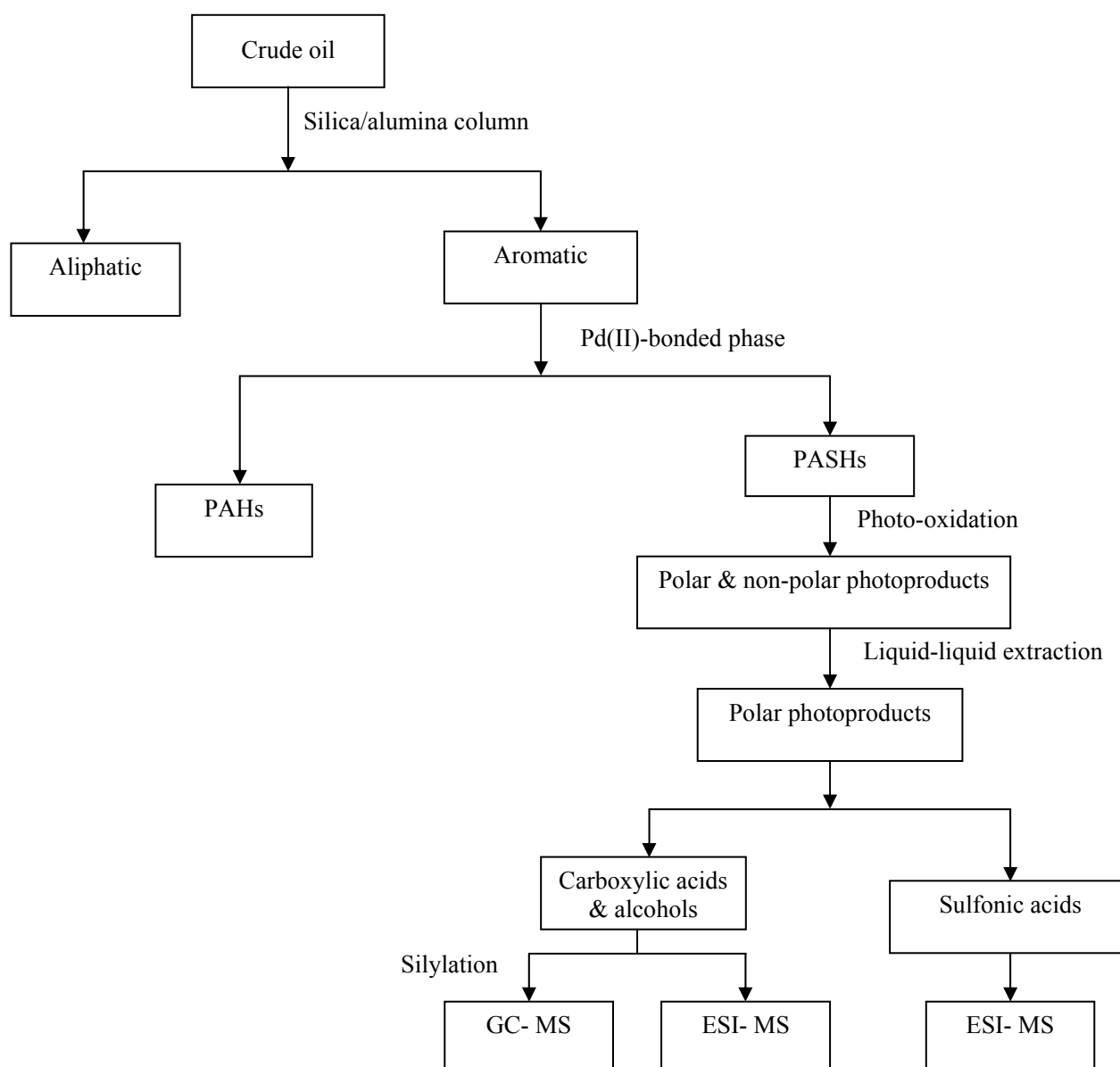


Figure 8.1. Analysis scheme of polar photoproducts of PASHs.

8.2. Results and discussion

8.2.1. Characterization of polar photoproducts 1

8.2.1.1. Derivatization

In order to analyze polar and thermolabile compounds by GC and GC-MS, they should be first derivatized. Derivatization usually improves the gas chromatographic properties of the compounds as it minimizes the undesirable and non-specific column adsorption and gives better peak shapes. As the chemical structure of the substance is changed after derivatization and, subsequently, the fragmentation pattern, high mass ions could be obtained and could be

then easily separated from the interferences either from the fragment ions of contaminants or from those due to column bleeding [196].

In addition, the introduction of groups with high electron affinity, such as halogen atoms, through derivatization can also enhance the detectability of a compound by GC-MS. Moreover, derivatization can be used to favour the formation of high stability fragments that can be used to monitor a common and characteristic fragment ion [197].

In order to accomplish a successful derivatization reaction, the following requirements are needed:

- a single derivative should be formed for each compound,
- the derivatization reaction should be simple and rapid and should occur under mild conditions,
- the derivative should be formed with a high and reproducible yield and should be stable in the reaction medium.

8.2.1.2. Silylation

Silylation is one of the most widely used derivatization procedures for GC-MS analyses [198]. An alkylsilyl group replaces an active proton in -OH, -SH or -NH groups leading to the elimination of hydrogen bonding and the formation of a silyl derivative. The order of increasing reactivity towards silylation is as follows: alcohols > phenols > carboxylic acids > amines > amides.

Trimethylsilylation is the most common silylation procedure currently used. In addition to the high thermal and chemical stability and high volatility of trimethylsilyl (TMS) derivatives, trimethylsilyl groups increase the total ion current and, hence, the sensitivity using positive ion mass spectra [199]. A variety of trimethylsilylating reagents with different properties (such as volatility, reactivity, selectivity, by-product formation, etc.) are nowadays used including trimethylhalosilanes, TMS-amines, TMS-esters and TMS-amides in which N-methyl-N-trimethylsilyl-trifluoroacetamide is the most volatile TMS-amide available [198]. Moreover, in order to derivatize sterically hindered functions or to enhance reaction rates, catalysts such as trimethylchlorosilane, trimethylsilylimidazole, trimethyliodosilane or potassium acetate have been added to the previous reagents to increase their silylating power

[200]. Furthermore, as all the above derivatization reagents can be injected directly into the GC-MS system, the time needed for the sample preparation is usually short.

8.2.1.3. Identification of polar photoproducts 1

PP1 can be divided into several classes of compounds based on their functional groups. They will be discussed here according to that pattern:

Carboxylic acids

In order to identify the polar photoproducts 1 of PASHs, after their extraction from water, they were dried and subjected to electrospray mass spectrometry in the negative mode. An electrospray tandem mass spectrometry analysis in the negative mode with a neutral loss of 44 amu corresponding to the loss of CO₂, which is characteristic of carboxylic acids, was produced from the parent peaks [201]. Figure 8.2 shows the negative ESI-MS/MS spectra of the photoproducts that have lost CO₂. As can be deduced from Figure 8.2, a large number of carboxylic acids were found among the PP1. Since the instrument used does not have a high enough resolution to deduce the elemental compositions from the masses recorded, additional information about the structure of the compounds is then required. Therefore, the acids were derivatized as trimethylsilyl derivatives and then analyzed by QuattroMicro GC-MS. The resulting gas chromatogram in Figure 8.3 displays many peaks, some of which may be derived from carboxylic acids and some from other polar products. The carboxylic acids can be selectively detected by recording the single ion chromatogram of m/z 132 (Figure 8.4). This mass is generated by the fragment [CH₂=C(OH)-O-SiMe₃]⁺ which is characteristic of McLafferty rearrangement in fatty acid trimethylsilyl esters. A series of regularly spaced peaks can be seen which were identified as the fatty acids from butanoic to hexadecanoic acid.

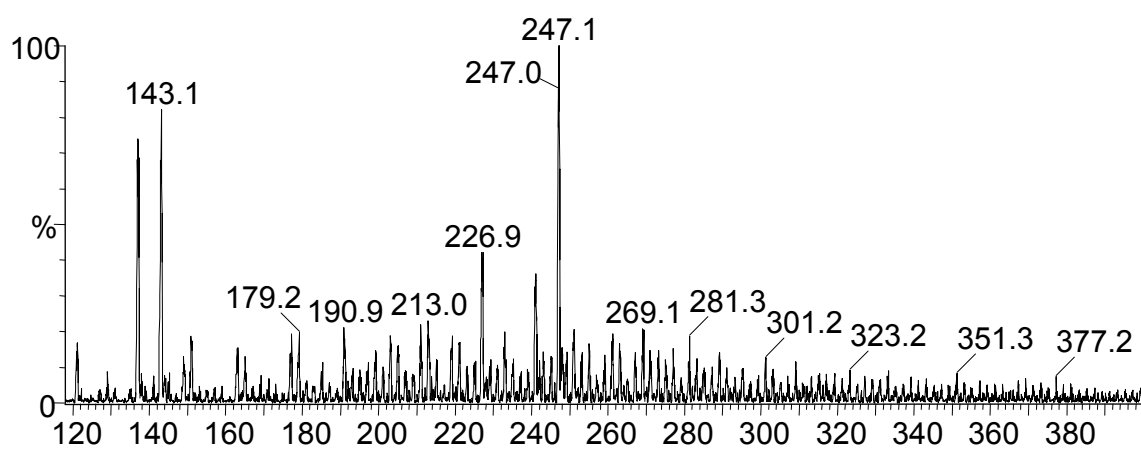


Figure 8.2. Negative ion ESI-MS/MS spectrum after the loss of m/z 44 from carboxylic acids.

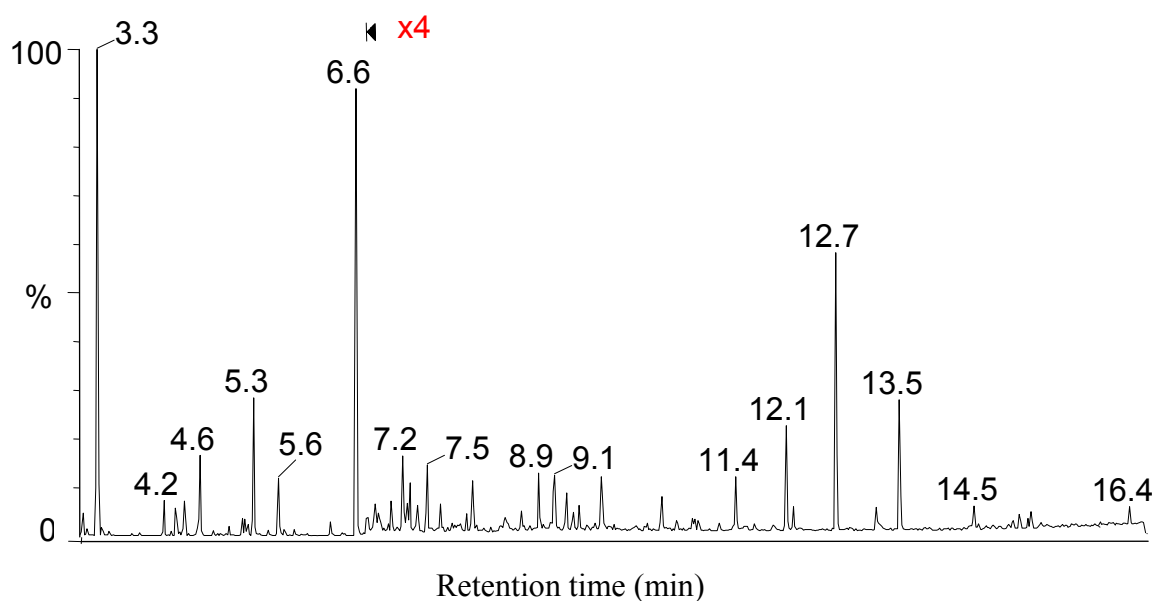


Figure 8.3. GC-MS chromatogram of carboxylic acids trimethylsilyl derivatives.

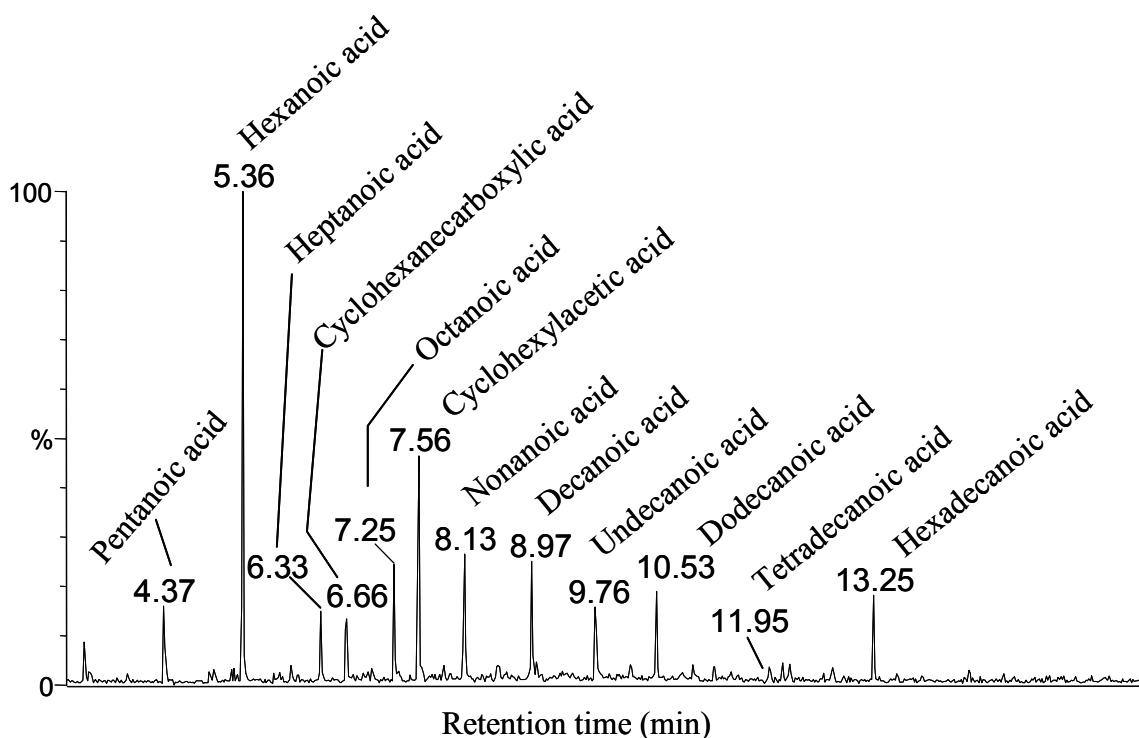


Figure 8.4. Mass chromatogram of m/z 132 of carboxylic acid trimethylsilyl derivatives.

The identification of the fatty acids was based on the following considerations, illustrated for the compound eluting at 7.25 min (Figure 8.4 and 8.5). The mass spectrum showed predominant ions at m/z 73, 75, 117, 132, 145 in addition to the ions 157, 173, 187, 201 and 216. The ion at m/z 201 represents the molecular ion less 15 mass units, a common fragment observed with TMS-derivatized compounds, suggesting the loss of a methyl group from TMS substituent. In general, electron ionization (EI) mass spectra of trimethylsilyl ethers or esters is characterized by the presence of the $[M-15]^+$ ion formed by loss of a methyl group bonded to silicon, which is usually used for the determination of the molecular mass. Moreover, it is commonly known that during the EI fragmentation process, many rearrangements may occur that are useful for the deduction of structures of unknown spectra [202]. Hence, in addition to M^+ and $[M-15]^+$, m/z 73 $[\text{Si}(\text{CH}_3)_3]^+$ and m/z 75 $[\text{Si}(\text{CH}_3)_2\text{OH}]^+$ are prominent in nearly all TMS spectra [198].

It was reported that the TMS ester group undergoes α -cleavage, β -cleavage with γ -hydrogen rearrangement and migration of a δ - or ϵ -hydrogen, with reciprocal hydrogen transfer and subsequent γ -cleavage [203] (Scheme 8.1). For instance, the peak at m/z 117 may arise from α -cleavage (ion a^+) or from the loss of a methyl radical by the ion b^+ (m/z 132) resulting from

β -cleavage (ion c^+) (Scheme 8.1). The fragment ion at m/z 129 was formed by the loss of methane from the ion d^+ (m/z 145) resulting from γ -cleavage. The formation of the highly stable ion e^+ (m/z 129) occurred through the movement of an electron pair from one of the Si-CH₃ bonds, with a concerted six centered movement of an electron pair from the H-O bond (Scheme 8.1). However, the transfer of a proton from the protonated carbonyl group to the oxygen of the trimethylsilyloxy group and the subsequent four-membered hydrogen rearrangement with charge retention were suggested as another formation pathway [202, 204].

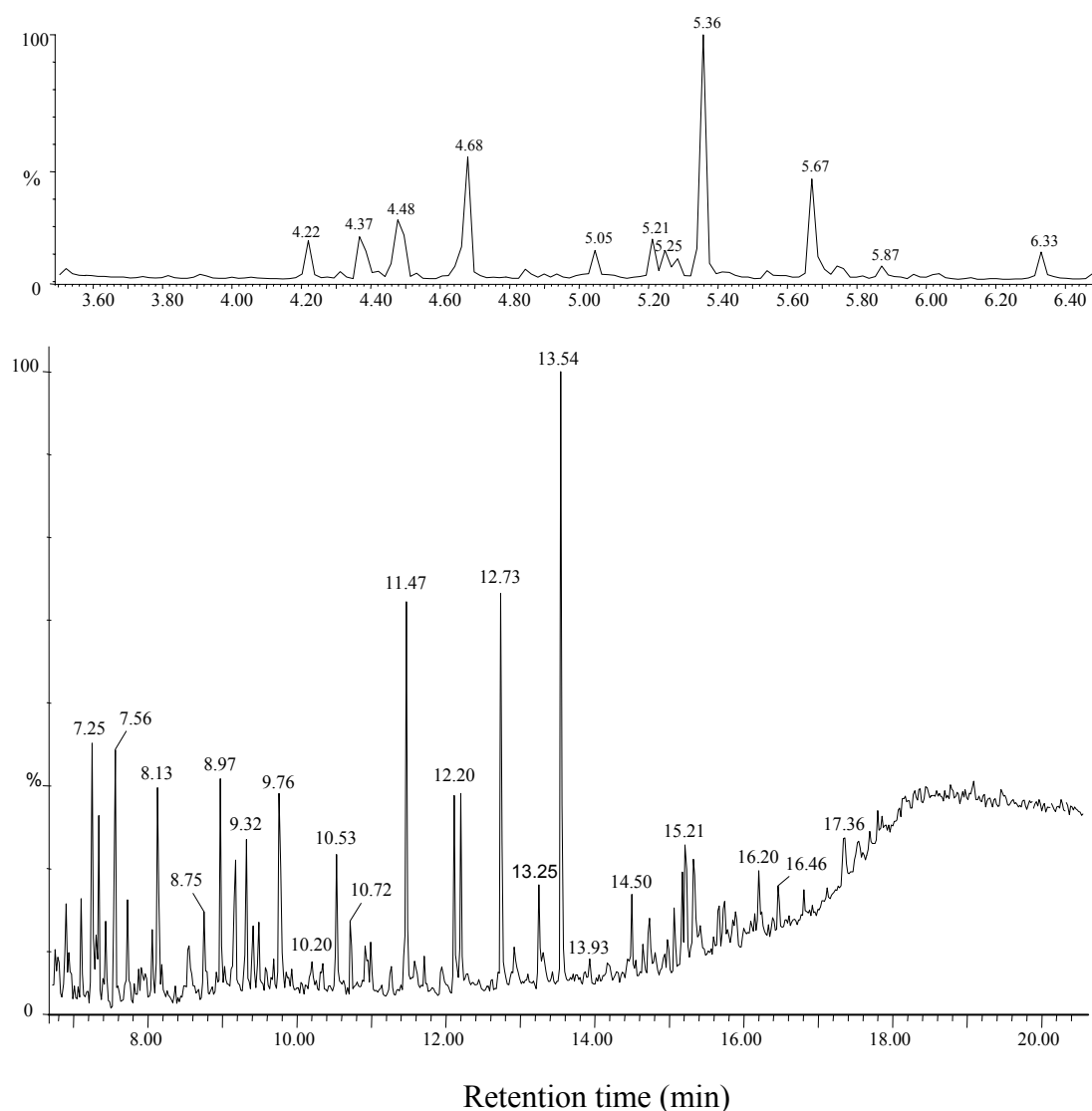
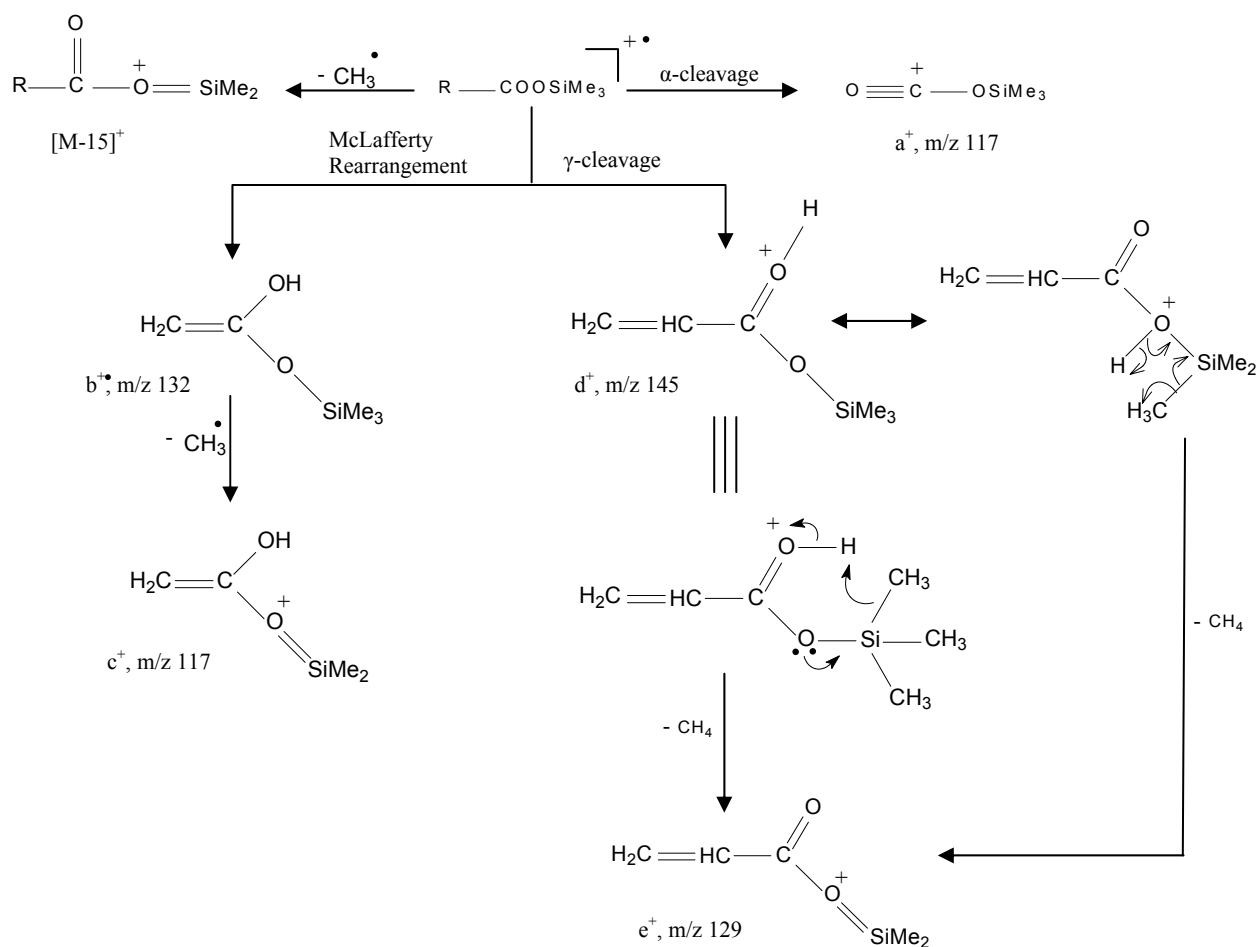


Figure 8.5. Total ion current partial expanded GC-MS chromatogram of carboxylic acids trimethylsilyl derivatives. Identifications are listed in Table 8.1.



Scheme 8.1. Proposed fragmentation of silylated carboxylic acids (from [204]).

The mass spectrum of the compound at 7.25 min coincided with that of the trimethylsilyl ester of octanoic acid in the NIST library and the retention time and the mass spectrum were identical with those of an authentic sample. The other alkanolic acids in Figure 8.4 were identified in a similar manner.

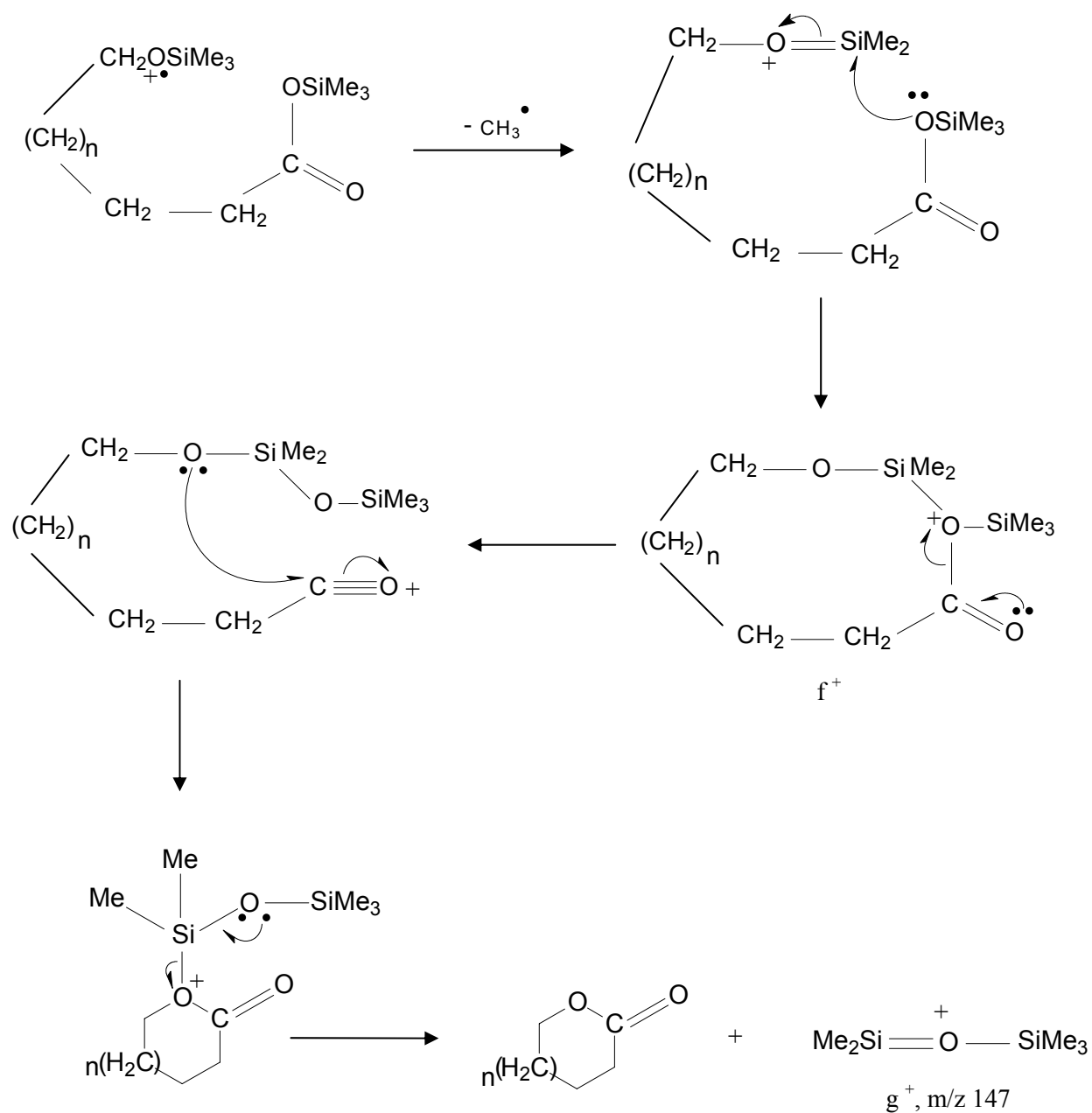
It should be noted that the peaks obtained at 12.10, 12.73 and 13.54 min (Figure 8.5) correspond to phthalates that may be originating from plasticizers and not from the photo-oxidation of PASHs.

Hydroxycarboxylic acids

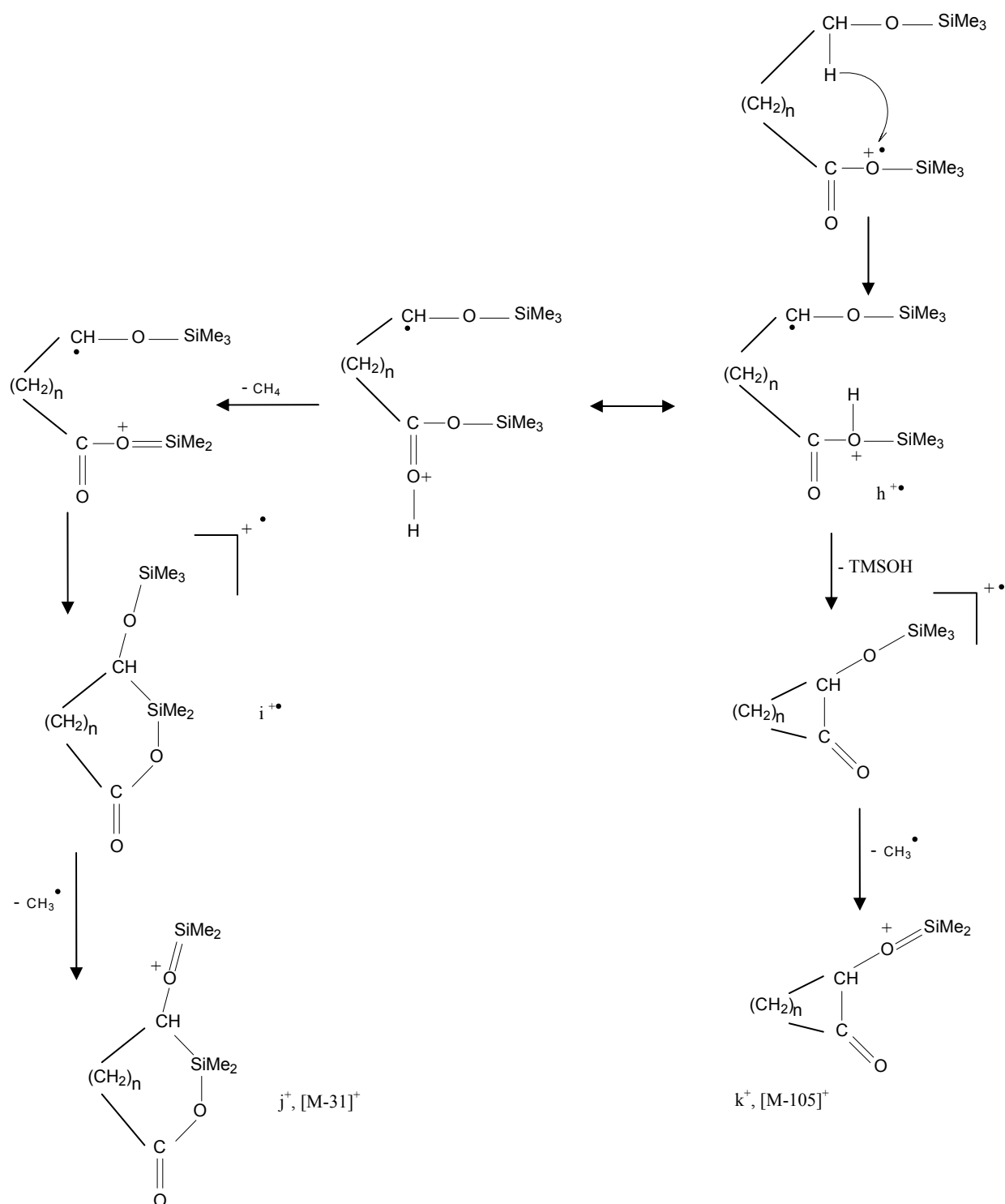
EI mass spectra of the compound at 8.75 min (Figure 8.5) showed fragment ions at m/z 103, 117, 129, 132, 145, 147, 171, 204, 217, 245, 261 and 276. The mass 103 $[\text{CH}_2=\text{O}-\text{SiMe}_3]^+$, which is formed through the cleavage of the alkyl chain, indicates the presence of a hydroxyl group. The m/z 261 and 276 represent the $[\text{M}-15]^+$ and $[\text{M}]^+$ respectively and the presence of m/z 103 together with the ions 129, 132 and 145 reveals the presence of a hydroxyl group and a carboxylic group respectively. In addition, the formation of the well known fragment ion g^+ at m/z 147 confirms the presence of more than one functional group (more than one silyl residue) [198], and the mechanism of its formation involves the loss of a methyl radical from one silyl group and subsequent rearrangement through a cyclic oxonium ion such as f^+ (Scheme 8.2) [204].

It is well known that through the interaction between the two functionalities in EI mass spectra of hydroxycarboxylic acid TMS derivatives, the ions $[\text{M}-31]^+$ and $[\text{M}-105]^+$ are formed (Scheme 8.3) [204]. Hence, this explains the formation of m/z 171 = $[\text{M}-105]^+$ and m/z 245 = $[\text{M}-31]^+$. Their formation pathways involve a hydrogen atom transfer from the primary carbon bearing the TMS ether group to the ionized ester group. A molecule of methane is then lost from the resulting ion h^+ (according to the mechanisms proposed in Scheme 8.1) to give after cyclization the radical ion i^+ which lose a methyl radical to yield the ion j^+ at $[\text{M}-31]^+$. A molecule of trimethylsilanol and a methyl radical are easily lost from the ion h^+ to give the ion k^+ corresponding to $[\text{M}-105]^+$ (Scheme 8.3).

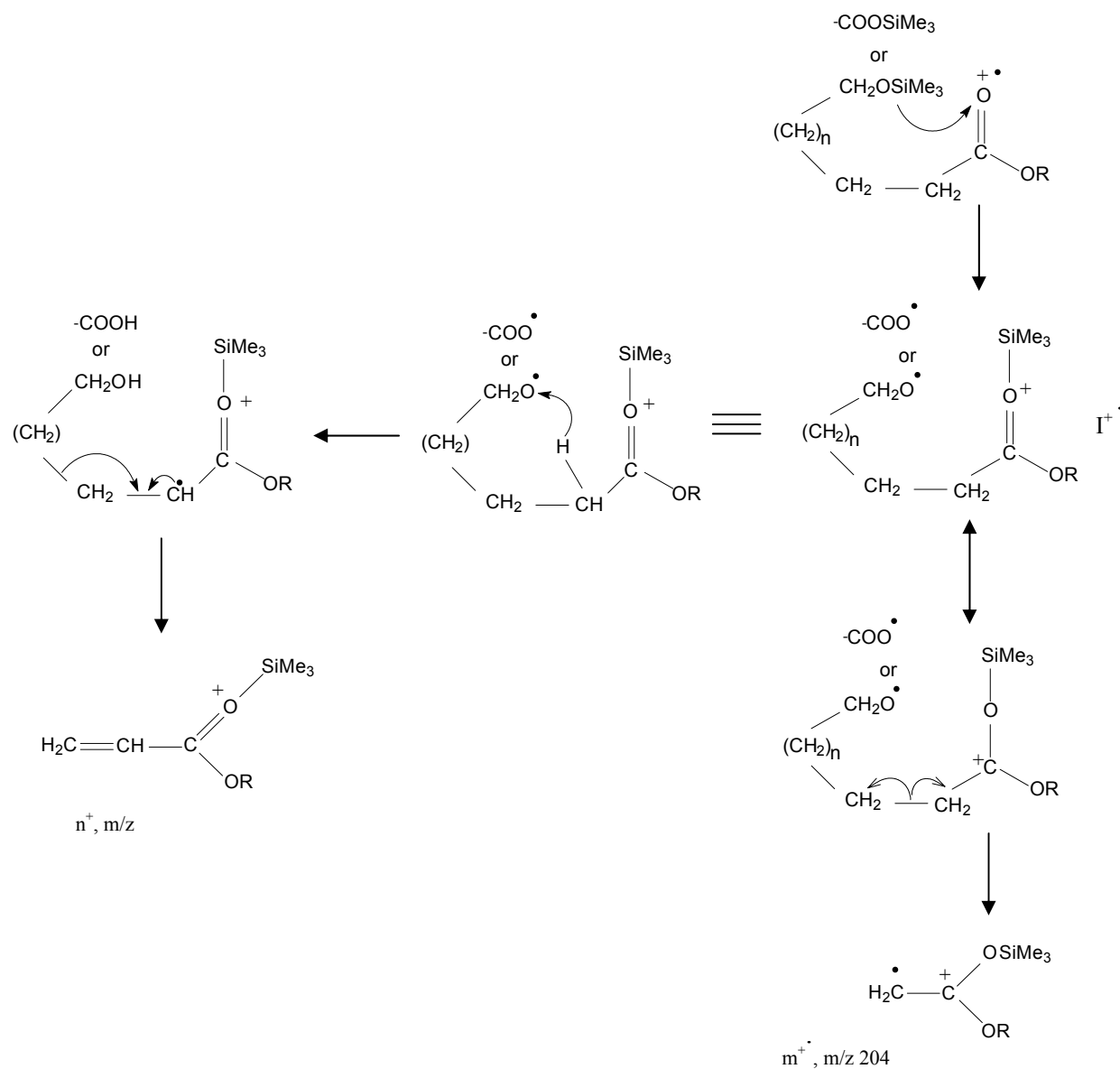
In addition to the fragmentations described above, the EI mass spectra of dicarboxylic acid and hydroxycarboxylic acid TMS derivatives show abundant ions at m/z 204 and 217. The ion 217 is important as it is independent of the chain length and is usually unaffected by the ionizing energy used [205]. The fragment ions at m/z 204 and 217 result from pathways similar to those described above as can be seen in Scheme 8.4 [204]. Due to the presence of all the above mentioned fragments and by comparison with the NIST data base, the compound at 8.75 min can be suggested to be a hydroxyhexanoic acid.



Scheme 8.2. Formation pathway of ion g^+ (at m/z 147) (from [204]).



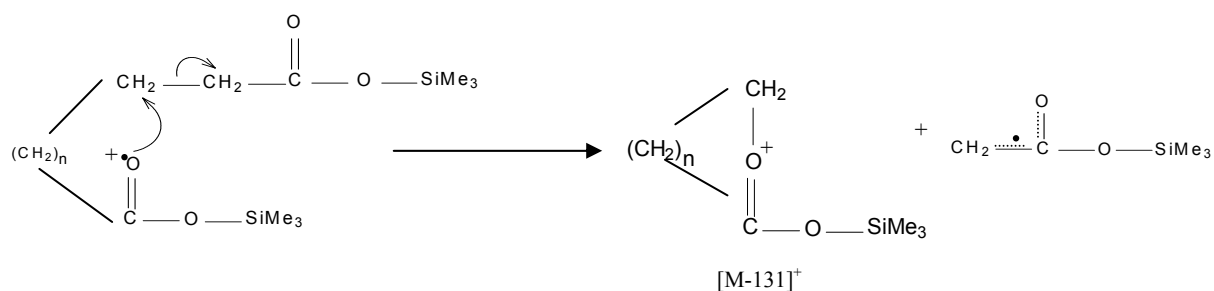
Scheme 8.3. Proposed formation pathways of ions $[M-31]^+$ and $[M-105]^+$ (from $[204]$).



Scheme 8.4. Proposed formation pathways of ions n^+ (at m/z 217) and m^+ (at m/z 204) involving trimethylsilyl transfer (from [204]).

Dicarboxylic acids

Based on the previously mentioned mechanisms, the compound eluting at 9.41 min (Figure 8.5), whose mass spectra contained m/z 275 as $[M-15]^+$ and each of m/z 73, 117, 147, 159, 172, 204 and 217 was identified as 1,6-hexanedioic acid. The mass fragment 159 corresponds to the $[M-131]^+$ which usually appears in the EI mass spectra of dicarboxylic acid TMS derivatives and is formed through the interaction between the two functionalities (Scheme 8.5). It is similar to the peak at $[M-73]^+$ (corresponding to the loss of the ester group plus C-2) which was observed in the case of dicarboxylic acid dimethyl esters [206].

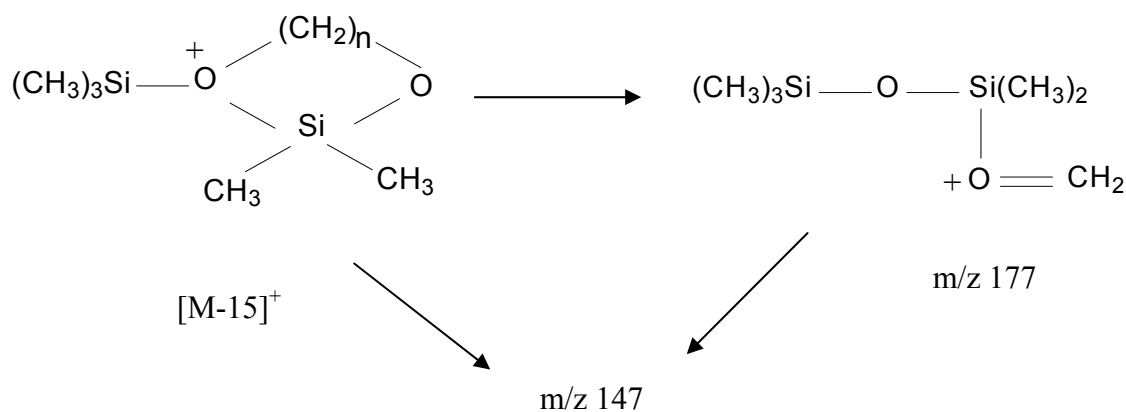


Scheme 8.5. Proposed formation pathway of ion $[M-131]^+$ (from [204]).

The MS profile of the compound at 11.57 min (Figure 8.5) contained the key fragment ions m/z 73, 117, 147, and 204, which are associated with two TMS derivatized carboxylic groups (m/z 73, 117, 147, and 204) and a succinyl moiety (m/z 172, 217, and 262, $[M-15]^+$) associated with alkylsuccinic acid derivatives from *n*-alkanes [207]. An $[M-15]^+$ ion with 2 mass units less than that predicted for a straight-chain alkylsuccinate was observed, suggesting a compound with one degree of unsaturation such as an alkene, or a cyclic alkane. A comparison of the mass spectrum with the database suggests that the compound may be cyclohexylsuccinic acid. The compound underwent a McLafferty rearrangement to give the ion at m/z 262 [202]. In this rearrangement, a bond cleavage between the cyclohexyl and succinic acid portions takes place, with transfer of a single proton from the cyclohexyl portion onto the nearest carbonyl group in the succinic acid portion. The resulting ion at m/z 262 has the same chemical composition as the di-TMS ester of succinic acid. This McLafferty rearrangement ion loses $\text{HOSi}(\text{CH}_3)_3$ (90 amu) to give the resulting ions at m/z 172. The ion at m/z 217 is 45 amu (CO_2H) smaller than the McLafferty rearrangement ion. The mechanism may involve a long-range migration of a TMS group [202].

Diols

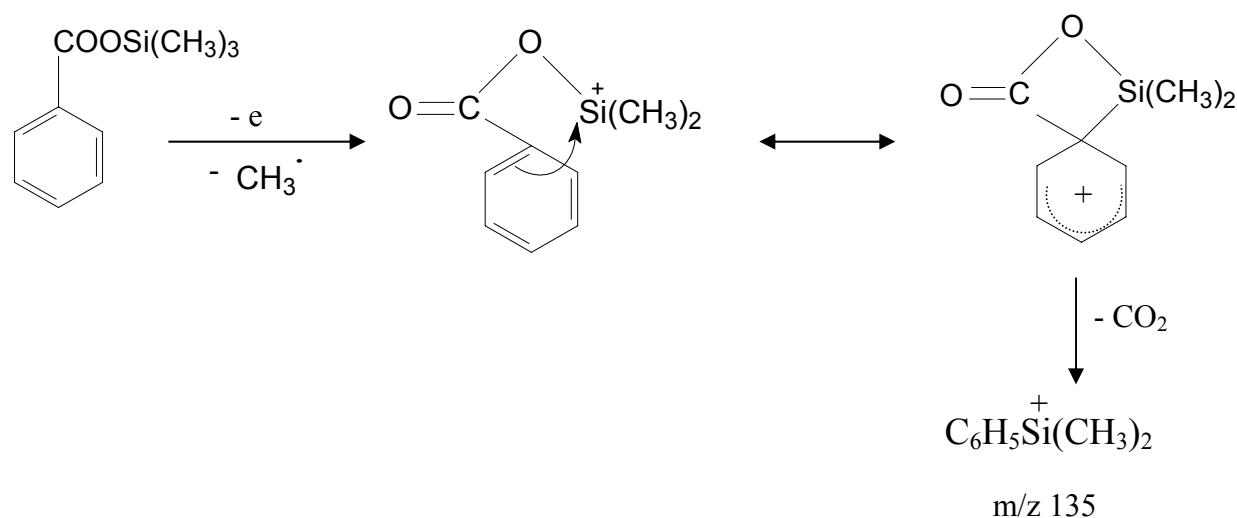
A compound appearing at 5.21 min (Figure 8.5) had the important fragments m/z 73, 103, 147, 177, 205 and was identified as 1,3-propane diol. The mass 103, $[\text{CH}_2=\text{O}-\text{SiMe}_3]^+$ previously mentioned, is commonly observed in TMS ether and diol spectra. However, diols are differentiated by the presence of m/z 147, $[(\text{CH}_3)_3\text{Si}-\text{O}=\text{Si}(\text{CH}_3)_2]^+$ [208]. In studies of TMS derivatives of terminal aliphatic diols ion m/z 147 has been shown to arise both from loss of CH_2O from m/z 177 and by a cyclic mechanism proceeding through $[\text{M}-15]^+$ [209]. On the other hand, in a study of related homologues ($\text{TMSO}(\text{CH}_2)_n\text{OTMS}$, $n = 3$ to 8), it was reported that both m/z 177 (Scheme 8.6) and 147 were derived from $[\text{M}-15]^+$, suggesting the presence of a cyclic oxonium ion form of $[\text{M}-15]^+$ as intermediate [210].



Scheme 8.6. Proposed formation pathway of ion $[(\text{CH}_3)_3\text{Si}-\text{O}=\text{Si}(\text{CH}_3)_2]^+$ m/z 147 (from [209]).

Aromatic acids

In addition to aliphatic products identified, aromatic compounds were also found, among them, the compound eluting at 7.10 min (Figure 8.5). It had the following fragment ions 73, 75, 77, 105, 135, 179 and 194 as $[\text{M}]^+$ and was identified as benzoic acid. It was demonstrated that the intense m/z 135 peak in the mass spectrum of trimethylsilyl benzoate arose by elimination of carbon dioxide from the $[\text{M}-\text{CH}_3]^+$ species as shown in Scheme 8.7 [211].



Scheme 8.7. Proposed formation pathway of m/z 135 (from [211]).

Likewise, many of the polar photoproducts obtained were identified and they are listed in Table 8.1.

By observing the polar photoproducts obtained, we can deduce that the first possible photodegradation pathway of PASHs is the oxidation of the terminal methyl group in the alkyl chain to CH_2OH , which is further oxidized to $-\text{CHO}$ and $-\text{COOH}$ followed by the cleavage of the alkyl chain. The identification of various aliphatic and aromatic acids and alcohols indicate that the alkyl side chains were susceptible to photo-oxidation. These results are in accordance with the work of Ehrhardt and Petrick [73] who investigated the photo-oxidation of 1-phenyl-*n*-tridecane among several other homologous of monoalkylated benzenes and identified 1-phenyl-1-tridecanone, 1-phenyl-tridecanol, 1-phenylethanone and benzaldehyde in addition to *n*-undecene-1, *n*-dodecane and *n*-decanal as photoproducts. Rontani et al. [72] also reported the formation of 1-phenyl-1-nonanone, 1-phenyl-1-nonanol, 1-phenylethanone, benzaldehyde, *n*-octane and nonanal resulting from the photo-oxidation of *n*-nonylbenzene on seawater, which shows that these results are fitting with the results of Ehrhardt and Petrick [73].

Table 8.1. Retention time (t_R) in Figure 8.5 and important fragment ions of carboxylic acids and alcohols as their trimethylsilyl derivatives by GC-MS analysis

Compound	t_R	Important mass spectral fragment ions
Butanoic acid	3.43	73, 117, 129, 145, 160
Pentanoic acid	4.37	73, 117, 129, 132, 145, 159, 174
Cyclohexanol	4.67	73, 101, 113, 129, 143, 157, 172
1,3-Propanediol	5.21	73, 103, 115, 130, 133, 147, 163, 177, 205
Cyclopentane carboxylic acid	5.24	73, 96, 117, 129, 142, 153, 171, 186
Hexanoic acid	5.36	73, 101, 117, 132, 145, 159, 173, 188
Heptanoic acid	6.33	73, 117, 132, 145, 159, 173, 187, 202
Cyclohexanecarboxylic acid	6.66	73, 117, 129, 145, 185, 200
Benzoic acid	7.10	73, 77, 105, 135, 179, 194
Octanoic acid	7.25	73, 117, 132, 157, 173, 201, 216
1,2-Cyclohexanediol	7.34	73, 81, 101, 117, 129, 142, 147, 155, 170, 245
Glycerol	7.43	73, 103, 117, 133, 147, 177, 191, 205, 218, 293
Cyclohexylacetic acid	7.56	73, 117, 132, 199, 214
2-Methyl benzoic acid	8.05	73, 77, 91, 119, 149, 193, 208
Nonanoic acid	8.13	73, 117, 132, 145, 171, 187, 215, 230
Hydroxyhexanoic acid	8.75	73, 103, 117, 129, 147, 171, 186, 245, 261, 276
Decanoic acid	8.97	73, 117, 132, 145, 185, 201, 229, 244
1,6-Hexanedioic acid	9.41	73, 83, 111, 117, 129, 147, 159, 172, 185, 275
2-Hydroxybenzoic acid	9.48	73, 91, 117, 147, 179, 193, 209, 221, 249, 267
Undecanoic acid	9.76	73, 89, 117, 132, 145, 185, 201, 243, 258
Dodecanoic acid	10.53	73, 99, 117, 132, 145, 159, 201, 257, 273
1,2-Benzenedicarboxylic acid	10.91	73, 91, 117, 147, 163, 207, 221, 235, 295, 310
Cyclohexyl succinic acid	11.57	73, 129, 147, 172, 217, 262, 329
Tetradecanoic acid	11.95	73, 95, 117, 132, 145, 285, 300
Hexadecanoic acid	13.25	73, 117, 132, 145, 187, 201, 269, 285, 313, 328

8.2.1.4. Identification of novel non-condensed cyclohexyl compounds

Two peaks seem to represent acids containing the cyclohexyl group were observed among the aliphatic acids obtained. The trimethylsilyl ester at 6.66 min (Figure 8.4) has the molecular mass 200, corresponding to a carboxylic acid of the composition $C_7H_{12}O_2$. There is therefore one double bond or one ring in the compound. Since unsaturated aliphatic chains are very rare in crude oils, either cyclohexanecarboxylic acid or methylcyclopentanecarboxylic acid would suggest itself. The retention time and the mass spectrum of this compound corresponded to those of the standard cyclohexanecarboxylic acid (Figure 8.6).

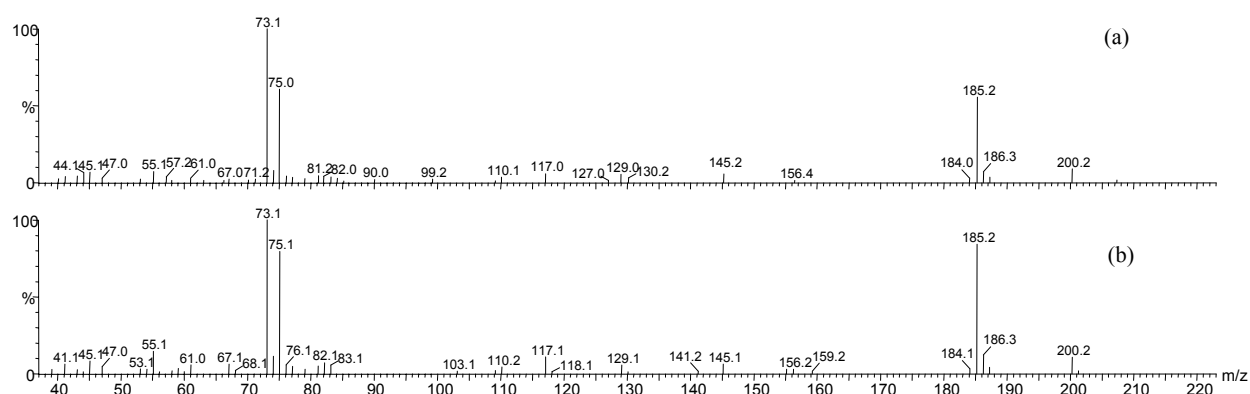


Figure 8.6. Mass spectral profiles of cyclohexanecarboxylic acid (a) found in the polar photoproducts and (b) as authentic standard (analyzed as TMS esters).

The acid represented by the peak at 7.56 min (Figure 8.4) has a molar mass of 214, 14 mass units more than cyclohexanecarboxylic acid. It may be cyclohexylacetic acid, a methylcyclohexanecarboxylic acid or an ethylcyclopentanecarboxylic acid. The retention time and the mass spectrum were identical with those of the authentic standard cyclohexylacetic acid (Figure 8.7).

The presence of the cyclohexyl group, in cyclohexanecarboxylic acid and cyclohexane acetic acid, among the aliphatic acids is significant since it indicates that polycyclic aromatic compounds in the crude oil contain this structural element in the side chain. High resolution mass spectrometry has established the profuse presence of aromatic compounds containing one or several saturated rings. MS does not distinguish between fused (e.g. cyclohexano) and substituted (e.g. cyclohexyl) rings but the photoproducts found here can only be derived from the latter.

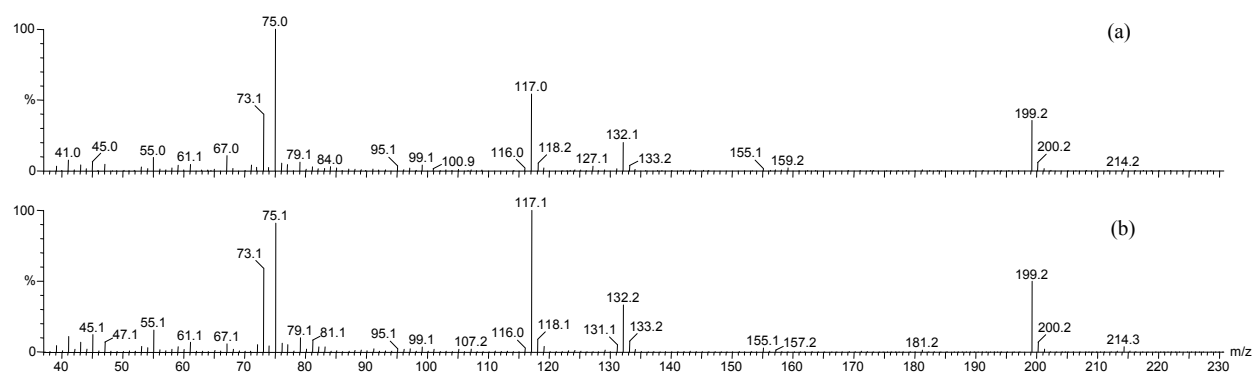


Figure 8.7. Mass spectral profiles of cyclohexylacetic acid (a) found in the polar photoproducts and (b) as authentic standard (analyzed as TMS esters).

Cyclohexylsubstituted aromatics do not seem to have been identified in crudes yet but cyclohexyltetralins have been shown to possess structural details that make them possible constituents of the unresolved complex mixture of petroleum [212]. The identification of the cyclohexyl containing acids among the photoproducts thus gives us new structural insights into the polycyclic aromatic compounds in crude oil.

8.2.2. Characterization of polar photoproducts 2 (PP2)

After the extraction of PP1, the aqueous phase remaining was evaporated and the PP2 were obtained in order to be analyzed by ESI-MS in the negative ion mode. First, the fragmentor voltage of the instrument was optimized using two standard compounds, p-toluene sulfonic acid and 2-sulfobenzoic acid, in order to achieve significant fragmentation of the quasi-molecular $[M-H]^-$ ion. Among the structurally important ions observed in the characterization of these standards by ESI-MS were those due to the loss of SO_3^- ion. This is in agreement with Alonso and Barcelo [213] who have found that the SO_3^- ion was observed in all sulfonic compounds, so that m/z 80 could be used as a diagnostic tool to indicate the presence of sulfonated aromatic compounds in any sample. Then the PP2 were then analyzed by ESI-MS/MS in which the parent peaks were subjected to the loss of m/z 80 fragment and Figure 8.8 shows the resulting mass spectrum of the daughter ions.

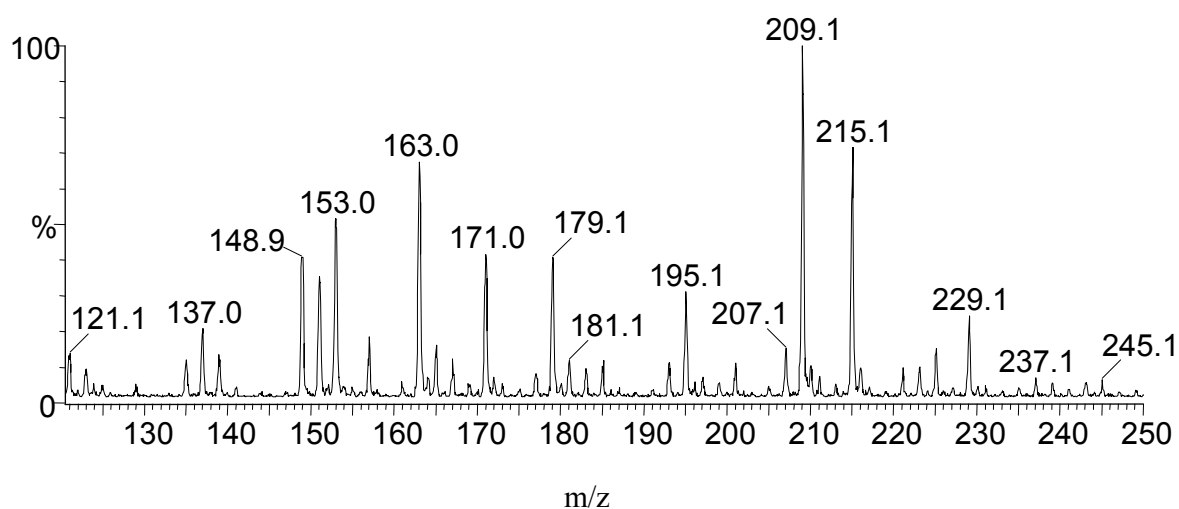


Figure 8.8. Negative ion ESI-MS/MS spectrum of precursor ions of SO_3^- of presumably all sulfonic acids.

Since the resolution of the instrument used is not high enough to deduce the elemental compositions of the sulfonic acids from the masses recorded, the PP2 were analyzed by the MicroTof MS in order to identify the various sulfonic acids. Accurate masses of the deprotonated sulfonic acid molecules were determined in the negative ionization mode and these were entered into the Elemental Composition program to calculate possible elemental compositions with a maximum deviation of ± 5 mDa from the measured mass. Parameter settings for all calculations were C: 0-10, H: 0-13, O: 0-7 and S: 0-1. The resulting elemental compositions were searched against the Merck Index and the NIST databases assuming the presence of a SO_3^- group. The double bond equivalent parameter was also used as an identification criterion in order to gain information about the aromaticity of the structure, whenever possible.

Selected examples

The m/z value of a deprotonated unknown compound was found to be 156.9953. The only elemental composition possible assuming the presence of a SO_3^- group and a benzene ring was $\text{C}_6\text{H}_5\text{O}_3\text{S}_1$. This corresponded to a benzene sulfonic acid. In a similar way, the m/z value of deprotonated unknown compounds was 171.0110 and 200.9852. Only one possibility resulted for each mass: $\text{C}_7\text{H}_7\text{O}_3\text{S}_1$ and $\text{C}_7\text{H}_5\text{O}_5\text{S}_1$ which indicated the presence of toluene sulfonic acid and sulfobenzoic acid respectively. The exact mass of an unknown compound was 185.0277. This elemental composition was found in the database, resulting in two possible isomers: a dimethylbenzene sulfonic acid or an ethylbenzene sulfonic acid. The

molecular weight of unknown compounds with their corresponding possible structure(s) identified are given in Table 8.2.

The sulfonic acids were also subjected to positive ESI-MS (Figure 8.9). The observed mass spectrum exhibited for instance the presence of significant peaks at m/z 69 $[C_5H_9]^+$, 71 $[C_5H_{11}]^+$ and 85 $[C_6H_{13}]^+$. Less significant peaks were present at m/z 55 $[C_4H_7]^+$, 57 $[C_4H_9]^+$ and 67 $[C_5H_7]^+$ (Figure 8.9). These peaks represent two alkylation series with peaks separated by m/z 14. These series represent $[C_nH_{2n-1}]^+$ and $[C_nH_{2n+1}]^+$ starting at $[C_4H_7]^+$ at m/z 55 and $[C_4H_9]^+$ at m/z 57 respectively. In addition to the previously mentioned series of peaks, clusters of peaks separated by m/z 2, which corresponds to successive losses of H_2 (i.e. addition of a ring or double bond) were also observed. It is assumed that these series were formed during the cleavage of the side alkyl chain. This is consistent with the previous studies of Ehrhardt and Petrick [73] who observed the formation of *n*-undecene-1 and *n*-dodecane from the photo-oxidation of 1-phenyl-*n*-tridecane as well as the formation of *n*-propene-1, *n*-nonene-1, *n*-decene-1, *n*-undecene-1 and *n*-dodecene-1 from the sensitized photo-oxidation of *n*-pentadecane [74]. Moreover, 1,3-pentadiene and *n*-butane were obtained as photoproducts from the photolysis of anthracene [214] and *n*-butylcyclohexane [215] respectively.

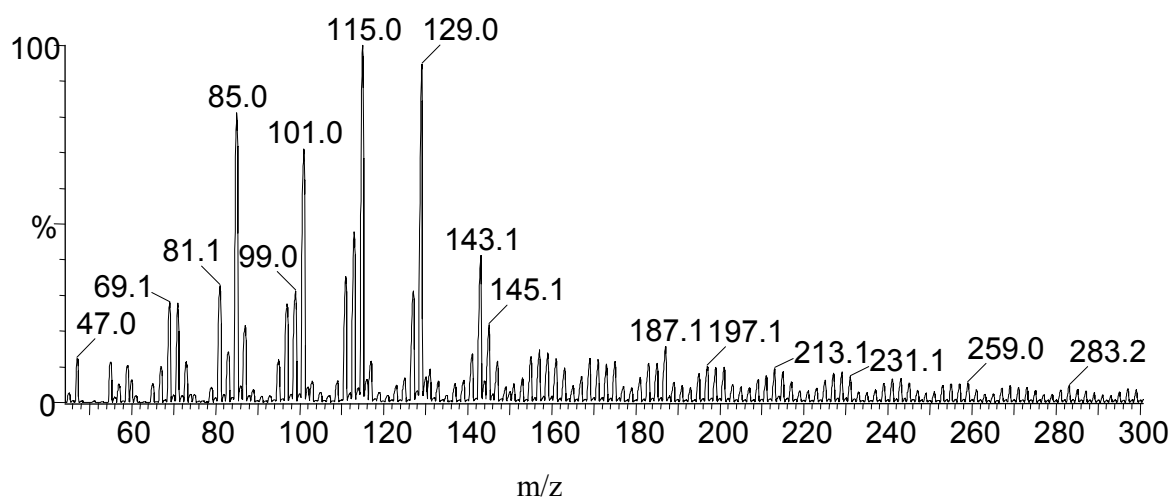
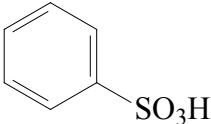
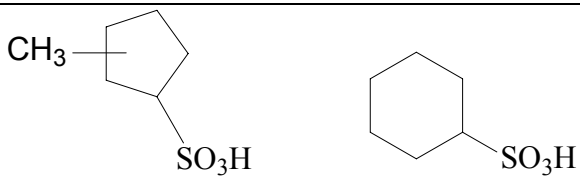
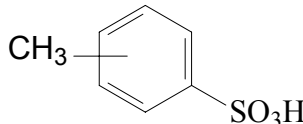

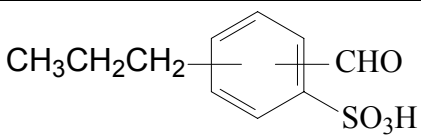
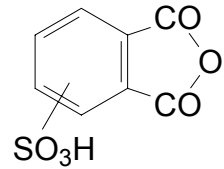
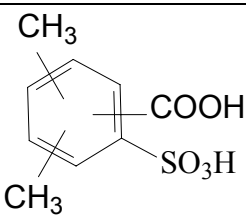
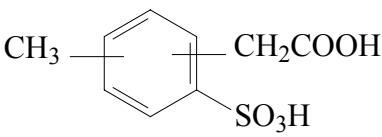
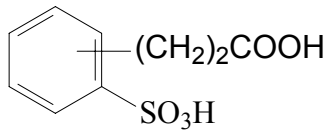
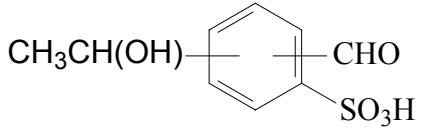
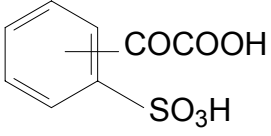
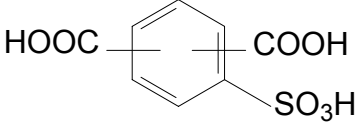


Figure 8.9. Positive ion ESI spectrum of sulfonic acids.

Table 8.2. Possible structures of sulfonic acids identified from the MicroTof mass spectra

Molecular weight	Molecular formula	Possible structures
136	$C_4H_8SO_3$	$CH_3-CH=CH-CH_2-SO_3H$ $CH_2=CH-(CH_2)_2-SO_3H$
138	$C_4H_{10}SO_3$ $C_3H_6SO_4$	$CH_3-CH_2-CH_2-CH_2-SO_3H$ $OHC-CH_2-CH_2-SO_3H$
152	$C_4H_8SO_4$	$OHC-CH_2-CH_2-CH_2-SO_3H$
154	$C_3H_6SO_5$	$HOOC-(CH_2)_2-SO_3H$
158	$C_6H_6SO_3$	
164	$C_6H_{12}SO_3$	
168	$C_4H_8SO_5$	$HOOC-(CH_2)_3-SO_3H$
172	$C_7H_8SO_3$	
186	$C_8H_{10}SO_3$	

202	$C_7H_6SO_5$	
208	$C_7H_{12}SO_5$	
216	$C_8H_8SO_5$	
222	$C_8H_{14}SO_5$	
228	$C_{10}H_{12}SO_4$	

	$C_8H_4SO_6$	 
230	$C_9H_{10}SO_5$	  
	$C_8H_6SO_6$	 
246	$C_7H_6SO_5$	

The second possible photodegradation pathway of PASHs is the oxidation of the aromatic ring. For instance, the ring oxidation was observed by Moza et al. [216] in a study of the photo-oxidation of naphthalene and phenanthrene as a liquid film on water. They have detected 3-phenyl-2-propenal and 2-carboxybenzaldehyde from naphthalene and 2-biphenyl carboxylic acid and 2-biphenyl aldehyde as photoproducts from phenanthrene. Furthermore, Lehto et al. [214] have studied the photodegradation of anthracene and benz[*a*]anthracene and detected 1(3H)-isobenzofuranone and 4-ethoxybenzaldehyde among the photoproducts of anthracene and 1(3H)-isobenzofuranone among those of benz[*a*]anthracene.

However, in the photo-oxidation studies of benzothiophene [94], monomethyl- and dimethylbenzothiophenes [99, 100] and dibenzothiophene [101, 102], thiophene dicarboxylic, tricarboxylic and tetracarboxylic acids were found as products from the benzo ring oxidation besides different sulfonic acids such as sulfobenzoic acids produced from the thiophene ring oxidation. As the PASHs were photo-oxidized for a long time (one month), it is assumed that the oxidized PASH compounds produced have undergone further photo-oxidation and were further photodegraded through the third photodegradation pathway, namely the oxidation of the thiophene ring. This is confirmed through the identification of a variety of aliphatic and aromatic sulfonic acids detected in the polar photoproducts in addition to the released sulfur atom, detected as sulfate ion (appearing as a peak with high intensity in negative ESI-MS at m/z 97 corresponding to $[\text{HSO}_4]^-$ [217]), which provides convincing evidence of the thiophene ring cleavage.

Moreover, the presence of a variety of aliphatic sulfonic acids may be explained based on the photo-oxidation studies of sulfides. It is known that the photo-oxidation reactions of dialkyl, alkylphenyl and diaryl sulfides with singlet oxygen ($^1\text{O}_2$), generated by the photosensitized conversion of triplet oxygen to $^1\text{O}_2$, yield the corresponding sulfoxide and sulfone [218]. However, Banchereau et al. [219] have photo-oxidized dimethylsulfide and dibutylsulfide in aqueous acetonitrile and reported the production of the corresponding sulfonic acid and sulphuric acid with the intermediate formation of the corresponding sulfoxide followed by the sulfone. In addition, methanoic and butanoic acids were also produced and were suggested to be formed by the oxidation of the corresponding alkyl radicals.

8.3. Summary

The production of many aliphatic and aromatic acids and alcohols in addition to various aliphatic and aromatic sulfonic acids reveal that the PASHs undergo three types of photodegradation pathways, including the oxidation of the alkyl chain, the oxidation of the benzo ring and the oxidation of the thiophene ring. The pathways discussed here which are independent of the aromatic ring structure, except those concerning the thiophene ring oxidation, should be equally relevant and hence applicable to polycyclic aromatic hydrocarbons.

9. Characterization of PASHs after photo-oxidation

Despite the fact that much attention was directed to the photo-oxidation of PAHs, only very little is so far known about the photo-oxidation of PASHs [94, 98-105] although they frequently constitute 10-30 % of the PAHs and that they are more readily bioconcentrated than sulfur-free PAHs [220] in addition to their important use as environmental source markers [221-223]. In the present work, we attempt to simulate the photo-oxidation of the PASH fraction of crude oil and to investigate the changes in the distributions of non-oxidized low- and high-molecular weight sulfur compounds that can take place in the marine environment after an oil spill using GC-MS and FT-ICR MS.

9.1. Characterization of PASHs after 10 days photo-oxidation by GC-MS

9.1.1. Experimental section

9.1.1.1. Crude oil fractionation

About 1 g of an Egyptian crude oil (1 % sulfur) was fractionated by column chromatography into saturates and aromatics as described in section (8.1.1). The saturate fraction was collected using 120 ml n-heptane as eluent and the aromatic one was eluted by 360 ml of a mixture of n-heptane and toluene (2:1).

9.1.1.2. Standard compounds

Most of the reference compounds used except a few were synthesized in our laboratory [224].

9.1.1.3. Fractionation of the aromatic fraction into PAHs and PASHs

The aromatic fraction of the Egyptian crude oil was separated into PAHs and PASHs by following the same procedure described in section (7.3.3.1).

9.1.1.4. Photo-oxidation of the PASH fraction

After the separation of the PASH fraction, about 15 mg was dissolved in 5 ml cyclohexane and added to 100 ml distilled water and was irradiated for 10 days by the mercury middle pressure lamp. A dark control containing 10 mg of the PASH fraction was prepared the same way but kept in dark.

9.1.1.5. Liquid-liquid extraction

After photo-oxidation, the polar photoproducts of the PASH fraction were separated from the non-polar ones by liquid-liquid extraction. In a separatory funnel, the photo-oxidized solution was made alkaline by adding sodium carbonate (till pH = 11) then the non-polar photoproducts were extracted using 60 ml dichloromethane (15 ml x 4). The solvent was then evaporated on a rotary evaporator till 3 ml and was then injected on GC-FID and GC-MS. The same procedure was also followed for the dark control and the PASH fraction was injected on GC-FID and GC-MS. The detailed analysis scheme is presented in Figure 9.1.

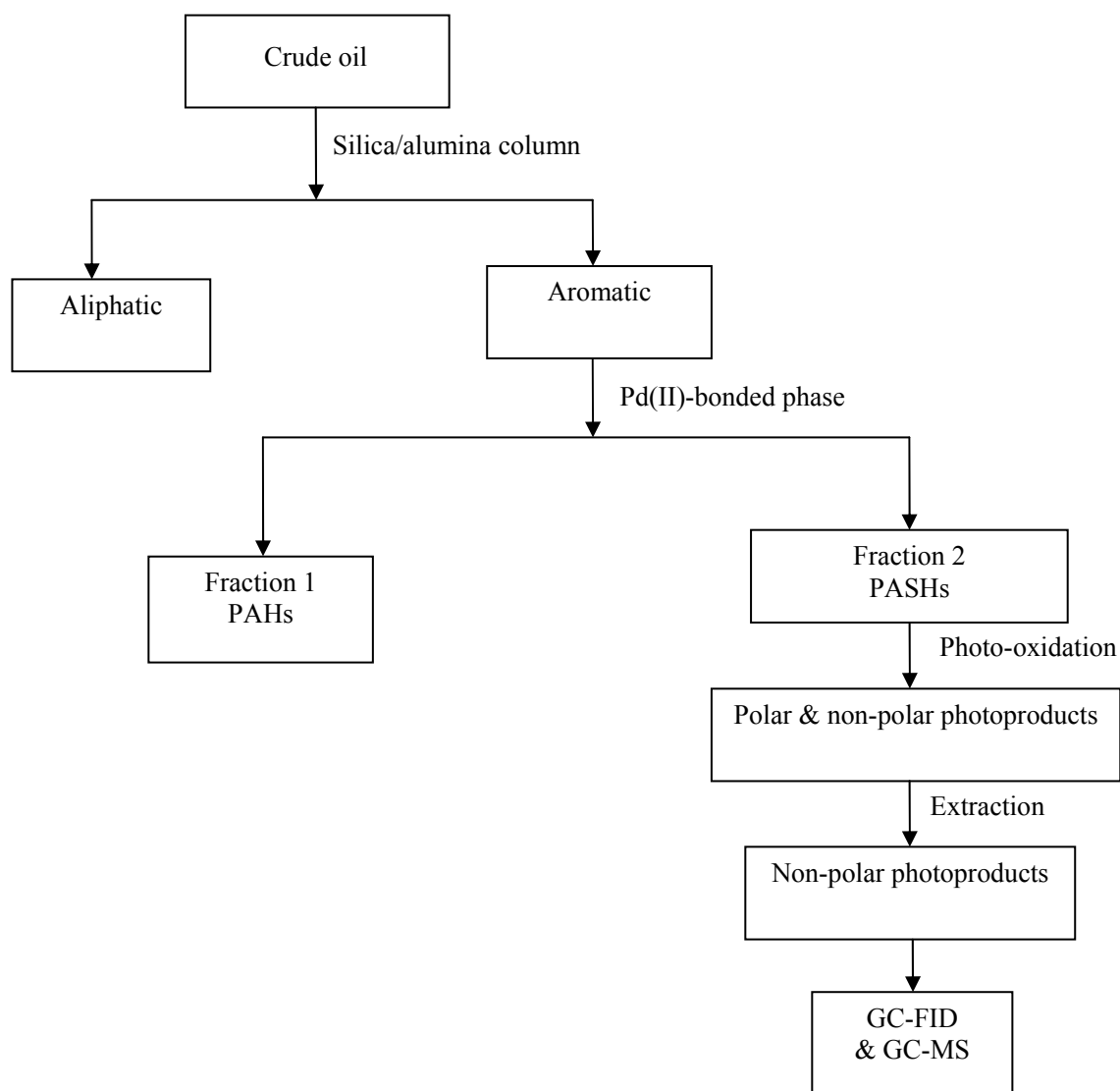


Figure 9.1. Analysis scheme of non-polar photoproducts of PASHs.

9.1.2. Results and discussion

9.1.2.1. The dark control

The GC-MS chromatogram (Figure 7.12 in chapter 7) of PASHs showed a mixture of substituted benzothiophenes and dibenzothiophenes. These sulfur aromatic heterocycles are mainly represented by isomers of mono-(MBT), di-(DMBT), tri-(TMBT) and tetramethylbenzothiophenes (TeMBT) as well as dibenzothiophene (DBT), mono-(MDBT), di-(DMDBT), tri-(TMDBT) and tetramethyldibenzothiophenes (TeMDBT). Identification of the benzothiophenes and dibenzothiophenes was based on comparison of their GC retention times with authentic standards synthesized in our laboratory and with published data [225, 226].

Benzothiophenes

Four characteristic groups of peaks found in the GC-MS chromatogram (Figure 9.2) correspond to MBT, DMBT, TMBT and TeMBT. By the close inspection of Figure 9.2, it is clear that the TMBTs have the highest abundance among the benzothiophenes. A closer inspection of the benzothiophenes distribution pattern (Figure 9.3) reveals that 3- + 4-MBT is more abundant than 2-MBT (see Table 9.1), 2,3-DMBT is the most abundant compound among the DMBTs and that 2,3,7-TMBT is the most abundant one among the TMBTs.

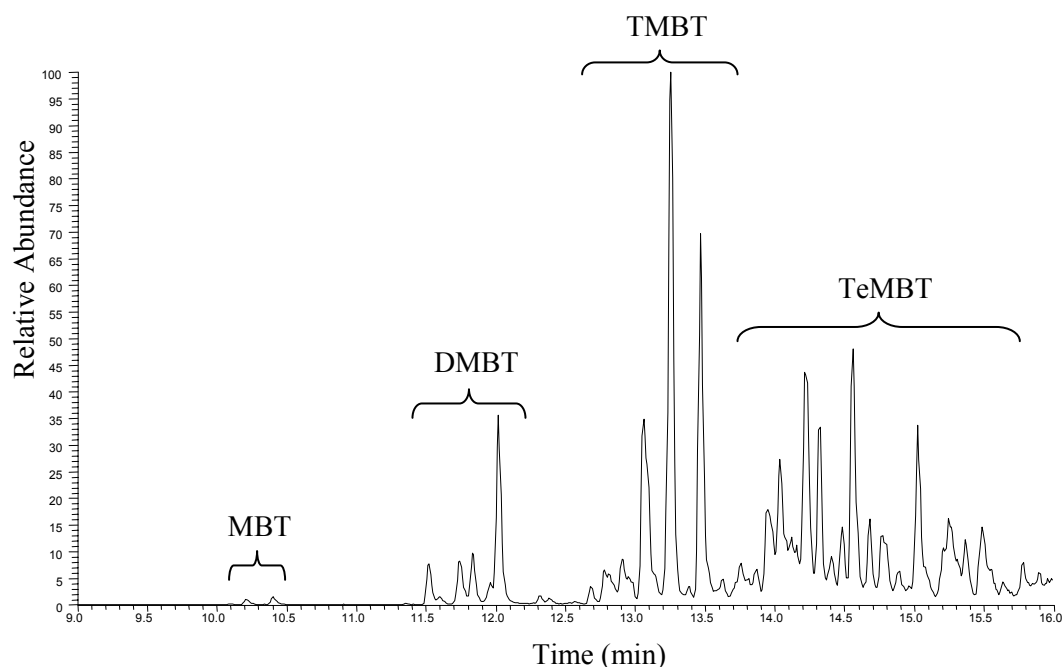


Figure 9.2. GC-MS chromatogram of benzothiophenes in the Egyptian crude oil.

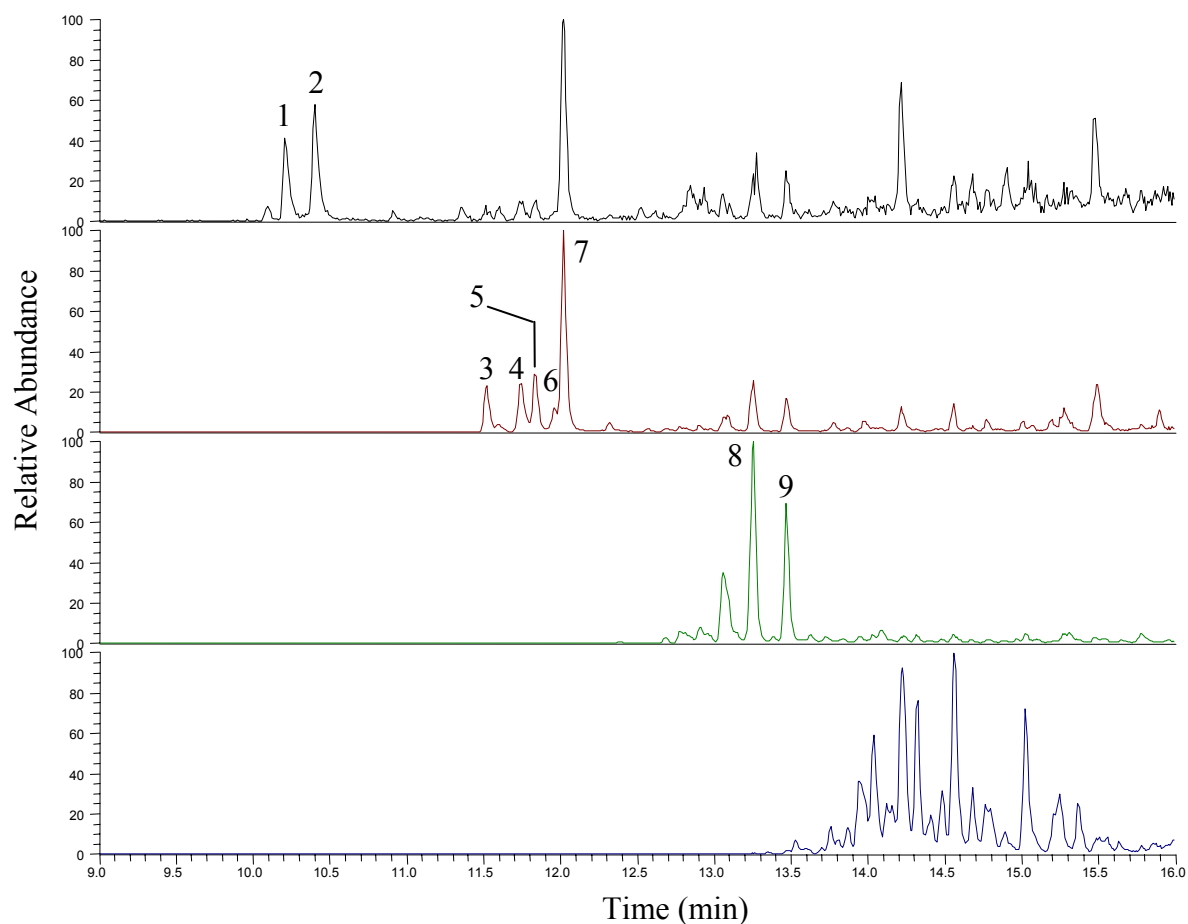


Figure 9.3. GC-MS chromatograms of benzothiophenes (m/z 148, 162, 176 and 190, from the top) of the Egyptian crude oil.

Table 9.1. List of benzothiophenes identified in the Egyptian crude oil

<i>Peak</i>	<i>Compound</i>
1	2-Methylbenzothiophene
2	3- + 4-Methylbenzothiophene
3	2,7-Dimethylbenzothiophene
4	2,6- + 3,7- + 4,7-Dimethylbenzothiophenes
5	4,6-Dimethylbenzothiophene
6	3,5-Dimethylbenzothiophene
7	2,3-Dimethylbenzothiophene
8	2,3,7-Trimethylbenzothiophene
9	2,3,5-Trimethylbenzothiophene

Dibenzothiophenes

Figure 9.4 shows the GC-MS chromatogram of dibenzothiophenes. Here, five characteristic groups of peaks can be observed, which can be attributed to DBT, MDBT, DMDBT, TMDBT and TeMDBT. Moreover, a close inspection of DBTs (Figure 9.5) shows that the abundance of the monomethyldibenzothiophenes is decreasing in the following order: 4-MDBT > 2- + 3-MDBT > 1-MDBT (see Table 9.2). In addition, the 3,6-DMDBT and 2,4,6-TMDBT are the most abundant compounds present among the dimethyldibenzothiophenes and trimethyldibenzothiophenes, respectively.

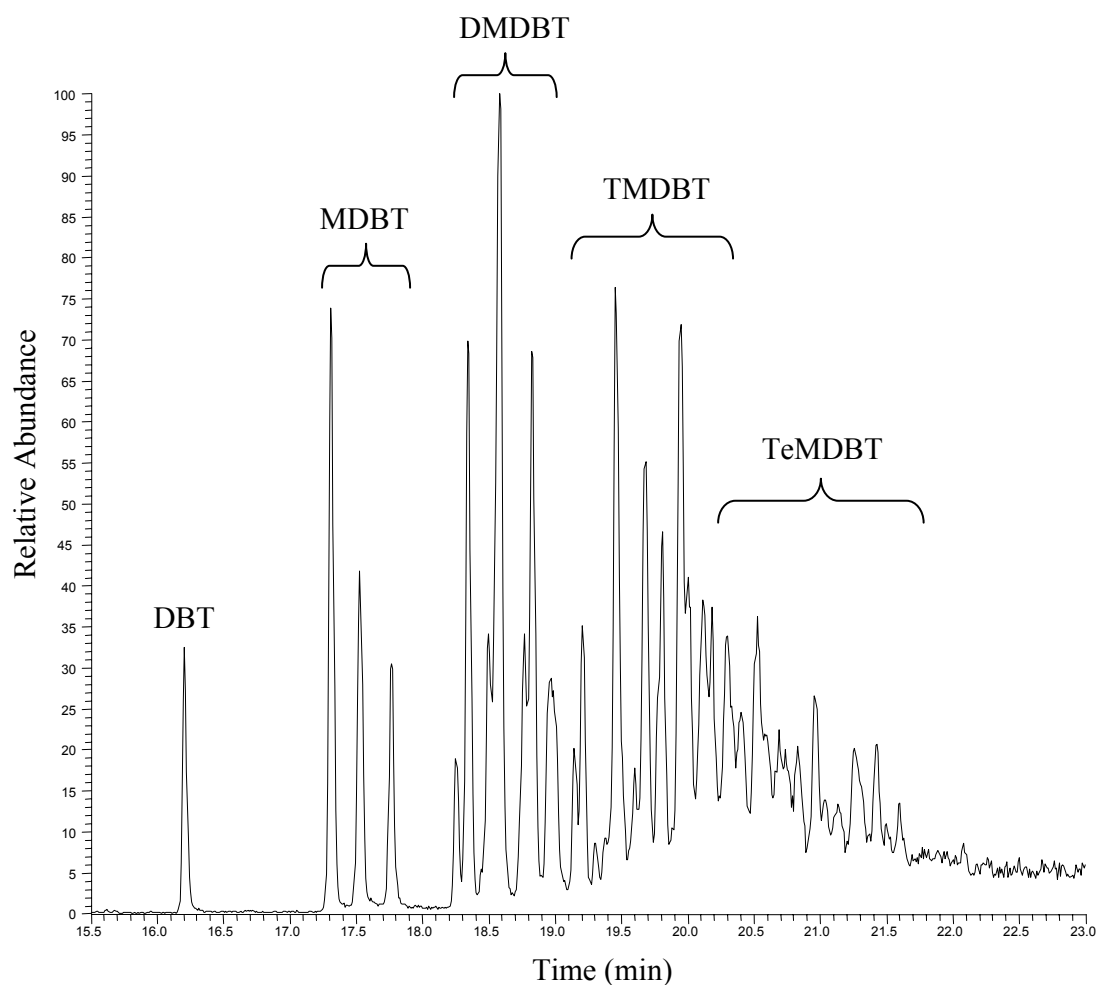


Figure 9.4. GC-MS chromatogram of dibenzothiophenes in the Egyptian crude oil.

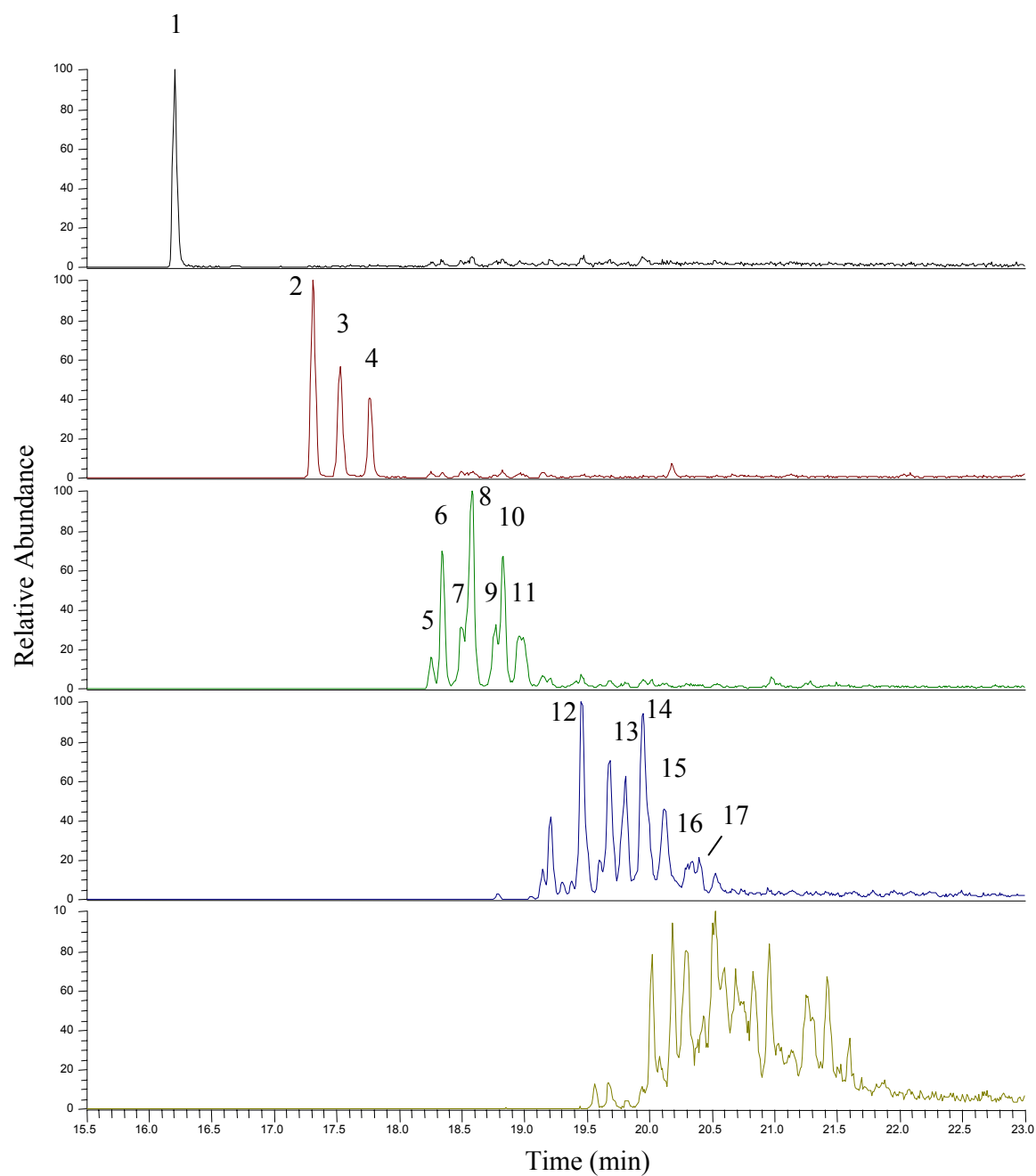


Figure 9.5. GC-MS chromatograms of dibenzothiophenes (m/z 184, 198, 212, 226 and 240, from the top) in the Egyptian crude oil.

Table 9.2. List of dibenzothiophenes identified in the Egyptian crude oil

<i>Peak</i>	<i>Compound</i>
1	Dibenzothiophene
2	4-Methyldibenzothiophene
3	2- + 3-Methyldibenzothiophenes
4	1-Methyldibenzothiophene
5	4-Ethyldibenzothiophene
6	4,6-Dimethyldibenzothiophene
7	2,4- + 2,6-Dimethyldibenzothiophenes + 2-Ethyldibenzothiophene
8	3,6-Dimethyldibenzothiophene
9	2,7- + 2,8- + 3,7-Dimethyldibenzothiophenes
10	1,4- + 1,6- + 1,8-Dimethyldibenzothiophenes
11	1,3- + 3,4- + 1,7-Dimethyldibenzothiophenes
12	2,4,6-Trimethyldibenzothiophene
13	2,4,7- + 2,4,8-Trimethyldibenzothiophenes
14	1,4,8-Trimethyldibenzothiophene
15	1,4,7-Trimethyldibenzothiophene
16	1,3,7-Trimethyldibenzothiophene
17	3,4,7-Trimethyldibenzothiophene

9.1.2.2. PASHs after 10 days photo-oxidation

The first impression that emerges from examining the GC-MS chromatograms of the PASH fraction in the dark control and that after 10 days photo-oxidation (Figure 9.6) is the obvious photodegradation of benzothiophenes in comparison to dibenzothiophenes. A closer inspection of the benzothiophenes distribution pattern after 10 days photo-oxidation is given in Figure 9.7. When the chromatogram of benzothiophenes from the dark control is compared with that after 10 days photo-oxidation, it is apparent that the photo-oxidation has nearly removed the 2-MBT and 3- + 4-MBT (peaks 1 and 2). For the dimethylbenzothiophenes, there has been some degradation of 2,3-DMBT and 2,6- + 3,7- + 4,7-DMBT as indicated by the relative reduction in the heights of the peaks 7 and 4, respectively. In case of trimethylbenzothiophenes, 2,3,5-TMBT was the most susceptible one to photodegradation followed by 2,3,7-TMBT and the compound A which can be easily recognized from the reduced peak heights of these compounds in the chromatogram after 10 days photo-oxidation in comparison with that of the dark control. A significant decrease in the peak heights of the

tetramethylbenzothiophene compounds B and C after 10 days photo-oxidation was also observed relative to those in the dark control.

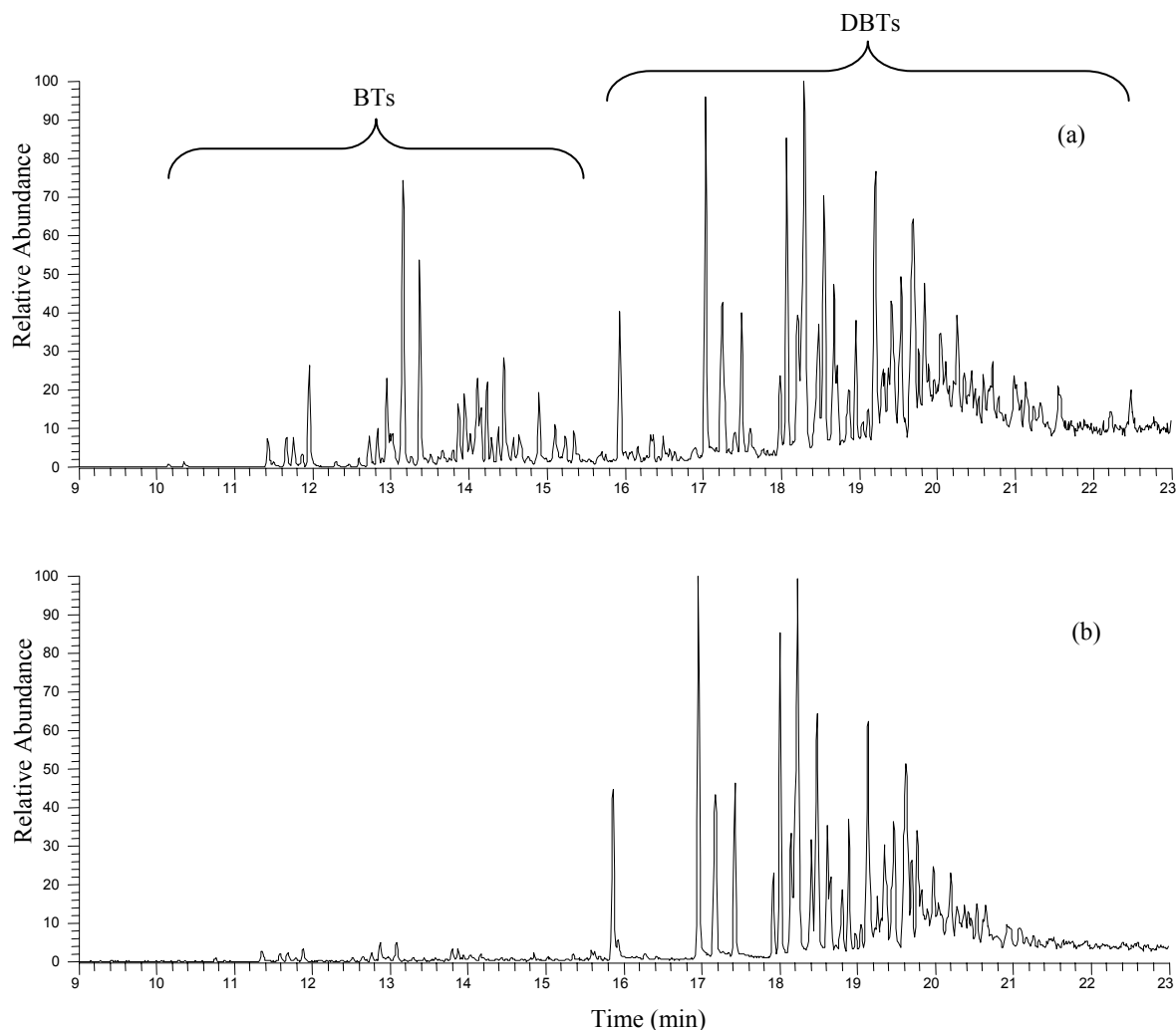


Figure 9.6. GC-MS chromatograms of the PASH fraction in the dark control (a) and after 10 days photo-oxidation (b).

The distribution pattern of the dibenzothiophenes after 10 days photo-oxidation is shown in Figure 9.8. It can be seen that very little changes have occurred to the dibenzothiophenes after 10 days photo-oxidation in comparison to the dark control. Moreover, the most pronounced photodegradation effect could be clearly seen in the trimethyldibenzothiophenes, namely in 2,4,6-TMDBT and 2,4,7- + 2,4,8-TMDBT (peak 12 and 13 respectively).

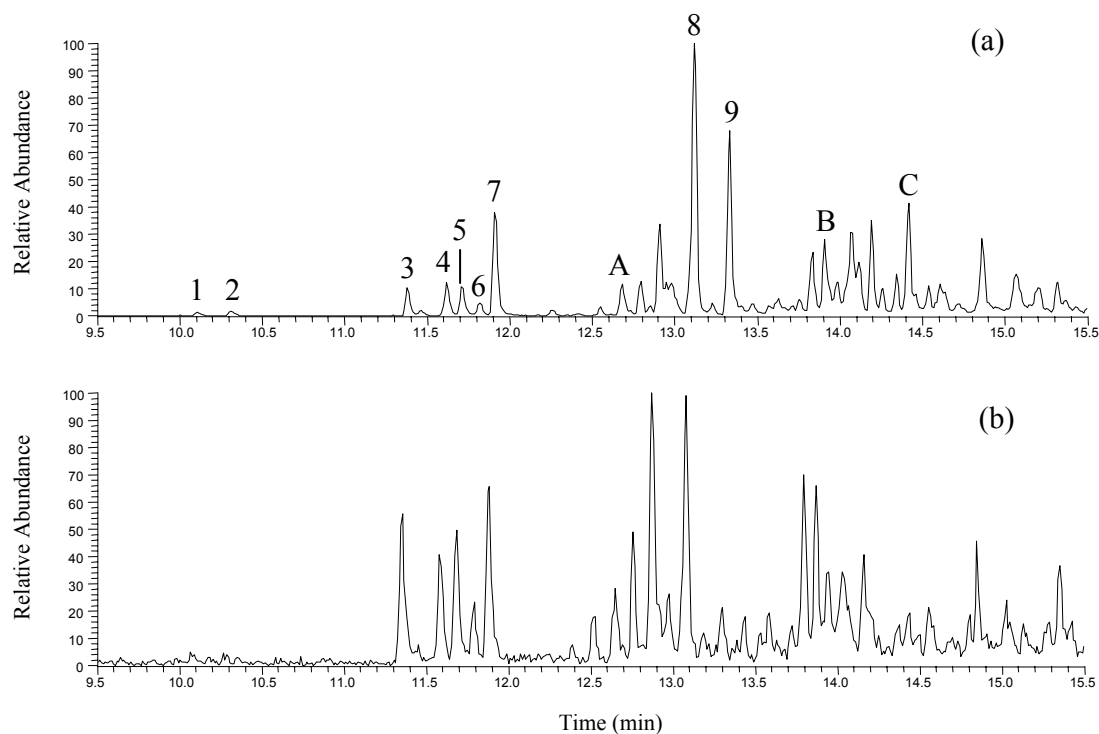


Figure 9.7. GC-MS chromatogram showing the benzothiophenes in the dark control (a) and after 10 days photo-oxidation (b). Numbered compounds are listed in Table 9.1.

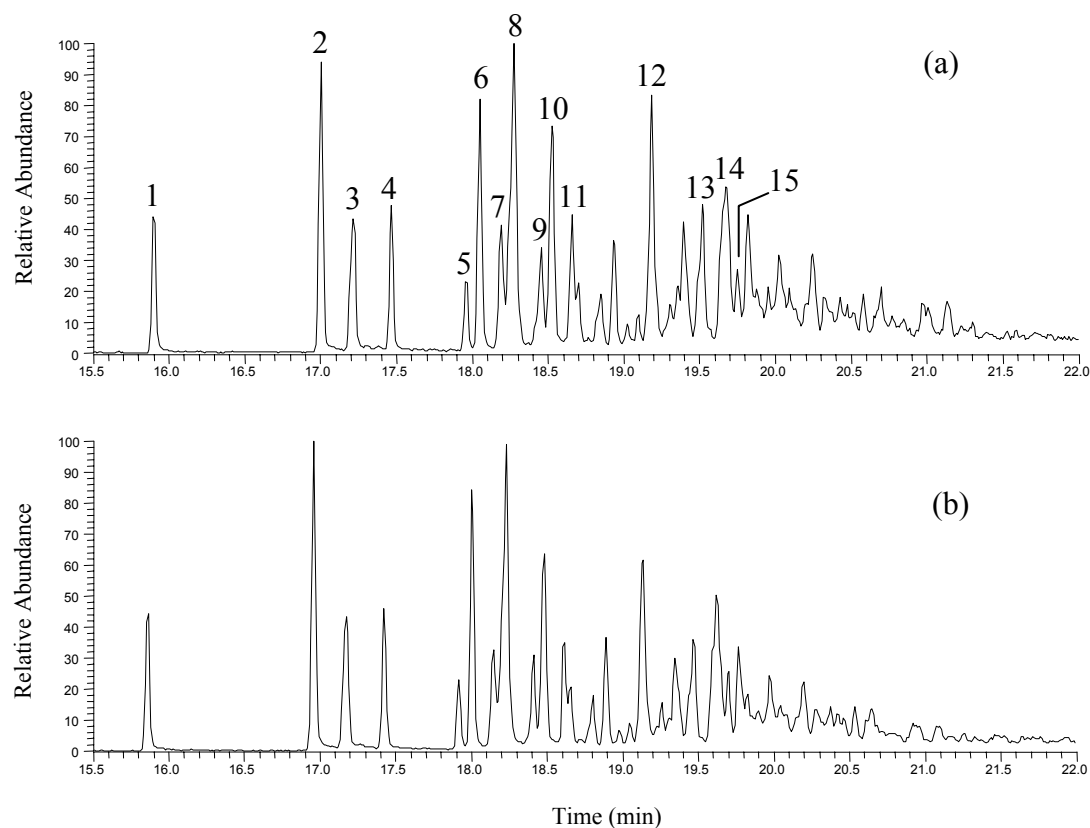


Figure 9.8. GC-MS chromatogram showing the dibenzothiophenes in the dark control (a) and after 10 days photo-oxidation (b). Numbered compounds are listed in Table 9.2.

Hence, by comparing the chromatograms of benzothiophenes and dibenzothiophenes in the dark control with those after 10 days photo-oxidation, it could be deduced that benzothiophenes are more susceptible to photo-oxidation than dibenzothiophenes. Moreover, it was observed that the alkylated benzothiophenes and dibenzothiophenes were more easily photodegradable than their parent compounds. This is in agreement with Ehrhardt et al. [227] and Prince et al. [228] who also showed that alkyl substituted polynuclear aromatic hydrocarbons are photo-oxidized more rapidly than the unsubstituted parent compounds. It can be also seen from the chromatograms of BTs and DBTs that increasing their alkylation renders them more susceptible to photodegradation. These results are also consistent with those of Ganjali et al. [195] who showed that increasing the alkyl substitution of naphthalene, phenanthrene and dibenzothiophene increased their sensitivity to photo-oxidation and lead to the photodegradation of 50 % of the trimethylated compounds.

9.2. Characterization of PASHs after 2 and 10 days photo-oxidation by FT-ICR MS

9.2.1. Experimental section

9.2.1.1. Crude oil fractionation

About 1 g of an Egyptian crude oil (1 % sulfur) was fractionated by column chromatography into saturates and aromatics. The saturate fraction was collected using 120 ml n-heptane as eluent and the aromatic one was eluted by 360 ml of a mixture of n-heptane and toluene (2:1) as described in section 8.1.1. The detailed analysis scheme is presented in Figure 9.9.

9.2.1.2. Photo-oxidation of the aromatic fraction

After the separation of the Egyptian crude oil into aliphatic and aromatic fractions, about 69 and 103 mg of aromatic fraction was dissolved in 2 and 5 ml cyclohexane and added to 100 ml distilled water and was irradiated, each one separately, for 2 days and 10 days, respectively by the mercury middle pressure lamp. A dark control containing 50 mg of the aromatic fraction was prepared in the same way but kept in dark.

9.2.1.3. Liquid-liquid extraction

After photo-oxidation for 2 and 10 days, the polar photoproducts of the aromatic fraction were separated from the non-polar ones by liquid-liquid extraction. In a separatory funnel, the photo-oxidized solution was made alkaline by adding sodium carbonate (till pH = 11) then the

non-polar photoproducts were extracted using 60 ml dichloromethane (15 ml x 4). The solvent was then evaporated on a rotary evaporator till 1 ml, and was further evaporated by a stream of nitrogen till dryness.

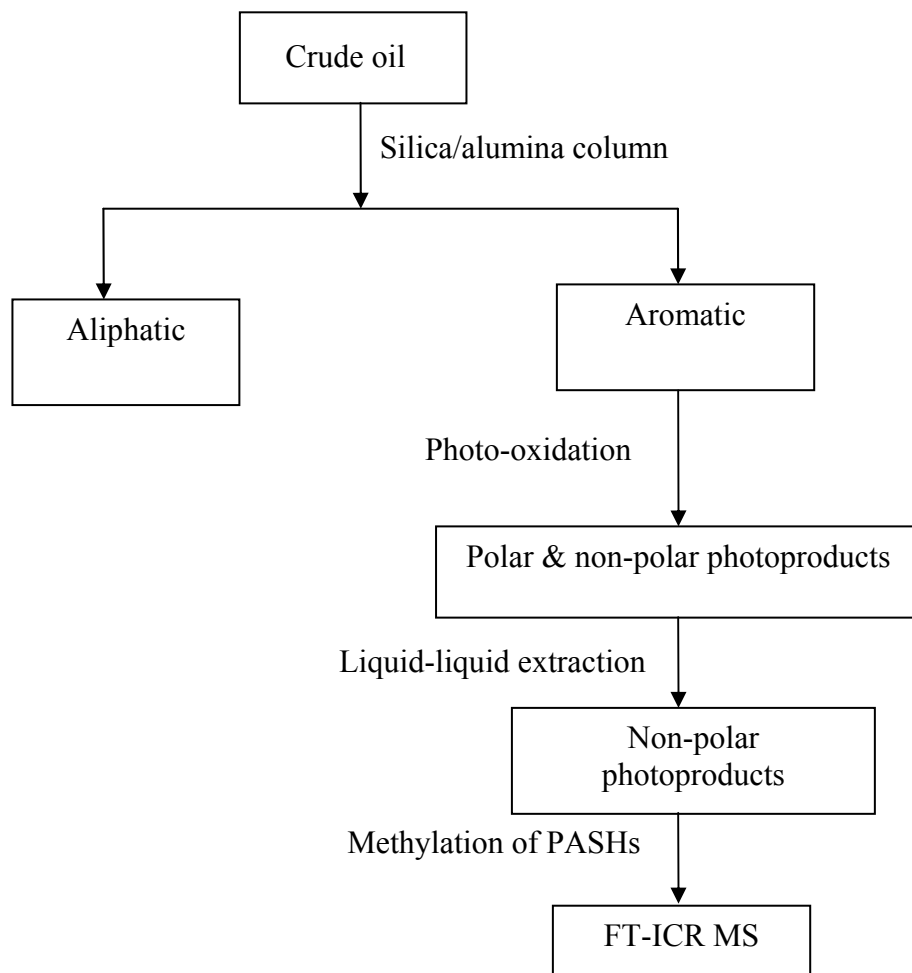


Figure 9.9. Analysis scheme of non-polar photoproducts of PASHs.

9.2.1.4. Sulfur selective methylation

To about 36 mg of the non-polar products of the aromatic fraction extracted after 2 and 10 days photo-oxidation, an excess of methyl iodide (50 μ l) and silver tetrafluoroborate (40 mg) was added in 3 ml of 1,2-dichloroethane. The mixture was stirred for 48 h at room temperature to ensure the complete methylation of all sulfur compounds in the sample. Then, the filtrate was collected and the solvent was evaporated by a stream of nitrogen to obtain methyl thiophenium salts [182, 229]. The same methylation procedure was performed on the dark control.

9.2.1.5. High resolution mass spectrometry

Mass spectra were acquired using an APEX III Fourier transform ion cyclotron resonance mass spectrometer (Bruker Daltonics, Bremen, Germany) equipped with a 7 T actively shielded super conducting magnet and an Agilent ESI source. The samples were introduced in a 1:1 (v/v) solution of dichloromethane/acetonitrile and injected in the infusion mode with a flow rate of 2 $\mu\text{l}/\text{min}$ detecting positive ions. The spray voltage was maintained at 4.5 kV. After ionization, the ions were accumulated for 0.5 s in the octapole before transfer to the cyclotron cell. For a better signal-to-noise ratio, at least 64 scans were accumulated. Internal and external calibrations were done using a mixture of the Agilent electrospray calibration solution of masses 622.02896 and 922.00980 with the addition of indolacrylic acid of masses 397.11589 $[2\text{M}+\text{Na}]^+$ and 584.17923 $[3\text{M}+\text{Na}]^+$ covering the whole range of masses in the samples. All the measurements by FT-ICR mass spectrometer were performed in collaboration with Max-Planck-Institute of coal research, Mülheim, Germany. Figure 9.10 shows the high resolution mass spectra of PASHs in the dark control and after 2 and 10 days photo-oxidation.

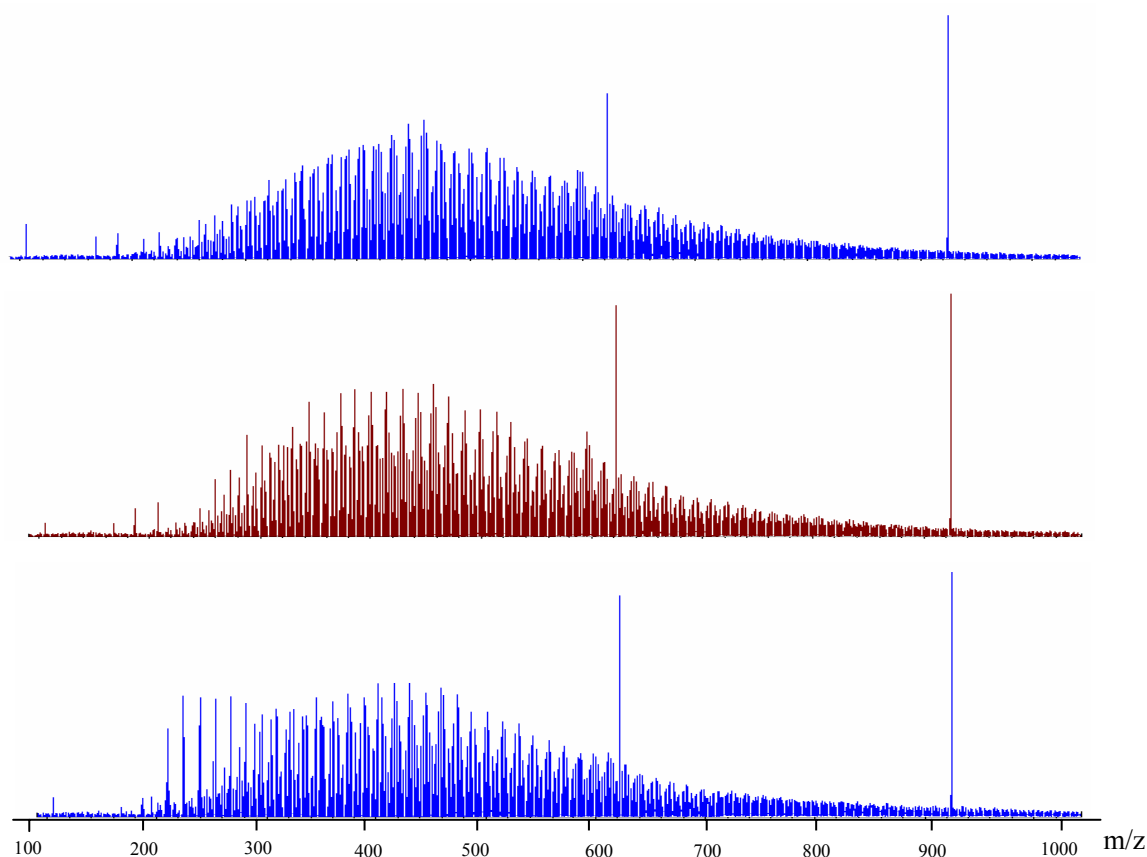


Figure 9.10. High resolution mass spectra of PASHs (from top to bottom): in the dark control, after 2 days photo-oxidation and after 10 days photo-oxidation.

9.2.1.6. Data analysis

All the data obtained from the mass spectrometer were imported into an Excel spreadsheet. Each signal in the mass spectrum corresponds to the methylated form of parent masses. In order to assign elemental composition of components present in crude oils, all the masses measured as $[M+CH_3]^+$ were converted to neutral masses by subtracting 15.02293 from the measured masses. Then IUPAC masses were converted to the Kendrick mass scale [174] and Kendrick masses were further sorted according to the procedure explained in Chapter 5.

9.2.2. Results and discussion

9.2.2.1. Characterization of monosulfur PASHs

9.2.2.1.1. Monosulfur PASHs in the dark control

The monosulfur PASHs of the aromatic fraction show a DBE value between 1 and 14 (Figure 9.11), which permits up to 5 condensed aromatic rings. The Egyptian oil clearly exhibits a wide alkyl carbon distribution as well as a high average number of alkyl carbons. The mass range for all monosulfur compounds in this oil goes from ca 172 Da to 940 Da.

It is important to note that for the lowest DBEs, practically only one parent ring system is likely (crude oils rarely contain appreciable amounts of alkenes so that the DBE is essentially made up of the number of rings and the number of aromatic double bonds), but for higher DBEs, several parent ring systems are a possibility. At $DBE > 9$, the number of possible parent systems becomes very large and a lack of published data on such high-boiling materials makes comparison difficult.

The first and second row in the Kendrick plot represent compounds having DBE value of 1 and 2 which are the tetrahydrothiophenes and dihydrothiophenes (see Table 9.3 for a description of the parent structures for the homologous series). The lowest mass recorded for tetrahydrothiophenes and dihydrothiophenes is 172 and 212, respectively, while the highest one for each is 578 and 660, respectively. These compounds have a relatively low abundance, as can be seen from the size of the circles in the Kendrick plot. The intensity of the mass spectrometric signals or the abundance of the compounds is represented in the Kendrick plot by the size of the circles.

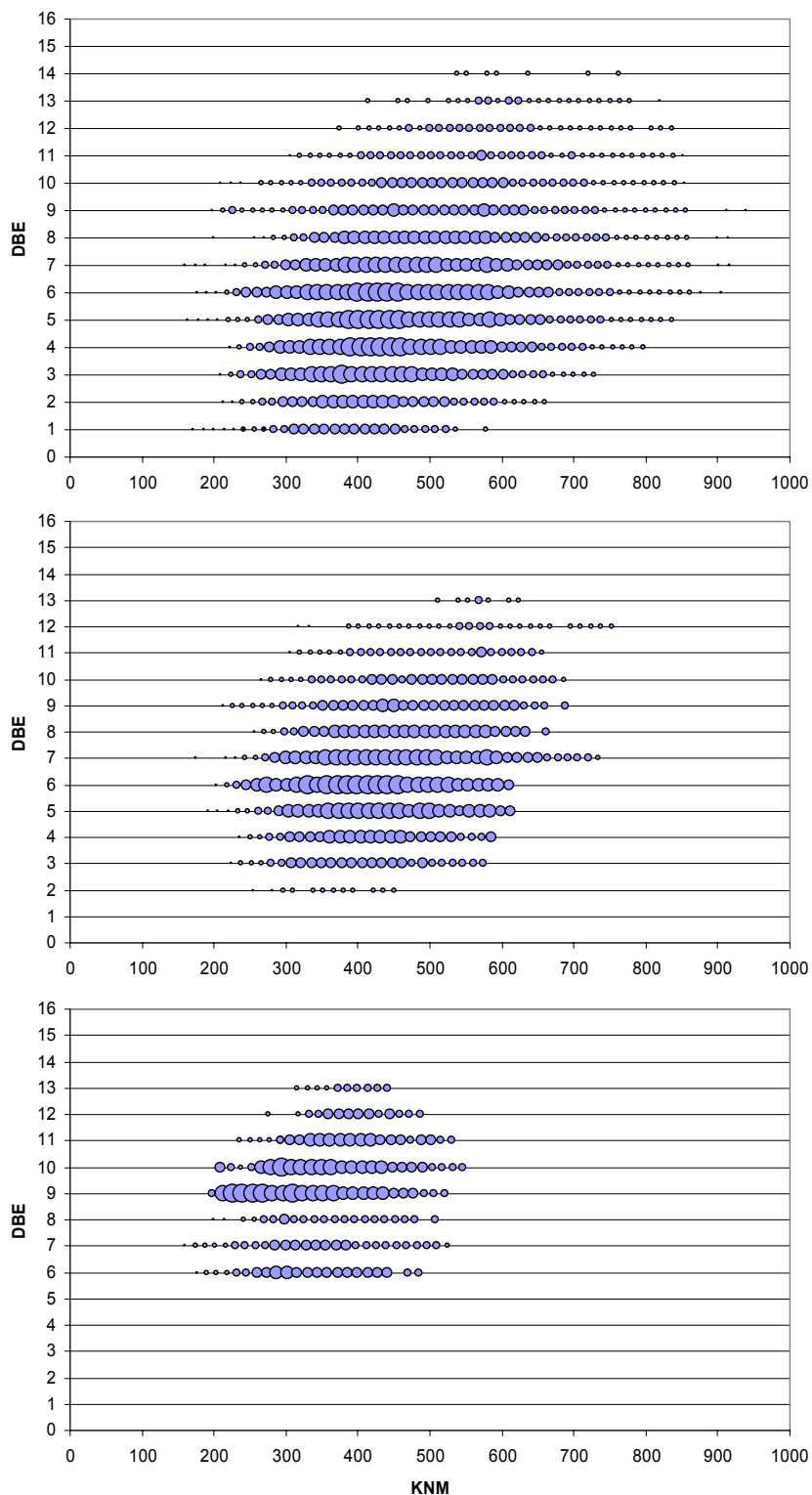


Figure 9.11. Kendrick plots of monosulfur PASHs (from top to bottom) in dark control, after 2 days photo-oxidation and after 10 days photo-oxidation.

Compounds with DBE value of 3, 4 and 5 are the thiophenes, naphthenothiophenes and cycloalkenothiophenes respectively. The mass range for each series reaches up to 728, 796 and 836 Da respectively.

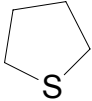
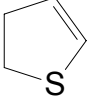
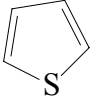
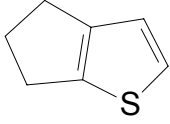
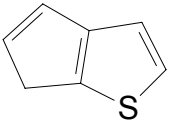
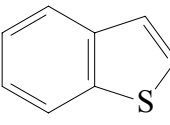
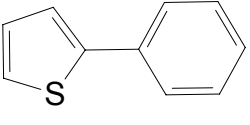
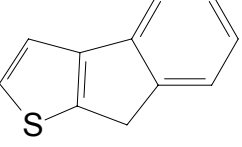
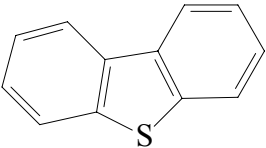
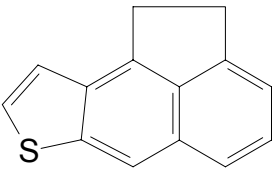
A major group of compounds appear at DBE = 6 as expected for benzothiophenes. Such compounds are among the most common sulfur species in crude oils. This series contains from 11 to 29 CH₂ groups in the side chains. The strong presence of benzothiophenes together with thiophenes, naphthenothiophenes and cycloalkenothiophenes illustrates that these compounds are the most abundant ones in this crude oil.

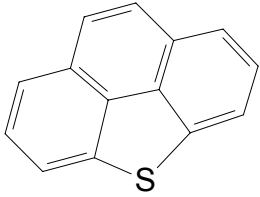
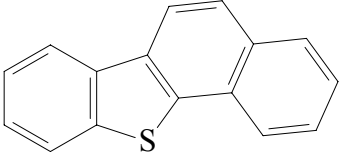
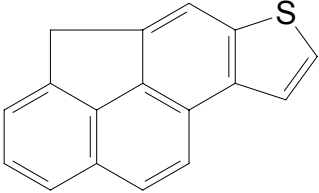
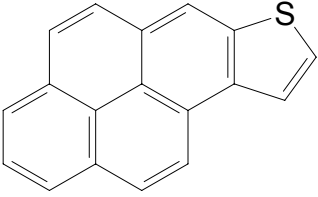
The next higher compound types of appreciable abundance having DBE equal to 7 are the phenylthiophenes together with the probability of other structures that contain non-condensed thiophenes. Compound classes with DBE = 8 include indenothiophenes and indanylthiophenes as well as benzothiophene with two naphthenic ring. Indenothiophenes can be regarded as bridged phenylthiophenes and indanylthiophenes are substituted thiophenes. Such compounds occur here in the mass range from 200 to 914 Da. Compounds of DBE 7 and 8 are observed as having fairly strong abundance in comparison to the remaining compounds having DBE values from 9 to 13.

DBE 9 most likely represent dibenzothiophenes (or benzothiophenes with 3 naphthenic rings) of KNM between 198 and 940 Da, indicating the presence of C₁- to C₅₄-dibenzothiophenes. They have a lower abundance compared to benzothiophenes. It should be noted that from mass spectrometric data alone, it is not possible to distinguish between dibenzothiophenes and the three isomeric naphthothiophenes, however, in crude oils naphthothiophenes are generally found in much lower quantities than dibenzothiophenes.

As the DBE increases, the probability of finding isomeric parent compounds increases to a greater extent. For instance, the next higher series (DBE = 10) might consist of acenaphthenothiophenes, benzothiophenes with a phenyl group as a substituent or dibenzothiophenes with a naphtheno ring. The compounds here have a KNM between 210 to 854 Da. DBE = 11 fits with phenanthrothiophenes, which are a class of compounds frequently found in fossil material. This series starts at a mass 306 and goes up to 852 Da.

Table 9.3. Parent structures for S1 homologous series, maximizing the number of aromatic rings

<i>Parent structure</i>	<i>Name</i>	<i>DBE</i>
	Tetrahydrothiophene	1
	Dihydrothiophene	2
	Thiophene	3
	Naphthenothiophene	4
	Cyclopentenothiophene	5
	Benzothiophene	6
	2-Phenylthiophene	7
	Indenothiophene	8
	Dibenzothiophene	9
	Acenaphthenothiophene	10

	Phenanthrothiophene	11
	Benzonaphthothiophene	12
	Phenanthronaphthenothiophene	13
	Pyrenothiophene	14

The next higher homologues are the benzonaphthothiophenes (DBE = 12) which are often identified in crude oils. The KNM of the compounds goes here from 374 to 836 Da. Here alkyl chains are found with 10 to 43 carbon atoms. DBE = 13 can correspond to benzonaphthothiophenes with one naphthene ring or dibenzothiophenes with one phenyl group as a substituent as well as several other parent systems. The lower KNM for a compound in this row is 414 Da while the highest one is 820 Da. Figure 9.11 indicates that from DBE = 10 to DBE = 13, the compounds in the different series have very low abundance.

The last class of compounds in this Kendrick plot is the class of pyrenothiophenes at DBE = 14. There are only relatively few points in Figure 9.11 that correspond to such ring systems.

It is noteworthy that the highest mass increases gradually starting from DBE 1 compounds having KNM equal to 578 Da till DBE = 9 class having KNM equal to 940 Da then it starts to decrease from the dibenzothiophene series till it reaches 762 Da in case of DBE 14. In this crude oil, the highest DBE value found for S1 compounds was 14 and the highest mass was 940 Da.

9.2.2.1.2. Monosulfur PASHs after 2 days photo-oxidation

By comparing the PASH distribution pattern after 2 days photo-oxidation with that of the dark control (Figure 9.11), it is obvious that photodegradation has a big impact on the high molecular weight compounds in the different classes with the preferential loss of long alkyl side chains (Table 9.4). A shift toward lower masses of high mass components (> 660 Da) is clearly evident.

Figure 9.11 shows that photo-oxidation of the crude oil after 2 days exhibited the complete depletion of two classes of compounds, namely DBE = 1 (tetrahydrothiophenes) and DBE = 14 (i.e. pyrenothiophenes).

Table 9.4. Depletion of monosulfur PASHs after 2 and 10 days photo-oxidation

<i>Series</i>	<i>Photodegraded compounds after 2 days (*)</i>	<i>Photodegraded compounds after 10 days (*)</i>
Tetrahydrothiophenes	All compounds	depleted after 2 days photo-oxidation
Dihydrothiophenes	C ₂₇ -C ₄₁	All compounds
Thiophenes	C ₃₆ -C ₄₆	All compounds
Naphthenothiophenes	C ₃₅ -C ₄₉	All compounds
Cycloalkenothiophenes	C ₃₆ -C ₅₁	All compounds
Benzothiophenes	C ₃₅ -C ₅₅	C ₂₆ -C ₅₅
Phenylthiophenes	C ₄₂ -C ₅₄	C ₂₇ -C ₅₄
Indenothiophenes	C ₃₆ -C ₅₃	C ₂₅ -C ₅₃
Dibenzothiophenes	C ₃₇ -C ₅₄	C ₂₅ -C ₅₄
Acenaphthenothiophenes	C ₃₅ -C ₄₆	C ₂₅ -C ₄₆
Phenanthrothiophenes	C ₃₃ -C ₄₆	C ₂₄ -C ₄₆
Benzonaphthothiophenes	C ₃₈ -C ₄₃	C ₁₉ -C ₄₃
Phenanthronaphthothiophenes	C ₂₈ -C ₄₁	C ₁₅ -C ₄₁
Pyrenothiophenes	All compounds	depleted after 2 days photo-oxidation

(*) Depletion is calculated relative to the dark control.

Interestingly, DBE 14 compounds (i.e. pyrenothiophenes) were the first condensed thiophenes to be completely photodegraded after two days followed by the photodegradation of the remaining sulfur heterocycles with variable rates. Hence, aromatic compounds are particularly sensitive to photo-oxidation and increasing the size of these compounds will increase their sensitivity to photochemical oxidation. These results are in accordance with those of Kochany and Maguire [230], Garrett et al. [231] and Guieysse et al. [232] who reported that compounds with higher molecular weight and more condensed aromatic rings have a higher rate of photolysis than smaller and less condensed ones. This is mostly due to the fact that the absorption maxima are shifted to longer wavelengths with increasing molecular size. Furthermore, Guieysse and Viklund [233] have studied the photodegradation of some polycyclic aromatic hydrocarbons and showed that the rate of their degradation was in the following order: benzo[*a*]pyrene > benzo[*a*]anthracene > fluoranthrene > pyrene > phenanthrene > fluorene. In addition, the photo-oxidation of an Arabian light crude oil for four weeks led to the photodegradation of about 95 % of di- and tri-*n*-alkylbenzothiophenes in the C₁₁-C₃₀ range [234].

Tetrahydrothiophenes showed also high reactivity towards photo-oxidation as they have been completely photodegraded after 2 days irradiation. This is in agreement with the studies of Banchereau et al. [219] on the photo-oxidation reactions of sulfides, in which the sulfides were easily photo-oxidized in the presence of oxygen yielding the corresponding sulfoxide, sulfone, and sulfonic acids and sulphuric acids as final products.

9.2.2.1.3. Monosulfur PASHs after 10 days photo-oxidation

An increase in the abundance of short alkyl chain dibenzothiophenes and acenaphthenothiophenes and a complete depletion of their long alkyl chain compounds were observed in comparison to the dark control (Figure 9.11). This reveals that these homologues appear to be quite resistant to photo-oxidation and thus can accumulate in the environment, whereas other species such as dihydrothiophenes, thiophenes, naphthenothiophenes and cycloalkenothiophenes were completely photodegraded after 10 days. Thus, it can be deduced that non-condensed thiophenes are very reactive toward photo-oxidation, and therefore were the first sulfur compounds to be completely depleted.

Furthermore, as can be seen in Figure 9.11, the most abundant classes are dibenzothiophenes and acenaphthenothiophenes. The relative abundance of the other homologues in this

Kendrick plot is in the following order: DBE 9 (dibenzothiophenes), DBE 10 (i.e. acenaphthenothiophenes) > DBE 6 (benzothiophenes), DBE 11 (i.e. phenanthrothiophenes) > DBE 7 (i.e. phenylthiophenes), DBE 8 (i.e. indenothiophenes) and DBE 12 (i.e. benzonaphthothiophenes) > DBE 13 (i.e. phenanthronaphthothiophenes).

9.2.2.2. Characterization of disulfur PASHs

Disulfur PASHs have been reported to be present in coal and shale oil [17, 235-240]. For instance, a series of C₁₅-C₂₄ 3,6-dialkyl-1,2-dithianes and two isomers of C₂₀ isoprenoid 1,2-dithianes have been identified in the bitumen of a bituminous shale from the Venio del Gesso basin (Italy) and in immature sediments from the Peruvian upwelling region and the Venio del Gesso basin, respectively [236, 237]. C₂₀ members of 5,5'-dialkyl-2,2'-bithiophenes and three C₂₀ isoprenoid bithiophenes have been also tentatively identified in Rozel Point seep oil [238] and in Rozel Point oils [17, 238, 239]. Furthermore, the latter compounds were also found in a number of other oils [240]. Moreover, small amounts of C₀-C₂ thienothiophenes and C₀-C₁ bithiophenes have been reported to be present in Rasa coal in addition to a series of C₀-C₆ thienobenzo[*b*]thiophenes, C₀-C₂ thienodibenzothiophenes and C₀-C₂ thienonaphthothiophenes [235]. However, as previously stated by Sinninghe Damste' and de Leeuw [235], the full identification of disulfur compounds is nearly impossible due to the increasing number of possible isomers with the increase in the number of alkylation. Moreover, there are no published data to show how these compounds are altered in the environment after spillage of petroleum, as in the case of monosulfur PASHs.

9.2.2.2.1. Disulfur PASHs in the dark control

Figure 9.12 shows the distribution of disulfur compounds as a function of DBE and KNM. The disulfur (S₂) PASHs detected were in the range 10 >DBE ≥ 5 with dominant KNM from 400 to 800 Da (Figure 9.12). The mass range for all disulfur compounds in this oil goes from ca 266 Da to 840 Da.

The disulfur PASHs fraction without photo-oxidation contains compounds having DBE = 5 series, which are most likely thienothiophene homologues (two condensed thiophene rings) with 7-48 additional methylene groups (see Table 9.5 for a description of some examples of the parent structures for the homologous series). The non-photooxidized disulfur fraction exhibits a DBE = 6 series with carbon numbers ranging from 14 to 17, most likely bithiophenes with KNM range from 306 to 810 Da, representing 10-46 additional methylene

groups. The lowest mass recorded for compounds with DBE = 7 is 402 Da and the highest one is 780 Da.

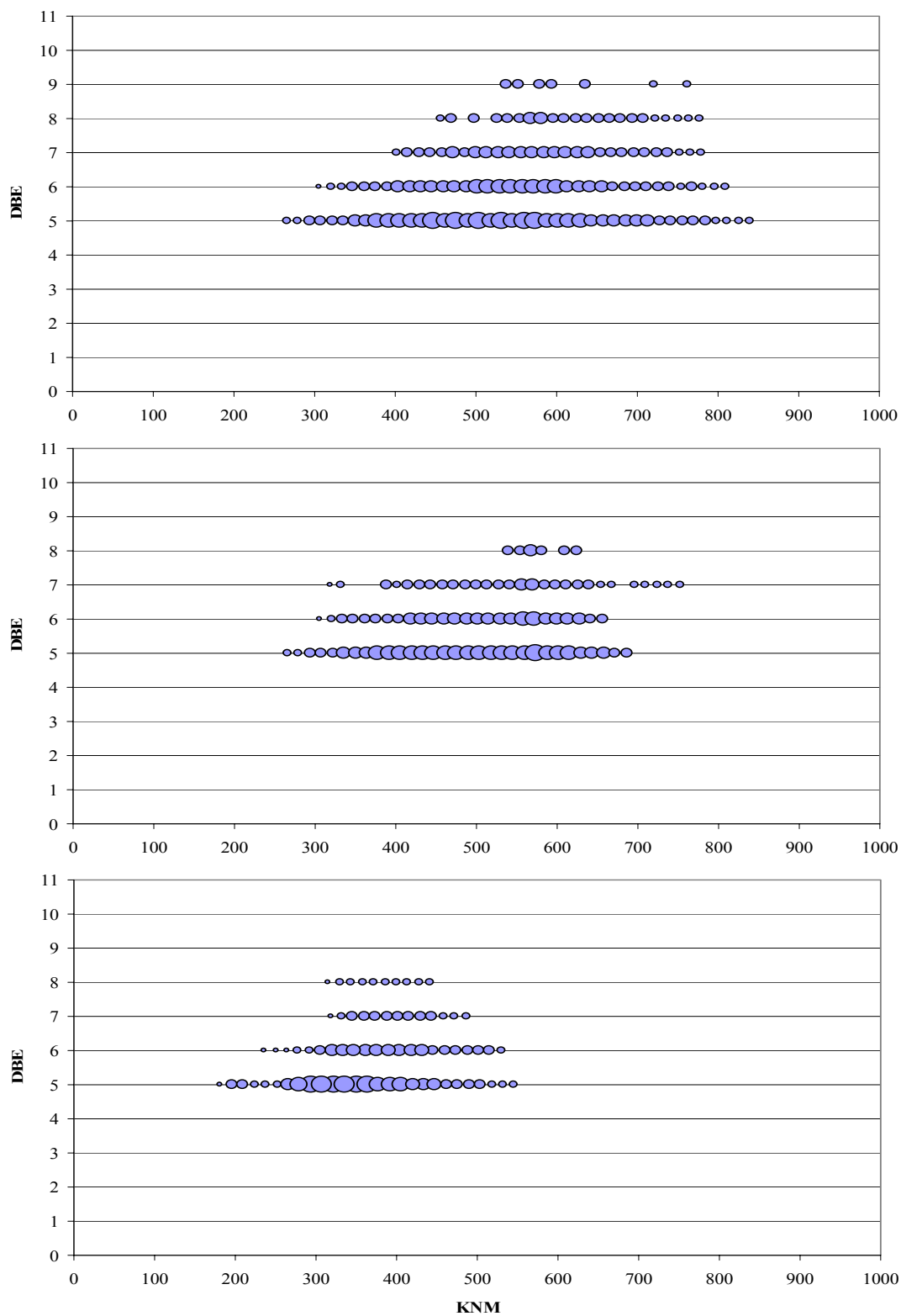


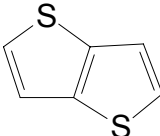
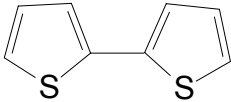
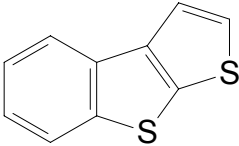
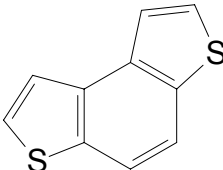
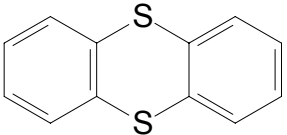
Figure 9.12. Kendrick plots of disulfur PASHs (from top to bottom) in dark control, after 2 days photo-oxidation and after 10 days photo-oxidation.

Compounds with DBE = 8 are likely thienobenzothiophenes (i.e., addition of one thiophenic ring to benzothiophene) or benzodithiophene having from 16 to 42 carbon atoms.

The most abundant disulfur PASHs are those having DBE 5 and 6 followed by the relatively abundant DBE series = 7 and 8. Low abundance species with DBE = 9, most likely thianthrenes, are also observed.

In this crude oil, the highest DBE value found for S2 compounds is 9 and the highest mass is 840 Da.

Table 9.5. Parent structure examples for S2 compounds

<i>Parent Structure</i>	<i>Name</i>	<i>DBE</i>
	Thieno[3,2- <i>b</i>]thiophene	5
	2,2'-Bithiophene	6
	Thieno[2,3- <i>b</i>]benzothiophene	8
	Benzo[1,2- <i>b</i> :4,3- <i>b'</i>]dithiophene	8
	Thianthrene	9

9.2.2.2.2. Disulfur PASHs after 2 days photo-oxidation

An inspection of S2 species after 2 days photo-oxidation (Figure 9.12) shows that the disulfur compounds range from $5 \leq \text{DBE} < 9$, with the highest abundance from $5 \leq \text{DBE} < 8$. Low abundance species with DBE = 8 are observed with carbon numbers of 25-31. DBE = 5, 6 and 7 series with carbon numbers ranging from 7 to 37, 10 to 35, 9 to 40 respectively were also

observed. Moreover, the photo-oxidation of the disulfur PASHs for 2 days lead to the complete depletion of DBE = 9 series.

The comparison of the disulfur PASH distribution pattern after 2 days photo-oxidation with that of the dark control (Figure 9.12) shows a shift of high mass components toward lower masses (e.g. from 840 to 686 Da for DBE 5; from 810 to 656 Da for DBE 6; from 780 to 752 Da for DBE 7; and from 778 to 624 Da for DBE 8) as can be seen in Table 9.6. This same trend of photodegradation was seen in monosulfur PASHs, which is the pronounced effect of photodegradation on the high molecular weight compounds in the different classes leading to the loss of long alkyl side chains.

9.2.2.2.3. Disulfur PASHs after 10 days photo-oxidation

The disulfur PASHs after 10 days photo-oxidation (Figure 9.12) exhibits the same DBE range as that after 2 days photo-oxidation. As can be seen in Figure 9.12, the most abundant disulfur species are those having DBE 5 and 6 followed by the relatively low abundant DBE 7 and 8. In addition, S2 compounds having DBE 5, 6, 7 and 8 showed the following carbon numbers: 1-27, 5-26, 9-21 and 9-18 respectively.

Table 9.6. Depletion of disulfur PASHs after 2 and 10 days photo-oxidation

<i>DBE</i>	<i>Photodegraded compounds after 2 days (*)</i>	<i>Photodegraded compounds after 10 days (*)</i>
5	C ₃₈ -C ₄₈	C ₂₈ -C ₄₈
6	C ₃₆ -C ₄₆	C ₂₇ -C ₄₆
7	C ₄₁ -C ₄₂	C ₂₂ -C ₄₂
8	C ₃₂ -C ₄₂	C ₁₉ -C ₄₂
9	All compounds	depleted after 2 days photo-oxidation

(*) Depletion is calculated relative to the dark control

A close inspection of S2 species after 10 days photo-oxidation reveals the photodegradation of species from different DBE series having mass range ~ 546-686 (Table 9.6) in comparison with those after 2 days photo-oxidation, indicating a shift to lower carbon number with increasing the irradiation time.

The previous results indicate that the disulfur PASHs in spilled oil are following the same photodegradative trend as that observed in monosulfur PASHs, in which the compounds undergo a consistent pattern of alkyl chain loss from the high molecular weight end of the homologue distribution. This suggests that a measurable increase in the concentrations of the homologues in the lower molecular weight range, a gradual lowering in carbon number of the homologue maximum, and a gradual decrease of the total homologue range from the high molecular weight end take place.

9.3. Summary

This study emphasizes the effect of photo-oxidation on the polycyclic aromatic sulfur heterocycles in crude oil. By using GC-MS and FT-ICR MS measurements, qualitative changes in the distributions of the low- and high-molecular weight PASHs after photo-oxidation were determined. For low-molecular weight PASHs, GC-MS indicated that benzothiophenes were more easily photodegradable than dibenzothiophenes. For high-molecular weight PASHs, our FT-ICR MS measurements showed the presence of homologous series of long side chain monosulfur and disulfur PASHs which were photodegraded in the same trend. For the monosulfur compounds, the tetrahydrothiophenes and the pyrenothiophenes have been preferentially photodegraded and completely depleted after two days photo-oxidation. However, benzothiophenes, phenylthiophenes, indenothiophenes, dibenzothiophenes, acenaphthenothiophenes, phenanthrothiophenes, benzonaphthothiophenes and phenanthronaphthothiophenes were generally more resistant to photodegradation than dihydrothiophenes, thiophenes, naphthenothiophenes and cycloalkenothiophenes which were completely degraded after 10 days photo-oxidation. For the disulfur compounds, DBE 9 species exhibited a particularly marked susceptibility to photodegradation which was manifested by their complete depletion after 2 days photo-oxidation. In addition, DBE 5 and 6 were more susceptible to photo-oxidation than those of DBE 7 and 8. Moreover, a decrease in the proportion of both long alkylated monosulfur and disulfur PASHs concomitant with an increase in the proportion of relatively short alkylated ones was observed indicating that the average length of aliphatic side chains in the PASHs decreased due to photodegradation. Hence, a shift to lower carbon number was observed for both monosulfur and disulfur compounds and this shift increased with increasing the irradiation time.

10. Summary

Liquid petroleum (crude oil and the products refined from it) plays a pervasive role in modern society. As the population of the world increases and developing countries become more industrialized, the demand for energy grows worldwide. Oil is currently the dominant energy source and it is expected to remain so over the next several decades. However, the worldwide extraction, transportation, and use of petroleum inevitably results in its release to the environment. Hence, oil spills have become a global problem.

As soon as a crude oil is released into the marine environment, it undergoes various physical processes including spreading, evaporation, dissolution, emulsification, dispersion and sedimentation that disperse the petroleum in the environment. Processes that transform such a material and therefore lead to its removal, and ultimate mineralization, include oxidation processes through microorganisms and sunlight. Such weathering processes strongly alter the physical and chemical properties of a crude oil. Hence, photochemical oxidation of petroleum and petroleum products is an important process in transferring organic material from the oil phase into the water column through the formation of a variety of oxidized compounds. As these compounds are water-soluble and hence bioavailable, they represent a real risk as they could be greatly toxic to the different organisms in the marine environment. In order to assess this risk, which is currently unknown, the identification of the main compounds responsible for the phototoxicity of crude oil is then mandatory. Nevertheless, this represents a major difficulty due to the complexity of crude oils as they are mixtures of thousands of different hydrocarbons and other organic molecules containing heteroatoms.

Therefore, in the present study, our goal was to determine the class of compounds responsible for the highest phototoxicity of petroleum and the identification of its components. First, a thin film of an Egyptian crude oil in aqueous solution was irradiated separately with sunlight and a mercury middle pressure lamp for 37 hours, placed in a cooling jacket of Duran glass to simulate the sunlight irradiation at the surface of the earth, and the toxicity of the photo-oxidized solutions was tested using the microcrustacean *Daphnia magna*. Next to these solutions, a third one was held in the dark, but treated in the same manner as the irradiated ones and its toxicity was also tested. The sunlight and lamp photo-oxidized solutions had similar toxicity which was higher in both cases than that of dark control.

Next, to achieve our aim, we sequentially reduced the complexity of crude oil by removing less toxic components in order to enable the chemical identification of the remaining major toxicants through a toxicity-based fractionation procedure. Hence, several chromatographic methods have been used for the separation of crude oil into classes and subclasses followed by their photo-oxidation for 37 hours using the mercury middle pressure lamp and the determination of the toxicity of their photoproducts using *Daphnia magna*. It should be noted that the irradiated solutions were placed in closed Duran-glass vessels to prevent the evaporation of volatile compounds and to maximize the photolysis yield. Thus, the Egyptian crude oil was fractionated on open column chromatography into aliphatic, monoaromatic and polyaromatic fractions which were irradiated separately by the mercury lamp and their photo-oxidized solutions were tested for their toxicity. As the polyaromatic fraction was the most toxic fraction, it was fractionated into polycyclic aromatic hydrocarbon fraction and polycyclic aromatic sulfur heterocycle fraction on a Pd(II)-bonded stationary phase using ligand exchange chromatography. The PAH and PASH fractions were irradiated and their photo-oxidized solutions were tested for their toxicity. The PASH fraction showed higher toxicity than the PAH one and therefore was further fractionated on a β -cyclodextrin column according to the number of condensed aromatic rings into two subfractions, one containing the benzothiophenes and the other the dibenzothiophenes and higher ring compounds. The two subfractions were photo-oxidized and the toxicity of the resulting solutions was determined. Seeing that both subfractions had equal toxicity, another alternative separation protocol was looked for, namely the separation of PASH photoproducts according to their polarity into polar and nonpolar photoproducts by liquid-liquid extraction. Although the experimental observations indicated that the toxicity of non-polar photoproducts is higher than that of polar ones after short-term (37 hours) photolysis, the photo-oxidation of the PASH fraction was continued for 10 days and the toxicity of the polar and non-polar products were investigated to ensure that possible long-term effects were not overlooked. After 10 days photo-oxidation, the polar fraction had the highest toxicity and this may be due to that by increasing the time of irradiation and subsequently, the photo-oxidation, the amount of polar products increases and the amount of parent PASH compounds decreases. Thus, finally it was clear that our key toxicants were the polar photoproducts of the polycyclic aromatic sulfur heterocycles. Accordingly, the next part of this study has focused on the identification of the individual components of the polar photoproducts and the investigation of the changes in the distributions of low- and high-molecular weight sulfur compounds after photo-oxidation using sophisticated chemical tools.

In order to identify the polar photoproducts, the PASH fraction of the Egyptian crude oil was photo-oxidized for one month as a film on the surface of water in the presence of anthraquinone acting as a sensitizer. Since the PASH fraction normally occurs with other polycyclic aromatic hydrocarbons in crude oil that may act as photosensitizers, we have used the anthraquinone which was previously found in the seawater for photosensitization, as it was concluded from a separate experiment that the photodegradation of the PASH fraction is very slow when it is irradiated alone. The polar photoproducts 1 (PP1) were extracted from water by liquid-liquid extraction while the polar photoproducts 2 (PP2) were obtained after the complete evaporation of the remaining aqueous phase and both of them were subjected to investigation.

The polar photoproducts 1 were subjected to electrospray tandem mass spectrometric (ESI-MS/MS) analysis in the negative mode in which a large number of compounds were detected by recording the loss of CO₂ from their molecular ions. Carboxylic acids were found among the PP1 and could be identified after esterification to the trimethylsilyl derivatives by gas chromatography-mass spectrometry. A series of regularly spaced peaks was observed which were identified as aliphatic fatty acids from butanoic acid to hexadecanoic acid besides cyclohexanecarboxylic acid and cyclohexylacetic acid. In addition, aromatic acids, dicarboxylic acids, hydroxyl carboxylic acids and diols were also observed.

The presence of the cyclohexyl group in the cyclohexanecarboxylic acid and cyclohexylacetic acid indicates that polycyclic aromatic compounds in the crude oil contain this structural element in the side chain. Although high resolution mass spectrometry has previously established the profuse presence of aromatic compounds containing one or several saturated rings, it does not distinguish between fused (e.g. cyclohexano) and substituted (e.g. cyclohexyl) rings. However, these acids found here can only be derived from the latter. These cyclohexylsubstituted aromatics do not seem to have been identified in crudes yet which make them possible constituents of the unresolved complex mixture of petroleum. Therefore, the identification of the cyclohexyl containing acids among the photoproducts gives new structural insights into the polycyclic aromatic compounds in crude oil.

Moreover, the polar photoproducts 2 were also subjected to ESI-MS/MS analysis in the negative mode in which a large number of sulfonic acids were detected by recording the loss of SO₃⁻ from their molecular ions. The sulfonic acids were analyzed by the time of flight mass

spectrometry and their accurate masses were determined and hence their elemental compositions and subsequently their structures could be identified.

In order to understand the fate of low- and high-molecular weight sulfur compounds and to simulate the changes in their distributions taking place in the marine environment after an oil spill, the aromatic fraction of the Egyptian crude oil containing the polycyclic aromatic sulfur heterocycles was irradiated as a film in aqueous solution with the mercury lamp for 2 and 10 days and the sulfur compounds were characterized by GC-MS and Fourier transform ion cyclotron resonance mass spectrometry, together with the aromatic fraction of a dark control. GC-MS showed that the benzothiophenes were easily photodegradable than dibenzothiophenes. Due to the non-polar nature of sulfur heterocycles, they were first sulfur-selectively derivatized via a methylation reaction targeting the sulfur atom and then analyzed by the ultra-high resolution and accuracy FT-ICR MS technique to investigate compounds up to 940 Da. After measurements, the data obtained from mass spectrometry were further sorted with multiple sorting procedures using Kendrick mass scale in order to extract useful information from the complex mass spectra. Series of long side chain mono- and disulfur compounds over a wide range could be identified and were found to undergo photodegradation in the same trend. However, it was clear that the reactivity of different classes of sulfur aromatics towards photo-oxidation depends on their parent aromatic structures. For the monosulfur compounds, the tetrahydrothiophenes and the pyrenothiophenes have been preferentially photodegraded and completely depleted after two days photo-oxidation. However, benzothiophenes, phenylthiophenes, indenothiophenes, dibenzothiophenes, acenaphthenothiophenes, phenanthrothiophenes, benzonaphthothiophenes and phenanthronaphthothiophenes were generally more resistant to photodegradation than dihydrothiophenes, thiophenes, naphthenothiophenes and cycloalkenothiophenes which were completely degraded after 10 days photo-oxidation. For the disulfur compounds, DBE 9 species, i.e. thianthrenes, exhibited a particularly marked susceptibility to photodegradation which was manifested by their complete depletion after 2 days photo-oxidation. In addition, DBE 5 and 6, i.e. thieno[3,2-*b*]thiophene and 2,2'-bithiophene respectively, were more susceptible to photo-oxidation than those of DBE 7 (i.e. thieno[2,3-*b*]benzothiophene) and 8.

Moreover, the disulfur PASHs are following the same photodegradative trend as that observed in monosulfur PASHs, in which the compounds undergo a consistent pattern of alkyl chain loss from the high molecular weight end of the homologue distribution. This was

observed through a decrease in the proportion of both long alkylated monosulfur and disulfur PASHs concomitant with an increase in the proportion of relatively short alkylated ones.

Furthermore, many of the reactions discussed in this work are independent of the aromatic ring structure so that these product studies should be equally relevant for polycyclic aromatic hydrocarbons. However, because of the sulfur atom in the PASHs, some products unique to this compound class were formed. The photodegradation trends discussed here could be also applicable to polycyclic aromatic hydrocarbons as well as to polycyclic aromatic sulfur heterocycles after an oil spill in the environment.

11. Zusammenfassung

Erdöl und seine Produkte spielen eine universelle Rolle in der heutigen Gesellschaft. Mit steigender Bevölkerungszahl und sich industrialisierenden Entwicklungsländern steigt der weltweite Energiebedarf. Öl ist die aktuelle und zumindest für die kommenden Jahrzehnte dominierende Energiequelle. Aufgrund der weltweiten Verwendung und des kontinuierlichen Transportes ereignen sich immer wieder unerwünschte Freisetzungen in die Umwelt. Somit haben sich Ölkatastrophen zu einem globalen Problem entwickelt.

Sobald Öl ins Meer gelangt, durchläuft es verschiedene physikalische Prozesse, z.B. Verteilung, Verdunstung, Lösen, Dispersion und Sedimentation. Auf diese Weise werden Ölbestandteile in der Umwelt verteilt. Zusätzlich erfolgen Umwandlung und Abbau, bzw. Mineralisation durch Mikroorganismen und Sonnenlicht. Solche Verwitterungen sorgen für massive Veränderungen der physikalischen und chemischen Eigenschaften eines Öls. Durch photochemische Oxidation werden seine Bestandteile besser wasserlöslich und lassen sich aus der Ölphase entfernen. Die Vielzahl der oxidierten Verbindungen erlangt so eine höhere Bioverfügbarkeit, wodurch aufgrund ihrer Giftigkeit ein vermehrtes Risiko für die Meereslebewesen einhergeht. Um das bisher unbekannte Risiko abschätzen zu können, ist die Identifikation der phototoxischen Erdölkomponenten erforderlich. Dies ist, aufgrund der Vielzahl der unterschiedlichen Kohlenwasserstoffe, sowie heteroatomhaltiger Verbindungen mit großen Schwierigkeiten verbunden.

Das Ziel dieser Arbeit war die Untersuchung der für die Phototoxizität verantwortlichen Substanzklasse, sowie die Identifizierung der Komponenten. Hierzu wurde ein dünner Film eines ägyptischen Erdöls in wässriger Lösung für 37 Stunden der Sonne, bzw. einer Quecksilbermitteldrucklampe zur Simulation der erdnahen Sonnenstrahlung ausgesetzt. Die Toxizität dieser photooxidierten Proben wurde an Kleinkrebsen der Gattung des Riesenwasserfloh (*Daphnia magna*) getestet. Zusätzlich wurden im Dunkeln gelagerte Blindproben auf ihre Toxizität geprüft. Die mit Sonnenlicht und Lampe bestrahlten Proben wiesen eine vergleichbare Giftigkeit auf, die in beiden Fällen die der Blindprobe übertraf.

Um die giftigsten Substanzen identifizieren zu können, wurden gemäß der Toxizität fraktioniert. Es wurden verschiedene chromatographische Verfahren zur Trennung des Öls genutzt, gefolgt von einer 37-stündigen Photo-oxidation mittels Quecksilberlampe und Toxizitätsbestimmung der Produkte an *Daphnia magna*. Die Belichtung erfolgt in

geschlossenen Duranglasgefäßen. So konnte Verdunstung verhindert und eine maximale Photolyseausbeute erzielt werden. Die Fraktionierung des Erdöls erfolgte über eine Schwerkraftsäule in eine aliphatische, eine monoaromatische und eine polyaromatische Fraktion, die der Photo-oxidation ausgesetzt wurden. Die giftigste Fraktion der Polyaromaten wurde mithilfe von Ligandenaustauschchromatographie über eine Säule mit immobilisierten Pd(II) in eine PAH und eine PASH-Fraktion unterteilt. Diese wurden ebenfalls separat bestrahlt. Erneut wurde die Fraktion mit der höheren Toxizität, in diesem Fall die PASH-Fraktion, weiter aufgetrennt. Dies erfolgte über eine β -Cyclodextrinphase anhand der Größe des aromatischen Systems. Man erhielt so wiederum zwei Fraktion, eine, die die Benzothiophene enthielt, eine zweite, in der sich die größeren PASHs befanden. Die Toxizitätsprüfung nach der Photo-oxidation ergab vergleichbare Werte, so dass eine alternative Trennung gesucht wurde. So wurden die Oxidationsprodukte durch Flüssig-Flüssig-Extraktion gemäß ihrer Polarität getrennt. Obwohl sich aufgrund experimenteller Beobachtung abschätzen lässt, dass nach kurzer Belichtungsdauer (37 Stunden) die unpolaren Photo-oxidationsprodukte giftiger sind als die polaren, wurde die PASH-Fraktion weitere zehn Tage bestrahlt, um mögliche Langzeiteffekte aufzudecken. Nach zehn Tagen konnte bei der polaren Fraktion die höchste Toxizität festgestellt werden, was sowohl aus der Erhöhung der Belichtungsdauer, als auch aus dem Anstieg der Mengen an polaren Produkten auf Kosten der PASH-Ausgangssubstanz hervorging. Somit konnte man erkennen, dass die giftigsten Substanzen aus der Photo-oxidation der PASHs der polaren Fraktion angehören.

Als nächstes Ziel wurden die Identifikation einzelner Verbindungen, sowie der Einfluss der Massenverteilung nach der Oxidation angegangen. Hierzu wurde die PASH-Fraktion des ägyptischen Erdöls als dünner Film auf Wasser mit Zusatz von Anthrachinon als Sensibilisator für einen Monat photooxidiert. Der Zusatz erfolgte, da die Oxidation der isolierten PASH-Fraktion sehr langsam erfolgt, das Anthrachinon soll so den fehlenden Einfluss der PAHs ausgleichen, die ebenfalls als Sensibilisator agieren können.

Die polaren Oxidationsprodukte 1 (PP1) wurden durch Flüssig-Flüssig-Extraktion isoliert, während die polaren Produkte 2 (PP2) nach der vollständigen Verdunstung der wässrigen Phase erhalten wurden. Beide wurden anschließend untersucht.

Die polaren Produkte 1 wurden mit Elektrospray Tandem Massenspektrometrie (ESI-MS/MS) im negativen Modus untersucht. So ließ sich eine große Anzahl von Substanzen nach dem Verlust von CO₂ erkennen. Es wurden Carbonsäuren in der PP1-Fraktion gefunden, die sich

durch Derivatisierung zu dem korrespondierenden Trimethylsilylether über GC/MS identifizieren ließen. Einer Reihe von regelmäßig auftretenden Signalen ließen sich die aliphatischen Fettsäuren von Butan- bis Hexadecansäure zuordnen, des weiteren Cyclohexancarbonsäure, so wie Cyclohexylelessigsäure. Außerdem konnten aromatische Säure, Dicarbonsäuren, Hydroxycarbonsäuren und Diole beobachtet werden.

Die Anwesenheit der Cyclohexylgruppe lässt darauf schließen, dass dieses Strukturelement in der Seitenkette polycyclischer aromatischer Kohlenwasserstoffe vorhanden ist. Auch wenn hochauflösende Massenspektrometrie die Anwesenheit zahlreicher gesättigter Systeme innerhalb der aromatischen Verbindungen aufzeigen konnte, ist diese nicht in der Lage zwischen kondensierten (z.B. Cyclohexano) und einfach gebundenen Ringen (Cyclohexyl-) zu unterscheiden. Die gefundenen Carbonsäure lassen sich allerdings nur durch die letztere Möglichkeit erklären. Da von dieser Art Substituent bisher nichts berichtet wurde, handelt es sich möglicherweise um einen Teil der nicht aufgelösten komplexen Mischung des Petroleums. Somit ist die Identifikation von cyclohexylbeinhaltenden Säuren ein weiterer Einblick in die Gruppe der PAHs.

Des Weiteren fanden sich in der Fraktion PP2 eine große Anzahl von Sulfonsäuren, die sich im ESI-MS/MS durch den Verlust eines Strukturelementes SO_3^- zeigten. Im Flugzeitmassenspektrometer wurden zusätzlich ihre akkuraten Massen bestimmt, so dass sich ihre Summenformel und anschließend mögliche Strukturen herleiten ließen.

Um die Entwicklung von leichten sowie schweren Schwefelverbindungen zu verstehen und ihren Verbleib in der Umwelt nach einer Ölkatastrophe zu simulieren, wurde die gesamte aromatische Fraktion des Erdöls als dünner Film in wässriger Lösung zwei, bzw. zehn Tage mit einer Quecksilberlampe bestrahlt und die Schwefelverbindungen mit GC-MS und Fourier Transform Ionen Cyclotron Massenspektrometrie untersucht, zusammen mit der aromatischen Fraktion einer Dunkelkontrollprobe. Eine Analyse mittels GC-MS zeigte, dass Benzothiophene leichter photolytisch abgebaut werden als Dibenzothiophene. Aufgrund der unpolaren Natur dieser Verbindungen, mussten sie schwefelselektiv durch Methylierung derivatisiert werden, um dann mit dem extrem hochauflösenden und akkuraten FT-ICR-MS untersucht zu werden.

Nach der Messung wurden die gesammelten Daten in das Kendrick Massen System umgeformt, um verwertbare Informationen aus den komplexen Massenspektren zu bekommen. Es wurden eine Reihe von langkettigen Mono- und Dischwefelverbindungen gefunden, die in ähnlichem Maß dem Photoabbau unterliegen. Die Reaktivität der verschiedenen Klassen an Schwefelverbindung hängt so in erster Linie von der Struktur des aromatischen Grundgerüsts ab. Die Monoschwefelverbindungen, die Tetrahydrothiophene, sowie die Pyrenothiophene waren nach zwei Tagen vollständig abgebaut. Benzothiophene, Phenylthiophene, Indenothiophene, Dibenzothiophene, Acenaphthenothiophene, Phenanthrothiophene, Benzonaphthothiophene and Phenanthronaphthothiophene erwiesen sich generell als resistenter gegenüber dem Photoabbau als Dihydrothiophene, Thiophene, Naphthenothiophene and Cyclopentenothiophene, die nach zehn Tagen vollständig abgebaut waren. Dischwefelverbindungen mit dem Doppelbindungsequivalent 9, z.B. Thianthren, zeigten teilweise eine große Empfindlichkeit gegenüber Photoabbau, was sich in dem vollständigen Abbau nach zwei Tagen zeigt. Ebenso sind die Doppelbindungsequivalente 5 und 6, z.B. Thieno[3,2-*b*]thiophen and 2,2'-Bithiophen reaktiver als die Spezies mit DBE 7 (z.B. Thieno[2,3-*b*]benzothiophen) und 8.

Ferner zeigten die Dischwefelverbindungen das gleiche Verhalten wie die Verbindungen mit einem Schwefelatom, den Verlust von Alkylgruppen ausgehend von den größten molekularen Massen einer homologen Reihe. Dieses wird gezeigt durch ein Rückgang des Anteils großer Monoschwefel und Dischwefel PASHs begleitet von einer Zunahme des Anteils an PASHs mit relativ kurzer Alkylkette.

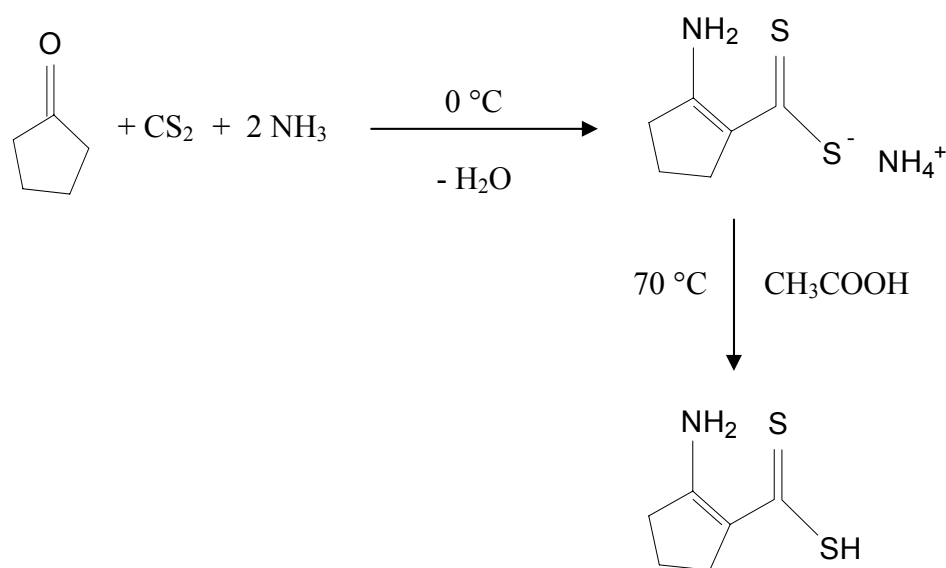
Viele der beschriebenen Reaktionen sind nicht von dem aromatischen System abhängig, so dass die erhaltenen Ergebnisse auch für PAHs relevant sein können. Einige Abbaureaktionen der PASHs gehen auf die Anwesenheit des Schwefels zurück. Der Verlauf des Photoabbaus, der hier diskutiert wird, kann sowohl für PAHs, sowie für PASHs nach einem Öleintrag in die Umwelt angewandt werden.

12. Appendix

12.1. Synthesis of Pd(II)-ACDA silica gel

12.1.1. Synthesis of 2-amino-1-cyclopentene-dithiocarboxylic acid (ACDA)

A mixture of cyclopentanone (12.5 g, 150 mmol), carbon disulfide (15 g, 195 mmol), and 150 ml of aqueous ammonia (25 %) was stirred at 0 °C for 8 h [242]. The yellow solid product was collected, washed with ether, and dried. The crude product was recrystallized from ethanol. 5 g of the ammonium salt of ACDA was dissolved in 50 ml of acetic acid at 70 °C. Ammonia gas evolved. The resulting solution was cooled and water was added until the solution became turbid. The yellow solid material which separated from the solution was collected and recrystallized from methanol.



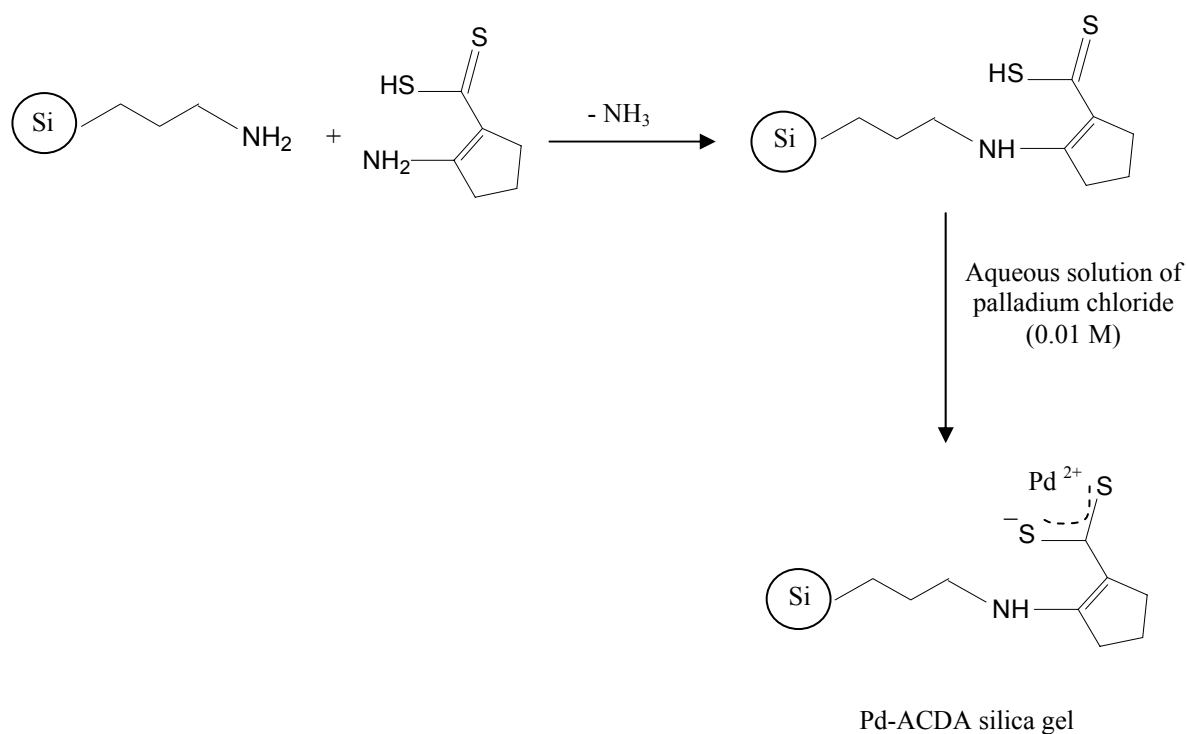
2-Amino-1-cyclopentene-1-dithiocarboxylic acid
(ACDA)

12.1.2. Synthesis of aminopropanosilica gel

10 g of LiChrosorb Si 100 (10 μm , dried at 130°C for 24 h) was refluxed with 12.5 ml of 3-aminopropanotrimethoxysilane in 50 ml dry toluene. The resulting product was filtered off and washed successively with toluene and methanol. The obtained aminopropano silica gel was dried at 50°C in oven.

12.1.3. Synthesis of ACDA-functionalized silica gel

10 g of aminopropano silica gel was added to a solution of 1.6 g of ACDA dissolved in 25 ml of methanol and refluxed for 5 hours [241, 242]. The apparatus was purged with nitrogen during the reaction. After cooling to room temperature, the ACDA-bonded silica was filtered off and washed with methanol.



2.5 g of ACDA-bonded silica was further treated with 250 ml aqueous solution of palladium chloride (0.01 M) in a 500 ml conical flask in order to obtain Pd(II)-ACDA silica gel.

12.2. Synthesis of Pd(II)-mercaptopropano silica gel

Silica gel (LiChrosorb Si 100, 10 μ m) was dried at 130 $^{\circ}$ C for 24 h. 10 g of dried silica gel was refluxed in a solution of 15 ml 3-mercaptopropanotrimethoxysilane in 50 ml dry toluene for 5 h. The resulting bonded silica gel was filtered off and was washed with toluene and methanol successively. The obtained mercaptopropano silica gel (MPS) was dried at 50 $^{\circ}$ C in an oven.

2.5 g of MPS was further treated with 250 ml aqueous palladium chloride solution (0.01 M) for 12 h. The palladium bonded silica phase was filtered off, washed successively with water, isopropanol and cyclohexane, and dried in vacuum at room temperature.

12.3. Instrumental parameters

12.3.1 HPLC instrumentation

Knauer Wellchrom

Knauer HPLC system consists of an interface box, four channel solvent degasser, two Ministar K 501 analytical pumps, a mixing chamber, an electrical injection valve and a variable wavelength detector. Instrument control and data recording were done with Chromgate version 2.8 (Knauer, 14163 Berlin, Germany).

HP 1050

Hewlett-Packard 1050 HPLC system with a quaternary pump, degasser, manual injection valve and a diode array detector set to record the UV spectra from 200 to 500 nm. Instrument control and data recording were done with Chemstation version 9.03 (Agilent, 71034 Böblingen, Germany).

12.3.2. Gas chromatographs

GC-FID

Gas Chromatograph :	Hewlett-Packard 5890 II
Auto sampler:	Gerstel MPS 2L
Injector:	Split/Splitless (60 s)
Injector temperature:	280 °C
Detector temperature:	300 °C
Capillary column	DB-5 MS (30m × 0.25 mm × 0.25 µm)
Carrier gas:	Hydrogen (4.8)
Temperature program:	60 °C -1 min - 10 °C/min - 300 °C - 10 min
Injection volume:	1 µl

GC-MS

Gas Chromatograph:	Finnegan MAT GCQ
Mass spectrometer:	Finnegan MAT GCQ Polaris MS
Auto sampler:	CTC A200S Liquid Sampler
Injector:	Split/Splitless (60 s)
Injector temperature:	260 °C
Detector temperature:	300 °C
Capillary column:	DB-5 MS (30m × 0.25 mm × 0.25 µm)
Transfer line:	275 °C
Carrier gas:	Helium (5.8)
Ionization conditions:	EI, 70 eV, Ion source 200 °C
Modus:	Full scan (50-600 amu)
Temperature program:	60 °C - 1 min - 10 °C/min - 300 °C - 10 min
Injection volume:	1 µl

The analyses on the following instruments were performed in the Mass Spectrometry Department, Institute of Organic Chemistry.

QuattroMicro GC-MS:

The tandem quadrupole GC-MS consists of an Agilent 6890 GC with a 30 m×0.32 mm×0.25 µm HP 5 column (Agilent) and a Waters Micromass (Manchester, U.K.) QuattroMicro mass spectrometer. It was operated with EI ionization at 70 eV in full scan mode from 40 to 800 amu and in SIM mode on m/z 132. The oven temperature was programmed as follows: 50 °C starting temperature, kept for 1 min, temperature ramp at 15 °C/min to 300 °C, kept for 10 min.

Quattro LCZ:

Tandem mass spectrometric analyses were performed on a Quattro LCZ triple quadrupole mass spectrometer (Waters-Micromass, Manchester, UK) operated in the electrospray positive and negative ion mode. In order to find the optimal parameter settings for maximum sensitivity, the cone voltage was varied between 20-30 V. The capillary voltage was 0.9-1.5 KeV. Argon was used as collision gas to obtain daughter ions. The system was controlled by MassLynx software.

MicroTof MS:

Experiments for the determination of elemental compositions of sulfonic acids were performed on a MicroTof (Bruker Daltonics, Bremen). The mass spectrometer was operated in the ESI-negative ion mode at a resolution of 9000 (FWHM). The capillary voltage was set at 4.5 KeV. Data were acquired in the continuum mode from 50 to 3000 Da and processed using MassLynx v. 4 software.

12.3.3. FT-ICR MS

Mass spectra were acquired using an APEX III Fourier transform ion cyclotron resonance mass spectrometer (Bruker Daltonics, Bremen, Germany) equipped with a 7 T actively shielded super conducting magnet and an Agilent ESI source. The samples were introduced in a 1:1 (v/v) solution of dichloromethane/acetonitrile and injected in the infusion mode with a flow rate of 2 $\mu\text{l}/\text{min}$ detecting positive ions. The spray voltage was maintained at 4.5 kV. After ionization, the ions were accumulated for 0.5 s in the octapole before transfer to the cyclotron cell. For a better signal-to-noise ratio, at least 64 scans were accumulated. Internal and external calibrations were done using a mixture of the Agilent electrospray calibration solution of masses 622.02896 and 922.00980 with the addition of indolacrylic acid of masses 397.11589 $[2\text{M}+\text{Na}]^+$ and 584.17923 $[3\text{M}+\text{Na}]^+$ covering the whole range of masses in the samples. All the measurements by FT-ICR mass spectrometer were performed in collaboration with Max-Planck-Institute of coal research, Mülheim, Germany.

12.4. Materials

Acetic acid	96 %	Merck
Acetone	Residue analysis	Fluka
3-Aminopropyltrimethoxysilane	97 %	Aldrich
Ammonia	25 %	Grüssing
Ammonium vanadate	p.a.	in house
9,10-Anthraquinone	98 %	Fluka
Benzoic acid	98 %	Merck
Biotin	> 99 %	BioChemika
Boric acid	p.a.	in house
<i>tert</i> -Butylmethyl ether	p.a.	Merck
Calcium chloride	p.a.	in house
Carbon disulfide	n.a.	Aldrich
Cobalt (II) chloride	p.a.	in house
Copper (II) chloride	p.a.	in house
Cyclohexane	99.8 %	Fluka
Cyclohexane carboxylic acid	98 %	Aldrich
Cyclohexyl acetic acid	> 99 %	Fluka
Cyclopentanone	99 %	Aldrich
Decanoic acid	98 %	Fluka
1,2-Dichloroethane	99.5%	Fluka
Dichloromethane	99.8 %	Riedel de Haen
Diethyl ether	p.a.	in house
Dimethylchlorosilane	98 %	Janssen Chimica
Dipotassium hydrogen phosphate	p.a.	in house
Ethanol	p.a.	in house
Helium	5.8	Institute supply
Helium	He GC BiP	Air products
<i>n</i> -Heptane	99 %	Grüssing
Hydrochloric acid	37 %	Grüssing
Isopropanol	99.8 %	Fluka
Lithium chloride	p.a.	in house
Magnesium sulfate (water free)	p.a.	in house
Magnesium sulfate	p.a.	in house

Manganese (II) chloride	p.a.	in house
Methanol	p.a.	in house
Methyl iodide	99 %	Merck
3-Mercaptopropyltrimethoxysilane	97 %	Aldrich
Nitrogen	Purity 4.6	Institute supply
N-methyl-N-(trimethylsilyl)-trifluoroacetamide	97 %	Acros Organics
Octanoic acid	98 %	Merck
Palladium (II) chloride	59 %	Acros Organics
<i>n</i> -pentane	99 %	Acros Organics
Potassium dihydrogen phosphate	p.a.	in house
Potassium chloride	p.a.	in house
Rubidium chloride	p.a.	in house
Silica gel 10 µm 100°A	for HPLC	Merck
Silica gel 60	for chromatography	Fluka
Silver tetrafluoroborate	98 %	Aldrich
Sodium bicarbonate	p.a.	in house
Sodium bromide	p.a.	in house
Sodium molybdate	p.a.	in house
Sodium nitrate	p.a.	in house
Sodium sulfate	p.a.	Merck
Strontium chloride	p.a.	in house
2-Sulfobenzoic acid	98 %	Aldrich
Tetradecane (olefin free)	> 99 %	Fluka
Tetradecanoic acid	97 %	Fluka
Toluene	99.8 %	Fluka
<i>p</i> -Toluene sulfonic acid	98 %	Fluka
Zinc chloride	p.a.	in house

12.5. Abbreviations

ACDA	2-Amino-1-cyclopentene-1-dithiocarboxylate
ANT	Anthracene
ATQ	Anthraquinone
BAP	Benzopyrene
BT	Benzothiophene
Da	Dalton
DBE	Double bond equivalent
DBT	Dibenzothiophene
DMBT	Dimethylbenzothiophene
DMDBT	Dimethyldibenzothiophene
EC ₅₀	Effective concentration causing 50 % immobilization
EEC	European economic community
EPA	US-American environmental protection agency
ESI	Electrospray ionization
FLA	Fluoranthene
FT-ICR	Fourier transform ion cyclotron resonance
FWHM	Full width at half maximum
GC-FID	Gas chromatography-flame ionization detector
GC-MS	Gas chromatography-mass spectrometry
h	hour
HDS	Hydrodesulfurization
HPLC	High performance liquid chromatography
IR	Infrared
ISO	International organization for standardization
KNM	Kendrick nominal mass
Log K _{ow}	Log octanol-water partitioning coefficient
MBT	Monomethylbenzothiophene
MDBT	Monomethyldibenzothiophene
m/z	Mass to charge ratio
NAP	Naphthalene
OECD	Organization for economic cooperation and development
PAHs	Polycyclic aromatic hydrocarbons
PASHs	Polycyclic aromatic sulfur heterocycles

PHE	Phenanthrene
PHEQ	9,10-Phenanthrenequinone
ppm	Parts per million
PYR	Pyrene
QSAR	Quantitative structure activity relationships
R	Resolution
TIE	Toxicity identification evaluation
TeMBT	Tetramethylbenzothiophene
TeMDBT	Tetramethyldibenzothiophene
TMBT	Trimethylbenzothiophene
TMDBT	Trimethyldibenzothiophene
TOF	Time of flight
UV	Ultraviolet
V	Visible
WAF	Water accommodated fraction

13. References

1. www.eia.doe.gov/oiaf/ieo/index.html, accessed 4 September 2007. Energy Information Administration (EIA), Sources: History: International Energy Annual 2004 (May-July 2006), Projections: EIA, System for the Analysis of Global Energy Markets (2007).
2. Kennish, M. J., *Pollution impacts on marine biotic communities*. CRC press: Florida, 1998; 310 p.
3. Clark, R. B., *Marine pollution*. Clarendon Press: Oxford, 1992; 3rd edition, 172 p.
4. National research council, *Oil in the sea III: Inputs, fates and effects*. The National Academies Press: Washington, D.C., 2003; 280 p.
5. Marshall, A. G.; Rodgers, R. P., Petroleomics: The next grand challenge for chemical analysis. *Accounts of Chemical Research* **2004**, 37, 53-59.
6. Wang, Z.; Stout, S. A.; Fingas, M., Forensic fingerprinting of biomarkers for oil spill characterization and source identification. *Environmental Forensics* **2006**, 7, 105-146.
7. Speight, J. G., *The chemistry and technology of petroleum*. Marcel Dekker, Inc: New York, 1999.
8. Severin, D.; Glinzer, O., In: *Characterization of heavy crude oils and petroleum residues*. Editions Technip: Paris, 1984, 19.
9. Orr, W. L., *Sulfur in heavy oils, oil sands and oil shales*. In: *Oil sand and oil shale chemistry*. Strausz, O. P.; Lown, E. M. (Eds). Verlag Chemie: New York, 1978; 223-243.
10. Peters, K. E.; Moldowan, J. M., *The biomarker guide. Interpreting molecular fossils in petroleum and ancient sediments*. Prentice Hall: Englewood Cliffs, New Jersey, 1993; 363p.
11. Francois, R., A study of sulfur enrichment in the humic fraction of marine sediments during early diagenesis. *Geochimica and Cosmochimica Acta* **1987**, 51, 17-27.
12. Gransch, J. A.; Posthuma, J., *On the origin of sulfur in crudes*. In: *Advances in organic geochemistry 1973*. Tissot, B.; Bienner, F. (Eds). Editions Technip: Paris, 1974; 727-739.
13. Rygle, K. J.; Feulmer, G. P.; Scheideman, R. F., Gas chromatographic analysis of mercaptan odorants in liquefied petroleum gas. *Journal of Chromatographic Science* **1984**, 22, 514-519.
14. Zygmunt, B.; Wardencki, W.; Staszewski, R., Gas chromatographic identification of thiols in the naphtha cut from Libyan crude oil. *Journal of Chromatography* **1983**, 265, 136-138.
15. Arpino, P. J.; Ignatiadis, I.; De Rycke, G., Sulfur-containing polynuclear aromatic hydrocarbons from petroleum. Examination of their possible statistical formation in sediments. *Journal of Chromatography A* **1987**, 390, 329-348.
16. Schmid, J. C.; Connan, J.; Albrecht, P., Occurrence and geochemical significance of long-chain dialkylthiacyclopentanes in petroleum. *Nature* **1987**, 329, 54-56.
17. Sinninghe Damsté, J. S.; de Leeuw, J. W.; Kock-van Dalen, A. C.; De Zeeuw, M. A.; De Lange, F.; Rijpstra, W. I. C.; Schenck, P. A., The occurrence and identification of

- series of organic sulfur compounds in oils and sediment extracts. I. A study of Rozel Point oil (USA). *Geochimica and Cosmochimica Acta* **1987**, 51, 2369-2391.
18. Payzant, J. D.; Montgomery, D. S.; Strausz, O. P., Sulfides in petroleum. *Organic Geochemistry* **1986**, 9, 357-369.
 19. Valisolalao, J.; Perakis, N.; Chappe, B.; Albrecht, P., A novel sulfur-containing C₃₅ hopanoid in sediments. *Tetrahedron Letters* **1984**, 25, 1183-1186.
 20. Sinninghe Damsté, J. S.; Van Koert, E. R.; Kock-Van Dalen, A. C.; de Leeuw, J. W.; Schenck, P. A. Characterization of highly branched isoprenoid thiophenes occurring in sediments and immature crude oils. *Organic Geochemistry* **1989**, 14, 555-567.
 21. Struck, H.; Felzmann, H.; Hopner, T., Oil-polluted Saudi-Arabian beaches. *Erdöl und Kohle-Erdgas-Petrochemie* **1993**, 46, 163-166.
 22. Ehrhardt, M. G.; Burns, K. A., Hydrocarbons and related photo-oxidation products in Saudi Arabian gulf coastal waters and hydrocarbons in underlying sediments and bioindicator bivalves. *Marine Pollution Bulletin* **1993**, 27, 187-197.
 23. http://en.wikipedia.org/wiki/Oil_spill, The Free Encyclopedia, accessed 5 July 2007.
 24. Sharma, V. K.; Hicks, S. D.; Rivera, W.; Vazquez, F. G., Characterization and degradation of petroleum hydrocarbons following an oil spill into a coastal environment of south Texas, USA. *Water, Air and Soil Pollution* **2002**, 134, 111-127.
 25. Fingas, M. F., *The evaporation of oil spills: Development and implementation of new prediction methodology*. In: *Proceedings of the 1999 international oil spill conference*. American Petroleum Institute, Washington, DC, 1999; p. 185-194.
 26. Payne, J. R.; Clayton, J. R.; McNabb, G. D.; Kirstein, B. E., *Exxon Valdez oil weathering and behavior, model predictions and field observations*. In: *Proceedings of the 1991 international oil spill conference*. American Petroleum Institute, Washington, DC, 1991; p. 641-654
 27. Douglas, G. S.; Owens, E. H.; Hardenstine, J.; Prince, R. C., The OSSAII pipeline spill: The character and weathering of the spilled oil. *Spill Science and Technology Bulletin* **2002**, 7, 135-148.
 28. Fingas, M., *Basics of oil spill cleanup*. CRC Press, LLC: Boca Raton, FL, 2000; 2nd edition, 233 p.
 29. Seymour, R. J.; Geyer R. A., Fates and effects of oil spills. *Annual Review of Energy and the Environment* **1992**, 17, 261-283.
 30. Fingas, M. F.; Fieldhouse, B.; Lane, J.; Mullin, J. V., *What causes the formation of water-in-oil emulsions*. In: *Proceedings of the 2001 international oil spill conference*. American Petroleum Institute: Washington, DC, 2001; p. 109-114.
 31. McLean, J. D.; Spiecker, P. M.; Sullivan, A. P.; Kilpatrick, P. K., *The role of petroleum asphaltene in the stabilization of water-in-oil emulsions*. In: *Structure and dynamics of asphaltene*. Mullins, O. C.; Sheu, E. Y. (Eds). Plenum Press: New York, 1998; p. 377-422.
 32. Fingas, M. F.; Fieldhouse, B.; Lane, J.; Mullin, J. V., *Studies of water-in-oil emulsions: Long-term stability, oil properties and emulsions formed at sea*. In: *Proceedings of the twenty-third arctic and marine oil spill program technical seminar*. Environment Canada: Ottawa, Ontario, 2000; p. 145-160.

33. Shiu, W. Y.; Bobra, M.; Bobra, A. M.; Maijanen, A.; Suntio, L.; Mackay, D., The water solubility of crude oils and petroleum products. *Oil and Chemical Pollution* **1990**, 7, 57-84.
34. Plummer, P. S., Origin of beach-stranded tars from source rock indigenous to Seychelles. *American Association of Petroleum Geologists Bulletin* **1996**, 80, 323-329.
35. Butler, J. N.; Wells, P. G.; Johnson, S.; Manock, J. J., Beach tar on Bermuda: Recent observations and implications for global monitoring. *Marine Pollution Bulletin* **1998**, 36, 458-463.
36. Gabche, C. E.; Folack, J.; Yongbi, E. C., Tar balls levels on some beaches in Cameroon. *Marine Pollution Bulletin* **1998**, 36, 535-539.
37. Prince, R. C., *Biodegradation of petroleum and other hydrocarbons*. In: *Encyclopedia of environmental microbiology*. Bitton, G. (Ed.). John Wiley: New York, 2002; p. 2402-2416.
38. Sugiura, K.; Ishihara, M.; Shimauchi, T., Physiological properties and biodegradability of crude oil. *Environmental Science and Technology* **1997**, 31, 45-51.
39. Atlas, R. M.; Bartha, R., *Hydrocarbon biodegradation and oil spill bioremediation*. In: *Advances in microbial ecology*. Marshall, K. C. (Ed.). Plenum Press: New York, 1992; p. 287-298.
40. Leahy, J. G.; Colwell, R. R., Microbial degradation of hydrocarbons in the environment. *Microbiology Review* **1990**, 54, 305-315.
41. Prince, R. C., Petroleum spill bioremediation in marine environments. *Critical Reviews in Microbiology* **1993**, 19, 217-239.
42. Bence, A. E.; Kvenvolden, K. A.; Kennicutt II, M. C., Organic geochemistry applied to environmental assessments of Prince William Sound, Alaska, after the *Exxon Valdez* oil spill. *Organic Geochemistry* **1996**, 24, 7-42.
43. Mackay, D.; McAuliffe, C. D., Fate of hydrocarbons discharged at sea. *Oil and Chemical Pollution* **1988**, 5, 1-20.
44. Daling, P. S.; Brandvik, P. J.; Mackay, D.; Johansen, O., Characterization of crude oils for environmental purposes. *Oil and Chemical Pollution* **1990**, 7, 199-224.
45. Ducreux, J.; Berthou, F.; Bodennec, G., Etude du vieillissement d'un pétrole brut répandu à la surface de l'eau de mer dans des conditions naturelles. *International Journal of Environmental and Analytical Chemistry* **1986**, 24, 85-111.
46. Thingstad, T.; Pengerud, B., The formation of "chocolate mousse" from Statfjord crude oil and seawater. *Marine Pollution Bulletin* **1983**, 14, 214-216.
47. ThomINETTE, F.; Verdu, J., Photo-oxidative behavior of crude oils relative to sea pollution. Part I. Comparative study of various crude oils and model systems. *Marine Chemistry* **1984**, 15, 91-104.
48. Desmaison, M.; Piekarski, C.; Desmarquest, J. P., Formation and stabilisation of reverse sea water petroleum emulsions: Role of interfacial tension and viscosity. *Revue de l'Institut Français du Pétrole* **1984**, 39, 603-615.
49. www.itopf.com/tip2.pdf. The International Tanker Owners Pollution Federation Limited (ITOPF), United Kingdom.

50. Scheier, A.; Gominger, D., A preliminary study of the toxic effects of irradiated vs. non-irradiated water soluble fractions of no. 2 fuel oil. *Bulletin of Environmental Contamination and Toxicology* **1976**, 16, 595-603.
51. Griffin, L. F.; Calder, J. A., Toxic effect of water soluble fractions of crude, refined, and weathered oils on the growth of a marine bacterium. *Applied and Environmental Microbiology* **1977**, 33, 1092-1096.
52. Gordon, D. C.; Keizer, P. D.; Hardstaff, W. R.; Aldous, D. G., Fate of crude oil spilled on seawater contained in outdoor tanks. *Environmental Science and Technology* **1976**, 10, 580-585.
53. Sydnes, L. K.; Burkow, I. C.; Stene, A.; Lonning, S., The formation of short-lived, toxic, water-soluble compounds during illumination of crude oil on seawater. *Marine Environmental Research* **1985**, 16, 115-126.
54. Klein, A. E.; Pilpel, N., The effects of artificial sunlight upon floating oils. *Water Research* **1974**, 8, 79-83.
55. Jordan, R. E., *Analytical photochemistry of Prudhoe Bay crude petroleum in simulated oil spills: Identification of major lower molecular weight photo-oxidation products*. Doctoral Thesis, San Diego State University, 1991; 185 p.
56. Sydnes, L. K.; Hemmingsen, T. H.; Skare, S.; Hansen, S. H., Seasonal variations in weathering and toxicity of crude oil on seawater under arctic conditions. *Environmental Science and Technology* **1985**, 19, 1076-1081.
57. Sydnes, L. K.; Hansen, S. H.; Burkow, I. C., Factors affecting photo-oxidation of oil constituents in the marine environment. I. Photochemical transformation of dimethylnaphthalenes in an aqueous environment in the presence and absence of oil. *Chemosphere* **1985**, 14, 1043-1055.
58. Larson, R. A.; Hunt, L. L.; Blankenship, D. W., Formation of toxic products from a no. 2 fuel oil by photo-oxidation. *Environmental Science and Technology* **1977**, 11, 492-496.
59. Larson, R. A.; Boil, T. L.; Hunt, L. L.; Rogenmuser, K., Photo-oxidation products of a fuel oil and their antimicrobial activity. *Environmental Science and Technology* **1979**, 13, 965-969.
60. Burwood, R.; Speers, G. C., Photo-oxidation as a factor in the environmental dispersal of crude oil. *Estuarine Coastal and Marine Science* **1974**, 2, 117-135.
61. Nicodem, D. E.; Fernandes, M. C. Z.; Guedes, C. L. B.; Correa, R. J., Photochemical processes and the environmental impact of petroleum spills. *Biogeochemistry* **1997**, 39, 121-138.
62. Zepp, R. G., *Environmental approaches to environmental photochemistry*. In: *The handbook of environmental chemistry*. Springer: Berlin, 1982; Vol. 2, Part B, p. 19-41.
63. Zepp, R. G.; Cline, D. M., Rates of direct photolysis in aquatic environment. *Environmental Science and Technology* **1977**, 11, 359-366.
64. Zafiriou, O. C., Natural water photochemistry. *Chemical Oceanography* **1983**, 8, 339-379.
65. Mill, T.; Hendry, D. G.; Richardson, H., Free-radical oxidants in natural waters. *Science* **1980**, 207, 886-889.
66. Foote, C. S., *Free radicals in biology*. Academic Press: New York, 1976; Vol 2, p. 85.

67. Sanniez, W. H. K.; Pilpel, N., Photo-oxidation of floating hydrocarbon oils in the presence of some naphthalene derivatives. *Journal of the Chemical Society, Faraday Transactions I* 1978, 74, 123-130.
68. Gesser, H. D.; Wildman, T. A.; Tewaru, Y. B., Photo-oxidation of n-hexadecane sensitized by xanthone. *Environmental Science and Technology* 1977, 11: 605-608.
69. Ehrhardt, M. G.; Bouchertall, F.; Hoff, H. -P., Aromatic ketones concentrated from Baltic sea water. *Marine Chemistry* 1982, 11, 449-461.
70. Ehrhardt, M. G., Photo-oxidation products of fossil fuel components in the water of Hamilton harbour, Bermuda. *Marine Chemistry* 1987, 22, 85-94.
71. Ehrhardt, M. G.; Weber, R. R., Formation of low molecular weight carbonyl compounds by sensitized photochemical decomposition of aliphatic hydrocarbons in seawater. *Fresenius' Journal of Analytical Chemistry* 1991, 339, 772-776.
72. Rontani, J. F.; Bonin, P.; Giusti, G., Mechanistic study of interactions between photo-oxidation and biodegradation of n-nonylbenzene in seawater. *Marine Chemistry* 1987, 22, 1-12.
73. Ehrhardt, M. G.; Petrick, G., On the sensitized photo-oxidation of alkylbenzenes in seawater. *Marine Chemistry* 1984, 15, 47-58.
74. Ehrhardt, M. G.; Petrick, G., The sensitized photo-oxidation of n-pentadecane as a model for abiotic decomposition of aliphatic hydrocarbons in seawater. *Marine Chemistry* 1985, 16, 227-238.
75. Rontani, J. F.; Giusti, G., Photosensitized oxidation of pristane in sea water: Effect of photochemical reactions on tertiary carbons. *Journal of Photochemistry and Photobiology A: Chemistry* 1987, 40, 107-120.
76. Rontani, J. F.; Giusti, G., Photosensitized oxidation of 3,6-dimethyloctane. *Tetrahedron Letters* 1988, 29: 1923-1926.
77. Ehrhardt, M. G.; Weber, R. R., Sensitized photo-oxidation of methylcyclohexane as a thin film on seawater by irradiation with natural sunlight. *Fresenius' Journal of Analytical Chemistry* 1995, 352, 357-363.
78. Larson, R. A.; Berenbaum, M. R., Environmental phototoxicity. *Environmental Science and Technology* 1988, 22, 354-360.
79. Wan, Z.; Jenks, W. S., Photochemistry and photophysics of aromatic sulfoxides. 2. Oxenoid reactivity observed in the photolysis of certain aromatic sulfoxides. *Journal of the American Chemical Society* 1995, 117, 2667-2668.
80. Whitehurst, D. D.; Isoda, T.; Mochida, I., Present state of the art and future challenges in the hydrodesulfurization of polyaromatic sulfur compounds. *Advances in Catalysis* 1998, 42, 345-471.
81. Shafi, R.; Hutchings, G. J., Hydrodesulfurization of hindered dibenzothiophenes: An overview. *Catalysis Today* 2000, 59, 423-442.
82. Nag, N. K.; Sapre, A. V.; Broderick, D. H.; Gates, B. C., Hydrodesulfurization of polycyclic aromatics catalyzed by sulfided CoO-MoO₃/γ-Al₂O₃: The relative reactivities. *Journal of Catalysis* 1979, 57, 509-512.
83. Chouhary, T. V.; Malandra, J.; Green, J.; Parrott, S.; Johnson, B., Towards clean fuels: Molecular-level sulfur reactivity in heavy fuels. *Angewandte Chemie-International Edition* 2006, 45, 3299-3303.

84. Houalla, M.; Broderick, D. H.; Sapre, A. V.; Nag, N. K.; De Beer, V. H.; Gates, B. C.; Kwart, H., Hydrodesulfurization of methyl-substituted dibenzothiophenes catalyzed by sulfided Co-Mo/ γ -Al₂O₃. *Journal of Catalysis* **1980**, 61, 523-527.
85. Kabe, T.; Ishihara, A.; Tajima, H., Hydrodesulfurization of sulfur-containing polyaromatic compounds in light oil. *Industrial and Engineering Chemical Research* **1992**, 31, 1577-1580.
86. Schade, T.; Andersson, J. T., Speciation of alkylated dibenzothiophenes in a deeply desulfurized diesel fuel. *Energy and fuels* **2006**, 20, 1614-1620.
87. Moza, P. N.; Hustert, K.; Leoff, S., Photochemical transformations of selected organic chemicals in two phase system. *Toxicology and Environmental Chemistry* **1991**, 31/32, 103-106.
88. Hirai, T.; Ogawa, K.; Komasaawa, I., Desulfurization process for dibenzothiophenes from light oil by photochemical reaction and liquid-liquid extraction. *Industrial and Engineering Chemical Research* **1996**, 35, 586-589.
89. Hirai, T.; Shiraishi, Y.; Komasaawa, I., Desulfurization process for light oil by photochemical reaction and liquid-liquid extraction: Removal of benzothiophenes and alkyl sulfides. *Journal of Chemical Engineering of Japan* **1997**, 30, 171-173.
90. Hirai, T.; Shiraishi, Y.; Ogawa, K.; Komasaawa, I., Effect of photosensitizer and hydrogen peroxide on desulfurization of light oil by photochemical reaction and liquid-liquid extraction. *Industrial and Engineering Chemical Research* **1997**, 36, 530-533.
91. Shiraishi, Y.; Hara, H.; Hirai, T.; Komasaawa, I., A deep desulfurization process for light oil by photosensitized oxidation using a triplet photosensitizer and hydrogen peroxide in an oil/water two-phase liquid-liquid extraction system. *Industrial and Engineering Chemical Research* **1999**, 38, 1589-1595.
92. Shiraishi, Y.; Hirai, T., Photochemical desulfurization and denitrogenation of light oil by using benzophenone-modified silica gel as a heterogeneous triplet photosensitizer. *Solvent Extraction Research and Development, Japan* **2003**, 10, 79-85.
93. Andersson, J. T., Polycyclic aromatic sulfur heterocycles. I. Use of hydrogen peroxide oxidation for the group separation of polycyclic aromatic hydrocarbons and their sulfur analogs. *International Journal of Environmental and Analytical Chemistry* **1992**, 48, 1-15.
94. Andersson, J. T.; Bobinger, S., Polycyclic aromatic sulfur heterocycles II. Photochemical oxidation of benzo[*b*]thiophene in aqueous solution. *Chemosphere* **1992**, 24, 383-389.
95. Lichtenthaler, R. G.; Haag, W. R.; Mill, T., Photo-oxidation of probe compounds sensitized by crude oils in toluene and as an oil film on water. *Environmental Science and Technology* **1989**, 23, 39-45.
96. Haines, W. E.; Cook, G. L.; Ball, J. S., Gaseous decomposition products formed by the action of light on organic sulfur compounds. *Journal of the American Chemical Society* **1956**, 78, 5213-5215.
97. Ali, L. N.; Mantoura, R. F.; Rowland, S. J., The dissolution and photodegradation of Kuwaiti crude oil in seawater. Part 2: Laboratory photodegradation apparatus and photodegradation kinetics of a model seawater soluble hydrocarbon (phenanthrene). *Marine Environmental Research*, **1995**, 40, 319-335.

98. Shiraishi, Y.; Hirai, T.; Komasa, I., Identification of desulfurization products in the photochemical desulfurization process for benzothiophenes and dibenzothiophenes from light oil using an organic two-phase extraction system. *Industrial and Engineering Chemical Research* **1999**, 38, 3300-3309.
99. Bobinger, S.; Andersson, J. T., Degradation of the petroleum components monomethylbenzothiophenes on exposure to light. *Chemosphere* **1998**, 36, 2569-2579.
100. Andersson, J. T.; Bobinger, S., Photochemical degradation of crude oil components: 2-methyl-, 3-methyl- and 2,3-dimethylbenzothiophene. *Polycyclic Aromatic Compounds* **1996**, 11, 145-151.
101. Bobinger, S.; Traulsen, F.; Andersson, J. T., Dibenzothiophene in crude oils: Products from the photochemical degradation. *Polycyclic Aromatic Compounds* **1999**, 14/15, 253-263.
102. Traulsen, F.; Andersson, J. T.; Ehrhardt, M. G., Acidic and non-acidic products from the photo-oxidation of the crude oil component dibenzothiophene dissolved in seawater. *Analytica Chimica Acta* **1999**, 392, 19-28.
103. Shemer, H.; Linden, K. G., Photolysis, oxidation and subsequent toxicity of a mixture of polycyclic aromatic hydrocarbons in natural waters. *Journal of Photochemistry and Photobiology A: Chemistry* **2007**, 187, 186-195.
104. Che, Y.; Ma, W.; Ren, Y.; Chen, C.; Zhang, X.; Zhao, J.; Zang, L., Photo-oxidation of dibenzothiophene and 4,6-dimethyldibenzothiophene sensitized by N-methylquinolinium tetrafluoroborate: Mechanism and intermediates investigation. *Journal of Physical Chemistry B* **2005**, 109, 8270-8276.
105. Che, Y.; Ma, W.; Ji, H.; Zhao, J.; Zang, L., Visible photo-oxidation of dibenzothiophenes sensitized by 2-(4-methoxyphenyl)-4,6-diphenylpyrylium: An electron transfer mechanism without involvement of superoxide. *Journal of Physical Chemistry B* **2006**, 110, 2942-2948.
106. IFP, *Petroleum products separation of saturates, aromatics, resins and asphaltenes fractions liquid adsorption chromatography*. Institut Français de Pétrole, 2002. method IFP 9305: p. 1-8.
107. Kerst, M.; Platthaus, M.; Andersson, J. T., Isolation of polycyclic aromatic compounds by normal-phase column chromatography with a colour indicator. *Polycyclic Aromatic Compounds* **2000**, 19, 209-216.
108. Andersson, J. T., Retention properties of a palladium chloride silica sorbent for the liquid chromatographic separation of polycyclic aromatic sulfur heterocycles. *Analytical Chemistry* **1987**, 59, 2207-2209.
109. Pyell, U.; Schober, S.; Stork, G., Ligand-exchange chromatographic separation of polycyclic aromatic hydrocarbons and polycyclic aromatic sulfur heterocycles on a chelating silica gel loaded with palladium (II) or silver (I) cations. *Fresenius' Journal of Analytical Chemistry* **1997**, 359, 538-541.
110. Schade, T.; Roberz, B.; Andersson, J. T., Polycyclic aromatic sulfur heterocycles in desulfurized diesel fuels and their separation on a novel palladium (II)-complex stationary phase. *Polycyclic Aromatic Compounds* **2002**, 22, 311-320.
111. Mitchell, C. R.; Armstrong, D. W., *Methods in molecular biology*. Humana Press Inc.: Totowa, NJ, 2004; p. 61.

112. Panda, S. K.; Schrader, W.; Andersson, J. T., β -Cyclodextrin as a stationary phase for the group separation of polycyclic aromatic compounds in normal-phase liquid chromatography. *Journal of Chromatography A* **2006**, 1122, 88-96.
113. Chmielowiec, J.; George, A. E., Polar bonded-phase sorbents for high performance liquid chromatographic separations of polycyclic aromatic hydrocarbons. *Analytical Chemistry* **1980**, 52, 1154-1157.
114. Colgrove, S. G.; Svec, J. H., Liquid-liquid fractionation of complex mixtures of organic components. *Analytical Chemistry* **1981**, 53, 1737-1742.
115. Tevini, M., *Molecular biological effects of ultraviolet radiation*. In: *UV radiation and ozone depletion*. Lewis: Boca Raton, FL, 1993; p. 1-15.
116. Cody, T. E.; Radike, M. J.; Warshawsky, D., The phototoxicity of benzo[a]pyrene in the green alga *Selenastrum capricornutum*. *Environmental Research* **1984**, 35, 122-132.
117. Bowling, J. W.; Leversee, G. J.; Landrum, P. F.; Giesy, J. P. Jr., Acute mortality of anthracene-contaminated fish exposed to sunlight. *Aquatic Toxicology* **1983**, 3, 79-90.
118. Allred, P. M.; Giesy, J. P. Jr., Solar radiation-induced toxicity of anthracene to *Daphnia pulex*. *Environmental Toxicology and Chemistry* **1985**, 4, 219-226.
119. Oris, J. T.; Giesy, J. P. Jr., The photoenhanced toxicity of anthracene to juvenile sunfish (*Lepomis* spp.). *Aquatic Toxicology* **1985**, 6, 133-146.
120. Oris, J. T.; Giesy, J. P. Jr., The photo-induced toxicity of polycyclic aromatic hydrocarbons to larvae of the fathead minnow *Pimephales promelas*. *Chemosphere* **1987**, 16, 1395-1404.
121. Newsted, J. L.; Giesy, J. P. Jr., Predictive models for photoinduced acute toxicity of polycyclic aromatic hydrocarbons to *Daphnia magna*, Strauss (cladocera, crustacea). *Environmental Toxicology and Chemistry* **1987**, 6, 445-461.
122. Gala, W. R.; Giesy, J. P. Jr., Photo-induced toxicity of anthracene to green alga, *Selenastrum Capricornutum*. *Archives of Environmental Contamination and Toxicology* **1992**, 23, 316-323.
123. Ren, L.; Huang, X. D.; McConkey, B. J.; Dixon, D. G.; Greenberg, B. M., Photoinduced toxicity of three polycyclic aromatic hydrocarbons (fluoranthene, pyrene, naphthalene) to duckweed *Lemna gibba* L. G-3. *Ecotoxicology and Environmental Safety* **1994**, 28, 160-177.
124. Rowland, S., Stratospheric ozone in the 21st century: The chlorofluorocarbon problem. *Environmental Science and Technology* **1991**, 25, 622-628.
125. Smith, R. C.; Pcezelin, B. B.; Baker, K. S.; Bidigare, R. R.; Boucher, N. P.; Coley, T.; Karentz, D.; MacIntyre, S.; Matlick, H. A.; Menzies, D.; Ondrusek, M.; Wan, Z.; Waters, K. J., Ozone depletion: Ultra-violet radiation and phytoplankton biology in Antarctic waters. *Science* **1992**, 255, 952-958.
126. Kerr, J. B.; McElroy, C. T., Evidence of large upward trends of ultraviolet-B radiation linked to ozone depletion. *Science* **1993**, 262, 1031-1034.
127. Hermens, J. L. M., *Quantitative structure-activity relationships of environmental pollutants*. In: *Handbook of environmental chemistry*. Hutzinger, O. (Ed). Springer Verlag: Berlin, 1989; volume 2E, p. 111-162.

128. Veith, G. D.; Broderius, S. L., Rules for distinguishing toxicants that cause type I and type II narcosis syndromes. *Environmental Health Perspectives* **1990**, 87, 207-211.
129. Schultz, T. W.; Holcombe, G. W.; Phipps, G. L., Relationships of quantitative structure-activity to comparative toxicity of selected phenols in the *Pimephales promelas* and *Tetrahymena pyriformis* test systems. *Ecotoxicology and Environmental Safety* **1986**, 12, 146-153.
130. Lipnick, R. L., Outliers: Their origin and use in the classification of molecular mechanisms of toxicity. *Science of the Total Environment* **1991**, 119/110, 131-153.
131. Hermens, L. L. M., Electrophiles and acute toxicity to fish. *Environmental Health Perspectives* **1990**, 87, 219-225.
132. Ariens, E. J., *Receptors: A tool in drug development*. In: *Innovative approaches in drug research*. Harms, A.F. (Ed). Elsevier Science Publishers: Amsterdam, 1986; p. 9-22.
133. Verhaar, H. J. M.; Van Leeuwen, C. J.; Hermens, J. L. M., Classifying environmental pollutants. 1. Structure-activity relationships for prediction of aquatic toxicity. *Chemosphere*, **1992**, 25, 471-491.
134. Zitko, V.; Hutzinger, O., Uptake of chloro- and bromobiphenyls, hexachloro- and hexabromobenzene by fish. *Bulletin of Environmental Contamination and Toxicology* **1976**, 16, 665-673.
135. Grote, M.; Schüürmann, G.; Altenburger, R., Modeling photoinduced algal toxicity of polycyclic aromatic hydrocarbons. *Environmental Science and Technology* **2005**, 39, 4141-4149.
136. Landrum, P. F.; Giesy, J. P. Jr.; Oris, J. T.; Allred, P. M., *Photo-induced toxicity of polycyclic aromatic hydrocarbons to aquatic organisms*. In: *Oil in freshwater: Chemistry, biology, counter measure technology*. Proceedings of a symposium of oil in freshwater, Edmonton, Alberta, Canada. Vandermeulen, J. H.; Hrudehy, S. E. (Eds.). Pergamon Press: New York, 1987; p. 304-328.
137. Boese, B. L.; Lamberson, J. O.; Swartz, R. C.; Ozretich, R. J., Photoinduced toxicity of fluoranthene to seven marine benthic crustaceans. *Archives of Environmental Contamination and Toxicology* **1997**, 32, 389-393.
138. Huang, X. -D; Dixon, D. G.; Greenburg, B. M., Impacts of UV radiation and photomodification on the toxicity of PAHs to the higher plant *Lemna gibba* (duckweed). *Environmental Toxicology and Chemistry* **1993**, 12, 1067-1077.
139. McConkey, B. J.; Duxbury, C. L.; Dixon, D. G.; Greenberg, B. M., Toxicity of a PAH photo-oxidation product to the bacteria *Photobacterium phosphoreum* and the duckweed *Lemna gibba*: Effects of phenanthrene and its primary photoproduct, phenanthroquinone. *Environmental Toxicology and Chemistry* **1997**, 16, 892-899.
140. Xie, F.; Koziar, S. A.; Lampi, M. A.; Dixon, D. G.; Norwood, W. P.; Borgmann, U.; Huang, X.; Greenberg, B. M., Photoinduced toxicity of polycyclic aromatic hydrocarbons to *Daphnia magna*: Ultraviolet-mediated effects and the toxicity of polycyclic aromatic hydrocarbon products. *Environmental Toxicology and Chemistry* **2006**, 25, 613-622.
141. Lampi, M. A.; Gurska, J.; McDonald, K. I. C.; Xie, F.; Huang, X.; Dixon, D. G.; Greenberg, B. M., Photoinduced toxicity of polycyclic aromatic hydrocarbons to *Daphnia magna*: Ultraviolet-mediated effects and the toxicity of polycyclic aromatic

- hydrocarbon photoproducts. *Environmental Toxicology and Chemistry* **2006**, 25, 1079-1087.
142. Huang, X. -D.; Dixon, D. G.; Greenberg, B. M., Increased polycyclic aromatic hydrocarbon toxicity following their photomodification in natural sunlight: Impacts on the duckweed *Lemna gibba* L. G-3. *Ecotoxicology and Environmental Safety* **1995**, 32, 194-200.
143. Mallakin, A.; J. McConkey, B. J.; Miao, G.; McKibben, B.; Snieckus, V.; Dixon, D. G.; and Greenberg, B. M., Impacts of structural photomodification on the toxicity of environmental contaminants: Anthracene photo-oxidation products. *Ecotoxicology and Environmental Safety* **1999**, 43, 204-212.
144. Mallakin, A.; Babu, T. S.; Dixon, D. G.; Greenberg, B. M., Sites of toxicity of specific photo-oxidation products of anthracene to higher plants: Inhibition of the photosynthetic activity and electron transport in *Lemna gibba*. *Environmental Toxicology* **2002**, 17, 462-471.
145. Ohe, T., Mutagenicity of photochemical reaction products of polycyclic aromatic hydrocarbons with nitrite. *The Science of the Total Environment* **1984**, 39, 161-175.
146. Ren, L.; Zeiler, L. F.; Dixon, D. G.; Greenberg, B. M., Photoinduced effects of polycyclic aromatic hydrocarbons on *Brassica napus* (Canola) during germination and early seedling development. *Ecotoxicology and Environmental Safety* **1996**, 33, 73-80.
147. Schirmer, K.; Herbrick, J.-A. S.; Greenberg, B. M.; Dixon, D. G.; Bols, N. C., Use of fish gill cells in culture to evaluate the cytotoxicity and photocytotoxicity of intact and photomodified creosote. *Environmental Toxicology and Chemistry* **1999**, 18, 1277-1288.
148. Norberg-King, T. J.; Durhan, E. J.; Ankley, G. T., Application of toxicity identification evaluation procedures to the ambient waters of the Colusa basin drain, California. *Environmental Toxicology and Chemistry* **1991**, 10, 891-900.
149. Casellas, M.; Fernandez, P.; Bayona, J. M.; Solanas, A. M., Bioassay-directed chemical analysis of genotoxic components in urban airborne particulate matter from Barcelona (Spain). *Chemosphere* **1995**, 30, 725-740.
150. Fernandez, P.; Grifoll, M.; Solanas, A. M.; Bayona, J. M.; Albaiges, J., Bioassay-directed chemical analysis of genotoxic components in coastal sediments. *Environmental Science and Technology* **1992**, 26, 817-829.
151. Brack, W.; Altenburger, R.; Ensenbach, U.; Möder, M.; Segner, H.; Schüürmann, G., Bioassay-directed identification of organic toxicants in river sediment in the industrial region of Bitterfeld (Germany) - A contribution to hazard assessment. *Archives of Environmental Contamination and Toxicology* **1999**, 37, 164-174.
152. Castillo, M.; Barceló, D., Identification of polar toxicants in industrial wastewaters using toxicity-based fractionation with liquid chromatography/mass spectrometry. *Analytical Chemistry* **1999**, 71, 3769-3776.
153. Reemtsma, T.; Fiehn, O.; Jekel, M., A modified method for the analysis of organics in industrial wastewater as directed by their toxicity to *Vibrio fischeri*. *Fresenius' Journal of Analytical Chemistry* **1999**, 363, 771-776.
154. Galassi, S.; Benfenati, E., Fractionation and toxicity evaluation of waste waters. *Journal of Chromatography A* **2000**, 889, 149-154.

155. Kosian, P. A.; Makynen, E. A.; Monson, P. D.; Mount, D. R.; Spacie, A.; Mekenyan, O. G.; Ankley, G. T., Application of toxicity based fractionation techniques and structure-activity relationships models for the identification of phototoxic polyaromatic hydrocarbons in sediment pore water. *Environmental Toxicology and Chemistry* **1998**, 17, 1021-1033.
156. Thomas, K. V.; Benstead, R. E.; Thain, J. E.; Waldock, M. J., Toxicity characterization of organic contaminants in industrialized UK estuaries and coastal waters. *Marine Pollution Bulletin* **1999**, 38, 925-932.
157. Brack, W.; Altenburger, R.; Küster, E.; Meissner, B.; Wenzel, K.; Schüürmann, G., Identification of toxic products of anthracene photomodification in simulated sunlight. *Environmental Toxicology and Chemistry* **2003**, 22, 2228-2237.
158. Lampi, M. A.; Huang, X. -D.; El-Alawi, Y. S.; McConkey, B. J.; Dixon, D. G.; Greenberg, B. M., Occurrence and toxicity of photomodified polycyclic aromatic hydrocarbon mixtures present in contaminated sediments. *ASTM Special Technical Publication, STP 1403 (Environmental toxicology and risk assessment: Science, policy and standardization-implications for environmental decisions)* **2000**, 10, 211-220.
159. Kim, S.; Rodgers, R. P.; Marshall, A. G., Truly "exact" mass: Elemental composition can be determined uniquely from molecular mass measurement at ~0.1 mDa accuracy for molecules up to ~500 Da. *International Journal of Mass Spectrometry* **2006**, 251, 260-265.
160. Yamashita, M.; Fenn, J. B., Electrospray ion source. Another variation on the free-jet theme. *Journal of Physical Chemistry* **1984**, 88, 4451-4459.
161. Jürgen, H. G., *Mass spectrometry - A text book*. Springer Verlag Berlin: Heidelberg 2004; p 101, 518 p.
162. Wiley, W. C.; McLaren, I. H., Time-of-flight mass spectrometer with improved resolution. *Journal of Mass Spectrometry* **1997**, 32, 4-11.
163. Guillhaus, M.; Mlynsky, V.; Selby, D.; Perfect timing: Time-of-flight mass spectrometry. *Rapid Communications in Mass Spectrometry* **1997**, 11, 951-962.
164. Mamyrin, B. A.; Karataev, V. I.; Shmikk, D. V.; Zagulin, V. A., Mass reflectron. New nonmagnetic time-of-flight high-resolution mass spectrometer. *Zhurnal Eksperimental'noi i Teoreticheskoi Fiziki* **1973**, 64, 82-89.
165. Morris, H. R.; Paxton, T.; Dell, A.; Langhorne, J.; Berg, M.; Bordoli, R. S.; Hoyes, J.; Bateman, R. H., High sensitivity collisionally-activated decomposition tandem mass spectrometry on a novel quadrupole/orthogonal-acceleration time-of-flight mass spectrometer. *Rapid Communications in Mass Spectrometry* **1996**, 10, 889-896.
166. Boyle, J. G.; Whitehouse, C. M., Time-of-flight mass spectrometry with an electrospray ion beam. *Analytical Chemistry* **1992**, 64, 2084-2089.
167. Wolff, J. C.; Eckers, Ch.; Sage, A. B.; Giles, K.; Bateman, R., Accurate mass liquid chromatography/mass spectrometry on quadrupole orthogonal acceleration time-of-flight mass analyzers using switching between separate sample and reference sprays. 2. Applications using the dual-electrospray ion source. *Analytical Chemistry* **2001**, 73, 2605-2612.
168. Zamfir, A.; Peter-Katalinic, J., Glycoscreening by on-line sheathless capillary electrophoresis/electrospray ionization-quadrupole time of flight-tandem mass spectrometry. *Electrophoresis* **2001**, 22, 2448-2457.

169. Henry, C., Electrospray in flight. Orthogonal acceleration brings the advantages of time of flight to electrospray. *Analytical Chemistry* **1999**, 71, 197A-201A.
170. Rodgers, R. P.; Schaub, T. M.; Marshall, A. G., Petroleomics: MS returns to its roots. *Analytical Chemistry* **2005**, 77, 20A-27A.
171. Wu, Z.; Jernström, S.; Hughey, C. A.; Rodgers, R. P.; Marshall, A. G., Resolution of 10000 compositionally distinct components in polar coal extracts by negative-ion electrospray ionization Fourier transform ion cyclotron resonance mass spectrometry. *Energy and Fuels* **2003**, 17, 946-953.
172. www.ivv.fraunhofer.de/ms/ms-analyzers.html.
173. Scheppele, S. E.; Chung, K. C.; Hwang, C. S., Computer processing of mass spectral data. I. Assignment of formulas to experimental masses, chemical and mathematical principles. *International Journal of Mass Spectrometry and Ion Physics* **1983**, 49, 143-178.
174. Kendrick, E., A mass scale based on $\text{CH}_2 = 14.0000$ for high resolution mass spectrometry of organic compounds. *Analytical Chemistry* **1963**, 35, 2146-2154.
175. Hsu, C. S.; Qian, K. N.; Chen, Y. N. C., An innovative approach to data-analysis in hydrocarbon characterization by online liquid chromatography mass spectrometry. *Analytica Chimica Acta* **1992**, 264, 79-89.
176. Zhan, D.; Fenn, J. B., Electrospray mass spectrometry of fossil fuels. *International Journal of Mass Spectrometry* **2000**, 194, 197-208.
177. Kujawinski, E. B., Electrospray ionization Fourier transform ion cyclotron resonance mass spectrometry: Characterization of complex environmental mixtures. *Environmental Forensics* **2002**, 3, 207-216.
178. Stenson, A. C.; Landing, W. M.; Marshall, A. G.; Cooper, W. T., Ionization and fragmentation of humic substances in electrospray ionization Fourier transform ion cyclotron resonance mass spectrometry. *Analytical Chemistry* **2002**, 74, 4397-4409.
179. Marshall, A. G.; Hendrickson, C. L.; Jackson, G. S., Fourier transform ion cyclotron resonance mass spectrometry: A primer. *Mass Spectrometry Reviews* **1998**, 17, 1-35.
180. Fenn, J. B.; Mann, M.; Meng, C. K.; Wong, S. F.; Whitehouse, C. M., Electrospray ionization principles and practice. *Mass Spectrometry Reviews* **1990**, 9, 37-70.
181. Rudzinski, W. E.; Zhou, K.; Luo, X. M., Mass spectrometric characterization of organosulfur compounds using palladium (II) as a sensitivity enhancing reagent. *Energy and Fuels* **2004**, 18, 16-21.
182. Acheson, R. M.; Harrison, D. R., The synthesis, spectra, and reactions of some S-alkylthiophenium salts. *Journal of the Chemical Society C: Organic* **1970**, 13, 1764-1784.
183. Green, T. K.; Whitley, P.; Wu, K. N.; Lloyd, W. G.; Gan, L. Z., Structural characterization of sulfur compounds in petroleum by S-methylation and carbon-13 NMR spectroscopy. *Energy and Fuels* **1994**, 8, 244-248.
184. Boese, B. L.; Ozretich, R. J.; Lamberson, J. O.; Cole, F. A.; Swartz, R. C.; Ferraro, S. P., Phototoxic evaluation of marine sediments collected from a PAH-contaminated site. *Archives of Environmental Contamination and Toxicology* **2000**, 38, 274-282.
185. Boese, B. L.; Lamberson, J. O.; Swartz, R. C.; Ozretich, R.; Cole, F., Photoinduced toxicity of PAHs and alkylated PAHs to a marine infaunal amphipod (*Rhepoxynius*

- abroniusj*). *Archives of Environmental Contamination and Toxicology* **1998**, 34, 235-240.
186. Little, E. E.; Cleveland, L.; Calfee, R.; Barron, M. G., Assessment of the photoenhanced toxicity of a weathered petroleum to the tidewater silverside. *Environmental Toxicology and Chemistry* **2000**, 19, 926-932.
187. www.caudata.org/daphnia/#anatomy. Accessed 5 October 2007.
188. Organisation for Economic Cooperation and Development, Paris, France (OECD), OECD guidelines for testing of chemicals. *Daphnia sp acute immobilisation test and reproduction test*. Guideline 202, 1996; Section 2.
189. European Economic Community (EEC), *A: Methods for the determination of ecotoxicity. C2. Acute toxicity for Daphnia*. EEC Directive 92/69/EEC, Official Journal of the EEC L383, 1992.
190. American Society for Testing and Materials (ASTM), *Standard guide for conducting renewal life-cycle toxicity tests with Daphnia magna*. In: *Annual book of ASTM standards*. ASTM: Philadelphia, E 1193, 1987; p. 765-781.
191. Elenndt, B. -P.; Bias, W. -R., Trace nutrient deficiency in *Daphnia magna* cultured in standard medium for toxicity testing. Effects of the optimization of culture conditions on life history parameters of *Daphnia magna*. *Water Research* **1990**, 24, 1157-1167.
192. International Organization for standardization (ISO), *Water quality-determination of the inhibition of the mobility of Daphnia magna (Cladocera, Crustacea)*. ISO 6341, 1982; 15 p.
193. Duxbury, C. I.; Dixon, D. G.; Greenberg, B. M., The effects of simulated solar radiation on the bioaccumulation of polycyclic aromatic hydrocarbons by the duckweed *Lemna gibba*. *Environmental Toxicology and Chemistry* **1997**, 16, 1739-1748.
194. Payne, J. R.; Phillips, C. R., Photochemistry of petroleum in water. *Environmental Science and Technology* **1985**, 19, 569-579.
195. Ganjali, S. T.; Niknafs, B. N.; Khosravi, M., Photo-oxidation of crude petroleum maltenic fraction in natural simulated conditions and structural elucidation of photoproducts. *Iranian Journal of Environmental, Health and Science Engineering* **2007**, 4, 37-42.
196. Segura, J.; Venturam, R.; Jurado, C., Derivatization procedures for gas chromatographic-mass spectrometric determination of xenobiotics in biological samples, with special attention to drugs of abuse and doping agents. *Journal of Chromatography B* **1998**, 713, 61-90.
197. Solans, A.; Carnicero, M.; de la Torre, R.; Segura, J., Comprehensive screening procedure for detection of stimulants, narcotics, adrenergic drugs, and their metabolites in human urine. *Journal of Analytical Toxicology* **1995**, 19, 104-114.
198. Evershed, R. P., *Handbook of derivatives for chromatography*. Blau, K.; Halket, J. M. (Editors), Wiley: Chichester, UK, 2nd edition, 1993; p.51.
199. Wells, R. J., Recent advances in non-silylation derivatization techniques for gas chromatography. *Journal of Chromatography A* **1999**, 843, 1-18.
200. Opfermann, G.; Schaenzer, W., *Trimethyl silylation*. In: *Recent advances in doping analysis (4)*. Schaenzer, W.; Geyer, H.; Gotzmann, A.; Mareck-Engelke, U. (Editors). Sport und Buch Strauss: Köln, Germany, 1997; p.17-22.

201. Bandu, M. L.; Watkins, K. R.; Bretthauer, M. L.; Moore, C. A.; Desaire, H., Prediction of MS/MS data. 1. A focus on pharmaceuticals containing carboxylic acids. *Analytical Chemistry* **2004**, 76, 1746-1753.
202. McLafferty, F. W., *Interpretation of mass spectra*. University Science Books: Mill Valley, California, 1980; 3rd Edition, 303 p.
203. Kraft, M.; Spiteller, G., Die β , γ -Spaltung von Carbonylver-Bindungen und derivaten als Allgemeingültige Hauptabbau-Reaktion im Massenspektrometer. *Organic Mass Spectrometry* **1969**, 2, 541-546.
204. Rontani, J. -F.; Aubert, C., Trimethylsilyl transfer during electron ionization mass spectral fragmentation of some ω -hydroxycarboxylic and ω -dicarboxylic acid trimethylsilyl derivatives and the effect of chain length. *Rapid Communications in Mass Spectrometry* **2004**, 18, 1889-1895.
205. Draffan, G. H.; Stillwell, R. N.; McCloskey, J. A., Electron impact-induced rearrangement of trimethylsilyl groups in long chain compounds. *Organic Mass Spectrometry* **1968**, 1, 669-685.
206. McCloskey, J. A., Mass spectrometry of lipids and steroids. *Methods in Enzymology* **1969**, 14, 382-450.
207. Rios-Hernandez, L. A.; Gieg, L. M.; Suflita, J. M., Biodegradation of an alicyclic hydrocarbon by a sulfate-reducing enrichment from a gas condensate-contaminated aquifer. *Applied and Environmental Microbiology* **2003**, 69, 434-443.
208. Petersson, G., Mass spectrometry of hydroxy dicarboxylic acids as trimethylsilyl derivatives. Rearrangement fragmentations. *Organic Mass Spectrometry* **1972**, 6, 565-576.
209. McCloskey, J. A.; Stillwell, R. N.; Lawson, A. M., Use of deuterium-labeled trimethylsilyl derivatives in mass spectrometry. *Analytical Chemistry* **1968**, 40, 233-236.
210. Diekman, J.; Thomson, J. B.; Djerassi, C. J., Mass spectrometry in structural and stereochemical problems. CLV. Electron impact induced fragmentations and rearrangements of some trimethylsilyl ethers of aliphatic glycols, and related compounds. *Journal of Organic Chemistry* **1968**, 33, 2271-2284.
211. Diekman, J.; Thomson, J. B.; Djerassi, C., Mass spectrometry in structural and stereochemical problems. CLXXIII. The electron impact induced fragmentations and rearrangements of trimethylsilyl esters of ω -phenoxyalkanoic acids. *The Journal of Organic Chemistry* **1969**, 34, 3147-3161.
212. Smith, E.; Wraige, E.; Donkin, P.; Rowland, S., Hydrocarbon humps in the marine environment: synthesis, toxicity and aqueous solubility of monoaromatic compounds. *Environmental Toxicology and Chemistry* **2001**, 20, 2428-2432.
213. Alonso, M. C.; Barceló, D., Tracing polar benzene- and naphthalenesulfonates in untreated industrial effluents and water treatment works by ion-pair chromatography-fluorescence and electrospray-mass spectrometry. *Analytica Chimica Acta* **1999**, 400, 211-231.
214. Lehto, K.; Puhakka, J. A.; Lemmetyinen, H., Photodegradation products of polycyclic aromatic hydrocarbons in water and their amenability to biodegradation. *Polycyclic Aromatic Compounds* **2003**, 23, 401-416.

215. Rontani, J. -F.; Giusti, G., Photosensitized oxidation of n-butylcyclohexane as a model for photochemical degradation of n-alkylcyclohexanes in seawater. *Journal of Photochemistry and Photobiology, A: Chemistry* **1989**, 46, 357-365.
216. Moza, P. N.; Hustert, K.; Kettrup, A., Photo-oxidation of naphthalene and phenanthrene in hexane as an oil film on water. *Chemosphere* **1999**, 39, 569-574.
217. Metzger, K.; Rehberger, P. A.; Erben, G.; Lehmann, W. D., Identification and quantification of lipid sulfate esters by electrospray ionization MS/MS techniques: Cholesterol sulfate. *Analytical Chemistry* **1995**, 67, 4178-4183.
218. Schenck, G. O.; Krausch, C. H., Zur Photosensibilisierten O₂-Übertragung auf Schwefel-Verbindungen. Neuer Weg zu Sulfoxyden. *Angewandte Chemie* **1962**, 74, 510-510.
219. Banchereau, E.; Lacombe, S.; Ollivier, J., Unsensitized photo-oxidation of sulfur compounds with molecular oxygen in solution. *Tetrahedron* **1997**, 53, 2087-2102.
220. Dillon, T. M.; Neff, J. M.; Warner, J. S., Toxicity and sublethal effects of no. 2 fuel oil on the supralittoral isopod *Lygia exotica*. *Bulletin of Environmental Contamination and Toxicology* **1978**, 20, 320-327.
221. Hegazi, A. H.; Andersson, J. T., *Characterization of polycyclic aromatic sulfur heterocycles for source identification*. In: *Oil spill environmental forensics: Fingerprinting and source identification*. Wang, Z.; Stout, S. A. (Eds). Elsevier: Amsterdam, 2007; p. 147-168.
222. Havenga, W. J.; Rohwer, E. R., The determination of trace-level PAHs and diagnostic ratios for source identification in water samples using solid-phase microextraction and GC/MS. *Polycyclic Aromatic Compounds* **2002**, 22, 327-338.
223. Douglas, G. S.; Bence, A. E.; Prince, R. C.; Mcmillen, S. J.; Butler, E. L., Environmental stability of selected petroleum hydrocarbon source and weathering ratios. *Environmental Science and Technology* **1996**, 30, 2332-2339.
224. www.pash-standards.de, accessed 29 September 2007.
225. Mössner, S. G.; Wise, S. A., Determination of polycyclic aromatic sulfur heterocycles in fossil fuel-related samples. *Analytical Chemistry* **1999**, 71, 58-69.
226. Hegazi, A. H.; Andersson, J. T.; El-Gayar, M. Sh., Application of gas chromatography with atomic emission detection to the geochemical investigation of polycyclic aromatic sulfur heterocycles in Egyptian crude oils. *Fuel Processing Technology* **2003**, 85, 1-19.
227. Ehrhardt, M. G.; Burns, K. A.; Bicego, M. C., Sunlight-induced compositional alterations in the seawater-soluble fraction of a crude oil. *Marine Chemistry* **1992**, 37, 53-64.
228. Prince, R. C.; Garrett, R. M.; Bare, R. E.; Grossman, M. J.; Townsend, T.; Suflita, J. M.; Lee, K.; Owens, E. H.; Sergy, G. A.; Braddock, J. F.; Lindstrom, J. E.; Lessard, R. R., The roles of photo-oxidation and biodegradation in long-term weathering of crude and heavy fuel oils. *Spill Science and Technology Bulletin* **2003**, 8, 145-156.
229. Müller, H.; Andersson, J. T.; Schrader, W., Characterization of high-molecular weight sulfur-containing aromatics in vacuum residues using Fourier transform ion cyclotron resonance mass spectrometry. *Analytical Chemistry* **2005**, 77, 2536-2543.

230. Kochany, J.; Maguire, R. J., Abiotic transformations of polynuclear aromatic hydrocarbons and polynuclear aromatic nitrogen heterocycles in aquatic environments. *Science of the Total Environment* **1994**, 144, 17-31.
231. Garrett, R. M.; Pickering, I. J.; Haith, C. E.; Prince, R. C., Photo-oxidation of crude oils. *Environmental Science and Technology* **1998**, 32, 3719-3723.
232. Guieysse, B.; Viklund, G.; Toes, A.; Mattiasson, B., Combined UV-biological degradation of PAHs. *Chemosphere* **2004**, 55, 1493-1499.
233. Guieysse, B.; Viklund, G.; Sequential UV–biological degradation of polycyclic aromatic hydrocarbons in two-phases partitioning bioreactors. *Chemosphere* **2005**, 59, 369-376.
234. Dutta, T. K.; Harayama, S., Analysis of long-side-chain alkylaromatics in crude oil for evaluation of their fate in the environment. *Environmental Science and Technology* **2001**, 35, 102-107.
235. Sinninghe Damsté, J. S.; White, C. M.; Green, J. B.; de Leeuw, J. W., Organosulfur compounds in sulfur-rich Rasa coal. *Energy and Fuels* **1999**, 13, 728-738.
236. Kohnen, M. E. L.; Sinninghe Damsté, J. S.; ten Haven, H. L.; de Leeuw, J. W., Early incorporation of polysulfides in sedimentary organic matter. *Nature* **1989**, 341, 640-641.
237. Sinninghe Damsté, J. S.; de Leeuw, J. W., Analysis, structure and geochemical significance of organically bound sulfur in the geosphere: State of the art and future research. *Organic Geochemistry* **1990**, 16, 1077-1101.
238. Schmid, J. C., *Marqueurs biologiques soufrés dans les pétroles*. Ph. D. dissertation 1986, University of Strasbourg.
239. Sinninghe Damsté, J. S.; de Leeuw, J. W., The origin and fate of isoprenoid C₂₀ and C₁₅ sulfur compounds in sediments and oils. *International Journal of Environmental Analytical Chemistry* **1987**, 28, 1-19.
240. Sinninghe Damsté, J. S.; Rijpstra, W. I. C.; de Leeuw, J. W.; Schenck, P. A., The occurrence and identification of series of organic sulfur compounds in oils and sediment extracts: II. Their presence in samples from hypersaline and non-hypersaline palaeoenvironments and possible application as source, palaeoenvironmental and maturity indicators. *Geochimica and Cosmochimica Acta* **1989**, 53, 1323-1341.
241. Pyell, U.; Stork, G., Preparation and properties of an 8-hydroxyquinoline silica gel, synthesized via Mannich reaction. *Fresenius' Journal of Analytical Chemistry* **1992**, 342, 281-286.
242. Seshadri, T.; Kettrup, A., Synthesis and characterization of silica gel ion exchanger bearing 2-amino-1-cyclopentene-1-dithiocarboxylic acid (ACDA) as chelating compound. *Fresenius' Zeitschrift für Analytische Chemie* **1982**, 310, 1-5.

Acknowledgement

First of all, I would like to thank my principal advisor Prof. Dr. Jan T. Andersson for his invaluable guidance and continuous support during my entire Ph. D. tenure. The successful completion of my research work was only possible by his informative suggestion and fruitful discussions in addition to his amicable nature and friendly attitude.

I would like to thank Prof. Dr. Hans-Ulrich Humpf and Prof. Dr. Uwe Karst for being my mentors for the dissertation committee.

In addition, I want to thank my colleagues: Dr. Thomas Schade, Dr. Benedikte Roberz, Dr. Kishore Sripada, Dr. Saroj Panda, Markus Penassa, Nina Kolbe, Magdalena Ulman, Daniel Plothe, Claudia Sill, Peni Hadayani, and Thies Nolte for their help, support and for providing a friendly working environment. Especially, I thank Ansgar Japes for the translation of the English summary and for his help concerning the printing of the thesis. There are also two members of our group whom I would like to acknowledge individually: Mrs. Marianne Lüttmann and Mrs. Karin Weißenhorn.

My sincere thanks to Dr. Wolfgang Schrader from Max Planck Institute, Mülheim, for performing the FT-ICR MS measurements.

I would like to thank the German Academic Exchange Service (DAAD) for providing the financial assistance for two and half years to carry out this work. Egyptian government is also acknowledged for presenting a six months grant to complete the work.

My appreciation to Agiba Petroleum Company, Egypt, for supplying the crude oil used in this study.

I would like to collectively thank all my friends in Germany and Egypt for their love and care.

Especially, I would like to convey my special thanks to my husband Dr. Abdelrahman Hegazi for his love, help and support which enabled me to complete this work and for correcting the first version of the thesis.

However, this thesis certainly would not have been possible without the love, continuous support and encouragement of my parents and my sister.